

University of Naples “Federico II”
Faculty of Science MM.FF.NN
Department of Chemistry

**TESI DI DOTTORATO IN
SCIENZE CHIMICHE XXIV ciclo**

**“Innovative processes for the production
of acetaldehyde, ethyl acetate
and pure hydrogen by Ethanol”**

Candidata: Dott. **Giuseppina Carotenuto**

Tutore: Ch.mo Prof. **Elio Santacesaria**

Relatore: Ch.mo Prof. **Mauro Causà**

Coordinatore: Ch.mo Prof. **Lucio Previtera**

**DOTTORATO DI RICERCA
IN SCIENZE CHIMICHE (SETTORE CHIM/03)
(XXIV CICLO)**

Novembre 2011

Table of Contents

Preface	i-iii
General Introduction: Literature review and background	1
i.1 Introduction.....	1
i.2 Ethanol production.....	4
i.3 Chemicals from ethanol	8
i.3.1 Acetaldehyde uses and global demand	10
i.3.2 Ethyl acetate and Hydrogen global market	11
i.4 Strategy and thesis contents	14
i.5 References	18
Section A	
Abstract: Ethanol Oxidative Dehydrogenation to acetaldehyde	20
Chapter 1: Acetaldehyde literature background	21
A-1.1 Introduction	21
A-1.2 Acetaldehyde production	22
A-1.2.1 Dehydrogenation.....	22
A-1.2.2 OxidativeDehydrogenation	27
A-1.3 Vanadia based catalysts preparation.....	31
A-1.3.1 Classical routes	22
A-1.3.2 Grafting techniques	27
A-1.4 Metal alkoxides.....	33
A-1.4.1 Adsorption isotherms	35
A-1.4.1.1 Support $\text{TiO}_2/\text{SiO}_2$	35
A-1.4.1.2 Support $\text{V}_2\text{O}_5/\text{TiO}_2\text{-SiO}_2$	38
A-1.5 References.....	45
Chapter 2: Techniques and equipment	46
A-2.1 Introduction	46
A-2.2 Catalysts preparation.....	47
A-2.2.1 Vanadia based catalysts prepared by grafting	47
A-2.2.2 Copper based catalysts prepared by impregnation	52
A-2.2.3 Copper based catalysts prepared by coprecipitation.....	52
A-2.2.4 Commercial copper compositions.....	52
A-2.3 Apparatus of reaction	53

A-2.4 References	57
Chapter 3: Experimental results	57
A-3.1 Introduction	57
A-3.2 Ethanol dehydrogenation with copper based catalysts	58
A-3.3 Oxidative dehydrogenation (ODH) with vanadia.....	66
A-3.4 Acetaldehyde an intermediate to produce Ethyl acetate	69
A-3.5 References	71
Conclusions	73
Section B	
Abstract: One step dehydrogenation to ethyl acetate.....	74
Chapter 1: Ethyl acetate literature background.....	74
B-1.1 Introduction	76
B-1.2 EA classical route of production	77
B-1.3 EA innovative way of production.....	81
B-1.3.1 Dehydrogenation	82
A-1.3.2 Main reaction	82
A-1.3.3 Active phases.....	86
A-1.3.2 Operative conditions	96
B-1.4 Hydrogen production	99
B-1.5 References.....	100
Chapter 2: Techniques and equipment	103
B-2.1 Introduction	103
B-2.2 Commercial Catalysts compositions	103
B-2.3 Catalysts characterization.....	105
B-2.4 Catalytic runs: operative conditions.....	111
B-2.4.1 Apparatus.....	114
B-2.4.2 Gas-chromatography.....	114
B-2.5 References.....	117
Chapter 3: Thermodynamic study	118
B-3.1 Introduction	118
B-3.2 Equilibrium constants evaluation	118
B-3.3 Aspen	122
B-3.4 Results and Discussion	125

B-3.5 References.....	134
Chapter 4: Experimental	135
B-4.1 Introduction	135
B-4.2 Catalysts characterization	137
B-4.2.1 Ex-Situ characterization	138
B-4.2.2 In-Situ characterization	153
B-4.3 Experimental runs	167
B-4.4 Discussion and mechanism of reaction	213
B-4.5 References.....	220
Chapter 5: kinetic study	226
B-5.1 Introduction	226
B-5.2 Diffusivity limits	231
B-5.2.1 Intraparticles transfer	231
B-5.2.2 Interphase transfer	233
B-5.3 kinetic study.....	234
B-5.3.1 Reaction mechanism.....	234
B-5.4 Models	238
B-5.4.1 Power Law	239
B-5.4.1.1 Mod.1.1	239
B-5.4.1.2 Mod.1.2	245
B-5.4.1.3 Mod.1.3	246
B-5.4.2 Adsorption Dual Sites	250
B-5.4.2.1 Mod.2.1	259
B-5.4.1.2 Mod.2.2	265
B-5.4.1.3 Mod.2.3	265
B-5.4.3 LHHW Mod.3	266
B-5.4.4 List of Symbols.....	280
B-5.5 References.....	281
Chapter 6: Plant Design.....	282
B-6.1 Introduction	282
B-6.1.1 Process Scale up.....	282
B-6.1.2 Process design	283
B-6.2 Project: main aspects.....	286
B-6.2.1 Simulation Hints.....	286
B-6.2.2 Process description	287
B-6.2.2.1 Section 100	291
B-6.2.2.2 Section 200	295

B-6.2.2.3 Section 300	297
B-6.2.2.4 Section 400	300
B-6.3 Summary	304
B-6.4 References	305
Conclusions	306

Section C

Abstract: OPX reactions for hydrogen production	312
Chapter 1: Hydrogen production literature background	312
C-1.1 Introduction	313
C-1.2 Steam reforming	314
C-1.2.1 Noble metals	315
C-1.2.2 Non noble metals	317
C-1.3 Reforming and partial oxidation	323
C-1.4 oxidative steam reforming	325
C-1.5 Innovative catalysts preparation: combustion synthesis	326
C-1.6 References	328
Chapter 2: Techniques and equipment	333
C-2.1 Introduction	103
C-2.2 Catalysts preparation: combustion synthesis	334
C-2.3 Catalysts characterization	336
C-2.4 Catalytic runs: operative conditions	340
C-2.4.1 Apparatus	340
C-2.4.2 Gas-chromatography	342
Chapter 3: Experimental	343
C-3.1 Introduction	343
C-3.2 Catalysts characterization	344
C-3.2.1 Ex-Situ characterization	345
C-3.2.2 In-Situ characterization	351
C-3.3 Experimental runs	356
C-3.3.1 Combustion catalysts	356
C-3.3.2 Commercial catalysts	369
C-3.4 Discussion	376
C-3.5 References	385

Conclusions	386
OVERALL CONCLUSIONS	388
Appendix A: Characterization techniques	387
Appendix B: Matlab code	404
Appendix C: Plant equipment.....	403

PREFACE

The research motivation

The aim of this research is the development of new heterogeneous catalytic processes to produce high commodities chemicals of industrial interest such as ethyl acetate, acetaldehyde and pure hydrogen from bio-ethanol.

Actually, the acetaldehyde is produced by dehydrogenation reaction of ethanol performed at high temperature and low pressure. The thermodynamic restriction of this reaction has been a starting point to study the oxidative dehydrogenation reaction of the ethanol. A challenge of this new process is represented by the individuation of a good alternative catalytic system to improve the acetaldehyde selectivity. At this purpose new catalytic systems have been prepared by grafting of vanadia on a multiple layers of titania supported on silica. The obtained results could be considered very promising and strictly correlated to the nature of the prepared catalysts. The grafting technique has, as main advantage, the possibility to obtain catalysts with a well dispersed active phase, a high resistance to sintering and a high mechanical strength.

Successively, our interest has been focused on the ethyl acetate production. The use, in the classical processes, of acetaldehyde and acetic acid, respectively, a toxic and corrosive solvents and the corresponding increase of the global demand of this solvent, has required the development of alternative production routes. In particular, the ethanol dehydrogenation reaction represents a possible alternative route to produce ethyl acetate with high yields. The main

peculiarities of the proposed process is the low cost of raw materials, of plant maintenance and the possibility to obtain in only one step of reaction the main product with an high degree of purity. The catalysts employed, to perform this reaction, are copper based ones supported and unsupported on Alumina. The catalysts are characterized by the presence of different promoters such as zinc oxide and chromia. The use of promoters is fundamental to improve the copper stability on the catalyst surface due to the low Huttig-Tamman temperature (300°C) of the copper. As matter of fact, the mobility of the copper particles became very significant at temperature higher than 180°C. The main advantage of this process is related to the possibility to obtain pure hydrogen, which could be recovered and used to feed fuel cells. This reaction has been studied in more details with the aim to realize a scale up of the process. At this purpose, various dimensionless criteria were evaluated to confirm there was not significant mass transfer limitation, and thus the experimental results represent intrinsic kinetics. Furthermore, a thermodynamic study was conducted using a Gibbs free energy minimization method to identify the effect of reaction conditions on ethanol conversion and ethyl acetate selectivity with the aim to evaluate the thermodynamically favorable operating conditions. The performances of different copper based catalytic systems have been studied in the ethanol dehydrogenation reaction. Moreover, the performances of these catalytic systems were correlated with their physical and chemical properties; in fact, a careful study of characterization was realized. A depth investigation has suggested that the individuation of the optimal conditions of temperature, pressure, residence time and feed composition is fundamental to improve the ethanol conversion and reach the desided industrial target of purity. By the depth kinetic study was identified the best model able to fit the experimental data: the Langmuir-Hinselwood-Hougen-Watson (LHHW). The examined model

was used to determine the activation energy, the order of reaction and the kinetics parameter useful for a process scale-up.

Moreover, the ethanol reforming and oxidative reforming reactions in presence of both commercial and prepared by combustion synthesis catalysts have been studied. The interest for this reaction is essentially due to the high global demand of hydrogen in the last few years. The high yield in hydrogen has been obtained in wide range of temperature (100-500°C) and atmospheric pressure. The use of catalysts highly resistant to sintering and with a very high thermal strength has been required to perform this reaction. At this purpose the use of catalysts promoted by chromia has been proposed. The catalytic performances of commercial catalysts have been compared with the ones prepared by combustion. The catalysts physical and chemical properties have been deeply investigated by using the common characterization techniques. The scope of this research is, thus, the development of new process able to convert, ethanol produced by renewable raw material, in high commodities chemicals and pure hydrogen.

INTRODUCTION

A general overview

This chapter provides general background information about the research carried out, including a general overview about the ethanol application in oxidative dehydrogenation, dehydrogenation and oxidative reforming reactions of ethanol, and around the catalysts selection, research methodology and objectives.

i-1 Introduction

In the last years, the main interest of the worldwide academic and industrial research is to attain *sustainable* chemical industry. Due to the reduced availability of non-renewable resources and the climate change caused by increasing the greenhouse effect, studies have been conducted with a view to gradual replacement of current energy sources based on fossil fuels to produce clean fuels from biomass. At this purpose an investigation of the potential of substituting bioethanol based processes to the fossil-based processes, has been realized in this project. In particular, in this research three processes were investigated, that share the use of ethanol as feedstock. Actually, the vast majority of fuels and carbon-containing chemicals are produced from fossil resources but on the other hand, many studies predict that most kinds of fossil resources will be depleted within the next century. Furthermore, the combustion of fossil fuels causes elevated levels of greenhouse gases (GHG) in the atmosphere, which is the main cause of the global warming effect [1]. Consequently, in the last years the growing concerns related to the safeguard of the world

by the greenhouse gas emissions and by the global warming have captured the attention of the worldwide multinational companies [2]. At this purpose, the aim of the nowadays society is a gradual change from an economy based on fossil resources to one based on sustainable resources. Biomass resource is widely acknowledged as a potential substitute of fossil resources for sustainable development. Many kinds of biomasses are potentially available at a large scale and are cost-competitive with petroleum whether considered on a mass or energy basis, and in terms of price on current, projected and mature technology [3]. Bio-ethanol has already been playing a role as a kind of bio-fuel replacing petroleum and, its large availability in the next future will make it as the main feedstock to produce many kinds of high commodity chemicals. Produced by various kinds of biomass renewable resources, bio-ethanol can be considered as a possible candidate that would contribute to solving some urgent environmental problems such as fossil depletion and climate change. However, the utilization of bio-ethanol cannot guarantee actual sustainability unless bio-ethanol based processes are examined from the viewpoints of not only renewability but also other sustainability indicators. Therefore, a comprehensive assessment of bio-ethanol based processes from the viewpoint of monetary and non-monetary issues, such as environmental impacts and safety hazards, is strongly needed considering the entire chain of production processes of both bio-ethanol and bio-ethanol based chemicals. This assessment is aimed to provide visions for further development and investment in bio-ethanol based chemical industry. It is noteworthy that with the proper technology it is possible to convert biomass to essentially all the high-value commodity chemicals and fuels currently available from fossil resources. There could even be some advantages using biomass compared to fossil fuels as a feedstock, e.g., for production of certain oxygenated chemicals since introduction of oxygen functionalities into hydrocarbons can be rather difficult, whereas many products derived from biomass already contain some oxygen [4]. However, this also

entails an increase in production costs for some of the non-oxygen-containing products, such as gasoline [5]. Figure 1 illustrates that, in relative terms, it is possible to produce some chemicals from biomass. Thus, fossil and renewable resources are not necessarily equally useful starting materials for all possible products.

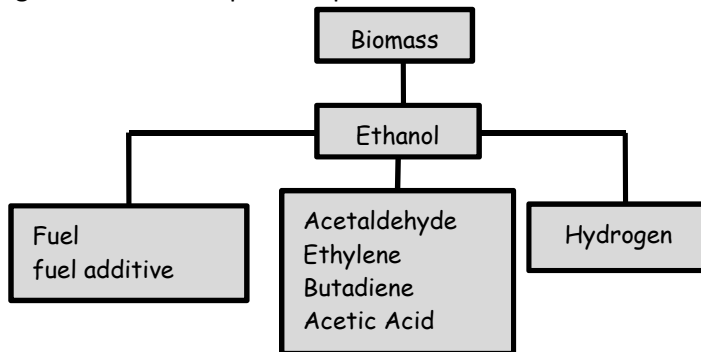


Figure 1: Bioethanol as new generation fuel and as feedstock for many high commodities chemicals and hydrogen.

In particular, the growing demands for CO₂-neutral transportation fuels and the desire to achieve a reduced dependence on fossil resources have been the major driving forces for the substantial increase in the amounts of bioethanol produced by fermentation of biomass. An interesting question is whether the optimal use of bioethanol as a fuel, or as a feedstock for producing higher-value chemical products. As well known, the ethanol is already widely used, as motor fuel or additive for gasoline in country such as Brazil and in the United States [6]. From 2007 to 2008, the share of ethanol in global gasoline type fuel use increased from 3.7% to 5.4%[6]. In 2010 worldwide ethanol fuel production reached 22.95 billion U.S. liquid gallons (bg) (86.9 billion liters), with the United States as the top producer with 13.2 bg (50 billion liters), accounting for 57.5 percent of global production [7]. Moreover, the ethanol is a potential sources for hydrogen considered as the fuel of the future that can be employed in fuel cells for auto vehicles application. The ethanol could be find application also in the production of an important industrial chemical

as acetaldehyde that can be used in turn as an intermediate in the production of acetic acid, acetic anhydride, ethyl acetate, butyraldehyde, crotonaldehyde, n-butanol and many other high value chemicals[8]. A potential source for low-cost ethanol production is to utilize waste means as lignocellulosic materials (crop residues, grasses, sawdust, woodchips, sludges, livestock manure) [9]. The feasibility of using these materials as a feedstock is often limited by the cost of bioethanol production, which is relatively high based on current technologies. The challenges are generally associated with the low yield and the high cost of the hydrolysis process [10]. In the next paragraph, a general framework on the bioethanol production and application will be discussed.

i-2 The oil market and the Ethanol innovative routes

As well known, the light olefins and in particular the propylene and ethylene represents some of the main building-blocks of the chemical industry. The great interest for these raw materials is related to their application for the production of important chemicals, commonly employed for the production of materials of large consume and fuels. The Figure 2 represents the common employments of the mentioned building block.

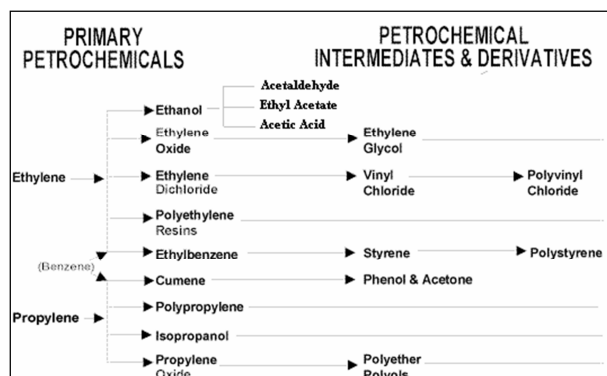


Figure 2: main products obtainable by ethylene and propylene

Ethanol is directly produced by ethylene, one of the main sub-products of the petroleum processing. The increasing of the global demand of the olefins required the necessity to develop new dedicated processes, such as the steam cracking and the catalytic cracking, for the processing of virgin naphtha. The Business Intelligence Committee (BIC) of APPE (Association of Petrochemicals Producers in Europe) [11] has estimated the global production of olefins by fossil raw materials and in particular, in Figure 3 a review of the market situation for ethylene as well as an analysis of the competitiveness of the European petrochemicals industry has been reported.

On the other hand the rapid rise of oil prices, that began in 2007 culminated in the middle of 2008 as in the last two years as shown by the trends represented in Figure 4, requires the development of alternative processes able to use raw materials of renewable nature for the production of ethanol, as alternative to the classical routes that employs ethylene derived by fossil sources.

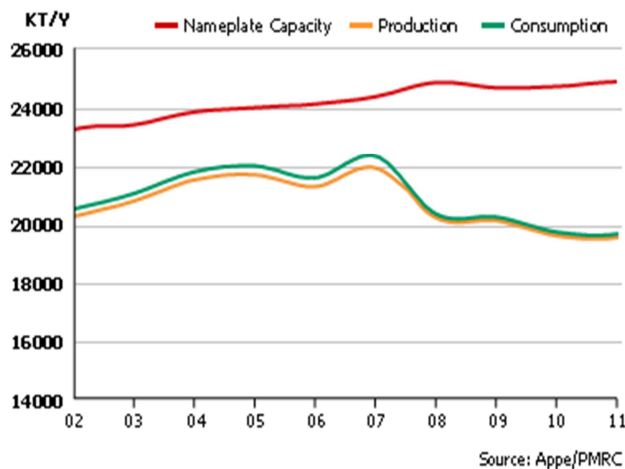


Figure 3: market situation for ethylene

Moreover, the worldwide interest for the safety of the planet and the new concept of environmental sustainability requires the individuation

of alternative sources to the fossil ones. The use of biomasses represents actually a great challenge for the research world. Supplies of ethanol have increased greatly in the last few years and the development of alternative technologies able to convert waste cellulosic residues in second generation bio-ethanol will generate its large supply in the next decades, which could be used as a gasoline substitute or fuel additive.



Figure 4: oil price revolution (INSEE Institut National de la Statistique et des Études Économiques)

Taking into account, this future large availability of bio-ethanol, the use of ethanol as feedstock for the chemical industry can also be foreseen. Brazil and many tropical countries use sugarcane or molasses, while France, the largest producer in Europe, uses mainly sugar beets. The United States and eastern Canada use mainly corn kernels; in western Canada, wheat is the main feedstock. In China, corn, cassava and sweet potatoes are the mostly used materials. In France and Italy, ethanol is also produced from waste from wine manufacture [12]. Actually, a considerable research is being focused on developing processes that can produce ethanol from low-cost, no-food feedstock. The industry is hoping to develop economical cellulosic ethanol, derived from the fermentation of cheap forms of

biomass. The main challenge is the development of advanced or 2nd generation production technologies. At this purpose the use of lignocellulosic materials to produce bioethanol represent a really advanced technology. In fact, the bio-ethanol can be produced by using several materials such as sugar, starch and lignocellulose-based materials but bioethanol is produced predominantly from sugarcane and corn. The use of lignocellulose represents a great challenge cause by the difficulties of pre-treatment of the raw materials than sugar-rich or starch-rich materials. On the other hand, the lignocellulosic materials are abundant almost all over the world and they can be used for bioethanol production because they have a high content of cellulose and hemicellulose. In more detail, the lignocellulose is composed of mainly cellulose, hemicellulose and lignin. Cellulose is a long-chain homogenous polysaccharide of D-glucose units linked by β -1,4 glycoside bonds and contains over 10,000 glucose units. Hemicellulose is a complex, heterogeneous polymer of sugars and sugar derivatives which form a highly branched network and the monomers include hexoses (glucose, galactose, and mannose) and pentoses (xylose and arabinose). It consists of about 100-200 sugar units. Lignin is a very complex heterogeneous mixture of mainly phenolic compounds and their derivatives. It is a main component in plant cell walls. Lignin holds the cellulose and hemicellulose fibers together and provides support to the plants. The great complexity of the lignocelluloses materials requires its conversion to ethanol by involving three steps: pretreatment, hydrolysis, and fermentation. The purpose of the pretreatment is to separate the lignin from the main polymeric components cellulose and hemicelluloses in the lignocellulose, reduce cellulose crystallinity, and increase the porosity of the material, so the hydrolytic enzymes can access their substrates (cellulose and hemicellulose) in the following enzymatic hydrolysis. The pretreatment technologies have been extensively investigated in the last three decades, including physical, chemical, and biological processes. The main drawback of the acid or alkaline hydrolyses

(chemical pretreatment) is due to corrosion and maintenance of the apparatus. Moreover the dilute acid pretreatment could get the formation of chemicals such as furfurals during the degradation of hemicelluloses that inhibit the following enzymatic hydrolysis and microbial fermentation. While during the alkaline pretreatment, although alkaline pretreatment could cut the bonds between lignin and cellulose or hemicelluloses, a significant portion of lignin still remains mixed with cellulose after the pretreatment. The existence of lignin may inhibit cellulase enzymes during the following enzymatic hydrolysis. An alternative methodology of pre-treatment is of biological typology by using microbes such as brown-, white- and soft-rot fungi to degrade lignin and hemicellulose in lignocellulosic materials. Although this process has positive economical feedback, it is also a very time consuming process in fact the pretreatment usually takes a few weeks. An innovative pretreatment is the physical one that includes low energy consumption pretreatment process using saturated water vapor to release polysaccharides rapidly and without chemicals. The pretreatment includes a previously mechanical comminution, steam explosion, ammonia fiber explosion, and pyrolysis. After the pretreatment process, of the lignocellulosic materials an enzymatic hydrolysis is employed to obtain hexoses (glucose, galactose, and mannose), from the cellulose fraction and pentoses (xylose and arabinose), from the hemi-cellulose fraction. The enzymatic hydrolysis is carried out in very mild conditions about pH=4.8 and 50°C, by using as catalytic system enzymes such as cellulase and hemicellulose. Finally the fermentation converts the clean sugars to ethanol using a modified by brewer's yeast (*Saccharomyces cerevisiae*). The fermentation step produces beer with a high ethanol concentration. In the last step of the process beer resulting from fermentation is treated in a separate column to separate ethanol from fermentation residues, mainly lignin. Since lignin has a high heating value it can be fed to a cogeneration unit to produce steam and electrical power, thus ensuring self-sustaining from an energy perspective.

i-3 The Bio-refinery: chemicals from Bio-ethanol

The exploitation of biomass as well defined in the previously paragraph represents a key technology toward a sustainable development. In particular the large supply of ethanol obtained by cellulosic residues could be used to produce commodity chemicals of great interest. In the last several years the main interest of the research world is to investigate the potential of substituting bioethanol based processes for fossil-based process to produce ethylene, acetaldehyde, acetic acid, ethyl acetate and pure hydrogen. As a matter of fact the technologies for producing chemicals from ethanol are well known and have been employed commercially for several decades. Ethylene production by ethanol dehydration, for example, was widely used in the United States and Western Europe during the first half of the 20th century, and in Brazil and India during the 1950s and 1960s. Thereafter, the steam cracking process, which employs petroleum fractions and natural gas as feedstock, emerged as the dominant method for large-scale ethylene production worldwide. As consequence of declining oil prices in the 1980s and 1990s and wide availability of olefins from steam cracking, most processes using ethanol as feedstock could no longer compete with their corresponding petrochemical routes, and the ethanol-based chemical industry went into decline.

With the recent boom in the market of ethanol as fuel, particularly in Brazil and the United States, the production of chemicals from ethanol has attracted renewed interest. Environmental concerns over the use of fossil-based resources and the concept of sustainability have also broadened the worldwide interest in renewable sources for both chemical feedstock and for energy. In the case of bio-derived ethanol, production costs declined significantly over the years as result of productivity improvements and scale economies. These, combined with the promise of new technologies from cheap cellulosic biomass, could make ethanol a competitive feedstock for chemicals in the

future. At this purpose this research work is focused on the development of alternative processes and innovative catalytic system for the production of chemicals from ethanol, with a special focus on acetaldehyde, ethyl acetate and pure hydrogen.

New catalytic systems for the acetaldehyde production by using the oxidative dehydrogenation of ethanol to acetaldehyde have been studied. The ethyl acetate represents another important commodity chemicals and a new process, by dehydrogenation of dry ethanol, for its production has been developed. In particular the production of ethyl acetate from ethanol by dehydrogenation is very economically competitive with the conventional esterification process. One of the main by-products of this process is pure hydrogen that could be easily separated from the other reaction by-products by condensations processes. Finally, the reactions of ethanol decomposition at high temperature and oxidative reforming have been investigated to produce hydrogen with high yield. The hydrogen is considered a fuel for fuel cells and in the future it could be substitute the gasoline. The ethanol for its versatility of application could be considered as a building block for the future biorefinery. In the next paragraphs, only a rapid survey will be done on the main applications of acetaldehyde, ethyl acetate and hydrogen and the aspect will be studied in depth in the next sections of this thesis.

i-3.1 The Acetaldehyde: uses, global demand and production.

Acetaldehyde is produced throughout the world primarily from ethylene, although some is still derived from ethanol and acetylene.

The worldwide demand for acetaldehyde has continued to decrease primarily because of less consumption for acetic acid manufacture.

For example, all manufacture of acetic acid from acetaldehyde in North America has been discontinued and in Europe, significant capacity for this process has been permanently shut down. Acetaldehyde use for acetic acid manufacture in Asia continues but is under pressure from the enduring establishment of methanol

carbonylation technology. In addition to the disappearance of use for acetic acid and plasticizer alcohols, acetaldehyde demand has also declined in the last few years because of mature end-use markets and the effects of the economic downturn on these acetaldehyde-derived products. There has also been continued substitution for acetaldehyde-based chemistries with other materials, which has further contributed to the drop in acetaldehyde use. In figure 5, the world consumption of acetaldehyde is reported.

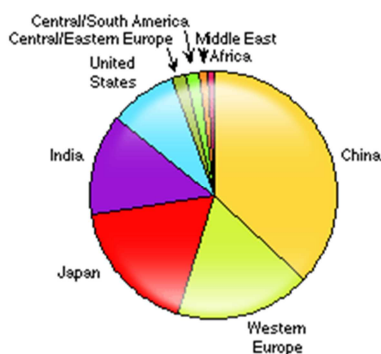


Figure 5: world consumption of acetaldehyde

Overall, the global market for acetaldehyde is expected to grow 2–3% annually during 2009–2014. However, some of this growth is actually a recovery from the significant decline experienced in 2009 (for example, China's use in the acetic acid market). Major regions including Japan, Western Europe and the United States will have low growth because of no use or no growth for acetic acid production, minimal growth in other acetaldehyde-consuming products, or continued product replacement of materials that consume acetaldehyde.

i-3.2 The Ethyl Acetate: uses, global demand and production

All current and potential processes producing ethyl acetate from bio-ethanol are analyzed, and their sustainability is comprehensively evaluated. Ethyl acetate is a colourless liquid with a characteristic

fruity odour. It is slightly soluble in water and soluble in most organic solvents, such as alcohol, acetone, ether and chloroform. It finds use as a solvent in a wide range of applications, across many industries. *Surface coating and thinners:* ethyl acetate is one of the most popular solvents and finds wide use in the manufacture of nitrocellulose lacquers, varnishes and thinners. It exhibits high dilution ratios with both aromatic and aliphatic diluents and is the least toxic of industrial organic solvents. *Pharmaceuticals:* Ethyl acetate is an important component in extractants for the concentration and purification of antibiotics. It is also used as an intermediate in the manufacture of various drugs. *Flavours and essences:* Ethyl acetate finds extensive use in the preparation of synthetic fruit essences, flavors and perfumes. *Flexible packaging:* Substantial quantities of ethyl acetate are used in the manufacture of flexible packaging and in the manufacture of polyester films. It is also used in the treatment of aluminum foils. *Miscellaneous:* Ethyl acetate is used in the manufacture of adhesives, cleaning fluids, inks, coated papers, explosives, artificial leather, photographic films and plates.

The main advantage of its use is related to the possibility to replace completely the aromatic compounds, in the sector previously listed, which cause serious damage to human beings and the environment.

Ethyl acetate is an active solvent that is available in three grades: 85-88%, 99% and 99.5%. The most popular grade, 99% is mainly used in industrial lacquers and surface coating resins. It is also used as an extraction solvent in the production of pharmaceuticals and food and as a carrier solvent for herbicides. About 60% of demand is in coatings. Process solvents, including pharmaceuticals and organic synthesis, account for 15% of demand, as does printing inks. Miscellaneous uses, including adhesives and cosmetics, account for 10% of consumption. In figure 6 the main sectors of application of this solvent have been reported.

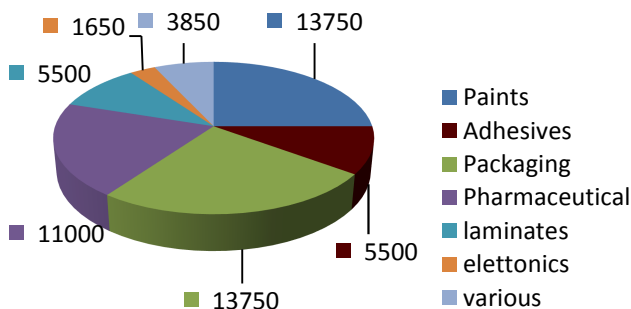


Figure 6: Distribution of ethyl acetate consume (ton/anno) [14]

Table 1: Source: Chemical Market Reporter

Producer	Annual capacity [million lbs]	Annual capacity [tons]
Celanese, Pampa, Tex	130	59.091
Eastman, Kingsport, Tenn	59	26.818
Eastman, Longview, Tex	51	23.182
Solutia, Springfield, Ma	30	13.636
Solutia, Trenton, Mich	24	10.909
Total	294	13.636

The demand for ethyl acetate in US was 71 Mtons in 2001 and 68 Mtons in 2002. Demand for the year 2006 was of about 81,000-tons. The historical growth during the period 1997-2002 was -5.3% per year. Therefore, the production of ethyl acetate catches many attentions in terms of improving productivity, saving cost etc. The identification of a sustainable bio-ethanol based production process of ethyl acetate has high contribution to the development of solvent industry.

i-3.3 The Hydrogen: uses, global demand and production

Bio-ethanol could constitute the raw material also for the production of H_2 by catalytic processes. It is a common opinion that H_2 will play a fundamental role in the future scenario of economy because it is a clean, renewable and non-polluting fuel. Fuel cell will supply the

energy that a global society requires to support the growing number of people that demanding on fuel cell technology using hydrogen. For that purpose, some fossil fuels, which have high hydrogen to oxygen ratio, were the best candidates to produce hydrogen. The hydrogen is cheap, easy to obtain, highly efficient, and its use releases less pollutant emissions. One of the primary uses, foreseen for the H₂, is in the fuel cell technology to generate clean energy at high yield [13]. Among different fuel cell technologies, molten carbonate fuel cell (MCFC), operating at high temperature (650 °C) allow to process H₂ stream even containing high concentration of carbon monoxide without any deactivation problems.

i-4 Strategy and contents of the thesis

The research work described in this thesis was realized at the research group NICL (Naples Industrial Chemical Laboratory), managed by Prof. E.Santacesaria, of University of Naples "Federico II". The aim of this thesis is to investigate the catalytic performances of vanadia and copper based catalysts in innovative processes such as the oxidative dehydrogenation, dehydrogenation and partial oxidative reforming reactions for the productions of high commodities chemicals such as respectively acetaldehyde, ethyl acetate and pure hydrogen. The use of bio-ethanol produced by second generation raw materials is actually the great challenge of the research world. By future forecasts the quantity of ethanol will be in the last few years increasing and the use of this "future building blocks" is useful to produce these chemicals. In a first phase of this research work, the study is focused on the development of new catalytic system and on the study of them in the oxidative dehydrogenation of ethanol to acetaldehyde. Indeed, the interest toward the acetaldehyde is due to its use for the production of ethyl acetate. The experimental results have shown that the redox mixed metal oxide V₂O₅/TiO₂-SiO₂ are very active and selective catalysts in the oxidative dehydrogenation of the ethanol to acetaldehyde. The same performances have not been obtained in the

dehydrogenation reaction in one step reaction for the ethyl acetate production. In matter of fact, the scarce performances of these catalytic systems have increased the research of innovative ones to promote the ethyl acetate preparation. At this purpose different commercial copper based catalysts have been studied in the dehydrogenation of ethanol to ethyl acetate. In the latter case a depth investigation on the mechanism and on the kinetic of reaction have been realized. Finally, a simulation and a scale-up of the process is realized. The main co-product of this reaction is pure hydrogen. Actually, the interest of the research is directly aimed to the development of new alternative processes for the hydrogen production. At this purpose the commercial copper based catalysts have been studied in the ethanol decomposition and partially oxidative reforming too. The performances of the commercial catalysts have been compared with the ones prepared by using the innovative combustion synthesis reaction. The prepared catalysts and the commercial ones have been investigated in more details by using different advanced characterization techniques. To easily understood, the organization and scheme of this thesis a brief summary of the chapters is thus reported. The present thesis is divided in three different dedicated sections:

- *Section A*: study of the performances of the Vanadia based catalysts in ethanol ODH (oxidative dehydrogenation) reaction.
- *Section B*: study of the performances of copper based catalysts in the ethanol dehydrogenation reaction for the ethyl acetate and pure hydrogen production.
- *Section C*: study of the hydrogen production by ethanol decomposition and oxidative reforming reactions.

Section A. In this section, as already above mentioned, the results of the performances of the vanadia catalytic systems in the oxidative dehydrogenation of ethanol to acetaldehyde will be discussed. In more details, in this section, the peculiarities of different vanadia based catalysts prepared by grafting technique have been studied. The

catalytic performances have been compared with the results obtained with commercial system in the dehydrogenation reaction by using copper based catalysts. The section A is organized in four main chapters.

A.1-Introduction and background information. In this section a systematic investigation of the most recent results reported in literature about the preparation, the characterization and the catalytic performances of vanadia based catalysts have been reported. In order to clarify the structure-property relationship of our investigation a clearly state of the art has been realized.

A.2-Apparatus and analytic methods. In this chapter the techniques employed to perform the reaction have been illustrated.

A.3-Experimental sections and discussion of the results. The performances of the vanadia based catalysts have been reported in the oxidative dehydrogenation reactions. The obtained results have been compared with the performances of the copper based catalysts in the dehydrogenation reaction.

Section B. The second section is completely dedicated to the investigation of an alternative process for the production of ethyl acetate. In particular, our intent is to develop a new process, very innovative and simple respect to the classical ones that would produce ethyl acetate in only one step reaction. In this section a depth investigation of the performances of different copper based catalysts have been realized. In particular a great interest is devoted to the use of different structural promoters with the aim to improve the catalytic performances in terms of activity and selectivity towards the ethyl acetate production. The section B consists of six chapters that would illustrate the main peculiarities of a developed process to produce ethyl acetate.

B.1- Introduction and background information. In this section a systematic investigation of the most recent results reported in literature about the preparation, the characterization and the catalytic

performances of the main active phases employed to perform the dehydrogenation reaction to produce ethyl acetate have been reported.

B.2- Experimental sections. A summary of the characterization techniques employed to investigate the chemical and structural has been reported. Moreover, the operative conditions, the peculiarities of the reaction apparatus and the analysis of products is illustrated.

B.3- Thermodynamic study. The reaction pathway was studied by using Aspen with the aim to evaluate the thermodynamics properties of each main reaction of the complex scheme of dehydrogenation reaction.

B.4-Experimental, characterization and discussion. In this chapter the results in terms of ethanol conversion, ethyl acetate selectivity at different temperature, residence time, pressure, hydrogen partial pressure have been studied. The catalysts have been characterized by employing commonly in-situ and ex-situ techniques with the aim to correlate their physical-chemical properties to their performances in ethanol dehydrogenation at high pressure.

B.5-kinetic study. The kinetic of reaction was also investigated by using a simple power law and more complex models focused on an assumed mechanism of reaction. The best model able to describe as well the experimental data is an adsorption model based on the Langmuir-Hinshelwood-Hougen-Watson (LHHW).

B.6-Industrial plant simulation. On the basis of a very simple power law kinetic model, an hypothesis of process was realized and investigated. The process consists of two different sections: of dehydrogenation of ethanol and azeotropic distillation to obtain a high purity degree final product.

Section C. Finally, the performances in the last section the performances of the copper based catalysts in the ethanol decomposition and oxidative dehydrogenation has been studied. This section, essentially divided in four main chapters, would give general

idea of the actual main process dedicated to the hydrogen production by bio-ethanol (C-1). The second chapter of this section (C-2) illustrates the characterization techniques and the products analysis obtained by ethanol dehydrogenation. The third chapter (C-3) is entirely dedicated to the illustration of the experimental results in terms of catalysts performances and characterizations. The final part of the current chapter is thus dedicated to the discussion of the obtained results.

The most significantly results have been summarized in the last chapter (conclusion) of this Ph.D thesis.

i.5 Reference

- [1] http://unfccc.int/kyoto_protocol/items/2830.php.
- [2] Jeppe Rass-Hansen, Hanne Falsig, Betina Jørgensen and Claus H Christensen* *J Chem Technol Biotechnol* 82:329–333 (2007).
- [3] R. L. Lynd, E. C. Wyman and U. T. Gerngross, 1999, Biocommodity Engineering, *Biotechnol. Prog.*, 15:77
- [4] Dale BE, *J Chem Technol Biotechnol* 78:1093–1103 (2003).
- [5] Kosaric N, Duvnjak Z, Farkas A, Sahm H, Bringer-Meyer S, Goebel O, *et al.*, Ethanol in *Ullmann's Encyclopedia of Industrial Chemistry* (7th edn). Wiley, Chichester (2006.). Additional data from www.icispricing.com, www.eia.doe.gov and www.dft.gov.uk.
- [6] "Towards Sustainable Production and Use of Resources: Assessing Biofuels". United Nations Environment Programme. 16 October 2009. Retrieved 24 October 2009.
- [7] F.O. Lichts. "Industry Statistics: 2010 World Fuel Ethanol Production". Renewable Fuels Association. Retrieved 30 April 2011.
- [8] PetrChladek*, Eric Croiset, William Epling and Robert R. Hudgins, *The Canadian Journal of Chemical Engineering*, Volume 85, December 2007, p. 917.
- [9] www.chemtex.com.

- [10] C. I. Macedo, E. A. J. Seabra and E. A. R. J. Silva, 2008, The 2005/2006 Averages. Prediction for 2020, *Biomass Bioenergy*, 32:582.
- [11] APPE web site <http://www.petrochemistry.net>.
- [12] P.Champagne Resources, Conservation and Recycling 50 (2007) 211–230.
- [13] SRI consulting Process Economics Program Report 235 Chemicals from Ethanol By Marcos Cesar Published November 2007.
- [14] Dutia, Pankaj (august 10th, 2004). “Ethyl Acetate: A Techno-Commercial Profile”. *Chemical Weekly* pp. 181-184.
- [15] Dolgov et al. *International Journal of Hydrogen Energy* 31 (2006) 1607.

SECTION A

Abstract

Oxidative Dehydrogenation

In the present chapter, the oxidative dehydrogenation of ethanol to acetaldehyde has been thoroughly investigated. A particular attention was dedicated to the performances of catalysts prepared by grafting vanadyl tri-isopropoxide on the surface of silica coated with TiO₂ that were found to be very active and selective. Together with acetaldehyde, small amounts of by-products were obtained, including acetic acid, acetals, ethyl acetate and CO₂. The kinetic behavior of the catalysts was studied in the temperature range 100-180 °C, by changing the ethanol residence time, the molar ratio between the reagents (EtOH:O₂), and the catalysts vanadium loading. Moreover, the performances of copper based catalysts in the dehydrogenation reaction have been studied. At the end of the chapter, a discussion about the more advantageous process for the acetaldehyde production was finally reported.

SECTION A

Chapter 1

Background info Literature Review

A-1.1 Introduction

There are several different ways to produce acetaldehyde and the precursors, commonly used, are ethylene or acetylene. Nowadays a great attention is dedicated to the use of ethanol. There are several reasons for which the ethanol is favored with respect to ethylene or acetylene. Ethylene is produced in the petrochemical industry and is hence not classified as a green product. The production of acetaldehyde, from acetylene, includes a catalyst containing mercury, hence also this method is discarded. The main route to produce acetaldehyde is the ethanol dehydrogenation but a large attention is dedicated also to the use of the oxidation reactions. The acetaldehyde production via the oxidative dehydrogenation (ODH) of ethanol could be a promising alternative to the Wacker process, occurring more simply in a single step and in tubular reactors, if high activities and selectivities can be achieved under mild conditions. The partial oxidation of ethanol over different catalytic systems has been studied by several authors [1-8]. In particular, supported V_2O_5 based catalysts have been found to be active and selective in promoting the oxidative dehydrogenation of ethanol to acetaldehyde. The chapter in exam was entirely dedicated to the explanation of the main characteristics of the vanadia catalysts and to their application in the ODH reactions. As well known, the preparation methodology can affect the final

performances in ODH reactions and at this purpose, a rapid overview on the peculiarities of grafting technique was made.

A-1.2 Acetaldehyde production

A-1.2.1 Dehydrogenation

An extensive amount of literature concerning acetaldehyde production via dehydrogenation is available. Acetaldehyde was first synthesized by ethanol oxidation in 1817 [9] and later was produced by hydration of acetylene. Armstrong and Hilditch [10] reported that the dehydrogenation process was developed and applied during the First World War, but more thorough investigation [11] was prompted by an increasing significance of acetaldehyde as one of the most important aliphatic intermediates in the production of acetic acid, acetone, ethyl acetate, C₄-aldehydes, 1-butanol, pentaerythritol and many other chemicals. The most popular metal, used for selective dehydrogenation of alcohols to aldehydes or ketones, is copper, mainly because of its ability to dehydrogenate ethanol without splitting the C-C bond, which would lead to the undesirable decomposition of acetaldehyde to CH₄ and CO. Various studies [13-17] have shown that it is metallic Cu⁰, formed by reduction of CuO, to act as an active phase in dehydrogenation. Other alternative phases to Cu, including Pt, Pd, Cr, Cd, Ni, Fe, Mn, Co, Zn and Ru, were proposed, but none of them matched the selectivity obtained with copper catalysts. However, Cu suffers from poor stability at high temperatures, where dehydrogenation is thermodynamically favorable. The reaction only approaches 100% equilibrium conversion at temperatures higher than 500°C, while Cu is reported to deactivate at temperatures as low as 220°C. The most probable mechanism of thermal deactivation of copper is sintering, which is expected to become significant in the temperature range of 177–400°C (Hüttig temperature - Tamman temperature – empirically determined temperatures, when metal particles become mobile on the catalyst

surface, $TH = 0.33 \cdot m.p.$, $TT = 0.5 \cdot m.p.$). Sintering as a deactivation mechanism was experimentally confirmed by the works of Tu et al. [13-17].

On the other hand, other researchers [11,19] reported deactivation by carbon formation, which may originate from ethanol dehydration or from polymerization of higher hydrocarbons formed in subsequent acetaldehyde reactions. In either case, the selection of catalyst preparation technique, suitable support and promoter can eliminate or significantly inhibit deactivation. Thus, notwithstanding the high activity of unsupported copper, as demonstrated [19], must be supported. However, unsupported copper suffers from lower thermal stability and, more importantly, from low metallic surface area, resulting in less acetaldehyde produced per g of copper than in any of the supported or promoted copper catalysts [18,19,21]. Therefore copper has been deposited on a variety of high surface area materials. In the middle of the 20th century, various naturally occurring materials were commonly used as supports. Church et al. [19] demonstrated the superior properties of asbestos and pumice for ethanol dehydrogenation. Nowadays, modified natural or synthetic materials with better-defined, more homogeneous structures and properties are employed. Iwasa and Takezawa [22] compared unsupported copper catalyst performance to copper supported on SiO_2 , ZrO_2 , Al_2O_3 , MgO and ZnO . ZrO_2 and ZnO supported catalysts were selective for ethyl acetate formation, while the use of Al_2O_3 support promoted undesired secondary reactions that resulted in higher amounts of diethyl ether and C_4 species. It was concluded that these by-products were formed on the acidic sites of Al_2O_3 , because selectivity to these by-products rapidly dropped after the support was doped with basic KOH. On the other hand, Church et al. [19] observed increased formation of undesired higher hydrocarbons not only with basic oxides promoters (ZnO , MgO) but also with Al_2O_3 and ascribed this formation to base-catalyzed aldol condensation. This observation was further confirmed

by Inui et al. [23] (2002) who reported that both Al_2O_3 and ZrO_2 additions to pure Cu completely switched selectivity from acetaldehyde to ethyl acetate, and diethyl ether and ethyl acetate, respectively. In contrast, the addition of ZnO had no effect on product distribution. Repeatedly and independently, SiO_2 was proven to be superior support by Iwasa and Takezawa [22] and White [24], in all cases exhibiting high activity and selectivity to acetaldehyde formation. These superior properties were related to its high surface area, allowing for a high dispersion of Cu and also to its inertness, resulting in the absence of active sites required for undesired parallel or secondary reactions. The only aspect in which SiO_2 may be lacking is thermal stability. SiO_2 -supported catalysts are commonly prepared by impregnation, a technique in which active metal is merely deposited in the pores and on the surface of the support, but not anchored in the support oxide lattice. From this perspective, hydrotalcites, i.e., a class of layered materials consisting of positively charged brucite $\text{Mg}(\text{OH})_2$ like sheets where several Mg^{2+} ions are replaced by trivalent Al^{3+} ions and the excess of positive charge is counterbalanced by anions, such as CO_3^{2-} or NO_3^- , in the interlayer plus water molecules, may provide a stable, high surface alternative to SiO_2 . Thus, Di Cosimo et al. [25] reported that small addition of Al to MgO (Mg/Al molar ratio > 5) leads to a creation of hydrotalcite material, which by itself was capable of producing significant amounts of acetaldehyde. When impregnated with Cu solution, Al^{3+} ions are exchanged by Cu^{2+} and copper is therefore incorporated in the support lattice as shown by Alejandre et al. [26]. Since the activity of copper catalyst quickly decreases with time on stream at temperatures higher than 300°C , most likely because of copper sintering, many researchers focused on improving the stability by adding a textural promoter to the catalyst formula, which would act mainly as a mechanical barrier decreasing copper particle mobility.

The common feature of the promoters studied was their irreducibility at the dehydrogenation reaction conditions, i.e., promoters were present on the catalyst surface in the form of metal oxides. Church et al.[19] evaluated the effect of 5-7 % addition of Cr_2O_3 , CoO , ZnO and MgO on Cu /asbestos catalyst performance. It was found that Zn and Mg alkaline oxides had a detrimental effect on the selectivity of reaction, promoting aldol condensation and thus forming undesirable higher hydrocarbons. Amphoteric Cr_2O_3 favored the creation of ethylene via dehydration of ethanol. Although deposition of 5% CoO slightly decreased the selectivity of dehydrogenation to acetaldehyde, its addition resulted in increased conversion of ethanol. To further improve the stability of Cu-CoO catalyst, 2% Cr_2O_3 was added to the catalyst formula. Indeed, Cr_2O_3 is the most popular of all additives considered in the literature as a potential stabilizer. Tu et al.[12,16] published two papers addressing the effect of Cr_2O_3 on the dehydrogenation activity of unsupported copper catalysts. Even trace amounts increased the metallic copper surface area and also increased the stability, though sintering was never completely suppressed at temperatures higher than 300°C . Below this temperature, the catalyst did not show any signs of deactivation, but the reaction did not achieve 100% conversion. At 310°C , a Cr/Cu ratio of 4/40 resulted in the smallest decrease in Cu surface area and consequently in activity after 8 h on stream. Overloading the catalyst with chromium, for example at a Cr/Cu ratio of 20/40, had a significantly negative effect on the catalyst activity, since a new catalytically inactive CuCr_2O_4 phase was formed. Kanoun et al.¹⁸ tested the influence of Cr and Al oxides addition on the catalyst properties and found that Al_2O_3 increased the total catalyst surface area while Cr_2O_3 increased specific copper surface area. Cr addition also increased the activity of catalyst per copper weight. However, if activity was defined per weight of catalyst, then any addition of Al or Cr led to a decrease. The authors then concluded that Cr is a better structural promoter. Unfortunately,

the low reaction temperature of 190°C and deliberately low ethanol conversion (<1%) made it impossible to determine the effect of promoters on either acetaldehyde selectivity (always 100%) or catalyst stability. The same mild experimental conditions served for testing of other promoters, namely Zr, V, and Zn oxides, by the same research group^{19,22} [18,21]. The highest amounts of acetaldehyde produced per grams of Cu were always obtained with the highest Cu dispersion, which was attained at the lowest Cu loading. A Cu-Zr catalyst exhibited the highest activity (but only 80% selectivity) of all three binary mixtures tested, while a ternary mixture of Cu-V-Zr was inferior in performance to a Cu-V-Zn catalyst. The highest amount of acetaldehyde produced for g of copper was achieved with a Cu-V-Zn catalyst with minimum Cu loading. But once again, pure Cu proved to be most active in terms of acetaldehyde produced per g of catalyst. Even at such mild temperature (190°C), the authors reported a steady decline in activity over 16 h on stream. From all three papers published by Kanoun et al.[18,21], it can be concluded that the total surface area decreases with the addition of promoters in this order: Al>Cr>Zr>V>Zn, while metallic copper surface area, which is responsible for the activity of the catalyst decreases with the additives in the following order: Cr>V=Zr>Al>Zn. Cr is thus the best structural promoter and also a good stabilizer. Chen [27] carried out series of tests on the effect of alkali metals (Na, K, Rb) and alkaline earth metals (Mg, Ca, Sr, Ba) as promoters on the performance of Cu/SiO₂ catalyst. The metal oxides of alkaline metals and alkaline earth metals did not undergo reduction at a reaction temperature of 300°C, neither did they contribute significantly to the dehydrogenation activity. While alkali metals created only slightly basic sites on the catalyst surface, all alkaline-earth-metals containing catalysts, with the exception of Mg addition, possessed both strong and weak basic sites. The presence of strong basic sites resulted in an extreme drop in activity after a short time on stream, thus deeming especially Ba and Sr as poor promoters.

MgO proved to be most stable of alkaline earth oxides, but even this additive did not prevent the catalyst from losing 20% of its initial activity after just 4 h on stream. Among the alkali metals, a K-doped catalyst displayed the highest resistance to sintering, losing only 8% of its activity after 4 h on stream. Thus, K was identified as the best promoter out of all metals tested, even though the initial ethanol conversion was 2% lower (68%) than the highest conversion obtained with a MgO promoter (70%). Though it is rather difficult to compare the effects of various promoters, because of different conditions used by researchers, there seems to be a general agreement throughout the literature that the best promoter is Cr_2O_3 .

This promoter did not eliminate sintering but merely decreased the rate of deactivation. It may therefore be impossible to achieve stable operation with complete conversion and selectivity to acetaldehyde, in which case the reaction will have to be operated at lower non-deactivating temperatures and then the use of a promoter would be superfluous. An alternative route to obtain acetaldehyde with high yields is the oxidative dehydrogenation.

A-1.2.2 Oxidative dehydrogenation

It seems that nowadays, for conversion of light alkanes, the oxidative dehydrogenation (ODH) reaction is more promising than direct dehydrogenation. Reactions are endothermic (e.g., for n-butane ΔH_r is about 134 kJ/mol) and in order to shift the equilibrium to product formation, reactions must be carried out at relatively high temperatures (from 400 to 500°C). As demonstrated by a literature thermodynamic study [28] a conversion of 100% was achieved at a temperature of almost 500°C. Moreover, the use of high temperatures in catalytic dehydrogenation presents several disadvantages. The difficulty in controlling undesirable reactions that decrease selectivity (such as cracking of hydrocarbons) and coke formation over the catalyst, which decreases activity, are the most significant. For all

these reasons, reactions of alcohols conducted in presence of oxygen are excellent alternatives in the synthesis of aldehyde. The formation of a very stable product such as water makes this reaction very thermodynamically favourable. Thus, in principle, practically complete conversion can be achieved even at low temperatures, getting enormous advantages from the economic and process engineering points of view. However, in such conditions selectivity also presents limitations. Notwithstanding all the above-mentioned advantages over dehydrogenation, ODH (as well as the majority of other catalytic-oxidation processes) has some drawbacks: due to its exothermic character it may require special care in reactor operation, some feed composition ranges can be explosive (leading to limitations in feed compositions or to multiple air inlets), and the desired product must be sufficiently stable in the reaction conditions in order to be removed from the product stream before it decomposes or undergoes other subsequent reactions. Thus, ODH reactions with high yield are a great challenge in catalysis.

The key-aspect of the technology is, therefore, the development of catalysts capable to favour the formation of acetaldehyde with high selectivity, starting from ethanol. Several reviews have discussed oxidation catalysts containing vanadium, but none is specifically concerned with the oxidehydrogenation reactions. The partial oxidation of ethanol over different catalytic systems has been studied by several authors [29-36].

In particular, supported V_2O_5 based catalysts have been found to be active and selective in promoting the oxidative dehydrogenation of ethanol to acetaldehyde [37]. The reaction occurs under very mild conditions of temperature (150-250 °C) and pressure (1 atm). Moreover, in contrast to other ODH reactions, such as the ODH of light hydrocarbons that occurs at higher temperature, the surface oxygen of V_2O_5 lattice is not directly involved in the ODH process, because the oxygen exchange reaction is too slow at the low temperatures used.

According to Oyama and Somorjai [38], unlike to the oxidative dehydrogenation of methanol to formaldehyde, the ODH of ethanol to acetaldehyde performed on V_2O_5 based catalysts supported on SiO_2 is not structure-sensitive. The same conclusion was reached by Lakshmi et al.[39] using V_2O_5 catalysts prepared by impregnation on mixed oxides. Inamaru et al.[40] studied ethanol dehydrogenation on V_2O_5 catalysts prepared by both impregnation and by chemical vapor deposition (CVD). They found that, in the latter case, the catalysts were more dispersed and more selective in the reaction. As well as the preparation method, also the support plays an important role. According to the literature, vanadia catalysts constitute a relevant example of the influence of the interaction between catalytically active metal oxide particles and oxide carriers. Several authors compared the properties of vanadia supported on different carriers (SiO_2 , Al_2O_3 , TiO_2 , MgO , ZrO_2) and concluded that the nature of the dispersed surface metal oxide phase enabling the vanadia, to become an effective catalyst for selective oxidation of aromatics, olefins and alcohols. Titania (anatase) interacts strongly with an immobilized vanadia layer, generating a molecular dispersion of V_2O_5 , but the system suffers from limited specific surface area and low resistance to sintering [35]. A way to obtain a titania surface with high, thermostable surface area and good mechanical properties is to support TiO_2 onto silica. Thus, vanadia based systems such as V_2O_5/TiO_2 and V_2O_5/SiO_2 catalysts have been studied for selective oxidation of alcohols. In particular, V_2O_5 and V_2O_5/SiO_2 are very active and selective for oxidation of ethanol to acetaldehyde. By a proper selection of the catalytic oxide system and to acetaldehyde, acetic acid, or ethyl acetate, all of which can be used either as final products or as intermediates in synthetic routes. Quaranta et al. [35] studied the ODH of ethanol to acetaldehyde on $V_2O_5/TiO_2/SiO_2$ catalyst by comparing the catalytic performances with those of V_2O_5/TiO_2 and V_2O_5/SiO_2 catalysts. A depth studies of the performances of vanadia

based catalysts was realized also by Santacesaria et al. [44]. As demonstrated, the coating of the silica carrier with a monolayer of TiO_2 increased substantially the activity of the catalyst. Despite the significant attention paid by various authors to the ODH of ethanol and to the action of vanadium-based catalysts, only one kinetic study has been published on this reaction, namely, the work by Gomez et al. using a VMgO as catalyst [45]. Tesser et al. [46] studied the kinetic of the ODH of ethanol on $\text{V}_2\text{O}_5/\text{TiO}_2/\text{SiO}_2$ catalyst, prepared by grafting vanadyl tri-isopropoxide onto a support of silica coated with TiO_2 . The $\text{TiO}_2/\text{SiO}_2$ support has been prepared according to the multi-step grafting procedure. The kinetic behaviour of the catalyst was verified by varying the reagent concentrations, the residence time, the temperature, the vanadium load, the acid and basic characteristics of the catalyst and the presence in the feed of reaction products such as water or acetaldehyde. A kinetic law for interpreting both the main reaction from ethanol to acetaldehyde and all other oxidations occurring in the reaction scheme was derived by assuming a redox mechanism occurring in the following four steps: (i) dissociative adsorption of ethanol on vanadium giving place to an ethoxy group, (ii) α -hydrogen withdrawal by the metal to form acetaldehyde and a hydride group, (iii) oxidation of the formed hydride, and (iv) dehydration of the vanadium site to restore the original active site. The kinetic law derived was found to be identical, in mathematical form, to the one that can be obtained from the classical Mars and van Krevelen mechanism [47]. As shown by the kinetic study realized by Tesser et al. [45], on the basis of the obtained values of activation energies, the $\text{V}_2\text{O}_5\text{-TiO}_2$ chemical environment is favorable to this reaction, in agreement with the suggestion made by other authors that V-O-support bonds are determinant for the activity and selectivity of different reactions, because the effect of the support is often dramatic. In the next paragraphs, the main techniques employed to prepare vanadia based catalyst have been reported. In particular, our

attention was focused on the grafting peculiarities and on the properties of the metal alkoxides.

A-1.3 Vanadia based catalysts preparation

A-1.3.1 Classical routes

The preparation of supported metal oxide catalysts is a very important step because it significantly affects the three most important characteristics of the final catalyst product, i.e., its catalytic activity, catalyst selectivity, and catalyst lifetime [48].

Despite the large number of patents and applications about catalyst preparation, the field of “catalyst design” can be still considered in continuous developing. It involves the precise control over the nature (oxidation state, coordination environment, dispersion, etc) of the supported active site at the molecular level in a reproducible manner. This far from easy, and future research has to be directed toward a better understanding of the basic aspects of catalyst preparation through the use of *in situ* and *operando* microscopic and spectroscopic techniques. Catalyst preparation is, thus, defined as the strategy domain in chemical industries. It is also a field with great potential because important improvements in catalyst performance can be obtained by simply fine-tuning the different preparation steps of a specific catalyst. There are two main stages in the preparation of supported metal oxides catalysts. In a first stage, the active metal component precursor is deposited on the oxidise support. The second stage consists of a transformation of the deposited metal precursor into a metal oxide dispersed at the support surface. This transformation process can be achieved by a heat treatment of the precursor material in oxygen or in air, often referred to as calcination step (formation of supported metal oxides). Supported vanadium oxide based catalysts can be prepared via several methods.

Impregnation

The most simple and widely used deposition method is impregnation, which refers to a procedure whereby a certain volume of an aqueous or non-aqueous solution containing the specific metal component precursor is totally adsorbed into the pores of an inorganic oxide. Two important impregnation procedures can be distinguished. If the support is dipped into an excess amount of solution, the process is called **wet impregnation**. More precise control over the vanadium oxide loading is achieved with a technique called **dry impregnation**, **pore volume impregnation** or **incipient wetness impregnation**. In this case, the support is contacted with a solution of appropriate concentration, corresponding in quantity to the total known pore volume of the support, or slightly less. This allows precise control of the concentration of the active vanadium oxide component on the support. However, the maximum loading obtainable in a single impregnation step is limited by the solubility of the reagent and if necessary multiple impregnation steps should be applied. V_2O_5 has a low solubility in aqueous and non-aqueous solutions and therefore, many authors prepare their supported vanadium oxide catalysts by impregnating the support with an aqueous solution of, e.g. NH_4VO_3 or NH_4VO_3 dissolved in aqueous oxalic acid [49]. The impregnation process is followed by a drying and heating step in which the vanadium oxide compound is chemically anchored onto the support oxide. Non-aqueous impregnation methods use vanadyl acetylacetonate ($VO(acac)_2$) as vanadium compound or $VO(OC_2H_5)_3$ or $VO(OC_3H_7)_3$ in methanol or another organic solvent [50]. After the impregnation step the material is calcined in air at high temperatures (e.g. 500 °C) and surface anchored vanadium oxides are formed.

Another route to prepare catalysts is a gas-phase technique is the **Atomic Layer Deposition** (ALD) that uses as precursor a volatile vanadyl acetylacetonate. A correlated technique is **Chemical Vapor Deposition** (CVD), which makes use of a volatile inorganic or organo-

metallic compound. Controlled reaction conditions are accomplished to stabilize the surface deposition sites on the support by heat treatment and by removing any physisorbed or unreacted molecules after each reaction by inert gas purge [51]. However, it is important to point out that the adopted preparation method influences the amount of supported vanadium oxides, which can be deposited on a particular support oxide without the formation of crystalline V_2O_5 . In this way, the preparation method may affect the vanadium oxide dispersion on the surface of the oxide support.

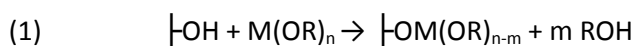
A-1.3.2 Grafting technique

Grafting is defined as the removal from solution of a compound containing vanadium through interaction with hydroxyl groups on the surface of an inorganic support. Several authors pointed out that grafting techniques lead to more dispersed catalysts that are stable when an opportune support is used. Multi-step grafting followed by calcination is, often, used to obtain a monolayer of vanadium oxide on the surface of a support oxide. In general, liquid phase deposition can be regulated by controlled reagent concentration and washing and drying procedures whereas in the gas phase, the key factors are the character of precursor, the reaction temperature and the number of active surface hydroxyl sites.

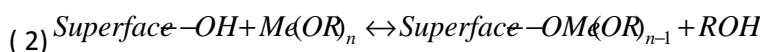
A-1.4 Metal Alkoxides as precursor to prepare supported metal oxides by *Grafting*

The alkoxides are largely employed to prepare catalysts and catalytic supports, that classically were produced by impregnation or coprecipitation [52]. The first methodology gets a not well dispersed active phase on the catalyst supports while with the coprecipitation the catalyst porosity is difficult to control. The grafting is an alternative preparation technique that involves a specific reaction between a metal alkoxide and a surface rich of hydroxides group [53,54]. A

number of literature works have shown the catalysts preparation and the main features of vanadia based catalysts supported on many different supports such as SiO₂, TiO₂, ZrO₂, Al₂O₃. The main advantage of the examined technique is the possibility to check and to improve the redox properties of the catalysts, the dispersion degree of the active phase on a support [55,56]. The grafting reaction is thus represented (1):

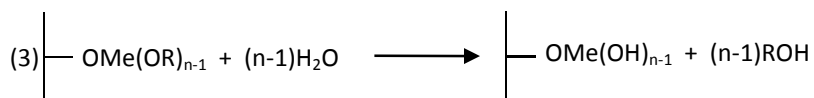


The support, previously calcinated to stabilize the surface and to eliminate trace of moisture, was put in contact with a solution of known concentration of the desired metal alkoxide in an anhydrous solvent and in inert environment. The hydroxyl groups represent the reactive sites able to anchoring the metal and during the reaction, the use of an apolar solvent is necessary to favor the strong anchoring of the metals to the supports. An intensively study, conducted in this research group [57-59], has shown that the use of alcohols, close to the used alkoxides, is useful to obtain a well dispersion of the active phase on the catalysts surface, as the equation (2) illustrates [27-29]:



The reaction in exam is of equilibrium and the removal of alcohol is fundamental to favor the mixed oxides formation. The alkoxides concentration that must be used to perform the reaction is evaluated on the basis of the quantity of active phase desired on the support. The strength of the bound between the metal oxide and the support is dependent by the acid-base characteristics of this last. A good catalytic system is characterized by a good dispersion of the active phase and the alkoxide must be has a very scarce tendency to oligomerization. An unavoidable operation is the steaming, that should be conducted after

the grafting reaction to eliminate the organic groups by the catalyst surface (3).



Alternatively, the burning in air and the calcination at 200°Cx2h could be used. After that, the catalyst surface must be stabilized by calcination at 500°C x2h. The grafting technique is advantageous because combines the thermal resistance of an ideal support to the redox and acid-base surface properties. The technique is versatile and by a simply changing of the alkoxide it is possible to obtain different loading of the active phase on the support [60]. In particular, low loading (sub-monolayer) gives a wide dispersion of the active phase. The monolayer loading favors the obtainment of catalysts with chemical properties quite different by the support by with the same mechanical strength of this last one. The multilayer loading, obtained by repeating several time the grafting, gives catalysts with particular properties related to their structure (structure sensitive).

A-1.4.1 Adsorption isotherms

A-1.4.1.1 Support TS

The critical factor regarding the preparation of supported TiO₂/SiO₂(TS) catalysts is the maximum surface coverage of the precursor molecules. Some factors such as the porosity, size, and morphology of the silica pores may influence the maximum surface coverage of a precursor. Very small pores may be inaccessible to large precursor molecules. Therefore, the maximum surface coverage of

precursor molecules is associated with the steric hindrance effect. Above the maximum surface coverage, extra precursor molecules do not react with the surface hydroxyls and remain on the surface after the solvent is removed. The unreacted precursor molecules either evaporates during calcination at elevate temperatures or remain on the surface and become oxidized into oxide phase. In order to determine the maximum surface coverage of silica by titanium alkoxide, a depth study of the grafting adsorption behaviour of titanium tetra-isopropoxide ($\text{Ti}(\text{O-Pr}^i)_4$) on the surface of silica support by contacting solutions of increasing concentrations of the mentioned alkoxide, dissolved in dioxane, was carried out. This approach resulted very interesting to investigate the chemical adsorption of titanium alkoxide until the surface saturation, by using the isotherm obtained, depicted in Figure 1[60].

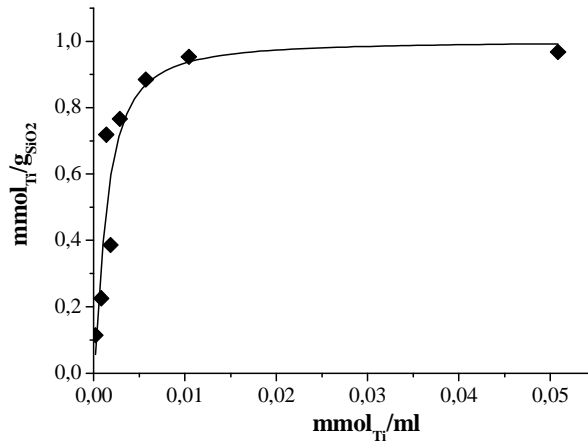


Fig.1: Adsorption isotherm of titanium tetra-isopropoxide ($\text{Ti}(\text{O-Pr}^i)_4$) adsorbed by grafting on the surface of SiO_2 .

As can be seen, the adsorption isotherm can be interpreted as a Langmuir isotherm in line with the following relation:

$$K = (1/C^{eq}) / (\Gamma^\infty / \Gamma^\infty - \Gamma^{eq}) \quad (4)$$

As shown, by regression analysis experimental points can be well fitted by using the following values of the parameters: $K = 710.89$ [L/mol] e $\Gamma^\infty = 1.02$ mmol_{Ti}/g_{SiO₂}. By the latter value approximately 8.14% by weight of TiO₂ adsorbed on support is calculated and this value corresponds to a monolayer. In the adopted preparation, due to the steric interference effect, the maximum surface coverage of the Ti(O-Prⁱ)₄ precursor in a one-step grafting has been found to be ~ 2.2 Ti atoms/nm², which is similar to the maximum trimethylsilyl (TMS) surface coverage of 2.2-2.7 groups/nm² [61]. On the basis of the results achieved, it is possible to classify the titanium silica-supported catalysts in two categories, depending on the content of titanium grafted on SiO₂, expressed as “titanium surface density” and defined as the number of titanium atoms per square nanometer of the catalyst (atoms_{Ti}/nm²): sub-monolayers (~ 2 atoms_{Ti}/nm²) and monolayers (TSM) ($\sim 4-6$ atoms_{Ti}/nm²). Another important observation is the strong affinity of titanium alkoxide with the silica surface, derived from the steep rise in the initial part of the adsorption isotherm. Saturation of the adsorbed alkoxide monolayer is reached at a relatively low alkoxide equilibrium concentration (0.01 mmol_{Ti}/ml). However, it is interesting to note that, after calcination treatment, not only some of Si-OH groups become re-exposed and can further react with more Ti(O-Prⁱ)₄ precursor molecules but also some of Ti-OH groups of Ti-species anchored in previous grafting steps. Thus, in order to completely cover the surface of silica with titania, the above-mentioned sequence of operations, i.e., grafting, filtering, drying, steaming and calcinating were repeated, under the same conditions, twice more on each sample. This strategy resulted very useful to charge on the surface of silica a sufficient amount of titanium to form a monolayer coating of silica characterized by a highly dispersed active phase, corresponding to both isolated and/or polymeric titanium species, as resulted from the characterization investigation reported in the next paragraphs. So, a higher loading of TiO₂ (TSM) ($\sim 20\%$ wt

TiO₂), which correspond to ~ 4 Ti atoms/nm², is reached by employing three grafting steps. As stated above, among the variables involved in the synthesis of this type of catalysts (TiO₂/SiO₂), also the nature of the solvent used for dispersing the titanium alkoxide before the grafting reaction, plays an important role. The yield of the grafting reaction, i.e. the maximum quantity of titanium alkoxide, expressed as % wt TiO₂, that is possible to charge on the silica surface by employing one grafting-step, is almost quantitative by using toluene. This is probably due to the fact that the grafting is an equilibrium reaction and, thus, the use of the parent alcohol as solvent reduces the anchorage efficiency.

1.4.1.2 System V₂O₅-TiO₂/SiO₂

Apart from the role of the inorganic oxide used as support, the molecular structure of vanadium oxide species on amorphous support oxides can be influenced also by the vanadium oxide loading. Several studies on the vanadia based catalysts have shown that the adsorption of vanadia depends strongly by the typology of employed support. In Figure 2 the adsorption of vanadia respectively on silica and on supports prepared by grafting respectively TSm (monolayer 7.29%wt TiO₂) and TSM (multiple layer 17,8% wt TiO₂) have been reported [53]. By comparing from a qualitative point of view the isotherms, reported in Figure 2, it is possible to note the greater affinity of the vanadyl tri-isopropoxide for a TiO₂ surface.

The steep rise of the curves obtained on TiO₂ surface denotes a strong interaction between the adsorbate and the adsorbent. The great affinity of the vanadyl alkoxide for TiO₂ surface is shown by the large value obtained for K that is about 30 times the value obtained for the interaction between titanium tetra-isopropoxide and silica surface.

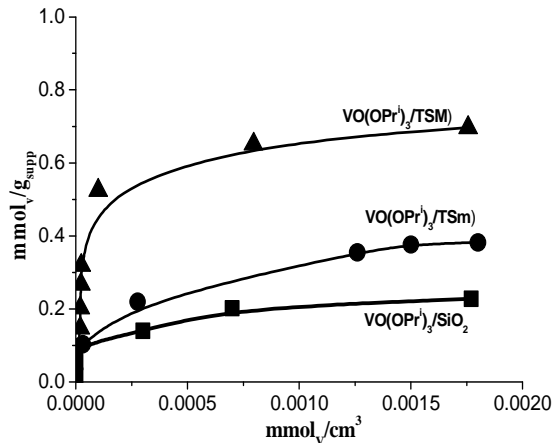
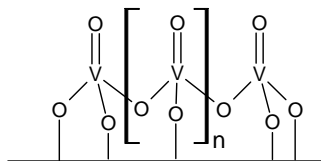
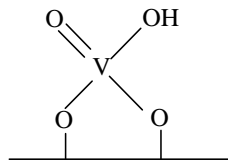


Figure 2: Comparison between the chemical adsorption isotherms of vanadyl alkoxides on: SiO₂, TSm and TSM.

The saturation value, corresponding to the monolayer, occurs for a surface density of 1.67 VO_x/nm², that is about 7% by weight of V₂O₅. It is interesting to observe that the overall stoichiometry for the monolayer is about 2OH/V. This means that we can have on the surface a mixture of oligomeric species of the type:



with the already seen monomeric species or alternatively a monomeric isolated specie of the type:



It is interesting to observe that also in this case by further increasing the vanadyl tri-isopropoxide concentration the adsorption increases

over the monolayer. This can be interpreted again by assuming the possibility of aggregation by vanadium (on the surface)-vanadium (in solution) interaction. Prepared catalysts and supports have been submitted to XRD analyses in order to verify the presence of crystallites and to have an estimation of the solids dispersion. In Figure 3, for example, XRD plots obtained for respectively pure V_2O_5 and V_2O_5 supported on silica at two different levels of concentrations (30% and 5% by weight) are reported.

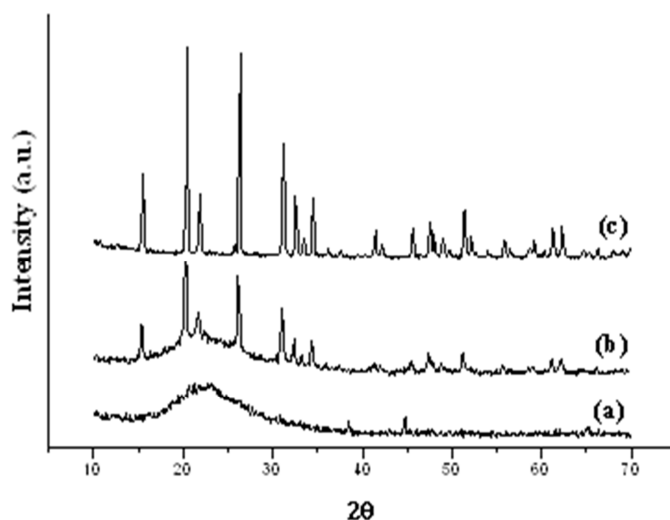


Figure 3: XRD spectra of vanadia catalysts supported on SiO_2 by and pure V_2O_5 : (a) 5 V_2O_5/SiO_2 ; (b) 30 V_2O_5/SiO_2 ; (c) pure V_2O_5 .

As can be seen, crystalline V_2O_5 is evident in the samples of pure V_2O_5 and in the samples containing 30% of V_2O_5 . For the lowest amount of V_2O_5 the catalyst shows a relatively good dispersion. The absence of crystallites of V_2O_5 has been observed for all the catalysts prepared by grafting on both SiO_2 and TiO_2-SiO_2 , independently of the amount of vanadium loaded. For catalysts of TiO_2-SiO_2 with 11.6% of V_2O_5 , an increase of the intensity of the anatase reflex, at 25° , can be observed

with respect to a catalyst prepared by grafting containing a comparable amount of V_2O_5 . This phenomenon has already been observed [62], that is, when vanadium is not uniformly dispersed on the surface it promotes the formation of anatase crystallites during the catalyst calcination. By concluding catalysts containing amounts of V_2O_5 lower than 10 % by weight don not show crystallites of this compound, in particular those prepared by grafting. Therefore, XRD analysis cannot give information about the molecular dispersion of V_2O_5 on the surface.

A-1.5 References

- [1] H. Idriss; E.G. Seebauer, *J. Mol. Catal. A: Chem.*, 2000, 152, 201.
- [2] S. Tsuruya; M. Tsukamoto; M. Watanabe; M. Masai, *J. Catal.*, 1985, 93, 303.
- [3] B. Parlitz; W. Hanke; R. Fricke; M. Richter; U. Roost; G. Ohlmann, *J. Catal.*, 1985, 94, 24
- [4] T.R. Ling; Z.B. Chen; M.D. Lee, *Appl. Catal. A: Gen.*, 1996, 136, 191.
- [5] V. Bagiev; G. Dadashev; K. Adzhamov; T. Alkhazov, *Kinet. Katal.*, 1992, 33 (3), 460.
- [6] S. Oyama; G.A. Somorjai, *J. Phys. Chem.* 1990, 94, 5022.
- [7] N.E. Quaranta; J. Soria; V. Cortes Corberan; J.L.G. Fierro, *J. Catal.* 1997, 171, 1.
- [8] E. Santacesaria; A. Sorrentino; R. Tesser; M. Di Serio; A. Ruggiero, *J. Mol. Catal. A: Chem.*, 2003, 204-205, 617.
- [9] Davy, H. Some new experiments and observations on the combustion of gaseous mixtures, with an account of a method of preserving a continued light in mixtures of inflammable gases and air without flame. *Philosophical Transactions of the Royal Society of London (1776-1886)* 107, 77-85. (1817).
- [10] Armstrong, E.F. & Hilditch, T.P. A study of catalytic action at solid surfaces. III. the hydrogenation of acetaldehyde and the dehydrogenation of ethyl alcohol in presence of finely-divided metals. *Proceedings of the Royal Society of London. Series A, Containing Papers of a Mathematical and Physical Character* 97, 259-264 (1920).

- [11] Franckaerts, J. & Froment, G.F. Kinetic study of the dehydrogenation of ethanol. *Chemical Engineering Science* 19, 807-818 (1964).
- [12] Tu, Y.-J., Li, C. & Chen, Y.-W. Effects of chromium promoter on copper catalysts in ethanol dehydrogenation. *Journal of Chemical Technology and Biotechnology* 59, 141-147 (1994b).
- [13] Tu, Y.-J. & Chen, Y.-W. Effects of alkaline-earth oxide additives on silica-supported copper catalysts in ethanol dehydrogenation. *Industrial and Engineering Chemistry Research* 37, 2618-2622 (1998).
- [14] Tu, Y.-J. & Chen, Y.-W. Effects of alkali metal oxide additives on Cu/SiO₂ catalyst in the dehydrogenation of ethanol. *Industrial and Engineering Chemistry Research* 40, 5889-5893 (2001).
- [15] Tu, Y.J., Chen, Y.W. & Li, C. Characterization of unsupported copper-chromium catalysts for ethanol dehydrogenation. *Journal of Molecular Catalysis* 89, 179-189 (1994a).
- [16] Tu, Y.J., Chen, Y.W. & Li, C. Characterization of unsupported copper-chromium catalysts for ethanol dehydrogenation. *Journal of Molecular Catalysis* 89, 179-189 (1994a).
- [17] Kanoun, N., Astier, M.P. & Pajonk, G.M. Dehydrogenation of ethanol and CO₂-H₂ conversion on newcoprecipitated Cu/Cr-Al catalysts. *Journal of Molecular Catalysis* 79, 217-228 (1993)
- [18] Kanoun, N., Astier, M.P. & Pajonk, G.M. New vanadium-copper-zinc catalysts, their characterization and use in the catalytic dehydrogenation of ethanol. *Applied Catalysis* 70, 225-236 (1991a).
- [19] Church, J.M. & Joshi, H.K. Acetaldehyde by dehydrogenation of ethyl alcohol. *Industrial and Engineering Chemistry* 43, 1804-1811 (1951).
- [20] Petr Chladek*, Eric Croiset, William Epling and Robert R. Hudgins, Volume 85, December 2007 *The Canadian Journal of Chemical Engineering* 917
- [21] Kanoun, N., Astier, M.P. & Pajonk, G.M. Selective dehydrogenation of ethanol over Cu catalysts containing Zr or V and Zr. *Reaction Kinetics and Catalysis Letters* 44, 51-56 (1991b).
- [22] Iwasa, N. & Takezawa, N. Reforming of ethanol - dehydrogenation to ethyl acetate and steam reforming to acetic acid over copper-based catalysts -. *Bulletin of the Chemical Society of Japan* 64, 2619-2623 (1991).

- [23] Inui, K., Kurabayashi, T. & Sato, S. Direct synthesis of ethyl acetate from ethanol over Cu-Zn-Zr-Al-O catalyst. *Applied Catalysis A: General* 237, 53-61 (2002).
- [24] Gole, J.L. & White, M.G. Supported catalysts prepared from mononuclear copper complexes: Catalytic properties. *Journal of Catalysis* 135, 81-91 (1992).
- [25] Di Cosimo, J.I., Díez, V.K., Xu, M., Iglesia, E. & Apesteguía, C.R. Structure and surface and catalytic properties of Mg-Al basic oxides. *Journal of Catalysis* 178, 499-510 (1998).
- [26] Alejandre, A., Medina, F., Salagre, P., Correig, X. & Sueiras, J.E. Preparation and study of Cu-Al mixed oxides via hydroxalite-like precursors. *Chemistry of Materials*. 11, 939-948 (1999).
- [27] Chen, S.P. & Voter, A.F. Reconstruction of the (310), (210) and (110) surfaces in fcc metals. *Surface Science* 244, L107-L112 (1991).
- [28] Petr Chladek, Phd thesis, University of Waterloo, 2007
- [29] H. Idriss; E.G. Seebauer, *J. Mol. Catal. A: Chem.*, 2000, 152, 201.
- [30] S. Tsuruya; M. Tsukamoto; M. Watanabe; M. Masai, *J. Catal.*, 1985, 93, 303.
- [31] B. Parltitz; W. Hanke; R. Fricke; M. Richter; U. Roost; G. Ohlmann, *J. Catal.*, 1985, 94, 24.
- [32] T.R. Ling; Z.B. Chen; M.D. Lee, *Appl. Catal. A: Gen.*, 1996, 136, 191.
- [33] V. Bagiev; G. Dadashev; K. Adzhamov; T. Alkhazov, *Kinet. Katal.*, 1992, 33 (3), 460.
- [34] S. Oyama; G.A. Somorjai, *J. Phys. Chem.* 1990, 94, 5022.
- [35] N.E. Quaranta; J. Soria; V. Cortes Corberan; J.L.G. Fierro, *J. Catal.* 1997, 171, 1.
- [36] E. Santacesaria; A. Sorrentino; R. Tesser; M. Di Serio; A. Ruggiero, *J. Mol. Catal. A: Chem.*, 2003, 204-205, 617.
- [37] M.F. Gomez; L.A. Arrua; M.C. Abello, *Ind. Eng. Chem. Res.*, 1997, 36, 3468.
- [38] S. Oyama; G.A. Somorjai, *J. Phys. Chem.* 1990, 94, 5022
- [39] J.L. Lakshmi; N.J. Ihasz; J.M. Miller, *J. Mol. Catal. A: Chem.*, 2001, 165, 199.
- [40] K. Inamaru; M. Misono; T. Okuhara, *Appl. Catal. A: Gen.*, 1997, 149, 133.
- [41] Y. Murakami, M. Inomata, K. Mori, T. Ui, K. Suzuki, A. Miyamoto and T. Hattori, p. 531, Elsevier, Amsterdam, 1983.

- [42] J. Kijenski, A. Baiker, M. Glinski, P. Dollenmeier and A. Wokaun, *J. Catal.*, 1986, **1**, 101.
- [43] I.E. Wachs and F.D. Hardcastle, *Chem. Inst. Canada, Ottawa*, 1988, **3**, 1449.
- [44] Santacesaria, E.; Sorrentino, A.; Tesser, R.; Di Serio, M.; Ruggiero, A. Oxidative dehydrogenation of ethanol on V₂O₅/TiO₂- SiO₂ catalysts obtained by grafting vanadium and titanium alkoxides on silica. *J. Mol. Catal. A: Chem.* 2003, **204-205**, 617.
- [45] M.F. Gomez; L.A. Arrua; M.C. Abello, *Ind. Eng. Chem. Res.*, 1997, **36**, 3468.
- [46] Tesser et al. *Ind. Eng. Chem. Res.* 2004, **43**, 1623-1633
- [47] P. Mars; D.W. van Krevelen, *Chem. Eng. Sci.*, 1954, **3**, 41.
- [48] B.M. Weckhuysen, P. Van Der Voort, G. Catana (Eds.), *Spectroscopy of Transition Metal Ions on Surfaces*, Leuven University Press, 2000 (The literature search is based on a Chemical Abstract search in the period 1967–2000).
- [49] Bert M. Weckhuysen, Daphne E. Keller, *Catalysis Today*, 2003, **78**, 25.
- [50] P. Van Der Voort, M. Baltes, E.F. Vansant, *Catalysis Today*, 2001, **68**, 121.
- [51] J. Keränen, A. Auroux, S. Ek, L. Niinistö, *Applied Catalysis A: General*, 2002, **228**, 213.
- [52] S. Klein, S. Thorimbert and W.F. Mayer, *J. Catal.*, 1996, **163**, 476.
- [53] M. A. Reiche, E. Ortelli, A. Baiker, *Appl. Catal. B: Environmental*, 23 (1999), 187-203.
- [54] E. Santacesaria, A. Sorrentino, M. Di Serio, R. Tesser, *Studies in Surface Science and Catalysis 143* E. Gaigneaux et al. (Editors), 2002 Elsevier Science
- [55] A. Sorrentino, Tesi di Dottorato, Preparazione di catalizzatori per grafting di alcossidi su ossidi misti e loro caratterizzazione, Dipartimento di chimica dell'Università degli Studi di Napoli, (2000)
- [56] M. Cozzolino, Tesi di Dottorato, "Preparation and characterization of heterogeneous catalysts obtained by Grafting", Dipartimento di chimica dell'Università degli Studi di Napoli, (2006)
- [57] P. Iengo et al., *Applied Catalysis A: General* 1998, **170**, 225.
- [58] P. Iengo et al. / *Applied Catalysis A: General*, 1999, **178** 97.

[59] P. Iengo, M. Di Serio, A. Sorrentino, V. Solinas, E. Santacesaria, *Appl. Catal. A*, 1998, *167*, 85.

[60] Santacesaria et al, *La Chimica e l'industria* n.10 Dicembre 2007, 112.

[61] R.C. Mehrotra, *Inor. Chim. Acta Reviews*, 1 (1967) 99

[62] Iannazzo, G. Neri, S. Galvagno, M. Di Serio, R. Tesser, E. Santacesaria; *Applied Catalysis A: General*, 246 (2003) 49-68.

SECTION A

Chapter 2

Techniques and equipment

A-2.1 Introduction

This chapter introduces some general aspects related to the catalyst prepared and to the reaction apparatus, employed to perform the ethanol dehydrogenation and oxidative dehydrogenation reactions in low pressure (1 bar) conditions and in mild range of temperature (140-200°C). In particular, in the following chapter the composition of vanadia catalysts supported on titania-silica by grafting, an available technique to obtain solids with a high dispersion of the active phase on support surfaces has been point out. Moreover, a list of the characterization techniques used to describe in details the chemical and physical properties of the examined catalysts have been described. Finally, the configuration of the equipment and of the operative condition has been reported. In this section, the study of the performances of several prepared vanadia based catalysts has been realized in the oxidative dehydrogenation and in dehydrogenation reaction too. The catalysts have been prepared by using different loading of Vanadia on a mixed oxide supports. In previously studies [1,2] the preparation of support by *grafting* $\text{Ti}(\text{O}-\text{Pr})_4$ on silica has been optimized by evaluating the influence of the nature of the solvent, used for dispersing the mentioned alkoxide, and of Ti-loading on the final surface catalyst dispersion. In this study the maximum surface monolayer coverage of silica (Grace S_{432} , specific surface area= $282 \text{ m}^2/\text{g}$, specific pore volume = $1.02 \text{ cm}^3/\text{g}$, hydroxyl groups = 0.92

mmol/g) by $\text{Ti}(\text{O}-\text{Pr})_4$ precursors was found to be ~ 2.2 Ti atoms/nm² by adopting a one-steps grafting procedure. The performances of these catalysts into the ethanol dehydrogenation reaction to acetaldehyde have been compared with the performances of several copper based catalysts. Moreover, several catalysts have been prepared by impregnation of copper nitrate on commercial support such as ZrO_2 and ZnO_2 (Sigma Aldrich). The coprecipitation technique has been used to prepare a copper catalyst incorporated in a structure of mixed oxide $\text{CuO-ZnO-Al}_2\text{O}_3\text{-ZrO}_2$. Finally, the performances of a K-310 catalyst have also studied in the mentioned reaction. The runs have an explorative character and have as main scope to individuate the possible active phase selective to produce acetaldehyde and ethyl acetate in low pressure conditions.

A-2.2 Catalysts preparation

A-2.2.1 Supported vanadia by grafting technique

The interest towards the study of the structure and composition of the surface active phases is progressively increased in the last few years and the individuation of the relationships between the surface characteristics of the catalysts and the preparation methodology is a topic of great concern. The main techniques used to prepare heterogeneous catalysts based by mixed metals oxide require two main steps:

1. The dispersion of the active phase on a catalytic support;
2. The calcination of the solid, to stabilize the active phases on a support too.

The deposition method involves, in the most cases, aqueous solutions of the catalytic active metal and the interaction between the precursor of active phase and the support occurs at the interphase liquid-solid [3]. In this chapter, the preparation modes of heterogeneous catalysts have been described by grafting of alkoxides on oxides surfaces. In

more detail, two different series of catalysts have been studied, at different loading of Vanadia respectively on a monolayer (Tsm) and triple layer (TSM) of titania supported on silica. Firstly, the two different supports have been prepared. The supports have been prepared by the contact of a commercial silica, at high specific surface area (Silica Grace, specific surface area $A_s=282\text{m}^2/\text{g}$), with a solution of titanium tri-isopropoxide ($\text{TiO}[\text{O-iPr}]_4$, Aldrich 99.999%, $d=0.963\text{g}/\text{ml}$) dissolved in anhydrous dioxane, of increasing concentrations. At first, the support has been characterized to evaluate the specific surface area ($A_s=280\text{m}^2/\text{g}$), the pore size distribution (mesoporous) and the density of the hydroxyls groups (see table 1).

Table 1: Commercial Silica Characteristics

Silica	Thermal treatment	Specific surface area (m^2/g)	Hydroxyles density (mmol/g)
Grace S432	500°CX 8h	282	0.92

The evaluation, by thermogravimetric measurements, of the density of hydroxyls groups is fundamental to evaluate, the exact quantity of alkoxides to employ to obtain the complete monolayer covering of silica support. For each $-\text{OH}$ group an alkoxides molecule reacts and to be sure, of the complete monolayer covering, an alkoxides excess of about 50% mol has been used.

The grafting reaction was performed for 5h in a well stirred glass reactor, under inert nitrogen atmosphere. The obtained solids were filtered, washed with dioxane, oven-dried at 120 °C overnight, heated at 200 °C and then calcined at 500 °C. The grafting operation was repeated for three times to prepare support of triple layer of titania on silica. Residual alkoxide groups were eliminated by burning. In table 2 the operative conditions used to prepare the supports Tsm, with a monolayer of about 7% in weight of TiO_2 , TSM_2 with a double layer of TiO_2 that correspond to 10% and TSM with a triple layer (15% wt of

TiO₂ , have been reported. In table 2, the composition for each prepared support is summarized.

Table 1: operative conditions to prepare TSm and TSM

Solvent/Support	Acronym	Ti(OR) ₄ (g)	SiO ₂ (g)	Dioxane (mL)
TiO ₂ /SiO ₂	TSm ₁	10.64	24.02	400
TiO ₂ /SiO ₂	TSm ₂ (doppio strato)	8.62	15.00	250
TiO ₂ /SiO ₂	TSM (triplo strato)	8.63	10.94	183

In Table 2 the weight percentage of anchored Titania on 3 grams of silica supports have been reported for each step of grafting reaction.

Table 2: TiO₂ loading at three different grafting steps.

Support	Step	TiO ₂ (mmol/g)	%TiO _{2wt}
TSm	I	1.00	7.44
TSm ₂	II	1.46	10.43
TSM	III	2.24	15.18

The values in table 2 show that in the first step the anchoring titania is of about the 7.44%. So, by speculating a stoichiometry of 1OH/1Ti, the complete monolayer loading is obtained, in agreement with previous works [4-6]. The chemical adsorption of the titanium alkoxides on the support surface has been studied to evaluate the adsorption isotherm of the titania on silica. As shown in literature work [7] the monolayer adsorption of TiO₂ on silica surface corresponds to a titania value of about 8%wt, that correspond to a surface concentration of 1mmols/g SiO₂ . By repeating two more times the grafting technique, a triple layer has been obtained. In all the mentioned cases, the amount of adsorbed titanium was determined by the colorimetric analysis suggested by Snell and Etre [8], by evaluating the quantity of titanium

remaining in solution after the grafting reaction. The amount of anchored active phase was also determined by realizing a mineralization of about 0.1 g of solid and by using a colorimetric method as described in Appendix A. The operative conditions used to prepare V_2O_5/TSm and V_2O_5/TSM are summarized in Table 3. The mixed oxides catalysts of vanadia V_2O_5/TiO_2-SiO_2 were prepared by grafting of vanadyl tetra-isopropoxide ($VO(O-iPr)_4$, Aldrich 99.999%, $d=0.963g/ml$) on two types TiO_2/SiO_2 supports: TSm (7.29 %wt TiO_2) and TSM (17.8 %wt TiO_2). The supports indicated with the acronyms TSm and TSM correspond, respectively, to the titanium tetra-isopropoxide monolayer and multilayer coverage of silica as above mentioned. In both the cases, a given amount of solid was contacted with solutions of vanadyl tri-isopropoxide ($VO(O-iPr)_3$, Aldrich 99.999%, $d=0.963g/ml$) dissolved in anhydrous dioxane of increasing concentrations. The grafting reaction was performed for 5h in a well stirred jacketed glass reactor, under inert helium atmosphere. The solids obtained were filtered, washed with dioxane, oven-dried at 120 °C overnight, heated at 200 °C and then calcined at 500 °C. Residual alkoxide groups were eliminated by burning. In Table 3 are summarized the operative conditions used respectively to prepare V_2O_5/TSm and V_2O_5/TSM catalysts.

Table 3: operative conditions adopted to prepare VTS_m and $VTSM$

Precursor/solvent/support	Acronym	$VO(O-iPr)_4$ (g)	Silica (g)	Dioxane (ml)	V_2O_5 Teor. %ww	V_2O_5 sper. %w
$VO(O-iPr)_4$ /diossano/TSm	1 V/TSm	0.08	3.0	50	0.99	0.98
$VO(O-iPr)_4$ /diossano/TSm	3 V/TSm	0.75	3.9	64	7.20	5.50
$VO(O-iPr)_4$ /diossano/TSM	1.5 V/TSM	0,12	3,00	50	1.5	1.5
$VO(O-iPr)_4$ /diossano/TSM	2.7 V/TSM	0,22	3,00	50	2.7	2.7
$VO(O-iPr)_4$ /diossano/TSM	8.8 V/TSM	0,89	3,00	50	11.0	8.8

The amounts of vanadium (%wt) adsorbed on silica (Table 3) have been determined by analysing residual vanadium on the filtration of water solutions, using UV-VIS spectroscopy. Moreover, the catalysts were mineralized by using sulphuric acid at high temperature (200°C) for about 4h; the details of the applied methodology are reported in Appendix A. The catalysts support is considered as an inert substance with an high specific surface area, ideal to support the metal oxide and to increase the mechanical strength of the catalysts. The activity, the selectivity and the life time of the catalysts have been affected by both the properties of the supports and by the preparation methodology of the catalytic systems. The TiO₂ favor the vanadia dispersion by the effect of the strong interaction between the titania and the supported vanadium oxide. On the other hand the TiO₂ supports have a very scarce thermal and mechanical strength and a low specific surface area (80m²/g), which is touchy to further decrease by the effect of sintering. The use of SiO₂ as support is necessary to increase the thermal and mechanical strength of the catalyst support. On the other hand, the acidic sites on the silica could promote an agglomeration of the vanadylic species, with a consequently decrease of the active phase dispersion. Thus, the use of a triple layer of titania on silica as support for vanadia is the best catalytic design ad already demonstrated in several previously papers [9-12]. The supports obtained by grafting the titania on silica are more stable to the high temperature, in fact the fusion temperature of silica is of about 1800°C. At the end catalysts with the same thermal and mechanical strength of silica and moreover, the use of titania favor a good dispersion of vanadia on titania [13,14]. The vanadia supported on a triple layer of TiO₂ coated SiO₂ is a possible candidate to perform the ODH of ethanol with high performances.

A-2.2.2 Supported Copper by impregnation

The most simple and widely used deposition method is impregnation, which refers to a procedure whereby a certain volume of an aqueous or non-aqueous solution containing the specific metal component precursor is totally adsorbed into the pores of an inorganic oxide. Two important impregnation procedures can be distinguished. If the support is dipped into an excess amount of solution, the process is called wet impregnation. More precise control over the vanadium oxide loading is achieved with a technique called dry impregnation, pore volume impregnation or incipient wetness impregnation. In this case, the support is contacted with a solution of appropriate concentration, corresponding in quantity to the total known pore volume of the support, or slightly less. This allows precise control of the concentration of the active vanadium oxide component on the support. The catalyst 30%Cu/ZnO e 30%Cu/ZrO₂ have been prepared by impregnating with a copper nitrate (Cu(NO₃)₂·2H₂O) solution two different supports ZnO (Aldrich) e ZrO₂ (Aldrich). For each 4g of a support a quantity of 4,4g di Cu(NO₃)₂·2H₂O has been dissolved in 6,8mL of water. The incipient wetness factor is determined to evaluate the quantity of water in which the salt of the active phase precursor must be dissolved. The obtained material was dried in oven at 100°C overnight and calcinated in air at 500°Cx3h to stabilize the surface. The operative conditions adopted to synthetize the catalysts have been summarized in Table 5.

Table 5: adopted operative condition to prepare catalysts by impregnation

Precursor/solvent/support	Acronym	CuO (%wt)
Cu(NO ₃) ₂ /H ₂ O/ZnO	30%Cu/ZnO	30
Cu(NO ₃) ₂ /H ₂ O/ZrO ₂	30%Cu/ZrO ₂	30

The copper catalysts have been previously reduced in hydrogen flow ($18 \text{ cm}^3/\text{min}$) for about 16-18h.

A-2.2.3 Copper catalyst by coprecipitation

The catalyst Cu-Zn-Zr-Al-O was prepared by coprecipitation of the corresponding metals nitrate by using sodium hydroxide as precipitating agent (3 mol dm^{-3}). Precisely, 9.7g of $\text{Cu}(\text{NO}_3)_2 \cdot 2\text{H}_2\text{O}$, 4g di $\text{Zn}(\text{NO}_3)_2$, 50.4g di $\text{Al}_2(\text{NO}_3)_2$ and 3.6g of zirconyl nitrate have been dissolved in 0.5 L of water. The obtained solid was filtered, washed, dried and calcined at $500^\circ\text{C} \times 3\text{h}$. The solid was reduced in hydrogen flow at $200^\circ\text{C} \times 4\text{h}$.

A-2.2.4 Copper commercial catalyst

The performances of two different commercial catalysts have also studied in the dehydrogenation and oxidative dehydrogenation of ethanol at low pressure. In table x the acronyms and the composition of the examined system has been reported. The studied catalysts are characterized by the presence of two different promoter ZnO and Chromia. Moreover, both of them contain alumina to increase the specific surface area.

Acronym	Composition given by the companies
BASF K-310	$\text{CuO-ZnO-Al}_2\text{O}_3$ (40-40-20 % b.w.)
BASF Cu-1234	$\text{CuCr}_2\text{O}_4\text{-CuO-Cu-BaCrO}_4\text{-Al}_2\text{O}_3$ (45-1-13-11-30 % b.w.)

A-2.3 Reaction Apparatus

The Kinetic runs were performed in a stainless steel tubular reactor with an internal diameter of 1 cm, kept isothermal with a fluidized bed of sand (Figure 1). Samples of powdered catalyst, generally 0.3 g, were placed inside the reactor on a bed of glass wool. Two thermocouples

located immediately upon and under the catalytic bed allowed the validity of the isothermal conditions to be controlled within ± 1 °C. Liquid ethanol was fed, by a syringe pump, into a vaporizer chamber kept at 250 °C and was then sent, after the addition of a stream of oxygen and helium, into a stainless steel coil kept at the same temperature of the reactor. All the fitting tubes are heated by heater at a temperature of 180°C to escape the condensation of products in the tube fitting. In Figure 2 the configuration of the apparatus has been represented.

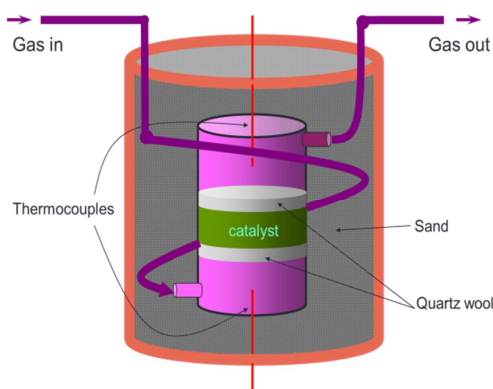


Figure 1: Reactor scheme

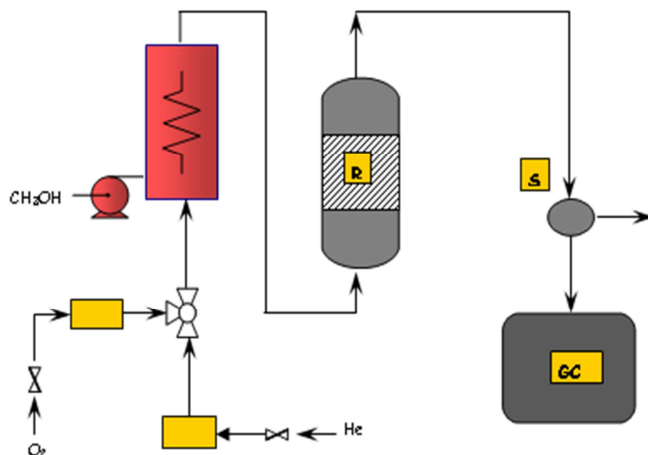


Figure 2: Schematic representation of the lab-scale plant used for the ODH of methanol to formaldehyde. R= reactor; S= sample valve; GC= gas-cromatograph.

The catalytic runs were conducted at atmospheric pressure (1 atm), by keeping constant the residence time and by changing the reaction temperature from 180 to 300 °C. Table 6 collects the operative conditions adopted for the catalytic screening.

Table 6: conditions used for the catalytic tests (Ethanol:Oxygen:Helium = 20:20:60 mol%)

Catalyst weight (g)	Helium Flow (ml/min)	Oxygen Flow (ml/min)	Ethanol Flow (ml/h)	W/F ($\text{g}_{\text{cat}} \cdot \text{h} / \text{mol}_{\text{MetOH}}$)
0.5-1.5	22.3	7.4	0.05-0.1	25.3

The composition of the gases at the outlet of the reactor was gas-chromatographically analysed by withdrawing a sample with an on-line sampling valve kept at 170°C. The GC used was an HP 5890 instrument, with a Restek RT-Q-Plot 30 m × 0.32 mm column. Helium was used as the carrier gas. The conditions used for the analyses were

as follows: temperature held at 40°C for 2 min, increased at a rate of 20°C/min to 100°C and then at a rate of 20°C/min to 180°C for 5 min, and finally kept at this temperature for 5 min. A TCD detector kept at 200°C was used. In Table 7 has been reported the retention times and the GC-factors determined for each component of the reaction mixture. The response factors of each compounds, have been evaluate by preparing solution of known concentration of two components. The solution contains always ethanol at which a factor 1 is attributed. The prepared mixture is then analyzed by gas-chromatograph with the aim to evaluate the response factor of the -i specie by using the following relation:

$$x_i = \frac{f_i A_i}{\sum_1^n f_i A_i} \quad (1)$$

f_i = response factor of - i specie

x_i = molar fraction of -i

A_i = GC area of - i specie

Table 7: retention times and the GC-factors determined for each component

Components	Retention Time	Response factors
Oxygen	5,11	1,9
CO ₂	5,32	0,8
Etylene	5,89	1
Water	9,16	6,45
1-butanol	10,42	-
Acetaldehyde	11,92	1,3
Ethanol	13,64	1
Propan-2-ol	16,37	-
Dietylether	17,55	0,4
1-propanol	18,99	-
Acetic acid	19,31	1,1
Ethyl acetate	25,5	0,8
Crotonaldehyde	30,60	-

Results are reported in terms of the ethanol conversion and product yields. The ethanol conversion and product selectivity is defined as:

$$X_{EtOH} = \frac{molEtOH_{reacted}}{molEtOH_{fed}}$$

$$S_i = \frac{mol\ products\ i\ produced}{molEtOH_{reacted}}$$

$$Yield_i = S \times C = \frac{mol\ prodotto\ i\ produced}{molEtOH_{fed}} \times a_i$$

A-2.4 References

- [1] A.Sorrentino et al. Journal of Molecular Catalysis A: Chemical 204–205 (2003) 617–627
- [2] M.Cozzolino, PhD thesis, University of Naples, 2008
- [3] H.F. Rase, Handbook of Commercial Catalysts, CRC Press, New York, 2000.
- [4]A. Comite et al., J. Molecular Catalysis A; Chemical, 2003,198, 151.
- [5]A. Sorrentino *et al.*, *Applied Catalysis A: General*, 2001, 209, 45.
- [6] R. Monaci *et al.*, *Applied Catalysis A: General*, 2001, 214, 203.
- [7] Santacesaria et al, La Chimica e l'industria n.10 Dicembre 2007, 112.
- [8] F.R.D. Snell and L.S. Ettre, *Enciclopedia of Industrial Chemical Analysis*, **1974**, 19, 107, Interscience, New York.
- [9] V. Iannazzo, G. Neri, S. Galvagno, M. Di Serio, R. Tesser, E. Santacesaria, *Appl. Catal. A General*, 2003, 246, 49.
- [10] E. Santacesaria, A. Sorrentino, R. Tesser, M. Di Serio, A. Ruggiero, *J. Mol. Catal. A Chem.* 204–205 (2003) 617–627.
- [11] E. Santacesaria, M. Cozzolino, M. Di Serio, A. M. Venezia , R. Tesser *Appl. Catal. A: Gen.* 270 (2004) 177-192
- [12] A. Comite, A. Sorrentino, G. Capanelli, M. Di Serio, R. Tesser,

- [13] M. Cozzolino *et al.*, *Studies in Surface Science and Catalysis*, E. Gaigneaux *et al.* (Eds.), 2006, 162, 299.
- [14] M. Cozzolino *et al.*, *Studies in Surface Science and Catalysis*, E. Gaigneaux *et al.* (Eds.), 2006, 162, 697.

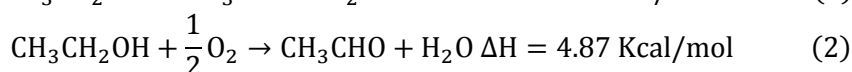
SECTION A

Chapter 3

Experimental Results

A-3.1 Introduction

As well known, the environmental concerns have increased the interest toward the development of new processes able to convert second-generation waste materials into ethanol. The main interest is its use as feedstock to produce acetaldehyde, ethyl acetate, acetic acid, ETBE and pure hydrogen. In this chapter, the interest is focused on the Acetaldehyde and pure hydrogen production. As well known, the importance towards acetaldehyde, considered as the most important aliphatic intermediates, is concerning to its use to produce acetic acid, acetone, ethyl acetate, C4-aldehydes, 1-butanol, pentaerythritol and many other chemicals. Actually, the ethanol dehydrogenation, oxidation and oxidative dehydrogenation, are the main routes to produce this compound, whose interest is related to its wide range of application in several industrial sectors [1,2]. The reaction steps by which is possible obtain acetaldehyde are reported below. The ethanol decomposition/dehydrogenation (1) is an endothermic reaction, the use of small amount of oxygen makes the reaction moderately endothermic (2). The use of a large excess of oxygen favour the ethanol combustion reaction (3).



In this chapter, the study of the dehydrogenation and oxidative dehydrogenation reactions, to produce acetaldehyde and pure hydrogen by ethanol, in mild temperature conditions and at low pressure, were carried out. In a first part of this chapter, the ethanol dehydrogenation by using copper/copper chromite catalysts have been lead. In order to successfully obtain acetaldehyde with high yield, it is necessary to identify an active, selective and stable catalyst system and also to find optimum conditions at which the production of hydrogen and acetaldehyde will be maximized and secondary reactions suppressed. At this purpose, the performances of Cu/ZnO, Cu/ZrO₂, Cu-ZnO-ZrO₂-Al₂O₃ and two others commercial Cu/ZnO/Al₂O₃ (K310) and CuCr₂O₄/CuO/BaCrO₄/Al₂O₃ have been studies. In a second section of this research work, the bearing of vanadia based catalysts prepared by grafting (see chp.2 section A) have been studied in the ethanol oxidative dehydrogenation reaction (ODH). At this purpose, a depth study on the mentioned reaction was realized in our research group and interesting results have been obtained by using redox catalysts of Vanadia supported on a triple layer of titania coated on silica. Thus, catalysts prepared by grafting of vanadyl tri-isopropoxide on the surface of silica coated with TiO₂ were found to be very active and selective to acetaldehyde in the oxidative dehydrogenation reaction [3-6]. The reaction occurs under very mild conditions of temperature (150-180°C) and at atmospheric pressure. The operative conditions and the characteristics of the catalysts have been reported in the chapter 2 of the current section. In correspondence with each experimental flow rate and temperature combination, different samples of the gaseous outlet mixture were withdrawn and sent to the GC for on line analysis, to evaluate the ethanol conversion and products selectivity. All the data reported in the tables mentioned above are averaged values for both the conversion and yields, evaluated under steady-state conditions.

A-3.2 Dehydrogenation

In this paragraph, the performances of copper based catalysts have been studied in low pressure and mild temperature (180-220°C) conditions. In more detail, the catalysts studied are:

- Catalysts of 30%_{wt} of copper impregnated on ZnO and ZrO₂.
- Catalysts of copper prepared by co-precipitation of metal nitrates 30% Cu/ZnO- ZrO₂-Al₂O₃.
- A typical low gas shift and steam reforming commercial catalyst supplied by BASF-K310 of Cu-ZnO-Al₂O₃ (40:40:20% b.w)
- A commercial catalyst of copper/copper chromite supplied by BASF-Cu-1234 of CuCr₂O₄-CuO-Cu-BaCrO₄-Al₂O₃ (45-1-13-11-30 % b.w).

The details on the preparation and compositions of the studied catalysts are reported in chapter 2 of this section.

All the copper based catalysts studied have been previously reduced in hydrogen flow 6% in nitrogen of 20 cm³/min, for about 16-18 h at 200°C of temperature. The runs have been performed by using 0.58 g of catalyst, ethanol flow 0.1cm³/h, a constant residence time of 478.8 ghmol⁻¹. In Table 1, the operative conditions and the results in terms of activity and selectivity for the catalysts prepared by coprecipitation (Cu-ZnO-ZrO₂-Al₂O₃) and by impregnation (Cu/ZnO and Cu/ZrO₂) have been summarized.

The catalysts studied have the same composition in copper, about 30% wt, and are mixed or supported with different oxides. As shown in table 1, the catalyst 30% Cu/ZnO has a relatively high conversion of about 50% at 260°C and of about 77% at 290°C. The use of so high reaction temperature is necessary to sustain the endothermic nature of the reaction and to activate the catalyst action. The acetaldehyde selectivity is high and corresponds to 95-98%. The catalytic activity of 30%Cu/ZrO₂ is

relatively low (10-18%) also at high temperature (350°C). On the other hand, the use of zirconia, instead of ZnO, favors the ethyl acetate formation (18-22%).

Table 1: catalyst prepared by coprecipitation (Cu-ZnO-ZrO₂-Al₂O₃) and by impregnation (Cu/ZnO and Cu/ZrO₂).

Catalyst	T°(C)	W/F (ghmol ⁻¹)	Conv. EtOH(%)	Sel. (%)	
				AcOEt	AcH
30%Cu/ZnO	260	478.8	47.7	4.5	95.4
30%Cu/ZnO	290	478.8	77.2	1.9	98.0
30%Cu/ZrO ₂	290	478.8	10.7	21.5	78.5
30%Cu/ZrO ₂	350	478.8	18.8	16.7	83.2
30%Cu/ZnO-ZrO ₂ -Al ₂ O ₃	290	478.8	16.7	14.0	85.9

This particular result is in agreement with those reported by Inui et al. [7], in which the product distribution over a series of catalysts with different composition is summarized. The quaternary system has a relatively poor activity also at high temperature (290°C). The main inconvenient of these systems is the rapid catalytic deactivation, after about 90 min of reaction, at this so high operating temperature. On the other hand only at T>250°C the examined catalysts show a significant activity.

More promising was the performances of a commercial low temperature gas-shift catalyst of Cu-ZnO-Al₂O₃. The performances of the catalyst (0.58 g) were studied by using mild temperature in the range of 180-190°C, low pressure (1 bar), a residence time of 290-583 ghmol⁻¹, an ethanol flow of F_{EtOH}=0.1mL/h-0.05mL/h and inert flow F_{He}=4cm³min⁻¹. In Figure 1 the ethanol conversion, the acetaldehyde and ethyl acetate selectivities profiles have been reported as function of the time-on-stream. The runs have been performed at a W/F=290 ghmol⁻¹, T=260°C, with ethanol flow of 0.1 cm³/min and inert flow of nitrogen of 5 cm³/min. As it can be appreciated by the profiles of Figure 1, the acetaldehyde selectivity is of about 89% and slightly decreases with the time on stream.

Table 2: operative conditions, selectivities and activities results for K-310. The catalytic runs were performed charging the reactor with 0.58g and by fed a nitrogen flow of 4 cm³/min as carrier.

Time (min)	T (°C)	F _{EtOH} (mL/h)	W/F (g _{cat} *h)/mol	Conversion (%)	Selectivity(%)		yield (%)	
					AcOEt	AcH	AcOEt	AcH
60	180	0.1	290	74.9	4.1	95.9	3.1	71.8
90	180	0.1	290	69.9	2.9	97.1	2.0	67.9
30	190	0.1	290	70.0	1.7	98.	1.2	69.3
60	190	0.1	290	70.4	2.0	98.	1.5	72.3
90	190	0.1	290	65.7	2.3	98.	1.5	64.2
60	260	0.1	290	72.7	10.9	89.1	7.9	64.8
90	260	0.1	290	64.3	10.7	89.3	6.9	57.5
120	260	0.1	290	56.9	11.5	88.5	6.5	50.4
160	260	0.1	290	55.3	12.1	88.	6.7	48.6
190	260	0.1	290	52.7	12.5	87.5	6.6	46.2
210	260	0.1	290	48.1	13.9	86.1	6.7	41.4
240	260	0.1	290	46.9	14.3	85.7	6.7	40.1
280	260	0.1	290	41.7	15.6	84.4	6.5	35.2
310	260	0.1	290	40.2	16.2	83.8	6.5	33.7
350	260	0.1	290	40.2	16.2	83.8	6.5	33.7
60	260	0.05	583	55.0	17.1	82.	9.4	45.5
90	260	0.05	583	42.0	23.6	76.4	9.9	32.2
120	260	0.05	583	36.5	26.4	73.6	9.6	26.9
150	260	0.05	583	32.0	27.7	72.3	8.9	23.1
180	260	0.05	583	28.0	29.2	70.7	8.2	19.9
190	260	0.05	583	29.2	29.5	70.5	8.6	19.9

On the other hand, the selectivity to ethyl acetate increases by 10 to 17% mol. This behavior could be an indicative guideline to understand the mechanism of reaction. The ethanol dehydrogenation results are in agreement with the literature [8,9]. In particular, condition of temperature, pressure, residence time and hydrogen partial pressure fed, the acetaldehyde can react with ethoxy group adsorbed in the catalyst surface to give ethyl acetate. This aspect will be thoroughly described in the section B of this thesis, completely dedicated to the ethyl acetate production by ethanol dehydrogenation under pressure.

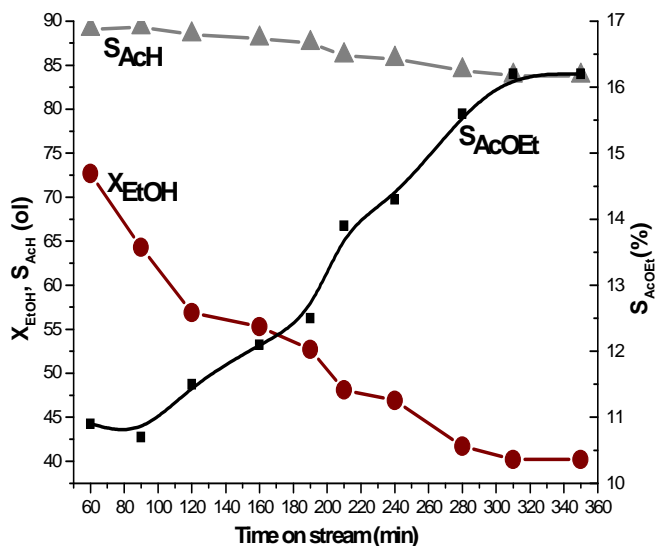


Figure 1: ethanol conversion, acetaldehyde and ethyl acetate selectivities for K-310. The runs have been performed at $W/F=290 \text{ ghmol}^{-1}$, $T=260^\circ\text{C}$, with ethanol flow of $0.1 \text{ cm}^3/\text{min}$ and inert flow of nitrogen of $5 \text{ cm}^3/\text{min}$.

One of the main disadvantages of this reaction is the prominent catalyst deactivation at temperatures higher than $200\text{--}220^\circ\text{C}$. A first hypothesis is the deactivation due to the fouling of the catalyst surface due to the coke deposition or acetaldehyde adsorption, which could polymerize. At this purpose, a flow of oxygen of about $1.5 \text{ cm}^3/\text{min}$ at a temperature of 200°C , was fed on the catalyst bed with the aim to burning the carbon residuals. This operation was not able to restore the catalyst activity. The reason of deactivation could be the possible copper sintering phenomena on the catalysts surface due to the low Hutting-Tamman temperature of the active phase ($T_{\text{Hugging}} < 300^\circ\text{C}$), as demonstrated [10] in literature. In Figure 2 the profiles of ethanol conversion, acetaldehyde and ethyl acetate selectivity for all the runs shown in Table 2 are reported.

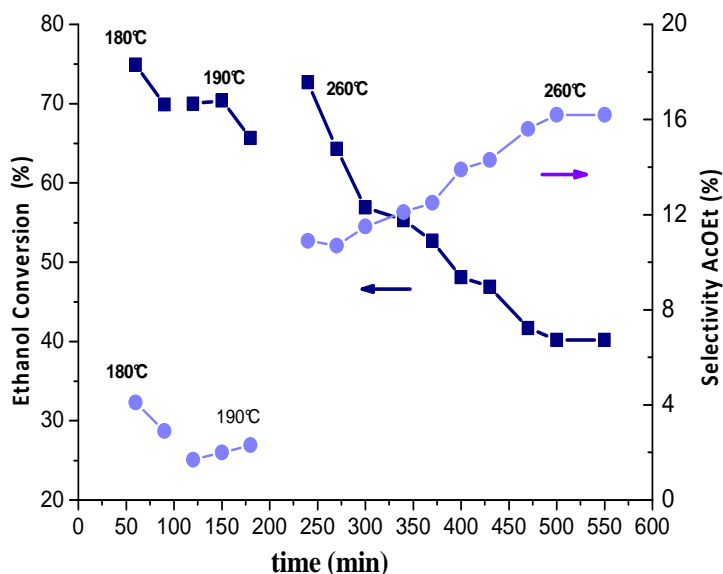


Figure 2: runs performed with K-310 catalysts at the operative conditions reported in table 2.

The profiles of Figure 2 suggest an increase of the ethyl acetate selectivity with the temperature of reaction and with the time on stream. A comparison also of the runs at two different residence times has been done. In figure 3, the comparison of the performances at respectively 290-583 ghmol^{-1} has been represented.

As it can be appreciated at higher residence time, 583 ghmol^{-1} , the ethyl acetate selectivity is of about 30% but on the other hand, the ethanol conversion is very low. The catalysts studied show high tendency to deactivate due to the effect of both the fouling of the catalysts surface, by coke deposition and acetaldehyde condensation, and the sintering of the active phase and growing of the copper metal particles with a consequently drastic reduction of the catalysts activity during the reaction.

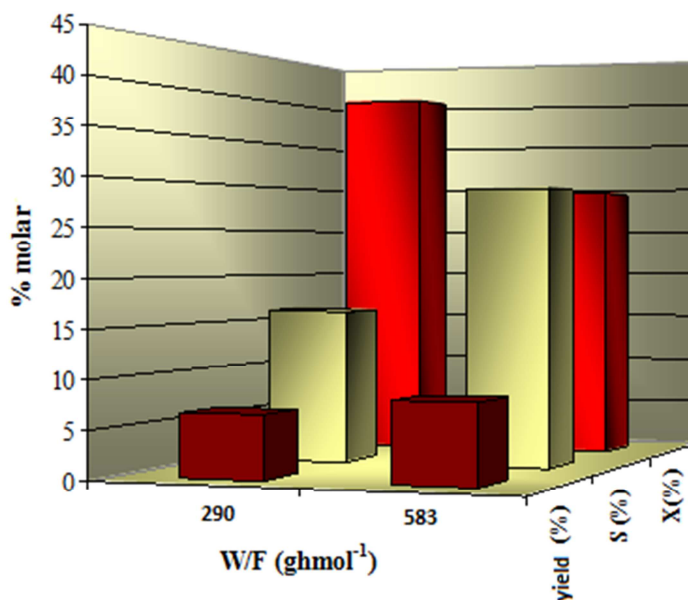


Figure 3: comparison of the performances at two different residence time 290-583 ghmol⁻¹. The runs have been performed at 260°C.

At last, the performances of another catalyst have been studied in this reaction. The catalyst examined is a commercial copper/copper chromite system composed by $\text{CuCr}_2\text{O}_4\text{-CuO-Cu-BaCrO}_4\text{-Al}_2\text{O}_3$ with the following compositions 45-1-13-11-30 % b.w. The catalyst has been studied at 220°C, at atmospheric pressure and at two very different residence times, of about 97.56 ghmol⁻¹ and 0.18 ghmol⁻¹.

The runs were performed by charging, in the first case ($W/F=97.56$ ghmol⁻¹), the reactor with 50 g of catalyst and by feeding 0.5 cm³/min of ethanol. In the second case ($W/F=0.18$ ghmol⁻¹) the reactor was charged with 0.4 g of catalyst and fed with 0.5 cm³/min of ethanol. Moreover the effect of the ethanol/oxygen ratio on the catalyst activity and acetaldehyde selectivity has been evaluated.

In Table 3, the operative conditions and the obtained results in terms of ethanol conversion, acetaldehyde and ethyl acetate selectivity have been summarized.

Table 3: Cu-1234 performances in ethanol dehydrogenation to produce acetaldehyde. The runs have been performed at a pressure of 1 atm at a temperature of 220°C. A mixture of hydrogen 6% in nitrogen of 25 cm³/min was previously mixed and successively fed to the reaction apparatus.

RUN	cat (g)	W/F (ghmol ⁻¹)	F _{EtOH} (cm ³ /min)	F _{O₂} (cm ³ /min)	X (%)	S _{CH₃CHO} (%)	S _{AcOEt} (%)	S _{Others} (%)
1A	50.00	97.56	0.5	-	49.55	12.17	40.40	47.43
2A	0.40	0.18	2.2	-	51	56.00	10.00	34.00
3A	0.40	0.18	2.2	1.2	53	85.11	4.5	10.39
4A	0.40	0.18	2.2	3.3	70	88.43	2.1	9.47

The runs 1A-2A have been performed in absence of oxygen, in dehydrogenation reaction at two very different residence times respectively of 97.56 ghmol⁻¹ and 0.18 ghmol⁻¹. Moreover, the behavior of the catalyst have been studied in partial oxidative dehydrogenation, reaction by feeding small amount of oxygen 1.2 cm³/min (O₂:EtOH=0.6) and 3.3 cm³/min (O₂:EtOH=1.2), by using a residence time of 0.18 ghmol⁻¹. The catalyst in exam has very important and interesting performances and mostly it was very stable and did not deactivate during the reaction. In figure 4, a comparison of the results obtained by operating at two different residence time, at a temperature of 220°C and at atmospheric pressure was reported. As it can be appreciated, the catalyst Cu-1234 shows at two different residence time more or less the same activity of about 50% molar conversion while a wide difference in the acetaldehyde selectivity has been obtained. The use of high residence time, of about 100 ghmol⁻¹, favors the acetaldehyde coupling reaction towards the ethyl

acetate production (40.40%), whilst at low residence time the acetaldehyde selectivity is of about 56%.

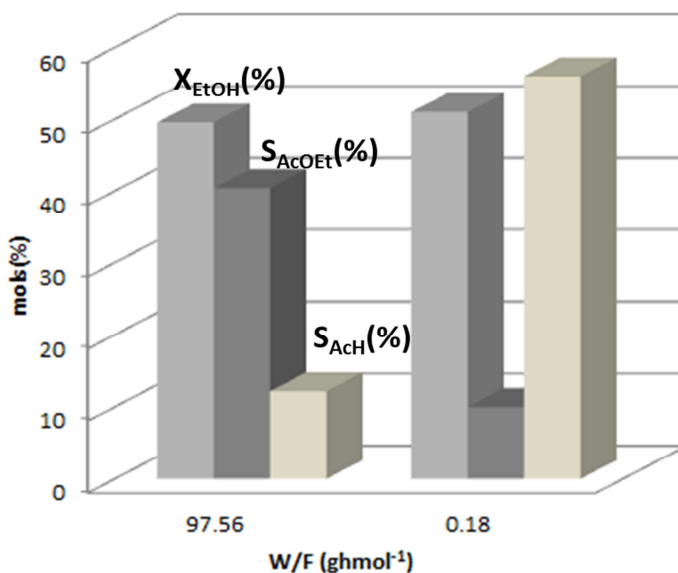


Figure 4: Cu-1234 performances in dehydrogenation reaction, performed at 220°C, at 1 bar, at 0.18-97.56 g_{mol}⁻¹.

The main advantage is to produce with high selectivity and a relatively high conversion, acetaldehyde and pure hydrogen as described in the reaction (1), at relatively mild temperature condition (220°C). By fed in the apparatus system a low amount of oxygen to have a ratio O₂:EtOH=0.6, the ethanol conversion is almost the same and acetaldehyde selectivity increase from 56 to 85.11%_{mol}. A further increase of the oxygen flow promotes a significantly increase of the ethanol conversion whilst the value of acetaldehyde selectivity is of about 88%. In spite of the good results obtained in partial oxidative dehydrogenation reaction, the main drawbacks are firstly related to the explosive nature of the reaction mixture and then to the several by-products CO_x, CH₄, H₂O that can reduce the purity of hydrogen. The use of dehydrogenation

reaction is more safety and flexible process, that, in presence of adequate catalytic system and of optimal operative conditions can favor the formation of other chemicals such as ethyl acetate (see section B).

A-3.3 Oxidative dehydrogenation

In this section the performances of two catalysts of vanadia supported on titania coating the silica, characterized by increasing amounts of active phase has been studied in the oxidative dehydrogenation reaction. In Table 4 the results in terms of activities and acetaldehyde selectivities of 2.7% of Vanadia supported on a triple coating of titania on silica has been reported. In this particular case the runs have been performed in a range of temperature of 100-200°C, at a residence time of 60 ghmol⁻¹, by charging the reactor with 0.3 g of catalyst. In this case the molar ratio between EtOH:O₂ is kept constant (1:3).

Table 4: 2.7-V₂O₅/TSM performance in ethanol ODH. The runs have been performed at 64.8ghmol⁻¹, by using 0.33 g of catalyst, at a constant ratio molar ratio EtOH:O₂=1:3. A flow of 0.30 mL/h and 0.7 mL/min of oxygen.

RUN	T (°C)	F _{EtOH} (cm ³ /h)	F O ₂ (cm ³ /min)	X (%)	S _{CH₃CHO} (%)	S _{AcOEt} (%)	S _{Others} (%)
1B	100	0.3	0.7	13.2	8.23	-	91.77
2B	120	0.3	0.7	12.9	15.4	-	84.6
3B	140	0.3	0.7	23.4	20.2	-	79.8
4B	160	0.3	0.7	48.4	39.9	-	60.1
5B	170	0.3	0.7	59.4	49.5	3.6	46.9
6B	180	0.3	0.7	62.3	54.3	4.4	41.3

In Table 5 the results in terms of activities and acetaldehyde selectivities of 8% of vanadia supported on a triple coating of titania on silica has been reported. In this particular case, the runs have been performed at 170-180°C, at a residence time of 60.80 ghmol⁻¹, by charging the reactor with

0.3 g of catalyst. In this case the molar ratio EtOH:O₂ is kept constant (1:3).

In figure 5 the profiles of ethanol conversion and acetaldehyde selectivities for both 2.7-VTSM and 8.8-VTSM have been reported.

Table 5: 8.8-V₂O₅/TSM performance in ethanol ODH. The runs have been performed at 64.8ghmol⁻¹, by using 0.33 g of catalyst, at a constant molar ratio EtOH:O₂=1:3. A flow of 0.30 mL/h and 0.7 mL/min of oxygen.

RUN	T (°C)	F _{EtOH} (cm ³ /h)	FO ₂ (cm ³ /min)	X (%)	S _{CH₃CHO} (%)	S _{AcOEt} (%)	S _{others} (%)
1C	170	0.3	0.7	68.4	53.9	3.6	42.5
2C	180	0.3	0.7	75.2	65.1	8.69	26.21

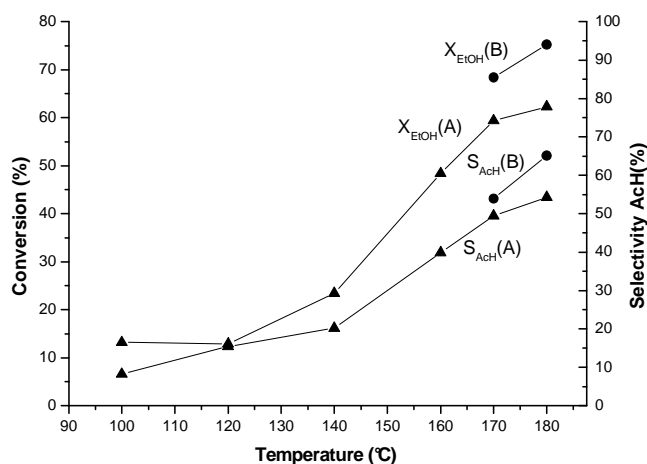


Figure 5: performances of 2.7-VTSM (A) and of 8.8-VTSM (B) in ODH by changing the temperature of reaction.

As it can be appreciated, by the profiles in Figure 5, by increasing the reaction temperature the ethanol conversion rise up from 12 to 64%. This effect is more evident for the catalyst with higher content of vanadia (B), where the ethanol conversion at a 180°C is of about 75%. At higher content of vanadia, the catalyst is more selective to acetaldehyde and in particular at 180°C the selectivity is of about 50% vs 40% obtained by 2.7-VTSM catalyst. In Table 6 the results in terms of activities and acetaldehyde selectivities of 8-VTSM has been reported at different molar ratio EtOH:O₂=1:3. In this particular case, the runs have been performed at 180°C, at a residence time of 60.80 ghmol⁻¹, by charging the reactor with 0.3 g of catalyst.

Table 6: 8-V/TSM performance in ethanol ODH. The runs have been performed at 64.8ghmol⁻¹, by using 0.33 g of catalyst, at a constant temperature of 180°C. An ethanol flow of 0.30 mL/h and an inert nitrogen flow of 25cm³/min.

RUN	F _{EtOH} (cm ³ /h)	F _{O₂} (cm ³ /min)	EtOH:O ₂ (mol)	X (%)	S _{CH₃CHO} (%)	S _{AcOEt} (%)	S _{others} (%)
1D	0.3	-	-	19.01	51.40	7.01	41.59
2D	0.3	2.5	1:1	33.90	57.91	3.51	38.58
3D	0.3	4.6	1:2	45.61	64.52	2.73	32.75
4D	0.3	7.7	1:3	75.90	75.10	1.01	23.89

In Figure 6, the effect of the oxygen partial pressure on the performance of the 8% V_2O_5/TiO_2-SiO_2 catalyst has been appreciated.

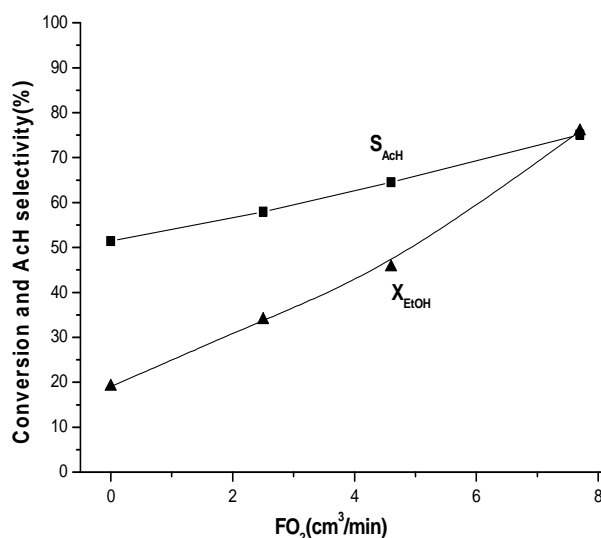


Figure 6: 8.8-V/TSM performance in ethanol ODH. The runs have been performed at 64.8 g/mol, by using 0.33 g of catalyst, at a constant temperature of 180°C. A flow of 0.30 mL/h and 0.7 mL/min of oxygen.

As it can be seen, the use of higher amount of oxygen favours the increase of the ethanol conversion also at lowest reaction temperature. The initially endothermic reaction becomes self-sustaining and able to produce acetaldehyde with high selectivities. The more drawback is the explosive nature of the reaction and the moreover the use, of higher ratio ethanol:oxygen than $EtOH:O_2=1:3$, favours the combustion reaction and consequently the formation of undesired CO_x . Very active and selective catalysts have been prepared by grafting vanadyl alkoxide onto a silica support coated with TiO_2 .

This type of catalyst (V_2O_5/TiO_2-SiO_2) gives rise to high conversion of ethanol to acetaldehyde at very low temperature (160-180 °C), which represents a useful perspective in view of industrial applications. The high dispersion of the catalyst strongly improves the selectivity and the activity is a linear function of supported vanadium amount. Acetaldehyde is relatively stable on this catalyst and this is the reason for the high selectivities observed. The acid and basic properties of the catalyst have a minimal influence on the catalyst performance in this reaction, and therefore, only the redox properties are responsible for the reaction. The mechanism of the reaction does not involve surface lattice oxygen, because, at the temperature used, the oxygen exchange reaction is too slow [11]. As demonstrated by several works the TiO_2 represent a favourable chemical environment for the vanadium catalytic reactions in the ODH of ethanol to acetaldehyde, in agreement with the suggestion made by other authors that V-O-support bonds are determinant for the activity and selectivity of different reactions, because the effect of the support is often dramatic.

A-3.4 Acetaldehyde: an intermediate of reaction to produce high commodities chemicals.

As demonstrated by several literature works, one of the main chemicals that could be produced by acetaldehyde is ethyl acetate. One of the section of this thesis will be completely dedicated to the study of the production of this important chemical, of great industrial interest for its wide range of applications [12,13]. The use of vanadia catalysts to produce acetaldehyde to convert successively into ethyl acetate could be an interesting study. The final section of this work was dedicated to the study of mechanical mixture of vanadia based catalysts prepared by grafting with ZnO , ZrO_2 with the aim to identify an eventual phase able to promote the ethyl acetate formation starting from acetaldehyde. Chan et

al. [14] suggests the use of physical mixture to promote the ethyl acetate formation. In this section two different mechanical mixtures of respectively 2.7-V₂O₅/TSM (2.7VTSM-ZnO) and 8.8VTSM (8VTSM-ZnO) with commercial ZnO (Aldrich 99,9%) and 8.8-VTM with ZrO₂(Aldrich 99,9%), almost the most used supports for the catalysts of dehydrogenation. The mechanical mixtures are 1:1 weigh %. The use of ZnO could be justified on the basis of many literature works that demonstrate that the active centers that favor the ethanol coupling reaction to form hemiacetal species, rapidly dehydrogenated to ethyl acetate are localized on the surface of a mixed oxide, which acts prevalently as a support (ZnO, ZrO₂, Al₂O₃) [15]. In Table 6 the operative conditions adopted and the results has been obtained by operating in mild condition of temperature (180°C) and pressure of 1 atm. The reactor was charged with about 3 g of catalyst and fed with 0.1 cm³/h of ethanol, 1.2 cm³/min of oxygen and 25 cm³/min of nitrogen as carrier.

Table 7: performances of a mechanical mixture of 2.7-VTSM-ZnO, 8.8-VTSM-ZnO and 8.8-VTSM-ZrO₂. The runs were performed at 180°C, at 1 atm, 0.1 cm³/h of ethanol flow.

Catalyst	W/F (ghmol ⁻¹)	X _{EtOH} (%)	Selectivity (%)	
			AcOEt	AcH
2.7VTSM-ZnO	156.85	37,9	6,5	88,0
8.8VTSM-ZnO	156.85	45,4	6,7	82,0
8.8VTSM-ZrO₂	156.85	41.4	32.10	57.24

At a temperature of reaction of 180°C the conversion is higher in case of catalyst with higher amount of vanadia supported and the selectivity is pretty the same (80-88%). The use of zirconia favors an evident increase of the ethyl acetate selectivity from 10 to 32%.

The effect of the temperature also was studied and in table 8 the results have been reported for the catalyst 8.8VTSM-ZnO.

Table 8: ODH 8.8-VTSM-ZnO. T=180-200°C, P=1 atm, 0.1 cm³/h of ethanol, 1.2 cm³/min of oxygen and 25 cm³/min of nitrogen

T (°C)	W/F (ghmol ⁻¹)	Conversion _{EtOH} (%)	Selectivity (%)	
			AcOEt	AcH
180	140.33	45,4	6,7	82,0
190	148.59	42,3	16,5	79,7
200	156.85	45,4	17,2	78,8

More probably, the coupling reaction is favored by the increase of the temperature reaction and as demonstrated by the results reported in Table 8 a significantly increase of the ethyl acetate selectivity was obtained by increasing the reaction temperature from 180 to 200°C. On the other hand, the use of high temperature and concentration of oxygen favors the combustion reaction, the formation of CO_x and consequently a decrease of selectivity to acetaldehyde.

A-3.5References

- [1] Acetaldehyde. In Ullmann's Encyclopedia of Industrial Chemistry, 6th ed.; Wiley-VCH: Weinheim, Germany, 2002; Vol. A1, pp 31-44.
- [2] A. Chauvel; G. Lefebvre; L. Castex, Technip, Paris, 1986; Vol. 2, p 33.
- [3] S. Oyama; G.A. Somorjai, J. Phys. Chem. **1990**, 94, 5022.
- [4] .E. Quaranta; J. Soria,; V. Cortes Corberan; J.L.G. Fierro, J. Catal. **1997**, 171, 1.
- [5] E. Santacesaria; A. Sorrentino; R. Tesser; M. Di Serio; A. Ruggiero, J. Mol. Catal. A: Chem., **2003**, 204-205, 617.
- [6] M.F. Gomez; L.A. Arrua; M.C. Abello, Ind. Eng. Chem. Res., **1997**, 36, 3468.
- [7] K.Inui et al. Applied catalysis A: general 237 (2002) 53-61.
- [8] N.Isawa et al.Bull.Chem.Soc.Jpn., 64, 2619-2623 (1991)
- [9] K.Inui et al. Journal of Catalysis **212**, 207–215 (2002)

- [10] M.V. Twigg, M.S. Spencer / Applied Catalysis A: General 212 (2001) 161–174
- [11] Santacesaria et al Ind. Eng. Chem. Res., Vol. 43, No. 7, 2004
- [12] K.Inui et al.Applied Catalysis A: general 237 (2002) 53-61
- [13] L.Wang et al. Chemistry Letters 1173-1176, 1986
- [14] Chang et al Applied Catalysis A: General 304 (2006) 30–39
- [15] Kanichiro Inui, Toru Kurabayashi, and Satoshi Sato, Naoki Ichikawa Journal of molecular catalysis 216 (2004) 147-156

SECTION A

Conclusion

The literature survey reported has shown that supported vanadium oxide catalysts are very complex inorganic materials that play an important role in most of heterogeneous catalytic processes. Their synthesis and catalytic design require a profound knowledge of both the solid-state chemistry and inorganic chemistry. Their application in heterogeneous catalysis results from the specific interaction between the support and the vanadium oxide. Insight into the preparation of supported vanadium oxides at the molecular level would be very important to an understanding of the different steps involved. It is also evident from this review/chapter that the support characteristics (i.e., structure and chemical composition) have a significantly influence on the properties of the supported vanadium oxide catalysts. This support–effect results in the formation of specific, often not-well defined, molecular structures of metal oxides with, for example, special redox properties. A better insight into the formation and local structure of these molecular structures can be only obtained by applying a battery of complementary characterization techniques, preferably under *in situ* conditions. Thus, the research has to be directed towards the use of an intelligent combination of preferably *in situ* spectroscopic techniques delivering both molecular and electronic information about the supported vanadium oxides. The results obtained about the ODH of ethanol to acetaldehyde, showed that vanadia supported by *grafting* on TiO₂-coated silica (V₂O₅/TiO₂-SiO₂) are very active and selective catalysts because able to promote the mentioned reactions under mild conditions of both temperature (140-

180°C) and pressure (1bar). This is due to the higher surface molecular dispersion of vanadium sites that is possible to achieve by using the grafting preparation method. By comparing the catalytic performances of supported vanadia catalysts in the ODH of ethanol to the corresponding aldehydes, the following considerations could be done:

- A high surface dispersion of supported vanadium sites is fundamental to improve both the activity and the selectivity to the desired products. It was found that the coating of the silica carrier with a monolayer of TiO_2 increases substantially not only the activity, but also the selectivity, as compared to those of the one supported on pure TiO_2 . This is in agreement with the literature, according to which the oxygen in the V–O–support bond is critical for these catalytic oxidation reactions.
- Only redox sites are responsible for the reactions. The acid and basic properties of the catalysts have a minimal influence on the catalyst performances.

The ODH reactions could have problem related to the safety due to the explosive nature of the reaction. Moreover the main drawback is the presence of co-feed oxygen that could drop significantly the selectivity to hydrogen and acetaldehyde and favor the combustion reactions to CO and CO_2 . The ethanol dehydrogenation, at this purpose, has shown promising results by using a catalyst promoted with chromia at low pressure and in mild conditions of temperature. Moreover, in total absence of oxygen, the possibility to improve the hydrogen selectivity and purity is very high. The dehydrogenation reaction suffers of the low life time of the catalyst and a depth study has been done to prove the high stability of copper catalyst promoted with chromia. Finally, by choosing particular range of temperature, pressure, residence time and initial hydrogen partial pressure the system could be improved and by ethanol, in only one step of reaction, towards acetaldehyde, the ethyl acetate could be produced

with high selectivity as it will be demonstrated in the section B of this thesis.

SECTION B

Abstract **High Pressure** **Dehydrogenation**

A novel catalytic process for producing ethyl acetate and high-purity, elevated-pressure hydrogen from synthesis gas was proposed and investigated. The process combines the advantages of low investment and operating costs with the flexibility to adapt to a small-scale operation. The process consists of one step ethanol dehydrogenation reaction by using a copper-chromite based catalyst. The main peculiarity of the developed process is the high selectivity to ethyl acetate, with respect to the conventional existed processes that requires another step of hydrogenation to convert the huge class of sub-products, mainly C₃-C₄ aldehydes and ketones, to ethanol. Another aspect is correlated to the possibility to obtain pure hydrogen, exempt of CO_x, which could be used directly as fuels for fuel cells. Various dimensionless criteria were evaluated to confirm there was no significant effect of mass transfer limitations and thus the experimental results represent true kinetics. Furthermore, a thermodynamic study was conducted using a Gibbs free energy minimization model to identify the effect of reaction conditions on ethanol conversion and determine the thermodynamically favorable operating conditions. Various commercial catalysts were characterized and screened for the reaction in exam in a down-flow, stainless steel fixed-bed reactor under pressure. The effects of temperature, pressure, residence time, and feed hydrogen partial pressure on ethanol conversion and product composition were determined.

Several kinetic models have been derived to describe the behavior of the reaction. On the basis of an empirical power law kinetic model a plant hypothesis has been finally realized. Finally an overall process simulation, made in ChemCAD, was used as a base for the sizing of the different units. The study shows the possibility to realize a plant to produce ethyl acetate and pure hydrogen by ethanol dehydrogenation. The plant capacity is of about 160 kton/year and by assuming an activity of 8000 hours/years. The hourly productivity is for ethylacetate of about 21 t/h and for hydrogen of 1 t/hour. An ethanol fed of 23 t/h is assumed.

SECTION B

Chapter 1

Background info Literature Review

B-1.1 Introduction

The first chapter of the section B is entirely dedicated to furnish a general background of the actually operative processes of production of the ethyl acetate by ethanol. In forecasting of the next future large supply of bioethanol, due to the use and the processing of cellulosic residues, new alternative processes able to produce commodities chemicals should be realized. Thus, taking in account this future large availability of bioethanol, the use of ethanol as feedstock for the chemical industry can also be foreseen. As well known the ethyl acetate is an industrially important high commodities chemical, alternative to the aromatics compounds, used primarily as a solvent in the paints, coatings, and inks industries. Actually it is produced commercially by classical routes such as the (i) esterification of ethanol by acetic acid [1], (ii) addition of ethane to acetic acid [2], or (iii) the dimerization of ethanol over alkaline solids by the Tischenko reaction. The use of acetic acid or acetaldehyde, respectively corrosive and toxic materials, has required the necessity to develop new processes at low environmental impact and characterized by low cost of maintenance. At this purpose a new process has been commercialized in which ethyl ethanoate can be synthesized without the need of acetic acid or ethanol, which consists of a one-step ethanol dehydrogenation reaction [3]. The scope of this chapter is to have a more detailed point of view about the advantages and disadvantages of the classical routes

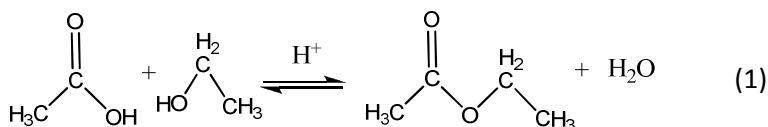
to produce this chemical with the aim to improve and develop in our research alternative, economically and at low impact ways of production.

B-1.2 Classical routes to produce ethyl acetate

Actually the commercial production of ethyl acetate is realized almost exclusively by esterification of acetic acid with ethanol. On the other hand several new technologies have been commercialized such as BP's new Avada process, employed in a new plant at Hull, UK, that uses ethylene and acetic acid with solid acid catalyst. Ethyl acetate is also produced as a by-product in the liquid phase oxidation of n-butane. In general the industrial processes related to the ethyl acetate production could be, thus, classify as follow:

1. *The Fisher esterification of acetic acid with ethanol [4,5].*
2. *Oxidation of ethanol*
3. *The oxidation of the ethylene to acetaldehyde and the Hoechst process based on Tischenko reaction [6,7].*
4. *Ethylene esterification with acetic acid [8].*
5. *Oxidative dehydrogenation reaction*
6. *One-step liquid phase esterification process over copper –based catalysts developed by Kvaerner-Technology Ltd.*

The acetic acid esterification with ethanol is a reversible reaction that occurs in presence of a homogeneous catalyst based on sulphuric acid as represented by the following reaction.



The use of acetic acid causes apparatus corrosion and consequently an increase of the total cost of the process of production. On the other

hand, although Tishchenko reaction uses only one feed and it involves a non-corrosive chemical, it is not considered as a green process due to the difficult of handling of acetaldehyde, considered a toxic chemical. Moreover, another aspect that absolutely should not be neglected is correlated to water production, which should be removed during the reaction because its presence could favor the shift of the reaction equilibrium to the formation of acetic acid rather than ethylacetate. In such circumstances, an *improved process* of ethyl acetate production is strongly desired and required by the industrial sectors.

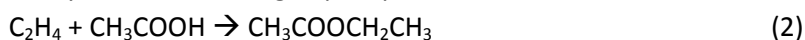
An alternative process consists of two different phases: an oxidation of the ethylene to acetaldehyde (Wacker) catalyzed by a palladium based catalyst and a condensation of acetaldehyde to ethyl acetate (Tischenko), by using a homogeneous catalyst of aluminium alkoxide. The use of homogeneous catalysts is not advantageous and the development of an alternative heterogeneous system could represent a solution to this aspect. Although the cationic exchange resins can solve both of these problems, this catalyst has a poor resistance to heating and could deactivate during the reaction. Another important drawback of this reaction is related to the thermodynamic limitations; in fact the overall yield to ethyl acetate is typically within 67% with equimolar reactants. The necessary separation processes, of ternary mixture ethanol-ethylacetate-water, involves high energetic consumption.

An example of *oxidation reaction* has been reported in the U.S.Pat.No 5,770,761[9]. In this work the oxidation of liquid ethanol in the presence of excess liquid ethanol and supported oxidation catalyst provided a one-step process for the production of ethyl acetate. During the reaction, the ethanol acid produced in the oxidation is adsorbed by the excess liquid ethanol which esterifies to ethylacetate. In more detail the first part of the process is the partial oxidation of

the acetic acid by air while the second step is the esterification of acetic acid with ethanol. The oxidation portion of the process is preferred with a metallic oxidation catalyst on a hydrophobic support such as Pd/C and the esterification portion with acidic solid ion exchange resin (amberlyst 15) to promote the esterification. This type of reaction is generally performed in a trickle bed reactor design[11]. Lemaski et al. [11] used this process with a multi-component catalysts consisting of Pd, Ti, and P ($\text{Pd}_a\text{M}_b\text{TiP}_c\text{O}_x$) where M is selected from Cd, Au, Zn, Tl, alkali metals and alkaline earth metals. In this process a mixture of acetic acid and ethyl acetate has been obtained.

Sano [12] also proposed that Pd supported on SiO_2 with some promoters, as for instance, W and Zn, is also able to generate ethyl acetate and acetic acid. Moreover, a Pd/ SiO_2 catalyst prepared by ionic exchange was also considered for the synthesis of ethyl acetate from ethanol by Appel et al. [13]. The results from the latter showed that high selectivity to acetate (70%) can be achieved at low ethanol conversions (50%). However, this process still showed some amount of acetic acid (30% selectivity). In the scientific literature, only two contributions, both using the liquid phase reaction and the oxidation process, can be quoted [14,15]. The first one employed a styrene-divinylbenzene copolymer (SDB) as support for the Pd catalyst that generated ethyl acetate and also acetic acid. The selectivities were similar to those of Pd/ SiO_2 . However, during the reaction, deterioration of the catalytic performance was observed and it was verified that it was mainly caused by the leaching of the Pd metal. The second one, by Jørgensen et al.[15], who used gold catalysts, synthesized acetic acid and also ethyl acetate. They showed that gold catalysts can be very active and selective to acetic acid. However, according to these same authors these catalysts should be improved as regard to acetate selectivity. Acetaldehyde, acetic acid and CO_2 are the main byproducts of the oxidation process.

Therefore, the purification procedures are straightforward and not expensive, and moreover the catalyst is very stable. However, due to the flammability and explosive limits of the ethanol/O₂ mixture, the oxidation process must be carried out using ethanol diluted in air, implying that high yields of ethyl acetate must be achieved. All in all, this contribution aims at further studying the oxidation of ethanol to ethyl acetate using PdO/SiO₂ catalysts. Anyway the main drawback of the oxidative process is the formation of high quantity of acetic acid [16]. The main inconvenient of this process is related to the necessity to perform the reaction in two different steps that cause the increase of the total cost of the process. One attempt to solve this inconvenient is by reacting of an aldehyde and an alcohol in presence of oxygen as described by Yan et al. [17]. In this case a bifunctional catalyst consisting of a metal as palladium supported on a zeolites acidic support, has been employed. These bifunctional catalysts are characterized by highly dispersed metals on adequate acid supports [18,19]. The palladium supported on zeolites or co-polymers of SDB (styrene-divinilbenzene) are considered very promising to realize this reaction [20]. The Hoechst process is based on the acetaldehyde condensation represented by Tischenko reaction, performed by using an aluminium alkoxides catalyst [21]. The Tischenko reaction is a dimerization of an aldehyde forming an ester, and catalyzed by solid base catalysts such as MgO, CaO, SrO under mild conditions. The main drawback is strictly related to the exothermic nature of the reaction and as consequence an intensive cooling is required. This process is complicated in operation procedures and equipment for the processing steps. The esterification of acetic acid with ethylene [22] is a further alternative to the ethyl acetate production. The reaction, as illustrated, is promoted by heterogeneous supported heteropoly acid catalysts such as a tungstophosphoric acid H₄SiW₁₂O₄₀.



Although the promising yields to desired reaction product, the necessity to use raw renewable materials, easy to handling and with low environmental and healthy impact is the main challenge.

A survey of the patent literature shows that it is possible to synthesize ethyl acetate from ethanol using an oxidative route, i.e., using ethanol in the presence of oxygen[23].The acetaldehyde was easily formed by oxidative dehydrogenation and reacted further with residual ethanol and oxygen to produce esters.

The common catalytic system employed to perform this reaction are mixed oxide metals such as of SiO_2 , TiO_2 , Fe_2O_3 , Fe_3O_4 , CaO , Bi_2O_3 , MoO_3 . Several works have shown the performances of these catalysts in the ODH reaction [24]. As reported by Idriss et al. [25] the mixed metals oxide and in particular Fe_2O_3 has a relatively high selectivity to ethyl acetate (about 40%), that decrease with the temperature of reaction in favor of the acetaldehyde production.

The great innovation is represented by Davy Process Technology (formerly Kvaerner) has licensed its ethanol-based process to Sasol. The main peculiarity of this process is the direct ethanol dehydrogenated to form ethyl acetate.

B-1.3 Innovative Route: Ethanol dehydrogenation

B-1.3.1 Introduction

The dehydrogenation reaction by using a single renewable feedstock, bio-ethanol, allows significant production cost benefits over other technologies. The elimination of acetic acid as a feedstock allows for lower grade materials of construction thereby reducing investment and maintenance costs. At this purpose Nguyen et al. [26] on the basis of a commercial process simulator, aspen plus, has modeled and calculated the mass and heat balance of the alternative processes, based on which production cost is evaluated. These processes are

designed to produce ethyl acetate with purity 99.95 wt% and productivity 100,000 tons/year.

Ethanol, as a renewable fuel, is playing an increasingly important role in both chemical and energy industries. Its mixture with water can be easily produced via fermentation of renewable sources such as corn, cane, fast-growing plants, or biomass waste. This product, containing up to 20% of ethanol, is then refined and can be used either as alternative fuel or a precursor in the synthesis of many important industrial chemicals. In the 2001 Davy techn, have developed a new process based on ethanol as unique raw material to produce in particular ethyl acetate. The great inconvenient of this process is related to the relatively low selectivity, during the dehydrogenation step, to the desired product of reaction. For this reason the process is equipped with an hydrogenation reactor to convert successively by-products, aldehydes and ketones, to corresponding alcohols, facilitating the purification of the target product. A schematic representation of this process is reported in Figure 1.

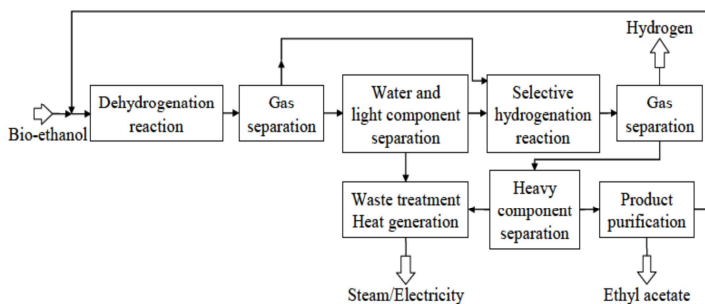


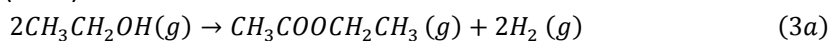
Figure 1: Ethanol dehydrogenation to ethyl acetate

Another aspect to take in account is that more recently, the importance of ethanol dehydrogenation as a source of hydrogen for fuel applications was recognized [27]. Our interest is focused on the identification of an active, selective and stable catalyst system as well

as the optimum conditions at which the production of hydrogen and ethyl acetate will be maximized and secondary reactions suppressed. At this purpose an in-depth study has been realized and considered further in the text in terms of the catalyst composition (nature of active metal phase, effect of promoters and supports, and effect of deposition techniques), reaction temperature and pressure, residence time, and feed composition.

B-1.3.2 Desiderable main reaction

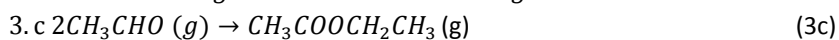
Ethanol dehydrogenation is a relatively fast endothermic reaction occurring at temperatures higher than 100°C. One mole of hydrogen is released per mole of ethanol reacted. The Acetaldehyde is the second main product, which can be separated by condensation (b.p. 21°C, at atmospheric pressure) and theoretically 100% pure hydrogen can thus be produced. The Ethyl acetate can be subsequently formed through different reaction pathways, with overall pathways as listed below (3.a-c).



$$\Delta H_{298K}^0 = 26.70 \frac{KJ}{gmol} \quad \Delta G_{298K}^0 = 9.16 \frac{KJ}{gmol}$$



$$\Delta H_{298K}^0 = -41.75 \frac{KJ}{gmol} \quad \Delta G_{298K}^0 = -25.82 \frac{KJ}{gmol}$$



$$\Delta H_{298K}^0 = -110.02 \frac{KJ}{gmol} \quad \Delta G_{298K}^0 = -60.80 \frac{KJ}{gmol}$$

Most authors[28-31] agree that its formation is enhanced by increasing residence times and ethanol conversions and by decreasing temperatures, because ethyl acetate is thermodynamically favored over acetaldehyde up to 200°C. In addition, ethyl acetate formation can be enhanced by increasing the size of the active metal particles on

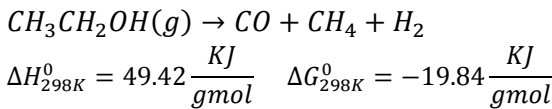
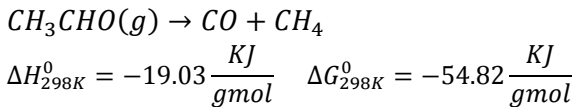
the catalyst surface [32]. In general one aspect to take in account that represent the main drawbacks of this reaction, is the poor selectivity to ethyl acetate caused by the several secondary reactions that can be divided into four main groups:

1. Acetaldehyde condensation reactions – main products of these reactions are generally higher C_3 and C_4 species, such as alcohols, aldehydes, ketones, acids and their esters.
2. Ethanol dehydration – main products are ethylene, ethane, diethyl ether and water.
3. Ethanol and acetaldehyde decomposition reactions – main products are simple C_1 species such as CO, CO_2 and CH_4 .
4. Fischer-Tropsch synthesis – syngas mixture in the second step of the cycle is commonly used for production of various hydrocarbons.
5. Ethyl acetate reaction with water to produce acetic acid [30].

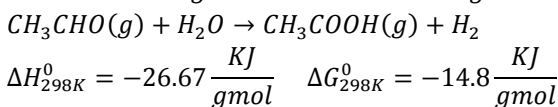
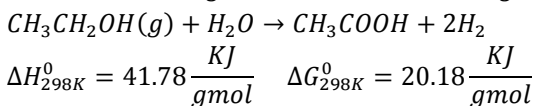
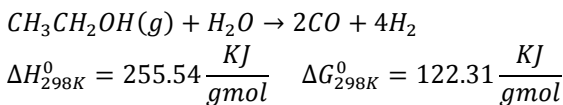
Finally the ethanol dehydration is also highly undesirable since the dehydration products can serve as precursors to coke formation, thus deactivating the catalyst.

A possible scheme of the main side reaction has been proposed by Inui et al [33] and reported in Figure 2.

Ethanol can undergo dehydration to diethyl ether (DEE) or ethylene which can polymerize on the catalyst surface and form carbon deposits. Dehydration has usually high activation energy and, therefore, is favored by high temperatures. For example, Freni et al [27] reported that, under his conditions, ethylene formation occurred on copper catalysts only at temperatures exceeding 500°C. Both ethylene and DEE formation are catalyzed by acidic sites present on the support, e.g., Al₂O₃. Thus, Iwasa and Takezawa (1991) detected DEE formation on supports with strong acidic sites.



Steam reforming of ethanol is a highly endothermic reaction resulting in conversion of ethanol to hydrogen and a mixture of CO₂ and CO. The reaction is not thermodynamically favorable below 327°C. As reported Isawa et al³³ [33], the selectivity to acetic acid increases by increasing ethanol conversion and residence time. The same authors reported that steam reforming of acetaldehyde also resulted in a mixture of acetic acid and hydrogen.



Nevertheless, the extent of the decomposition side-reactions can be significantly reduced by the choice of catalyst. For example, as early as 1920, Armstrong [34] compared two common active metals, Ni and Cu, in both ethanol dehydrogenation and acetaldehyde hydrogenation, and found Cu incapable of splitting the C-C bond. Therefore, by using copper catalyst supported on appropriate support and running the reactions at mild temperatures in order to avoid thermal decomposition, the extent of decomposing and reforming reactions should be minimized, preferably to virtually 0%. Mixtures of carbon monoxide and hydrogen can be used for the production of a large variety of organic compounds. The product distribution is affected mainly by reaction conditions and type of catalyst. Copper catalysts, especially when mixed with ZnO, are commonly used for methanol synthesis.

B-1.3.3 Active phases: employed catalysts

The choosing of an adequate active phase is fundamental to obtain high yields in ethyl acetate. Several processes illustrate the ethanol dehydrogenation to esters but selectivity to ethyl acetate is not sufficiently high to obtain a final product that not requires further steps of purification. Several studies have shown that the most popular metal used for selective dehydrogenation of alcohols to aldehydes or ketones is copper, mainly because of its ability to dehydrogenate ethanol without splitting the C-C bond, which would lead to the undesirable decomposition of acetaldehyde to CH₄ and CO. Various studies [36,37] have shown that it is metallic Cu⁰ formed by reduction of CuO, which acts as an active phase in dehydrogenation. Other alternatives to Cu, includes Pt, Pd, Cr, Cd, Ni, Fe, Mn, Co, Zn, Zr and Ru. For example the US patent 4,052,424 describes the esters production by ethanol vaporization on silver-cadmium alloy catalyst. Summerville et al. [38] has shown the

possibility to produce esters involving a mixture of alcohols and aldehydes in vapor phase with a reduced silver-cadmium-zinc-zirconium catalyst composition. Sanchez et al. [39] has shown the direct transformation of ethanol to ethyl acetate over supported palladium catalysts with low palladium content (1%, w/wPd) at 1 MPa pressure. In particular the effect of the used supports, such as SiO₂, Al₂O₃, ZnO, SnO₂ and WO₃-ZrO₂ (29%, w/w WO₃) on the catalytic performances has been studied. By using palladium (1_wt%) supported catalyst in the dehydrogenative process that the support changes the catalytic behavior. They verified that palladium supported on SnO₂ and ZnO are the most selective catalysts for the ethyl acetate synthesis. which can easily lead to alloyed palladium phases.

As matter of fact the necessity to individuate a stable and highly selective catalytic system, is correlated to the difficulty to separate the ethyl acetate by the several by-products derived by the acetaldehyde condensation reaction such as the methyl ethyl ketone (MEK). The MEK in the products gets a serious problem in the purification of ethyl acetate due to its formation of azeotropic mixture with ethanol. At this purpose no one of the alternative phases above proposed, has matched the selectivity obtained with copper catalysts. But on the other hand Cu suffers of poor stability at high temperatures, where dehydrogenation is thermodynamically favorable. Nevertheless, several studies about the performance of copper catalysts are reported in literature with the aim to individuate adequate structural promoters that favor the ethyl acetate formation and able to improve the thermal and mechanical stability of the copper phase. The use of copper based catalysts for the alcohols dehydrogenation to esters has been reported in several literature works. The formation of ethyl acetate from ethanol over a heterogeneous catalyst such as Raney copper was reported in 1953. After the discovery, some researchers reported the formation of ethyl acetate from ethanol over various

copper catalysts. Catalysts such as pure Cu, Cu-Al-Zn-O, and Cu-Zr-O have the ability to form ethyl acetate from ethanol. The selectivity to ethyl acetate is at most 56% under atmospheric pressure. In particular Isawa⁴⁹ et al have studied the performances of several copper based catalysts on supported on SiO₂, ZrO₂, Al₂O₃, MgO and ZnO. The use of supports has a significantly influence on the final product selectivity. As shown the Cu/ZrO₂ and Cu/ZnO are highly selective for ethyl acetate production while C₄-species are produced appreciably on the acidic sites of Cu-Al₂O₃. On the other hand, Menon et al have studied the performances of Cu-Al₂O₃ catalyst and demonstrated that no ester is obtained when copper or alumina alone is used as a catalyst, or when they are used separately in two reactors connected in series, but even a mechanical mixture of copper and alumina gives a good yield of the ester. Bolt et al [45] has shown the possibility to dehydrogenate alcohol fractions in the C₃ and C₄ alcohol boiling ranges to determine whether the process would be suitable to produce different types of oxygenated compounds (esters and ketones), which could find application as solvents. The reaction was conducted in the presence of a Cu/Zn/Al₂O₃. More specifically Inui et al. [33,46,47] have studied the dehydrogenative process using Cu/ZnO/Al₂O₃/ZrO₂ by investigating the catalytic performances also under high pressure conditions. The main aim of the Inui research is to investigate the effect of additive metal like oxides as Al₂O₃, ZnO, and ZrO₂, which are effective supports for the Cu catalyst, on the ethyl acetate production in the process of dehydrogenative dimerization of ethanol, to improve the selectivity to ethyl acetate. As showed by Inui et al. the pure copper catalyst gives low conversion of ethanol; selectivity to ethyl acetate is very low and the major product is acetaldehyde. The dehydrogenation is an equilibrium reaction and at a temperature of almost 260°C the ethanol conversion is about 35% at 533 K. It is reasonable that the low conversion is limited by the equilibrium between ethanol and

acetaldehyde because the pure copper catalyst has low ability for ester formation. The addition of ZnO into the pure copper catalyst has no significant effect on the catalytic reaction while including Al_2O_3 the conversion of ethanol and moderately also the selectivity to ethyl acetate can be promoted. A metal quaternary system of Cu-Zn-Zr-Al-O has shown high performances, with an evident reduction of the MEK. The addition of ZrO_2 to copper greatly increases the yield of ethyl acetate. ZrO_2 component is essential to the efficient ethyl acetate formation. The addition of Al_2O_3 increases the dehydrogenation ability of Cu and the yield of ethyl acetate, due to the decreased size of CuO particles.

Since the dehydration reaction of acetaldol occurs over acidic surfaces, the surface acidity of the catalyst probably decreases by increasing the Cu content. This behavior has been confirmed by the Iwasa and Takezawa reporting that the doping of KOH on a Cu/ Al_2O_3 catalyst decreased the formation of C_4 -species such as butanal, MEK, and 1-butanone [48]. They concluded that the C_4 -species were produced by acid-catalyzed reaction. Judging from the results of the treatment with K_2CO_3 solution after and before reduction, the post-treatment affects the acid–base sites that formed after reduction. Especially, the alkaline treatment suppresses the formation of methylethylcheton (MEK. This result is probably caused by masking of surface acid sites, and the treatment decreases the dehydration ability. This assumption is supported by complete suppression of DEE formation in the alkaline treatment. In the dehydrogenative dimerization of ethanol, we can summarize the roles of acid sites on the metal oxide surface, which are to: (a) assist the formation of ethyl acetate via hemiacetal (b) promote the aldol addition, which may be deactivated by all the alkaline treatments, and (c) perform the dehydration of alcohols. Appel et al.[49,50] have studied the synthesis of ethyl acetate by ethanol dehydrogenation at atmospheric pressure from ethanol working with

physical mixtures or by using a double bed reactor (Cu/ZnO/Al₂O₃ + ZrO₂) and suggested that: firstly, acetaldehyde is generated on the Cu/ZnO/Al₂O₃ catalyst; then it migrates towards the oxide (spillover) and reacts with ethanol or ethoxide species generating hemiacetal, which is then dehydrogenated producing ethylacetate. In more details these authors have studied the properties of a commercial Cu/ZnO/Al₂O₃ mixed physically with ZrO₂ (monoclinic), CeO₂, Al₂O₃ and SiO₂.

By using a physical mixture of Cu-Zn-Al and ZrO₂ displays the highest selectivity towards ethyl acetate and the lowest to acetaldehyde. Another important effect should be noticed by this work is that the catalysts of Cu-Zn-Al-O physically mixed with ZrO₂, that has shown the high yield to Ethyl acetate, has an higher ethanol consumption rate ($\text{mmol}_{\text{EtOH}}/\text{g}_{\text{cat}}\cdot\text{min}^{-1}$). In matter of fact, taking in account the thermodynamic study related to the dehydrogenation of ethanol to acetaldehyde, it is possible conclude that by using exclusively Cu-Zn-Al-O the ethanol conversion results are closed to the thermodynamic equilibrium. By using a promoter, the ethyl acetate and condensation reactions are favored and consequently the equilibrium of dehydrogenation is shifted. By using a double catalytic bed the selectivities to ethyl acetate are much lower and to acetaldehyde higher. The ethanol consumption rates of the double bed reactors are low and similar to the ones observed for Cu-Zn-Al-O. This behavior is due to the possible re-adsorption of acetaldehyde or ethanol on the oxide bed. The same work shows moreover the correlation between the total number of basic sites, on a catalysts surface, and the selectivity to ethyl acetate at a conversion of about 30%. It can be verified that, as the number of basic sites increases, the selectivity increases as well.

Therefore, strong basic sites are much more relevant than medium and weak ones for the ethyl acetate synthesis. According to Inui et

al.[33], basic sites are associated to the generation of ethoxide species. Therefore, the results obtained suggest that the ethoxide formation is a very important step of the ethyl acetate synthesis and might be the rate limiting step under these conditions.

One of the main drawbacks of the copper based catalysts is related to the loss in activity of copper with time-on-stream at temperatures higher than 300°C, most likely because of copper sintering [52]. For metals, the predominant sintering mechanism in the bulk is vacancy diffusion, which suggests a relationship with cohesive energy. Hughes [53] gave the following increasing order of stability for metals:

Ag < Cu < Au < Pd < Fe < Ni < Co
< Pt < Rh < Ru < Ir < Os < Re

It is, therefore, not surprising the copper-based catalysts are more susceptible to sintering than other commonly used metallic catalysts, for example, the nickel and iron catalysts used in ammonia and hydrogen plants based on the steam reforming of hydrocarbons. This is also shown by copper's low Hüttig temperature [54], which reflects a relatively low melting point (1083°C), compared with, for example, that of iron (1535°C) and nickel (1455°C). In more detail the so-called Hüttig ($T_{\text{Hüttig}} = 0.3T_{\text{melting}}$) indicate the temperature at which sintering starts. The following semi-empirical relations for Hüttig and Tamman temperatures are more commonly used.

Therefore, copper-based catalysts have to be operated at relatively low-temperatures, usually no higher than 300°C. In more detail the catalyst deactivation at high temperatures is due to the loss of catalytic surface area by the effect of crystal growth of the catalytic phase, the loss of wash-coat area due to a collapse of pore structure, and/or chemical transformations of catalytic phases to non-catalytic phases. The first two processes are typically referred to as sintering, and the third as the solid-solid phase transition at high temperatures [55]. In the case of supported metal catalysts, reduction of the active

surface area is stimulated the agglomeration and coalescence of small metal crystallites into larger ones [56]. Two different models have been proposed for sintering i.e., the atomic migration and the crystallite migration models. As such, sintering occurs either due to metal atoms migrating from one crystallite to another via the surface or gas phase by diminishing small crystallites in size and increasing the larger ones (atomic migration model). Sintering can also occur via migration of the crystallites along the surface, followed by collision and coalescence of two crystallites (crystallite migration model). Figure 3 represents a schematic representation of atomic migration and crystallite migration models.

Many researchers focused on improving the stability by adding a textural promoter to the catalyst formula, which would act mainly as a mechanical barrier decreasing copper particle mobility. At this purpose as demonstrated by Peppley et al [57], the catalyst of $\text{Cu/ZnO/Al}_2\text{O}_3$ is prone to deactivation at operating temperatures between 220 and 260°C. The time scale for deactivation, as measured by the time for the catalyst to lose one-half its initial activity, varies considerably with temperature [58].

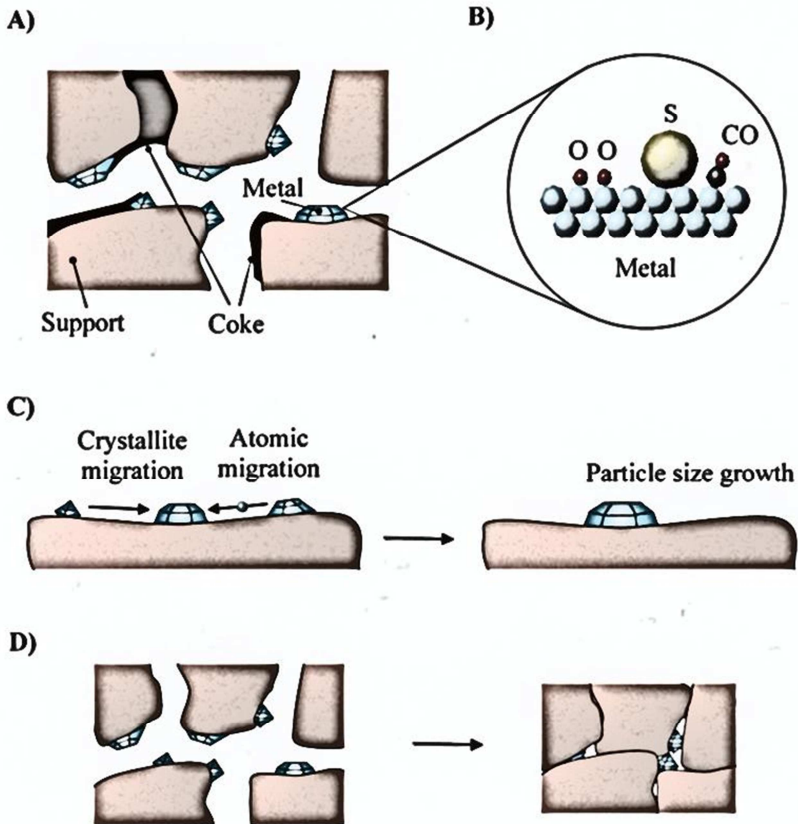


Figure 3: scheme of the sintering process

To overcome this inconvenience, a low operating temperature is necessary to slow deactivation, but this is synonymous of a lower catalyst activity so that a higher mass of catalyst is needed to improve the yield. Details of the mechanism of the thermal sintering of Cu catalysts emerged from in situ EXAFS studies [59].

The local structure of the Cu/ZnO catalyst was studied under hydrogen at elevated temperatures. The structure around the Cu atoms

assumed several forms depending on the temperature, and was best explained by assuming three structures.

1. Below 127°C, a quasi-two-dimensional layer epitaxially developed over the ZnO support.
2. Between 127°C and at least 227°C, small copper metal clusters dispersed over the ZnO.
3. At higher temperatures, large copper metal crystals dispersed on the support.

Activities in both reactions were markedly superior than those of catalysts derived from biphasic systems containing additional CuO (that is, CuO/Cu_xZn_{1-x}O). The enhanced activity in the former case was ascribed to very finely divided Cu crystallites present in intimate contact with the zinc oxide matrix. The Copper catalysts are not widely used for organic dehydrogenation reactions. In many cases, especially with hydrocarbon feedstock, thermodynamic limits on conversions [60,36] force the use of high temperature for which copper catalysts are inappropriate. The common feature of the promoters studied was their irreducibility at the dehydrogenation reaction conditions, i.e., promoters were present on the catalyst surface in the form of metal oxides. New formulations were developed containing Cr₂O₃, and later Al₂O₃, in addition to CuO and ZnO in the unreduced catalyst. The thermal stability of these catalysts was significantly higher. Chromium is known to be an effective specie for copper catalyst in the dehydrogenation reactions [60,61].

As reported by Shiao et al. [62] chromium cannot only stabilize the dispersion of copper but can also prevent copper from reacting with aluminum support to form aluminate. In this study, the addition of chromium has a similar promoting effect. However, for the electroless plated copper catalysts, the promoting extent of chromium depends not only on the chromium loading but also on the addition procedure that is reflected on the catalyst activity. The key factor for the copper

catalyst activity depends on the amount of added chromium that can penetrate into the copper layer. This is because only the penetrated chromium could play a positive promoting role to disperse the copper and consequently to enhance the reaction activity. But the copper catalyst activity is also influenced by the chromium remained on the copper surface, which, on the contrary, would play a negative role due to its occupation of some active sites on the copper surface and would cause the activity to decrease. Increasing chromium loading might also increase the amount of surface chromium for the ic-series catalysts and further decrease the catalyst activity. Church et al [63] evaluated the effect of 5-7 % addition of Cr_2O_3 , CoO , ZnO and MgO on Cu/asbestos catalyst performance. It was found that Zn and Mg alkaline oxides had a detrimental effect on the selectivity of reaction, promoting aldol condensation and thus forming undesirable higher hydrocarbons. Indeed, Cr_2O_3 is the most popular of all additives considered in the literature as a potential stabilizer. The first study about the potentiality of the copper chromite catalysts have been reported by the works of Adkins [64]. The main peculiarity of this catalyst is related to the possibility to hydrogenate aldehydes and ketones in the correspondent alcohols.

The properties and the wide application of the copper chromite based catalysts are well known. In matter of fact the copper chromite is a versatile catalyst which not only catalyzes numerous processes of commercial importance and national program related to defense and space research but also finds applications in the most concerned problem worldwide i.e. environmental pollution control. Several other very useful applications of copper chromite catalysts are in production of clean energy, drugs and agro chemicals, etc. In view of the globally increasing interest towards copper chromite catalysis, reexamination on the important applications of such catalysts and their useful preparation methods is thus the need of the time [65,66].

The main process in which the copper chromite (CuCr_2O_4) find applications as catalyst are: hydrogenation, dehydrogenation, hydrogenolysis, oxidation. Furthermore, copper chromite has been proved as promising catalyst for the production of H_2 a clean energy carrier, by conversion of alcohols [67].

The Copper chromite catalysts are often stabilized by the incorporation of barium oxide, typically about 10%, but it is not clear how this promoter functions. The activity of copper chromite catalysts is influenced by the oxidation state of Cr and Ba oxide inhibits its reduction, so stabilizing the catalysts [68]. It is also possible that BaO could influence the populations of Cu(0) and Cu(I) sites [69]. Kanoun et al. [37] tested the influence of Cr and Al oxides addition on the catalyst properties and found that Al_2O_3 increased the total catalyst surface area while Cr_2O_3 increased specific copper surface area. Cr addition also increased the activity of catalyst per copper weight. However, if activity was defined per weight of catalyst, then any addition of Al or Cr led to a decrease. The authors then concluded that Cr is a better structural promoter. By concluding the total surface area decreases with the addition of promoters in this order: $\text{Al} > \text{Cr} > \text{Zr} > \text{V} > \text{Zn}$, while metallic copper surface area, which is responsible for the activity of the catalyst decreases with the additives in the following order: $\text{Cr} > \text{V} = \text{Zr} > \text{Al} > \text{Zn}$. Cr is thus the best structural promoter and also a good stabilizer.

Tu and Chen [36] carried out series of tests on the effect of alkali metals (Na, K, Rb) and alkaline earth metals (Mg, Ca, Sr, Ba) as promoters on the performance of Cu/SiO_2 catalyst. The metal oxides of alkaline metals and alkaline earth metals did not undergo reduction at a reaction temperature of 300°C , neither did they contribute significantly to the dehydrogenation activity. While alkali metals created only slightly basic sites on the catalyst surface, all alkaline-earth metals containing catalysts, with the exception of Mg addition,

possessed both strong and weak basic sites. The presence of strong basic sites resulted in an extreme drop in activity after a short time on stream, thus deeming especially Ba and Sr as poor promoters. MgO proved to be the most stable among alkaline earth oxides, but even this additive did not prevent the catalyst from losing 20% of its initial activity after just 4 h on stream. Among the alkali metals, a K-doped catalyst displayed the highest resistance to sintering, losing only 8% of its activity after 4 h on stream. Thus, K was identified as the best promoter out of all metals tested, even though the initial ethanol conversion was 2% lower (68%) than the highest conversion obtained with a MgO promoter (70%). However, it is rather difficult to compare the effects of various promoters, because of different conditions used by researchers, there seems to be a general agreement, throughout the literature, that the best promoter is Cr₂O₃. At this purpose, the Kvaerner process technology announced a new ethyl acetate production process by using a commercial Cu-Cr-O catalyst, whereas space-time yield (STY) of ethyl acetate is not so high: ethanol conversion, 27.9%; selectivity to ethyl acetate, 94.6% at 496K and 2.86MPa [70]. Moreover in the open literature there are some contributions related to this technology, as for instance, the work published by Colley et al. [71] using Cu/Cr₂O₃.

B-1.3.4 Operative conditions

The individuation of the best operative conditions in terms of temperature, pressure, and residence time and feedstock composition is fundamental to obtain the desired results of activity and selectivity.

In this particular case the individuation of the best temperature of reaction is correlated with the enthalpy of formation of the ethyl acetate. At this purpose, as already reported, the ethanol dehydrogenation to ethyl acetate is a partially endothermic reaction. The temperatures of reaction to improve the yield to ethyl acetate

should not particularly high and a range of 200-300°C could represent a good compromise. The choice of the temperature of reaction is also limited by the nature of active phase, in matter of fact the copper based catalysts are subjected to a rapid deactivation most likely because of sintering phenomena at temperature higher than 300°C. Another important aspect to take in account is the operating pressure. Elementary reactions in the process are divided into three types: (a) reactions preferred by high pressure, (b) reactions preferred by low pressure, and (c) reactions that do not depend on pressure. The dehydrogenative dimerization of ethanol to ethyl acetate is a combination of dehydrogenation, which is preferred by low pressure, and dimerization, which is preferred by high pressure.

In particular the acetaldehyde formation is favored at low pressure (1 atm) as suggested by the Le Chatelier's principle. Moreover, in this case, in great part of the research literature works the use of diluted feedstock is necessary to further decrease the partial pressure of ethanol. In particular several works demonstrate the necessity to use high pressure of reaction to favor the esters formation [46,73]. In particular the experimental runs obtained operating at different temperatures and at different pressure shown a decrease of the equilibrium conversion with the increase of the reaction pressure. High-pressure operation suppresses both the ethanol conversion and the formation of by-products such as butanone and 1-butanol, derived from acetaldehyde, which can be rationalized by the decrease in the partial pressure of acetaldehyde caused by a shift in equilibrium among ethanol, acetaldehyde, and hydrogen at high pressure. Consequently, a high selectivity to ethyl acetate is achieved by suppressing the acetaldehyde partial pressure in the initial elementary reaction rather than by suppressing each elementary reaction for the by-products.

The formation of ethyl acetate proceeds stepwise via acetaldehyde, which is an intermediate. Inui et al.[33] has reported that the dehydrogenation step is not a rate-determining step in the formation of ethyl acetate from ethanol, because the product distribution in the reaction of acetaldehyde in H₂ flow is similar to that observed in the reaction of ethanol. The ethyl acetate could be formed by two different possible routes:

1. the Tishchenko reaction that consist into the coupling of acetaldehyde.
2. dehydrogenation followed by addition of ethanol to acetaldehyde.

In the formation of ethyl acetate from ethanol, the stepwise reaction requires a prolonged contact time, whereas much longer contact times cause by-products to form. When acetaldehyde has a high partial pressure in the reactor, an acetaldehyde molecule reacts with another acetaldehyde molecule to form acetaldol through aldol addition. The residence time affects both the conversion of ethanol and the composition of the outlet stream. Several authors [38] reported an increase in conversion with increasing residence time. However, the higher the contact time, the lower the selectivity towards acetaldehyde, which is subject to subsequent reactions¹. Generally, it is rather difficult to extract information on residence time from different articles, because of a non-uniform nomenclature as well as the omission of the values for catalyst loadings and/or feed flow rates. It is also questionable whether the W/F (mass of catalyst/active phase to gas feed rate) ratio should be based on the amount of catalyst or active phase. Another important factor, to take in account, for the necessity to individuate the effect of the water in the feedstock, which can have a side-effect on the purity of the final reaction products. The use of high residence time and of feed stocks contained water could enhance the formation of acetic acid, another undesirable product of

reaction. Similarly, Marino et al. [73] observed that the presence of water improved acetaldehyde and hydrogen selectivities. Water, as well as hydrogen, improved the stability of the catalyst but slightly decreased the conversion of ethanol by 2-3%. On the other hand, the presence of even small amount of acetaldehyde (acetaldehyde/ethanol = 0.1) in an inlet stream had a more detrimental effect, lowering the conversion by 4-6% depending on reaction temperature and feed composition.

B-1.4 Hydrogen production by ethanol dehydrogenation

The use of bioethanol for hydrogen production is a very promising way allowing to produce hydrogen from renewable sources. Several approaches for the development of a reliable method of hydrogen production from bioethanol have been proposed recently [74].

Dolgykh et al. [75] have shown the results of hydrogen productivity by testing the catalytic activity of dehydrogenation industrial catalysts in the process of hydrogen production by steam reforming of bioethanol. In this study a range of hydrogen productivity of 5-25 $\text{g}_{\text{H}_2}\text{Kg}_{\text{cat}}^{-1}\text{h}^{-1}$ has been obtained by operating in a range of temperature of 200-300°C, of ethanol residence time of 1.8-2.5 $\text{g}_{\text{cat}}\text{h mol}^{-1}$ and by using a molar ratio $\text{C}_2\text{H}_5\text{OH} : \text{H}_2\text{O} : \text{N}_2 = 1 : 18.5 : 17.5$. The use of dehydrogenating catalysts is advantageous to limits the decomposition of acetaldehyde, that is in this case the main product containing carbon, to CO-CO₂-H₂O.

B-1.5 References

- [1]G. Hangx, G. Kwant, H. Maessen, P. Markusse and I. Urseanu, 1999, Project No. GRD1 CT1999 10596.
- [2]W. Fullerton and J. A. Miller, 2007, US Patent No.2007/0255072 A1.
- [3]W. S. Colley, R. C. Fawcett, C. Rathmell, and M. W. M. Tuck, 2004, Process for the Preparation of Ethyl Acetate, US Patent No. 6 809 217 B1

- [4]K. Weissermel, H.-J. Arpe, Industrielle Organische Chemie, Bedeutende Vor- und Zwischenprodukte, 4th Edition, Verlagsgesellschaft, 1994.
- [5]J.A. Monick, Alcohols, Vol. 19, Reinhold Book Corporation, New York, 1968, p. 45.
- [6]J. March, Advanced Organic Chemistry, Reactions, Mechanism, and Structure, 4th Edition, Wiley, New York, 1992.
- [7]Y. Ogata, A. Kawasaki, Tetrahedron 26 (1969) 929].
- [8]T. Sato, T. Hagiwara, Tokuyama Sekiyu Kagaku K.K. Jpn. Kokai Tokkyo Koho JP11,140,017 (1999). [9]U.S.Pat.No 5,770,761
- [10]PCT WO 98/21173, LIN, Tzong-Bin et al.
- [11]M.F. Lemanski, J.B. Hazen, P.R. Blum, BR9105300-A, JP4300851-A (1992), The Standart Oil Company.
- [12]K. Sano, US 2003/0092936 A1 (2002), Showa Denko K.K.
- [13]L.G. Appel, R.M.S. Ramos, E.K. Libergott, S.E.C. Pereira, V.C. Almeida, BR 91 04562 (2000), Instituto Nacional de Tecnologia.
- [14]T. Lin, D. Chung, J.R. Chang, Ind. Eng. Chem. Res. 38 (1999) 1271.
- [15]B. Jørgensen, S.E. Christiansen, M.L.D. Thomsen, C.H. Christensen, J. Catal. 251 (2) (2007) 332.
- [16]A.B. Gaspar, A.M.L. Esteves, F.M.T. Mendes, F.G. Barbosa, L.G. Appel, Applied Catalysis A: General 363 (2009) 109–114.
- [17]US patent 6,399,812.
- [18]Y. Yan et al. production of aliphatic esters United States Patent 6,399,812 B1 (2002).
- [19]Lin et al. process for ethyl acetate production, United States Patent 5,770,761.
- [20]J.F. Lee, F.S. Zheng and J.R. Chang, J. Phys. Chem. B 2001, 105, 3400-404.
- [21]Wright, Jr. et al. US Patent n.3,714,236 .
- [22]US. patent n.4,275,228; U.S. patent n. 5,241,106] [PCT WO 2005/110966 A1.
- [23]T. Mallat and A. Baiker, Chem. Rev. 2004, 104, 3037-3058]
- [24]L. Wang, K. Eguchi, H. Arai and T. Seiyama chemistry letters pp.1173-1176, 1986]
- [25]H. Idriess, G. Seebauer Journal of molecular catalysis 152 (2000) 201-212]

- [26]Thuy Nguyena, Yasunori Kikuchia, Masaru Nodab, Hirokazu Sugiyamac and Masahiko Hiraoa- 20th European Symposium on Computer Aided Process Engineering – ESCAPE20 S. Pierucci and G. Buzzi Ferraris (Editors)]
- [27]Freni,S., Mondello,N., Cavallaro,S., Cacciola,G., Parmon,V.N. & Sobyanin,V.A. Hydrogen production by steam reforming of ethanol: A Two Step Process. *Reaction Kinetics and Catalysis Letters* **71**, 143-152 (2000).
- [28]Franckaerts,J. & Froment,G.F. Kinetic study of the dehydrogenation of ethanol. *Chemical Engineering Science* **19**, 807-818 (1964).
- [29] Fujita,S.I., Iwasa,N., Tani,H., Nomura,W., Arai,M. & Takezawa,N. Dehydrogenation of ethanol over Cu/ZnO catalysts prepared from various coprecipitated precursors. *Reaction Kinetics and Catalysis Letters* **73**, 367-372 (2001).
- [30]Iwasa,N. & Takezawa,N. Reforming of ethanol - dehydrogenation to ethyl acetate and steam reforming to acetic acid over copper-based catalysts -. *Bulletin of the Chemical Society of Japan* **64**, 2619-2623 (1991).
- [31] Raich,B.A. & Foley,H.C. Ethanol dehydrogenation with a palladium membrane reactor: An alternative to Wacker chemistry. *Industrial and Engineering Chemistry Research* **37**, 3888-3895 (1998).
- [32]Kenvin,J.C. & White,M.G. Supported catalysts prepared from mononuclear copper complexes: Catalytic properties. *Journal of Catalysis* **135**, 81-91 (1992).
- [33]Inui,K., Kurabayashi,T., Sato,S. & Ichikawa,N. Effective formation of ethyl acetate from ethanol over Cu-Zn-Zr-Al-O catalyst. *Journal of Molecular Catalysis A: Chemical* **216**, 147-156 (2004).
- [34]Armstrong,E.F. & Hilditch,T.P. A study of catalytic action at solid surfaces. III. the hydrogenation of acetaldehyde and the dehydrogenation of ethyl alcohol in presence of finely-divided metals. *Proceedings of the Royal Society of London.Series A, Containing Papers of a Methemathical and Physical Character* **97**,259-264 (1920)
- [35]Davidson,J.M., McGregor,C.M. & Doraiswamy,L.K. Mechanism of palladium-catalyzed decomposition of ethanol-a comparison of

- chemical kinetic and surface science studies. *Industrial and Engineering Chemistry Research* **40**, 108-113 (2001b).
- [36]Tu, Y.-J., Li, C. & Chen, Y.-W. Effects of chromium promoter on copper catalysts in ethanoldehydrogenation. *Journal of Chemical Technology and Biotechnology* **59**, 141-147 (1994b).
- [37]Kanoun, N., Astier, M.P. & Pajonk, G.M. Dehydrogenation of ethanol and CO₂-H₂ conversion on newcoprecipitated Cu/Cr-Al catalysts. *Journal of Molecular Catalysis* **79**, 217-228 (1993)
- [38]US patent 4,440,946 Apr.3, 1984
- [39]Adriana Bonilla Sanchez, Narcis Homs, J.L.G. Fierro, Pilar Ramí rez de la Piscina, *Catalysis Today* 107–108 (2005) 431–435
- [40]J. Deschamps, *Compt. Rend.* (1953) 1285.]
- [41]K. Takeshita, S. Nakamura, K. Kawamoto, *Bull. Chem. Soc. Jpn.* 51 (1978) 2622.
- [42]D.J. Elliot, F. Pennella, *J. Catal.* 119 (1989) 359.]
- [43]N. Iwasa, N. Takezawa, *Bull. Chem. Soc. Jpn.* 64 (1991) 2619]
- [44]P. G. MENON AND J. PRASAD *JOURNAL OF CATALYSIS* 17, 23&244 (1970)
- [45]F. H. A. Bolder *Ind. Eng. Chem. Res.* 2008, 47, 7496–7500]
- [46]K.Inui, T.Kubabashi, S.Sato, *Journal of Catalysis* 212, 207–215 (2002)]
- [47]K.Inui, T.Kubabashi, S.Sato *Applied Catalysis A: General* 237 (2002) 53–
- [48]N. Iwasa, N. Takezawa, *Bull. Chem. Soc. Jpn.* 64 (1991) 2619]
- [49]A.B. Gaspar, F.G. Barbosa, S. Letichevsky, L.G. Appel, *Appl. Catal. A* 380 (2010) 113–117]
- [50]P.C.Zonetti, J.Celnik, S.L.Alexandre B.Gaspar, L.G.Appel* *Journal of Molecular Catalysis A: Chemical* xxx (2010) xxx–xxx]
- [51]W. Dai, L. Ren, in: G. Ertl, H. Knozinger, F. Schuth, J. Weitkamp (Eds.), *Handbook of Heterogeneous Catalysis*, vol. 7, 2nd ed., Wiley-VCH, Weinheim, 2008, pp. 3256–3265 (Chapter 14)]
- [52]Martyn V. Twigg, Michael S. Spencer *Applied Catalysis A: General* 212 (2001) 161–174
- [53]R. Hughes, *Deactivation of Catalysts*, Academic Press, New York, 1994.]
- [54]M.S. Spencer, *Nature* 323 (1985) 685.

- [55] (Butt & Petersen 1988, Somorjai 1994, Bartholomew 2001, Moulijn et al. 2001).
- [56] (Gunter et al. 1997, Stakheev & Kustov 1999)
- [57]C.P. Thurgood, J.C. Amphlett, R.F. Mann, and B.A. Peppley, Topics in Catalysis Vol. 22, Nos. 3–4, April 2003, 253.
- [58]J.C. Amphlett, R.F. Mann, B.A. Peppley and C.P. Thurgood, Catalyst Deactivation (2001), Vol. 139, J. Spivey (ed.) 950 pp.]
- [59]K. Tohji, Y. Udagawa, T. Hizushima, A. Veno, Phys. Chem. 89 (1985) 5671.]
- [60] Y.S. Prasad, B.D. Padalia, S.K. Raman, J. Chem. Tech. Biotechnol. 35A (1985) 15–20]
- [61] Doca, E. Segal, Rev. Roum. Chim. 32 (2) (1987) 199–202.
- [62]C.-Y. Shiau, Y.R. Lee / Applied Catalysis A: General 220 (2001) 173–180]
- [63]Church,J.M. & Joshi,H.K. Acetaldehyde by dehydrogenation of ethyl alcohol. *Industrial and Engineering Chemistry* **43**, 1804-1811 (1951).
- [64]Adkins, H.; Connor, R. 1931. The catalytic hydrogenation of organic compounds over copper chromite. *J. Am. Chem. Soc.* 53: 1091-1095.
- [65]Ram Prasad *, and Pratchi Singh, Bulletin of Chemical Reaction Engineering & Catalysis, x (x), 2011, p.1 - p.51.
- [66]Rao, R.; Dandekar, A.; Baker, R.T.K.; and Vannice, M.A.; 1997. Properties of Copper Chromite Catalysts in Hydrogenation Reactions. *J. Catal.* 171: 406-419.
- [67]Valde´s-Soli´s, T.; Marba´n, G.; Fuertes, A.B. 2006. Nanosized catalysts for the production of hydrogen by methanol steam reforming. *Catal. Today* 116: 354-360.
- [68]C.L. Bianchi, M.G. Cattania, V. Ragaini, Surf. Interface Anal. 19 (1992) 533]
- [69]R.S. Rao, R.T.K. Baker, M.A. Vannice, *Catal. Lett.* 60 (1999)]
- [70]DAVY patent n°. ZA2004/9535 25 nov.2004][DAVY PATENT EP 1 117631 B1.
- [71]S.W. Colley, J. Tabatabaei, K.C. Waugh,M.A. Wood *Journal of Catalysis* 236 (2005) 21–33.
- [72]Fawcett, C. R., Tuck, M. W. M., Rathmell, C., and Colley, S. W.,Kvaerner Process Tech., Ltd., EP 0990638 (2000).]

[73]Marino,F., Boveri,M., Baronetti,G. & Laborde,M. Hydrogen production via catalytic gasification of ethanol. A mechanism proposal over copper-nickel catalysts. *International Journal of Hydrogen Energy* **29**, 67-71 (2004).

[74]Deluga C, Salge J, Schmidt L, Verykos X. Renewable hydrogen from ethanol by autothermal reforming. *Science* 2004;303:993–7

[75]L. Dolgykh et al. / *International Journal of Hydrogen Energy* 31 (2006) 1607 – 1610]

SECTION B

Chapter 2

Techniques and equipment

B-2.1 Introduction

This chapter introduces some general aspects related to the catalyst employed, their characterization and to the reaction apparatus employed to perform the reaction. In particular in the present chapter the commercial copper based catalysts composition has been reported. Moreover a list of the characterization techniques used to describe in details the chemical and physical properties of the examined catalysts have been reported. Finally the configuration of the experimental device and of the operative conditions has been described.

B-2.2 Catalysts composition

Five different commercial catalysts have been employed for the study of ethanol dehydrogenation reaction, respectively supplied by BASF and Sud Chemie Companies, that are:

- 1) The BASF K-310, which contains $\text{CuO}/\text{ZnO}/\text{Al}_2\text{O}_3$ (40:40:20% b.w.), is a catalyst normally employed to promote the low temperature gas shift reaction or the steam reforming of methanol [1]. It is constituted by cylindrical pellets of regular size 4.5 mm of diameter and 4.5 mm of height. Also the performances of an improved catalyst composition supplied by the same company BASF Sg-9601 $\text{CuO}:\text{ZnO}:\text{Al}_2\text{O}_3$ 37:37:26% b.w. has been studied. As well known, and also showed by BASF [2], the active species, in the low temperature shift catalyst skills, consist of small metallic copper crystallites which are not

thermodynamically stable. Over time, they have a tendency to aggregate reducing both surface area and catalytic activity. A temporary overheating, due for example to plant upset, can accelerate this aging process. To withstand the effect of aging, the catalyst is formulated to begin with both high copper content and high density.

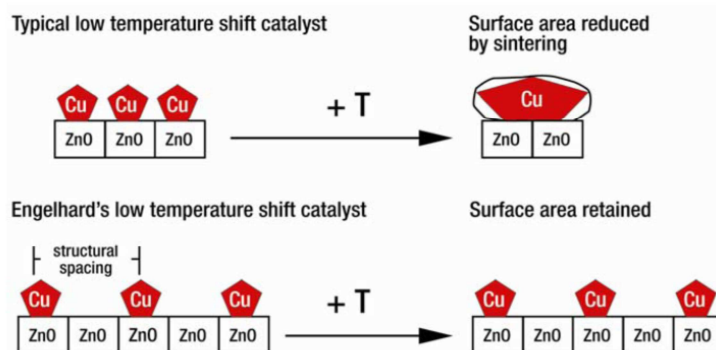


Figure 1: increased zinc oxide content in BASF low temperature shift catalysts acts as structural spacer to reduce sintering [BASF brochure www.BASF.com/syngas].

Due to these built-in performance reserves, the technology is able to retain its activity longer and under more extreme process conditions. In addition, the increased zinc oxide content also acts as a structural spacer for the copper crystallites spreading them out and improving their resistance to sintering resulting in increased temperature resistance and longer life (Figure 1).

2) The Sud-Chemie T-4466, a copper/chromium based catalyst containing CuO (53%) and Cr₂O₃ (45%), is constituted by regular tablets (3x3 mm). This catalyst is usually employed for the hydrogenation reactions of fatty acids to fatty alcohols. The performances of copper chromite catalyst supplied by sud-chemie have been compared with the ones of the copper chromite supplied by BASF Cu-0203 containing an higher amount of CuO (64%) and lowest amount of chromia (36%)

3) The BASF Cu-1234-1/16-3F is a pre-reduced copper chromite catalyst supported on alumina and containing BaCrO₄ as promoter.

The catalyst composition, provided by the supplier, is $\text{CuCrO}_4/\text{CuO}/\text{Cu}/\text{BaCrO}_4/\text{Al}_2\text{O}_3$ (45:1:13:11:30% b.w.) although being this a pre-reduced catalyst BaCrO_4 , very probably, is present in a reduced form as barium chromite or $\text{BaO}/\text{Cr}_2\text{O}_3$. The catalyst shape is characterized by cylindrical extrudate with 1.8 mm of diameter and irregular heights of 3-5 mm. All the examined catalysts were previously pre-reduced for 16-18h in a mixture of hydrogen in nitrogen ($\text{H}_2/\text{N}_2=6/94$ mol/mol) with a flow of $25 \text{ cm}^3/\text{min}$, keeping constant the temperature at 200°C . These catalysts have been selected because the first one contains free copper oxide supported on alumina and ZnO, while, the second one is characterized by the presence of unsupported copper chromite and the third one contains supported copper chromite. The properties, the performances and the drawbacks of these three different catalysts have been evaluated, compared and discussed.

B-2.3 Catalysts characterization

Physical and chemical properties of catalysts and their precursors were determined by various instrumental techniques. The following paragraph contains all techniques utilized in this work, the details of the experimental parameters can be found in Appendix Different techniques were used for the catalysts characterization, such as: BET, copper dispersion determination with N_2O treatment, X-ray diffraction (XRD), temperature programmed reduction (TPR) with a mixture of H_2 (6%) in N_2 , temperature programmed desorption of ammonia (NH_3 -TPD) and temperature programmed desorption of carbon dioxide (CO_2 -TPD) on a previously pre-reduced catalysts

Textural analyses were carried out by using a Thermoquest Sorptomatic 1990 Instrument (Fisions Instrument) by determining the nitrogen adsorption/desorption isotherms at 77 K. The samples were thermally pre-treated under vacuum overnight up to 473K (heating

rate=1 K/min). Specific surface area (S_{BET}) and pore size distributions were determined by using respectively the BET [3,4] methods (see appendix A).

The determination of the copper surface area and copper dispersion has been performed, with the N_2O method. A known amount of the catalyst, about 100 mg, was first of all reduced with a flow stream of $25 \text{ cm}^3/\text{min}$ of a mixture of 5% v/v H_2 in N_2 at 300°C for 2 hours. Afterwards, a flow stream ($45 \text{ cm}^3/\text{min}$) of pure N_2 was sent for about 20 minutes to remove residual hydrogen and water and then the catalyst was cooled to 60°C maintaining constant this temperature during the oxidation experiment. Specific Cu surface area and dispersion were measured by the well-known N_2O chemisorption method based on the reaction:



The N_2O experiments were conducted utilizing a pulse method. Precisely several pulses of 1 cm^3 of 5% N_2O in N_2 were injected into a carrier stream of N_2 flowing at $50 \text{ cm}^3/\text{min}$ until no further N_2O was reacted. Uptake of N_2O was monitored with a gold plated tungsten filament thermal conductivity detector (TCD) with a current of 130 mA. Dispersion and Cu specific surface area [5] were calculated assuming a Cu surface atomic density of $1.47 \cdot 10^{19} \text{ atoms}/\text{m}^2$ (Appendix A).

X-ray diffraction (XRD) patterns were obtained using a Philips powders diffractometer. The scans were collected in the range $5\text{-}80^\circ$ (2θ) using Cu $\text{K}\alpha$ radiation with a rate of 0.01° (2θ)/s. The X-ray tube operated at 40KV and 25mA (Appendix A).

The TPR experiments were carried out using a quartz U-tube reactor with an internal diameter of 10 mm. The powdered catalyst was loaded on a sintered quartz wool disk placed inside the reactor. The catalyst formed a bed of less than 5 mm in thickness (0.1-0.2 g) on which a glass wool plug was added. The samples were initially

pretreated in N₂ flow of 20 cm³/min, at a temperature of 100°C, for about 1 h, to remove any trace of moisture. The samples were then cooled at room temperature. Always under nitrogen stream the temperature was then gradually increased with a scanning rate of 10°C/min until reaching 300°C. After this pre-treatment the hydrogen TPR were performed using a flow stream of 6% of H₂ in N₂ (60 cc/min). The gas stream was split in two flows one leading to the reference arm of a thermal conductivity detector (TCD) and the other one passing through the reactor before going to the detector. The water produced during the TPR was trapped by a dry trap located between the detector and the reactor. After the reduction pre-treatment the catalysts were subjected to a Programmed Desorption of NH₃ or to a Programmed Desorption of CO₂ to evaluate respectively the overall surface acidity and basicity of the studied catalysts. The overall surface acidity of the prepared catalysts was determined by a Temperature-Programmed Desorption of ammonia (NH₃-TPD) in a fixed-bed continuous flow micro-reactor system. Before the NH₃-TPD measurement, a sample of powdered catalyst (0.1-0.2g) was out-gassed in a flow of pure helium (20 ml/min), at 300 °C for 30 minutes. Then, the sample was cooled at 40 °C and saturated with a stream of 10% NH₃ in He (20 ml/min) for about 30 min. Afterward, the catalyst was purged in a helium flow until a constant baseline was attained. The ammonia desorption was determined in the temperature range of 40–500 °C with a linear heating rate of 10 °C min⁻¹ in a flow of He (10 ml/min). Desorbed NH₃ was detected by a thermal conductivity Detector (TCD). Then, the surface basicity of the prepared catalysts was determined by TPD of CO₂ performed in the same fixed-bed micro-reactor used for ammonia TPD. The fresh catalysts were subjected to a pre-reduction, as previously described. Before the CO₂-TPD measurement, a sample of powdered catalyst (0.1-0.2 mg) was out-gassed in a flow stream of pure helium (20 ml/min), at 300 °C for

30 min. Subsequently, the sample was cooled at 40 °C and saturated with a stream of CO₂ (10 ml/min) for about 30 min. Then, the catalyst was purged with a helium flow until a constant baseline level was attained. The carbon dioxide desorption was evaluated in the temperature range of 100–500 °C with a linear heating rate of 10 °C min⁻¹ in a flow stream of He (20 ml/min). Desorbed CO₂ was detected by a thermal conductivity detector (TCD) (Appendix A).

X-ray photoelectron spectroscopy (XPS) is a quantitative analysis technique that is widely used in catalyst research because of its ability to analyze the surface (depth ~10 nm) of solid materials. However experiments must take place under ultra-high vacuum (UHV) conditions to ensure electrons reach the detector. The XPS experiments were conducted by using a Kratos XSAM-800 instrument with an Al-Kα X-ray source operating at 1486.6 eV and a 90-degree takeoff angle. The binding energies (BE) were calibrated with the C 1s peak fixed at 285.0 eV as an internal reference standard.

Fresh ground powder catalyst samples were adhered to brass mounts with double-sided carbon tape prior to loading into the analysis chamber. Samples were left to degas overnight while the vacuum system maintained a pressure less than 1×10^{-8} torr. Control and data collection was done using Vision2 software running on Sun workstations. Normally each element of interest was scanned 10 times with a range of ~20 eV and an acquisition time of ~1 minute, elements with low concentrations were scanned more times. Raw data was processed with CasaXPS software package, with relative sensitivity factors obtained from the Kratos XSAM library (Appendix A). The Scanning Electron Microscopy Scanning electron microscopy (SEM) was used to study the microstructure of certain catalyst particles. The microscope column is evacuated to approximately 10^{-6} torr, to minimize electron scattering by gas molecules. The generated electrons are accelerated to a proper voltage, depending on the type

of experiment, typically 0.1-30 keV using electromagnets. Magnetic lenses are able to focus the electron beam to a spot on the specimen less than 10 nm in diameter. Scanning coils are used to raster the beam across the surface of the sample. Due to scattering, both backscattered and secondary electrons escape from the sample surface and can be detected. Prior to analysis powder samples were finely ground and mounted on carbon tape on a stainless steel sample mount. Alternatively, to improve the particle dispersion on the holder, approximately 2 mg of sample was diluted in distilled water to form a suspension. Then, a single drop was set on the clean holder surface and evaporated at room temperature. The analysis was done in a Hitachi S4500 field emission SEM at 30 keV under a vacuum of 10^{-6} torr for the samples (Appendix A). X-rays are an important tool to probe the structure of solids. During X-ray absorption experiments, an X-ray having a given wavelength, or monochromatic beam, is directed into a sample. Then, the energy of the X-ray beam is gradually increased in order to reach the absorption energy of the photoelectrons of the element being analyzed. Depending on the energy range beyond the ionization edge, the absorption spectrum is classified between 5 and 150 eV as X-ray absorption near edge structure (XANES), and above 150 eV as X-ray absorption fine structure (EXAFS). The XANES region provides information of the oxidation state of the atom and the local geometry around the atom.

The EXAFS region provides detailed information on the local environment of the target atom, coordination numbers and scattering lengths. Measurements using extended x-ray absorption spectroscopy including extended x-ray adsorption fine structure and x-ray absorption near edge spectroscopy have been used. The measurements were made in transmission mode with ionization chambers optimized for the maximum current with linear response ($\sim 10^{10}$ photons detected/sec). A cryogenically cooled double-crystal Si

(111) monochromator with resolution (ΔE) better than 2.5 eV at 8.979 keV (Cu K edge) was used in conjunction with a Rh-coated mirror to minimize the presence of harmonics. The integration time per data point was 1-3 sec, and three scans were obtained for each processing condition. Standard procedures based on WINXAS97 software were used to extract the EXAFS data. Phase shifts and backscattering amplitudes were obtained from EXAFS data for reference compounds: CuO and Cu₂O for Cu-O and Cu foil for Cu-Cu. The sample was previously pressed into a cylindrical holder with a thickness chosen to give an absorbance ($\Delta\mu x$) of about 1.0 in the Cu edge region. Due to the high density of the Cu based catalysts, fresh powder was diluted by a factor of 10 with silica fume prior to being pressed into a wafer. The sample holder was centered in a continuous-flow EXAFS quartz reactor tube 18 inches long and 0.75 inches diameter. The tube was fitted at both ends with polyimide windows to allow transmission of the x-ray beam with gas valves fitted perpendicular to the tube. This entire apparatus was fitted into a clamshell style electrical furnace, which was controlled and monitored with three type K thermocouples located inside the reactor tube and furnace assembly. This furnace, window, and valve configuration allowed isolation of the reactor from the atmosphere and the ability to flow various reducing, reactant, and oxidizing gas mixtures at elevated temperatures, all while being probed by the x-ray beam. The Catalysts were studied via XANES spectroscopy under reaction and reducing conditions. Usually the spectrum was first recorded with the catalyst in its untreated state in air. All samples were reduced by heating in a reducing atmosphere of pure H₂ to a temperature of 300°C, and then scanned after cooling to room temperature. For reaction studies under ethanol decomposition reaction conditions the temperature was changed to the desired set point and a reaction mixture of 2.2 cm³/min of CH₃CH₂OH in He was flowed over the catalyst for 30 minutes. After that the EXAFS spectrum

has been recorded with the aim to evaluate the eventually variation of the oxidation state during the reaction (Appendix A).

Fourier Transform Infrared (FTIR) spectrometers are widely used to study the infrared absorption of adsorbed species on solid surfaces. Transmission IR can be obtained with samples that are partially transparent to IR radiation. When the sample is opaque and infrared transmittance is low, spectra can be collected in diffuse reflectance mode, better known as diffuse reflectance infrared fourier transform spectroscopy or DRIFTS.

The diffuse reflectance infrared spectra (DRIFTS) of ethanol on copper based catalysts were obtained in a Bruker Equinox 55 spectrometer equipped with a DTSG KBr detector. For ethanol adsorption experiments, a pressed disk of catalyst powders, in mixture with fuse silica, were used. A conventional manipulation/outgassing ramp connected to the IR cell equipped with a calcium fluorite window were used. In particular the IR cell has connections for inlet and outlet flows, and thermocouples connected to a temperature controller to monitor and control its temperature. The samples were thermally pre-treated by heating under Helium flow ($25 \text{ cm}^3 \text{ min}^{-1}$), after that it has been reduced at 300°C in a flow of 20% H_2 in He for about 1h. The system was rapidly cooling and the adsorption of ethanol procedure involves contact of the pre-treated sample disk with Ethanol at three different temperature $100\text{-}300^\circ\text{C}$, at atmospheric pressure. For each spectrum 128 sample scans in the range $4000\text{-}370 \text{ cm}^{-1}$ were recorded with a resolution of 4 cm^{-1} (Appendix A).

B-2.4 Catalytic activity

B-2.4.1 Apparatus

A wholly automated experimental apparatus built in-house, depicted in Figure 2, was used for the evaluation of catalyst activity of ethanol dehydrogenation.

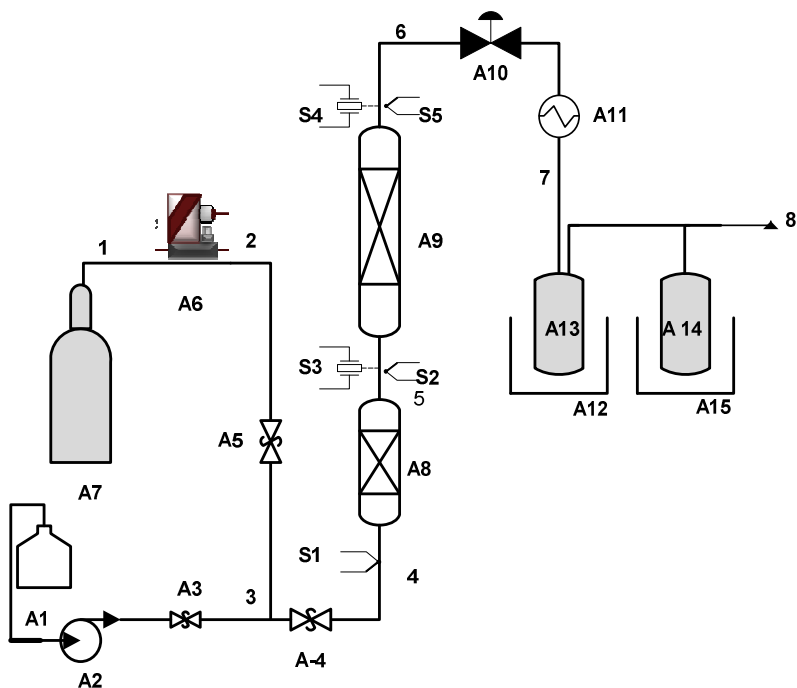


Figure 2: A1-Ethanol Tank, A2- ethanol hplc pump, A3/A5-check valves, A4-rielef valve, A6-flow mass controller, A7-cylinder containing a gases mixture of H₂ in N₂, A8-preheater,A9-stainless steel packed bed tubular reactor, A10-back pressure regulator, A11-heat exchanger, A13/A14-products tank raising, A12/A15-liquid nitrogen dewars, S1/S2/S5-temperature probes, S3/S4- pressure transducers.

The catalytic tests were performed in a stainless steel packed bed reactor of about 30 cm of length and 1inch of external diameter. In figure 3 the scheme of the reactor employed has been reported.

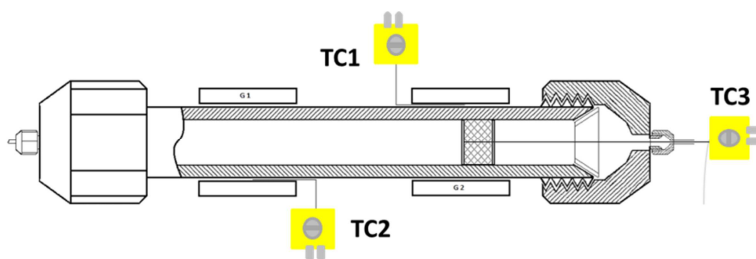


Figure 3: reactor scheme

As it can be seen by the reactor scheme the temperature of reactor was measured by using two different thermocouples (TC1 e TC2), inserted between the walls of the reactor and the heaters (series thinband). A third thermocouple has been placed inside the reactor to estimate the variation of the temperature along the catalyst bed. The thermocouples (TC1 e TC2) works by the action of thermo-regulators equipped with relay system. All the connecting pipes were heated by using electrical heaters kept at a constant temperature of 200°C to avoid the condensation of high boiling point compounds.

The pressure has been regulated by using a backpressure regulator able to operate in a range of 0-100 bars (Swagelok KBP1N Cv=0.06). The pressure of reaction has been monitored by using two different pressure transducers respectively placed at the inlet and at the outlet of the reactor. The apparatus consists of separate gas and liquid delivery sections. The liquid ethanol reactant (Fluka 99.8%), was pumped, by using an HPLC pump (flow of 0.0001-10 cm³/min and max. pressure limited to 100 bars) into a pre-heater kept at a temperature of 200°C, filled with inert material (glass balls) and mixed with the carrier flow of Nitrogen. The reaction has always been conducted in the presence of a hydrogen stream. The flow of the carrier mixed with a 6%wt of hydrogen was regulated by using a mass flow controller (Bronkhorst) able to operate at 1-50 cm³/min and at pressure up to 100 bar. On each connecting pipes to the instruments several check

valves have been placed. The resulting gaseous mixture was, after passing through a pre-heater zone, directed to a standard fixed-bed down-flow quartz reactor.

A weighed amount of catalyst (2-10-50 gr), in pellets, was charged in the reactor and, before the catalytic test, was submitted, for 18 h, to a pretreatment with a flow stream of H₂-N₂ mixture (H₂/N₂=6:94 mol/mol) 25 cm³/min, at a temperature of 200°C.

Table 1: reactor, catalyst bed and operative properties for a catalytic bed of 50g

Reactor Property		Catalytic bed		Operative conditions	
Reactor vol.	89 cm ³	Bed weight	50 g	Pressure	1-30 bar
Height	35 cm	Void fraction	0.4	Temperature	200-260°C
internal diameter	1.8 cm	Bed Length	17-18 cm	EtOH Liquid Flow	0.1-1.5 cm ³ /min
		Bed volume	48 cm ³	H ₂ 6% N ₂ Gas Flow	5-25 cm ³ /min

After the pretreatment, the catalyst was heated to the desired reaction temperature. The reaction was carried out at different temperatures in the range 200-260°C and different pressures in the range 10-30 bars

The ethanol contact time W/F has been taken in the range 5-950 g h mol⁻¹, where W and F are respectively the catalyst weight and the ethanol molar flow rate. The un-reacted ethanol and the condensable obtained products were collected in a trap cooled with liquid nitrogen. The reaction products were periodically analyzed by a gaschromatograph.

B-2.4.2 Gaschromatographic method

The gaschromatograph used was an HP 6890 with a Restek Rt-Q Plot 30m*0.32mm column, pure hydrogen has been used as carrier gas.

The conditions used for the analyses were as follows: the initial temperature of 80°C was increased at a rate of 10°C/min up to 220°C and then maintained at this value for 10 minutes. The flame ionization detector (FID) was kept at 280°C. The split-splitless injector was kept at 250°C. The response factors and the retention times for each products of reaction have been reported in Table 2.

Table 2: summary of the retention time and of the adopted response factors for each detected compound.

Component	Retention time (min)	Response factor
Acetaldehyde	3.80	1.7
Ethanol	4.50	1.0
Propan-2-ol	6.40	0.71
Acetone	6.60	0.76
Dietilether	7.30	0.91
1-propanol	-	-
Acetic acid	-	-
Butanon (Mek)	9.30	0.79
Ethyl acetate	9.60	1.09
Crotonaldehyde	10	0.75

The response factors have been evaluated on the basis of the internal normalization. Each gas-chromatographic area has been corrected on the basis of the specific obtained response factor for that compound. The response factors have been evaluated by using solution at well-defined concentration of the compound in exam. In more detail the ethanol has response factor assumed equal to 1. Several mixture of well-known weigh ratio of the compound (acetaldehyde, ethyl acetate, ethylene) with ethanol have been prepared and analyzed to the gas-chromatograph. By the ratio of the gas-chromatographic area and the

concentration of the mixture compound analyzed it's possible to obtain the response factors.

By using the equations (2)-(4) the quantity of each component and the correspondent area has been correlated.

$$g_{std} = f_{std} * A_{std} \quad (2)$$

$$g_{sample} = f_{sample} * A_{sample} \quad (3)$$

By the ratio (4) between the two above reported equations (2) and (3) an evaluation of the response factor (5) of each compound was done.

$$\frac{g_{sample}}{g_{std}} = \frac{f_{sample} * A_{sample}}{f_{std} * A_{std}} \quad (4)$$

$$f_{sample} = \frac{g_{sample} * A_{std} * f_{std}}{g_{std} * A_{sample}} \quad (5)$$

Known the response factor and the gas-chromatographic area the molar fraction for each component is evaluated by the reported equation (6):

$$x_i = \frac{f_i A_i}{\sum_i^n f_i A_i} \quad (6)$$

Where f_i , x_i and A_i represent respectively the response factor, the molar fraction and the gas-chromatographic area of the i -iesim compound. Different sets of runs were performed in order to evaluate the effect of the temperature, the pressure and the ethanol residence time on the catalysts performances. Results are reported in terms of ethanol conversion and products selectivity. Moreover on the basis of the obtained conversion and selectivity's to the compound containing hydrogen, its productivity has been calculated. The ethanol conversion is defined as (7):

$$x_{EtOH} = \frac{\text{mols EtOH}_{reacted}}{\text{mols EtOH}_{fed}} = 1 - \left(\frac{1}{\sum \frac{nC_i}{nC_{EtOH}} \frac{Ac_i}{Ac_{EtOH}}} \right) \quad (7)$$

while the selectivities, determined on the basis of a carbon balance for each component, are determined as (8):

$$S = \frac{\text{mols product}_i \text{ formed}}{n_{EtOH} \text{ reacted}} * \frac{nC_i}{nC_{EtOH}} \\ = \frac{nC_i}{nC_{EtOH}} \frac{Ac_i}{Ac_{EtOH}} \left(\frac{1 - x_{EtOH}}{x_{EtOH}} \right) \quad (8)$$

Where nC_i and nC_{EtOH} represent respectively the numbers of carbon atoms in the component i and in the ethanol fed, while Ac_i and Ac_{EtOH} are the normalized chromatographic peaks areas. The hydrogen productivity has been expressed as the $g_{H_2}/Kg_{cat} \cdot h$ and has been calculated by equation (9).

$$\text{Productivity } H_2 = \frac{F_{EtOHin}(\text{mol/h}) * X_{EtOH} * [S_{AcH} + S_{AcOEt}]}{Kg_{cat}} \quad (9)$$

B-2.5 References

- [1] E. Santacesaria and S. Carrà *Applied Catalysis*, 5 (1983) 345-358.
- [2] www.basf.com/syngas.
- [3] G. Leofanti, M. Padovan, G. Tozzola, B. Venturelli *Catalysis Today* 41 (1998) 207-219E] and Dollimore-Heal.
- [4] D. Dollimore and G.R. Heal, *J. Appl. Chem.* 14 (1964) 109.E.
- [5] Bond, G.C. & Namijo, S.N. *Journal of Catalysis* 118, 507-510 (1989).

SECTION B

Chapter 3

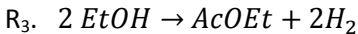
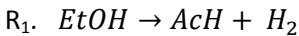
Thermodynamic study

B-3.1 Introduction

The ethanol dehydrogenation reaction, as well known, is generally used to produce acetaldehyde [1,2]. As demonstrated by Inui et al. [3] by employing the optimal operative conditions in terms of temperature, pressure and residence time the equilibrium of reaction could be shifted to the production of ethyl acetate and the acetaldehyde has been exploited as intermediate to produce the desired product of reaction. The shifting of the equilibrium reaction is not so easy because of several collateral reactions such as acetaldehyde condensation and ethanol dehydration. At this purpose, a thermodynamic analysis of dehydrogenation reaction for ethyl acetate production has been carried out by application of the Gibbs free energy minimization method. In advance, the optimum conditions for ethyl acetate productions have been identified: reaction temperatures between 200 and 260°C, pressure of 10-30 bar and relatively high residence time to favors the ethyl acetate production respect to the several reaction by-products. Under the optimal conditions, as will be demonstrated in chapter 4, a conversion of ethanol of about 60-65%, a selectivity of 98.8% to ethyl acetate has been obtained.

B-3.2 Determination of the equilibrium constants

By the minimization of the free energy it's possible to individuate the composition at equilibrium for each reactive system at an established pressure and temperature [4]. As already said, the dehydrogenation reaction to esters could be simplified in three different steps of reactions: R₁. dehydrogenation of ethanol to acetaldehyde; R₂. acetaldehyde could react with the unreacted ethanol to form ethylacetate and finally a third step, R₃., of direct production of ethyl acetate by ethanol. The three mentioned reactions are below reported.



For each reaction, the equilibrium constant, at atmospheric temperature and pressure, has been evaluated by considering both the Gibbs energy of formation and the standard enthalpy. The determination of the equilibrium constant is related to the energy of Gibbs according to the equation 1[5].

$$\ln K = -\frac{\Delta G^0(T)}{RT} \quad (1)$$

The evaluation of the equilibrium constants, for each reaction, at several temperature of reaction has been realized by applying the equation 2:

$$\ln \frac{k_a(T_2)}{k_a(T_1)} = -\frac{\Delta H^0}{R} \left(\frac{1}{T_2} - \frac{1}{T_1} \right) \quad (2)$$

At this purpose a first evaluation of respectively Gibbs energy and enthalpy of formation ΔG_f^0 e ΔH_f^0 have been calculated. In Table 1 the values at a 298.15K, obtained by the CHEMCAD library for each reactions have been reported.

Table 1: Chemcad Library value of Entalphy and Gibbs energy of formation of the different components of ethanol dehydrogenation

	ΔG_f^0 (Kcal/mol)	ΔH_f^0 (Kcal/mol)
Acetaldehyde	-30.79	-39.70
Ethanol	-40.09	-56.12
Ethyl acetate	-78.34	-106.17
Hydrogen	0	0

In Table 2 the values of the Gibbs energy ΔG_r^0 , enthalpy ΔH_r^0 of reaction and of equilibrium constant K_a at a temperature $T_0=298.15$ K have been reported.

Table 2: calculated values of ΔG° , ΔH° and K_a at 298 K for the three reactions R_1, R_2, R_3

	R₁	R₂	R₃
ΔG_r^0 (Kcal/mol)	9.30	-7.46	1.84
ΔH_r^0 (Kcal/mol)	16.42	-10.35	6.07
K_a (T= 298 K)	1.51E-07	2.96E+5	4.48E-02

According to the equation (2), the equilibrium constant have been evaluated at atmospheric pressure and at reaction temperature of 100-500°C. In figure 1 the profiles of $\ln(k_a)$ vs $1/T$ have been represented.

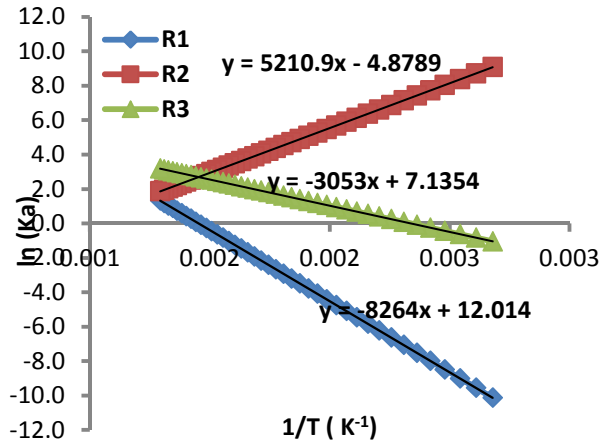


Figure 1: logarithmic profile of the equilibrium constant as function of the reaction temperature.

In Figure 2 the profiles of the logarithm $\ln(K_a)$ vs temperature for each reaction (R_1 - R_2 - R_3), obtained by applying the equation 3 have been also reported.

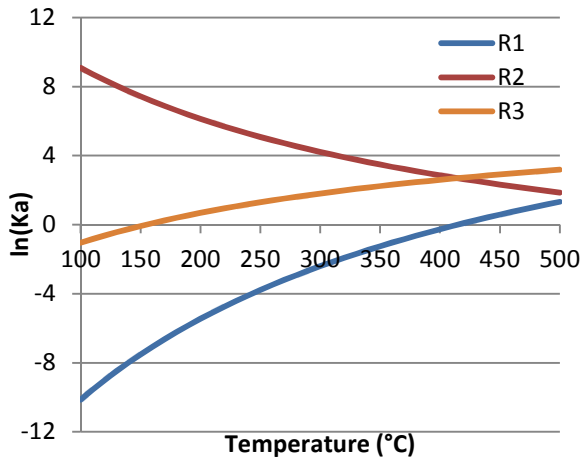


Figure 2: Equilibrium constant profiles of the three main reaction steps to produce ethyl acetate as function of the temperature.

The profiles of Figure 2 show that the reaction R_1 , related to the acetaldehyde formation by ethanol dehydrogenation is an endothermic reaction and therefore is favored at a temperature higher than 300°C. The ethyl acetate is produced by reaction R_2 , a coupling reaction between an acetylic fragment and an ethoxy group, formed by adsorbed ethanol. This reaction is favored by relatively low temperature of reaction because of its exothermicity. As matter of fact at low temperature of reaction (<300°C) the equilibrium constant is higher. The global reaction R_3 is a moderately endothermic. At this purpose to favor the ethyl acetate product of reaction, the dehydrogenation has been realized at temperature lower than 300°C. The obtained information are in agreement with the literature studies. Thus, the obtained equilibrium constants have applied in some of the kinetics models developed, as it will be illustrated in chapter 5.

B-3.3 Aspen simulation

In the present study, in order to evaluate the equilibrium compositions, the Gibbs energy minimization method was used. The total free energy of the system, regarded as an ideal gas phase, may be expressed, by taking in account the dependence of the equilibrium constants by the temperature of reaction, as:

$$nG = \sum_{i=1}^{Nc} n_i \bar{G}_i = \sum_{i=1}^{Nc} n_i G_i^0 + RT \sum_{i=1}^{Nc} n_i \ln \frac{f_i}{f_i^0} \quad (3)$$

where:

$$df_i = \varphi_i y_i P$$

$$f_i^0 = 1 \text{ bar}$$

$$G_i^0 = 0 \text{ elements}$$

The oportune substitutions transform the equation 3 in equation 4.

$$nG(n_i S, T, P) = \sum_{i=1}^{Nc} n_i \Delta G_i^0 + \sum_{i=1}^{Nc} RT \ln P + \sum_{i=1}^{Nc} n_i RT \ln \varphi_i \quad (4)$$

The aim is to minimize nG maintaining constant the temperature and pressure reaction with the bond:

$$\sum_{i=1}^{Nc} n_i a_{ji} = b_j \quad j = 1 \dots K \quad (5)$$

The nonlinear programming model, comprising the objective function to be minimized is solved by using PSRK (short for Predictive Soave-Redlich-Kwong)[8] that is an estimation method for the calculation of phase equilibria of a non-ideal mixtures of chemical components, contained in ASPEN, process modeling tool. In the present work, calculations were made considering an equilibrium reactor, fed with 1 Kmol/h of ethanol, a fixed pressure, respectively of 1-20-30 bar, and in a range of temperature of 0-500°C.

Precisely, the results of the components compositions obtained by the minimization of the free Gibbs energy have been reported for the reaction R_2 in non-ideal case at different pressure of reaction 1-10-20-30 atm., in the mentioned range of temperature.

In the calculation of the equilibrium constants the relation between the partial pressure, the total pressure and the molar fractions have been taken in account. For each Kmol/h of fed ethanol it is possible to extract the Kmol/h of all the products of reaction such as acetaldehyde, ethyl acetate and hydrogen and of the not react ethanol. It is important to specify that the eventually production of by-products of reaction, derived by acetaldehyde condensation, has been neglected. Moreover the reaction has been considered to occur in gas phase while, in the reality, the reaction occurs in an heterogeneous system between two phases: the gas phase of the reagents and the solid catalyst. Also the adsorption steps have been neglected. All this simplification could contribute to an error between the experimental data and the calculated ones.

The molar fraction of each components produced during the reaction have been calculated taken in account the fed of ethanol and the mols of each component in the outlet stream of the equilibrium reactor. The molar fractions were expressed as (6a-d):

$$y_{EtOH} = \frac{n_{EtOH,out}}{n_{TOT}} \quad \text{Residual ethanol} \quad (6a)$$

$$y_{AcH} = \frac{n_{AcH,out}}{n_{TOT}} \quad \text{acetaldehyde} \quad (6b)$$

$$y_{H_2} = \frac{n_{H_2,out}}{n_{TOT}} \quad \text{hydrogen} \quad (6c)$$

$$y_{AcOEt} = \frac{n_{AcOEt,out}}{n_{TOT}} \quad \text{ethyl acetate} \quad (6d)$$

The total mols in inlet stream is equal to the mols of each components and of not reacted ethanol in the outlet stream $n_{TOT} = n_{EtOH} + n_{AcH} + n_{H_2} + n_{AcOEt}$ (7)

By the composition of the several compounds in the outlet stream, the ethanol conversion and the selectivities of ethyl acetate, hydrogen and acetaldehyde at equilibrium has been defined by the equation (8 a-d).

$$X_{EtOH} = \frac{y_{EtOH,in} - y_{EtOH,out}}{y_{EtOH,in}} \quad (8a)$$

$$S_{AcOEt} = \frac{y_{AcOEt,out} * n_{TOT}}{X_{EtOH}} \quad (8b)$$

$$S_{AcH} = \frac{y_{AcH,out} * n_{TOT}}{X_{EtOH}} \quad (8c)$$

$$S_{H_2} = \frac{y_{H_2,out} * n_{TOT}}{X_{EtOH}} \quad (8d)$$

Where, $y_{EtOH,in}$ and $y_{EtOH,out}$ are respectively the molar fraction of fed ethanol and in the outlet stream. While $y_{AcOEt,out}$, $y_{AcH,out}$ and $y_{H_2,out}$ are respectively the molar fraction of ethyl acetate, of acetaldehyde and hydrogen in the outlet stream of

the equilibrium reactor. The selectivities, for each products containing carbon, were calculated by considering a mass balance on the carbon.

B-3.4 Results and discussion

The ethanol conversion and the compounds selectivity have been evaluated on the basis of thermodynamic considerations. The profiles of the molar fraction, of ethanol conversion and of the selectivities of the several products of reaction at a constant pressure of 20 bars, as example, have been represented. As suggested by the profiles of Figure 3, at a constant pressure of 20 bars, by increasing the temperature of reaction, the molar composition of ethanol in the effluents decrease up to completely consume at a temperature of about 600°C. Moreover the figure shows the significant effect of the temperature on the selectivities to the desired product of reaction.

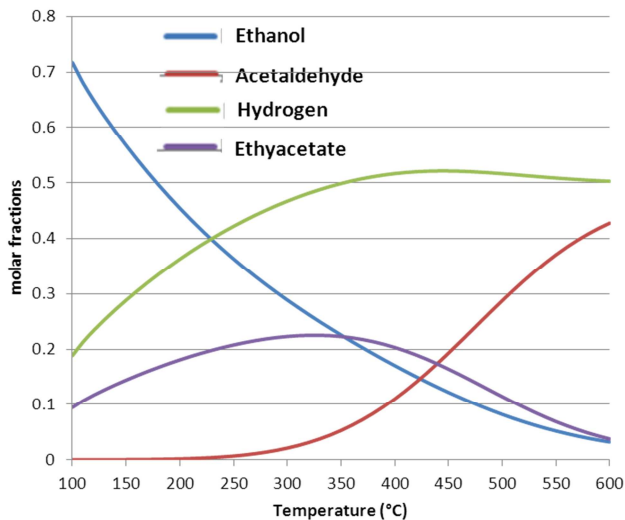


Figure 3: molar fractions for each compound at 20 bars, at different temperature.

In fact to maximize the ethyl acetate production the range of temperature 200-300°C should be used. By increasing the temperature of reaction, the ethyl acetate composition rising up to a maximum (340-350°C), after that the acetaldehyde becomes the main reaction product. In Figure 4, the profiles, of conversion of the ethanol and of selectivities of the three main products of reaction, at different temperature of reaction and at a constant pressure of 20 atm have been represented.

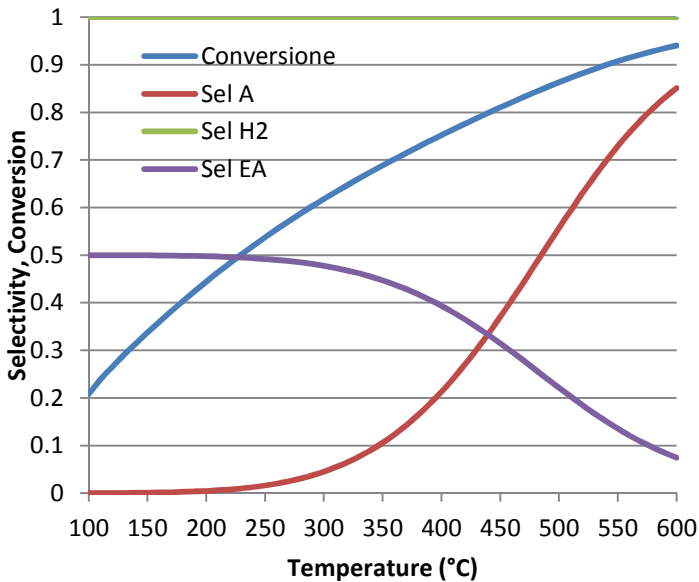


Figure 4: conversion and selectivities profiles at 20 bar.

An ethanol conversion of about 100% has been obtained at operating temperature higher 600°C. The maximum selectivity to ethyl acetate of about 0.5%, regardless carbon balance, was obtained at a temperature of 220-230°C. The ethanol conversion, in each case, increase with the temperature but on the other hand by increasing the pressure, it is necessary to increase the temperature to obtain the

100% of conversion. By operating at atmospheric pressure to obtain a 100% of ethanol conversion, a temperature of 500°C is required. At an intermediate temperature of reaction of about 300°C conversion of about 85% has been obtained vs the 70%, 62% and 55% obtained with an increase of the pressure until 30 bars.

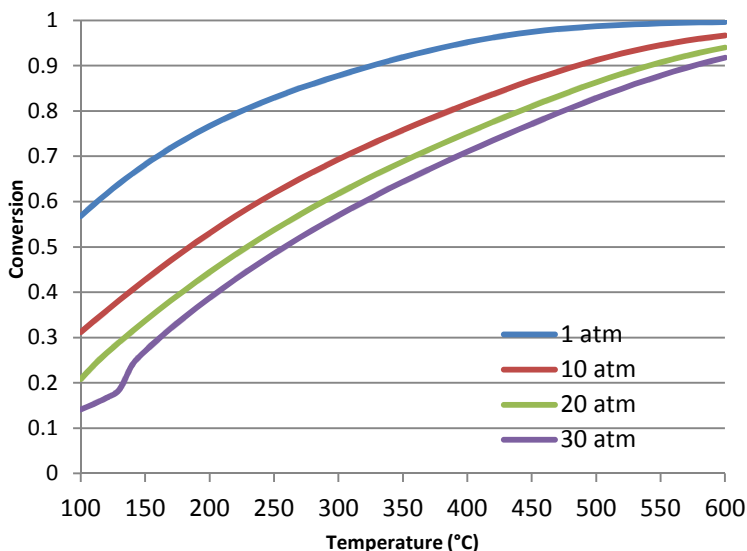


Figure 5: profiles of conversion variation with the pressure of reaction.

In Figure 6 the profile of selectivities to ethylacetate as function of the reaction temperature at different operating pressure have been reported. At temperature of reaction higher than 250°C, an evident increase of acetaldehyde selectivity was observed. The acetaldehyde formation by ethanol dehydrogenation is an endothermic reaction and for this reason favored by higher temperature. The effect of the decrease of selectivity of ethyl acetate at higher temperature is more evident at lower pressure. The increase of the operative pressure from 1 to 10 gives a significantly increase of the ethyl acetate yields. But a

further increase of the pressure from 10 to 30 atm doesn't affect significantly the ethyl acetate selectivity. In Figure 7 the profiles of selectivity to acetaldehyde as function of the temperature, at different pressure have been represented. The acetaldehyde selectivity has favored at low pressure and at temperature higher than 300°C. As the thermodynamic study suggests at temperature higher than 600°C the selectivity to acetaldehyde could rising up to 100%. Of course, the real situation is far from the ideal case, obtained with an equilibrium reactor.

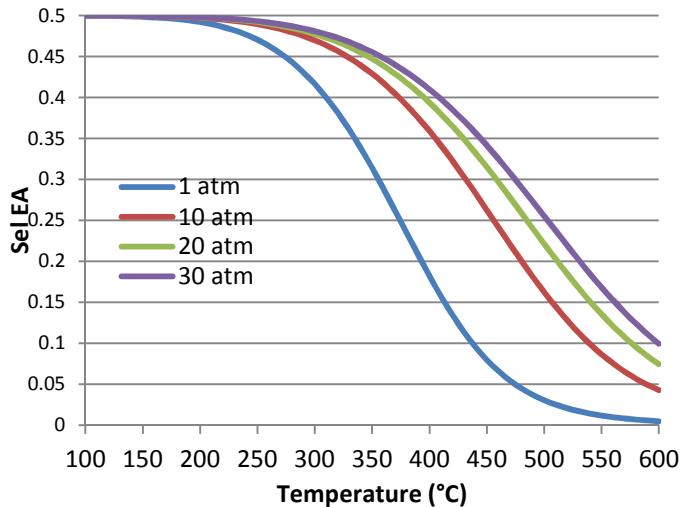


Figure 6: ethyl acetate selectivities profiles obtained at different pressure of reaction.

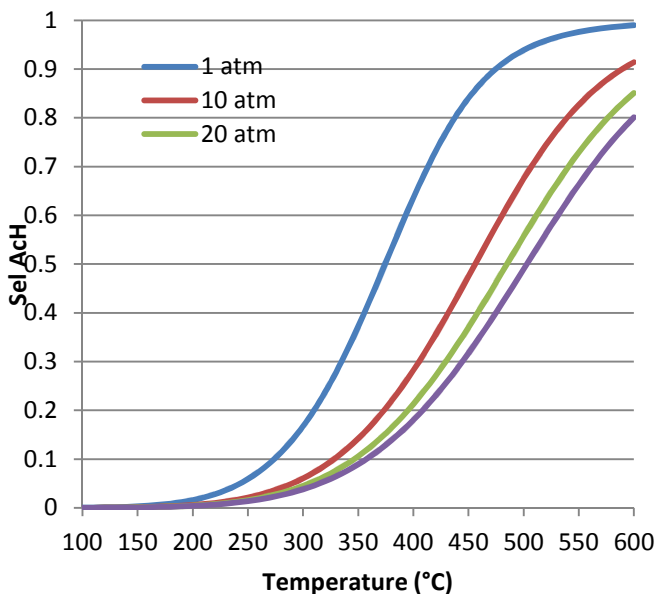


Figure 7: selectivities profile to acetaldehyde vs temperature at different pressure

Once the theoretically curves of equilibrium ethanol conversion and ethyl acetate/acetaldehyde selectivities have been individuated by the application of the free energy of Gibbs minimization, a comparison of them with the experimental results have been realized. The theretically profiles of compositions, selectivities, conversion are in perfect agreement with the thermodynamic study reported by Chadlek [9]. On the other hand, the theoretical compositions at equilibrium, predicted with the PSRK method, are in direct contradiction with our experimental data, as demonstrated also in the chapter 3-section A of this thesis. As demonstrated by our experimental works the acetaldehyde was produced also at relatively low temperature and this experimental results are in agreement with those reported in literature [10,11]. The acetaldehyde production can be obtained, during the dehydrogenation reaction also at low

temperature, when the adopted residence time is very low, as in our experimental runs, of about $0.18\text{-}20\text{ ghmol}^{-1}$. In fact the thermodynamics model, obtained by using the free Gibbs energy minimization with ASPEN, has shown that:

1. At low temperature, until 300°C , the thermodynamic doesn't favor the acetaldehyde production, the selectivity is less than 5%, without considering mass balance on the carbon.
2. In the same range of temperature $100\text{-}300^{\circ}\text{C}$ the ethyl acetate should be the main reaction product.

These two considerations are in direct contradiction with both the experimental results that we will discuss in the chp.4 but also with the literature results. As shown by Zonetti et al.[12] at a temperature of 200°C , for an ethanol conversion of about 55% a selectivity to acetaldehyde of about 60% has been obtained. This contradiction is related to the competition between the ethanol dehydrogenation to acetaldehyde and ethyl acetate. Thermodynamically the acetaldehyde is more favorable species up to 340°C . Once this results can be explained by the infinite residence time assumption used in Gibbs free energy minimization. In reality the residence time is finite and therefore only part of the acetaldehyde formed by dehydrogenation reaction, which is the first and fastest reaction to occur, gets converted to ethyl acetate.

At this purpose in Figure 8 a comparison of the theoretically profiles of conversion, obtained by the previously thermodynamic evaluation, with the experimental results obtained at two different residence time respectively of 4.07 ghmol^{-1} e 97.45 ghmol^{-1} have been reported. The experimental results have been obtained at a constant pressure of 20 bars at different reaction temperature of $200\text{-}260^{\circ}\text{C}$.

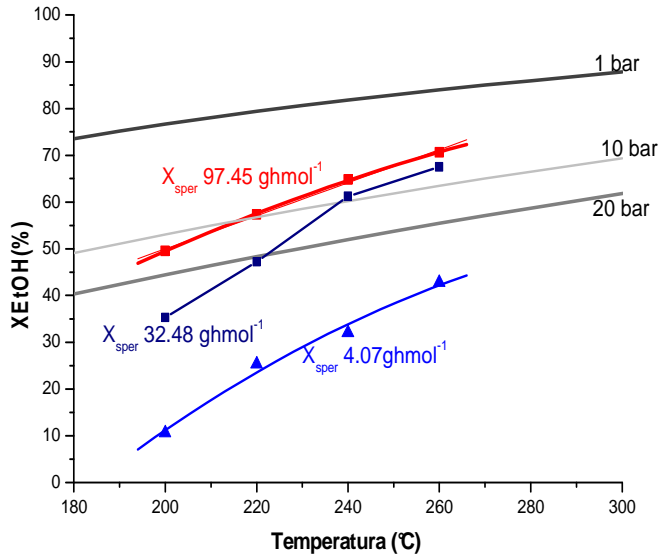


Figure 8: comparison of the experimental (20 bars) and theoretical profiles.

A first evaluation, has shown different behaviors at different residence time. At lowest residence time $W/F=4.07 \text{ ghmol}^{-1}$, the ethanol conversion, obtained by changing the reaction temperatures, is far from the ones obtained at equilibrium, imposed by the thermodynamic restrictions. At higher residence time the experimental ethanol conversion is higher than the ones obtained by the thermodynamic study. Nevertheless, the actual ethanol conversion is greater than the equilibrium conversion. Since the produced acetaldehyde is further converted to other by-products, such as butanone and butanol, at high temperatures, the actual conversion is greater than the equilibrium conversion of ethanol to ethyl acetate. On the other hand the experimental conversion is so different by the theoretical also for the several considered approximations: the reaction is more complex than the simplified represented and the sub-

product produced during the reaction could have such influence on the equilibrium.

Moreover this system is heterogeneous so a reaction of a gas phase with a solid catalytic surface has occurred, but all the phenomena of adsorption and how they could influence the thermodynamic equilibrium have been neglected. In Figure 9 the ethyl acetate selectivity theoretical and experimental profiles, obtained in the above described conditions, as function of the temperature have been compared.

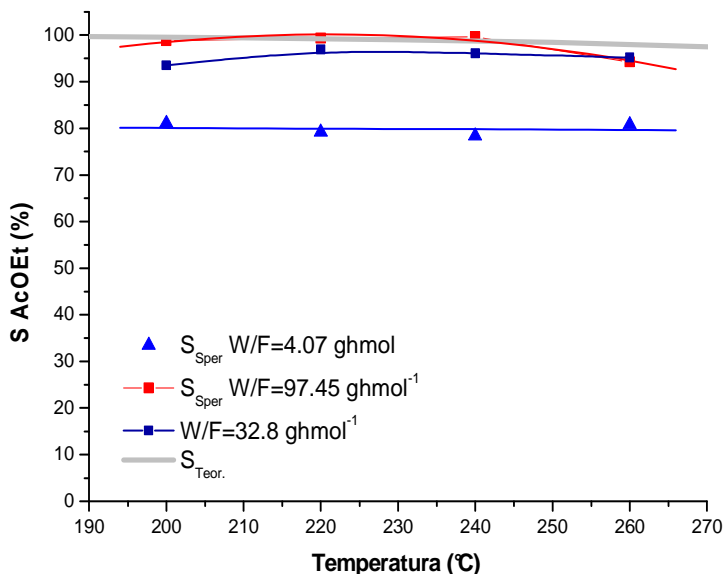


Figure 9: comparison of the ethyl acetate experimental selectivities profiles at 20 bar with the thermodynamic values.

The selectivities profiles show that at low residence time the experimental selectivity to ethyl acetate is of about 80%, a value less than the theoretical ones (100%), obtained at equilibrium in the examined range of temperatures (200-260°C). At high residence time a

good agreement between the experimental (96-98%) and theoretical values (100%) has been obtained. At high residence time the equilibrium selectivity value, imposed by the thermodynamic constrains, has been considered.

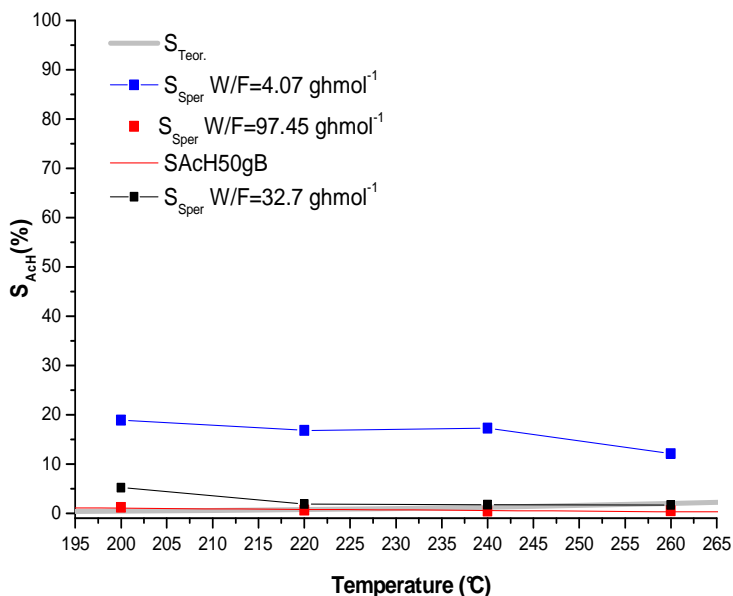


Figure 10: comparison of the experimental acetaldehyde profiles obtained at a pressure of 20 bar with the theoretical ones.

The acetaldehyde selectivity at lowest residence time is more favored (16-19%) than by operating at higher residence time. This behavior is in good agreement with which suggested by the thermodynamics studies. The high-pressure operation suppresses both the ethanol conversion and the formation of by-products such as butanone and 1-butanol, derived from acetaldo, which can be rationalized by the decrease in the partial pressure of acetaldehyde caused by a shift in equilibrium among ethanol, acetaldehyde, and hydrogen at high pressure. Consequently, a high selectivity to ethyl acetate is achieved

by suppressing the acetaldehyde partial pressure in the initial elementary reaction rather than by suppressing each elementary reaction for the by-products. Finally in Figure 10 the acetaldehyde profiles of selectivities have been compared with the theoretical ones. The thermodynamic study of ethanol dehydrogenation reaction at high temperature and pressure has suggested how to maximize the main desired product of reaction, ethyl acetate, by choosing the optimal range of operative condition. A total conversion of ethanol should be obtained at a temperature of about 600°C, at which the acetaldehyde selectivity is higher. At this purpose to favor the ethyl acetate formation reaction a temperature of reaction of about 220-240°C should be used. As well, the pressure has a great influence on the final ethanol conversion, in fact the increase of the reaction pressure could decrease the ethanol conversion that achieved a conversion of 100% at higher temperature. The increase of pressure favors the ethyl acetate selectivity with respect to acetaldehyde. The last product is favored at low pressure and high temperature of reaction (>300°C). By comparing the experimentally ethanol conversion profiles with the theoretically ones a discrepancy has been observed, in fact the experimentally conversion is higher than the conversion observed at equilibrium. This behavior could be justified taken in account the simplification made on the models, as already above discussed. A good agreement has been obtained, at higher residence time, between the theoretically and experimental selectivities of both ethyl acetate and acetaldehyde.

B-3.5 References

- [1] R.Tesser, V.Maradei, M.Di Serio, E.Santacesaria *Ind.Eng.Chem.Res.* 2004, 43, 1623-1633.
- [2] E.Santacesaria, M.Di Serio, A.Sorrentino, R.Tesser *Journal of molecular catalysis*, 2003, 204-205, 617-627.
- [3] Balci, *Ind.Eng.Chem.Res.* 2006, 45, 3496-3502.
- [4] Inui,K., Kurabayashi,T., Sato,S. & Ichikawa,N. Effective formation of ethyl acetate from ethanol over Cu-Zn-Zr-Al-O catalyst. *Journal of Molecular Catalysis A: Chemical* **216**, 147-156 (2004).
- [5] Perry RH, Green DW, Maloney JO.Perry's chemical engineers' handbook, New York, McGraw-Hill- 1999.
- [6] J.M.Prauniz, *The properties of gases and liquids*, fifth edition.
- [7] Franckaerts,J. & Froment,G.F. Kinetic study of the dehydrogenation of ethanol. *Chemical Engineering Science* **19**, 807-818 (1964).¹
- [8] G. Soave, *Chem. Eng. Sci.* 27, 1197 (1972)
- [9] PhD.Thesis, Petr Chladek, University of Waterloo.
- [10] Kanichiro Inui 1,2 Toru Kurabayashi, and Satoshi Sato *Journal of Catalysis* **212**, 207–215 (2002).
- [11] Priscila C. Zonetti, Johnatan Celnik, Sonia Letichevsky, Alexandre B. Gaspar, Lucia G. Appel* *Journal of Molecular Catalysis A: Chemical* 334 (2011) 29–34.
- [12]P.C. Zonetti et al. / *Journal of Molecular Catalysis A: Chemical* 334 (2011) 29–34.

SECTION B

Chapter 4

Experimental Results

B-4.1 Introduction

The ethanol dehydrogenation to ethyl acetate and pure hydrogen, in one-step reaction, has been studied by using several commercial copper-based catalysts.

The use of copper catalysts is fundamental to limit the undesirable decomposition of acetaldehyde to CH_4 and CO , in fact copper is able to dehydrogenate ethanol without splitting the C-C bond.

The early literature works related to the ethanol dehydrogenation to ethyl acetate date back to Dolgov et al. [1] that studied the performances of $\text{Cu/ZnO/Al}_2\text{O}_3$ (Cr_2O_3) and $\text{Cu-Cr}_2\text{O}_3$ catalysts. Many other researchers have then studied the same reaction using copper based catalysts and we can distinguish two different classes of such catalysts containing respectively copper/copper chromite [2-4] and copper metal supported and/or promoted by different oxides such as: Al_2O_3 , Cr_2O_3 , ZnO , ZrO_2 , SiO_2 [5-10].

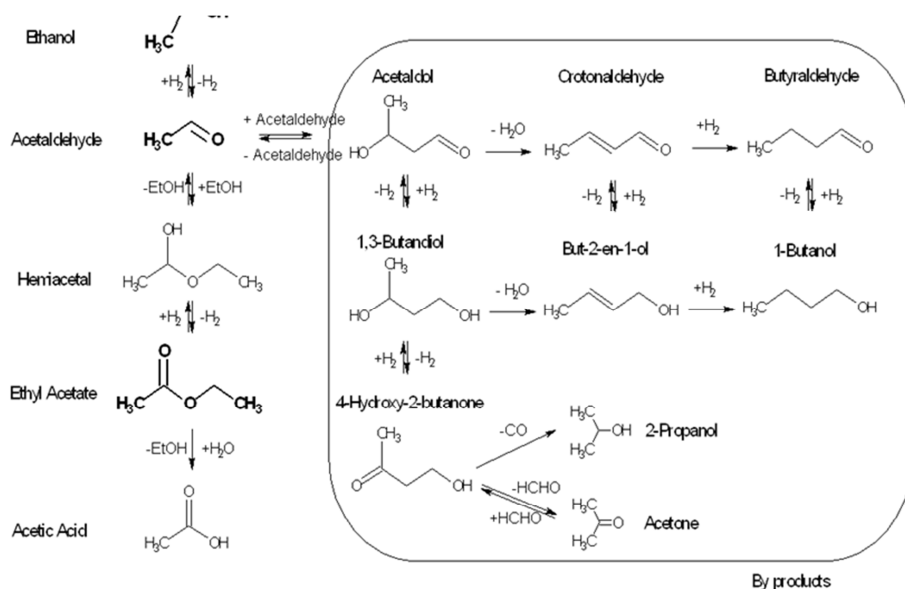
In particular, the copper chromite containing catalysts are useful for a variety of chemical reactions and one of the major applications of this system includes hydrogenation of fatty acids to fatty alcohols, without hydrogenating the eventual double bonds. Supported and promoted copper catalysts are used in many reactions of industrial interest and methanol synthesis, methanol steam reforming, low temperature wa-

ter gas shift reaction are significant examples. The presence of oxide compounds has, in some cases, the scope of slowing down the catalyst deactivation, because of copper sintering. The physical properties of copper chromite have been deeply investigated by several authors [11-18].

By reacting ethanol, according to the adopted type of catalyst and to the operative conditions, acetaldehyde or ethyl acetate as main products were obtained. Moreover, in some cases many by-products, essentially deriving from acetaldehyde, can also be attained. The pathways of the ethanol dehydrogenation are illustrated in Scheme 1 [8]. The challenge of this research work is to individuate an alternative catalytic system able both to resist to the high temperature and pressure of reaction and to give high selectivity to desired product by suppress the collateral reactions.

At this purpose, the reaction has been conducted in a conventional packed bed tubular reactor, by exploring a temperature range of 200-260°C and a pressure range of 10-30 bars. The best results have been found by using a commercial copper/copper chromite catalyst, supported on alumina and containing barium chromite as promoter, operating at 220-240°C, 20 bars and 98 (grams hour/mol) of ethanol contact time.

In these conditions, a conversion of 65 % with selectivity to ethyl acetate of 98-99% has been obtained. Another aspect to take in account is the production of high yield of pure hydrogen exempt by CO_x impurities. Therefore, this catalyst is a good candidate for developing a new process [19] and the optimal operative conditions have been individuated. In this section, several commercial copper based catalysts, promoted with zinc and chromia, unsupported and supported on alumina in the ethanol dehydrogenation reaction to produce ethyl acetate and pure hydrogen have been studied. The details related to the catalysts composition, the apparatus of reaction and the operative conditions were reported already in Chapter 2 of the current section.



Scheme 1: pathways of the ethanol dehydrogenation reaction

The main aim of this chapter is to show the chemical/structural properties of copper based catalyst, their performances in the ethanol dehydrogenation and finally to correlate the performances of the examined catalysts to their structural and chemical features, evaluated on the basis of ex-situ and in-situ characterization techniques. At the end of this chapter, the obtained results have been discussed on the basis of an hypotized and reliable reaction mechanism.

B-4.2 Catalysts characterization

The techniques employed to characterize the prepared catalysts could be classified in two different categories: ex-situ characterization such as BET, X-ray diffraction (XRD), scanning electron microscopy (SEM)

and X-ray photoelectron spectroscopy (XPS) and in-situ ones diffuse reflectance infrared fourier transform (DRIFT) in presence of ethanol and X-ray adsorption near edge spectroscopy (XANES). A detailed description of the equipment employed to characterize these materials and of the operative conditions used to pretreat the materials and to analyze, the same have been reported in APPENDIX A. The optimization of the operative conditions is a key of crucial interest to optimize and study in depth the physical and chemical characteristics of the materials with the scope to correlate them to the performances of the catalysts in the reaction of interest, the ethanol dehydrogenation to ethyl acetate.

B-4.2.1 Ex-situ characterization

The specific surface area, the pores volume and pores distribution of the employed catalysts are reported in Table 1. The table reports also the copper dispersion and copper surface area for the best catalytic systems. The calculations, employed to evaluate the dispersion and the copper surface area, are reported in APPENDIX A.

The results of Table 1 show that the BASF copper chromite catalyst Cu-1234-1/16-3F, supported on alumina, has a specific surface area, of $127 \text{ m}^2/\text{g}$; this value is much higher than the specific surface area of the both unsupported Cu/copper chromite catalyst supplied by Sud-Chemie ($21 \text{ m}^2/\text{g}$) and Cu-0203 ($13 \text{ m}^2/\text{g}$) by BASF company.

In Figure 1, the N_2 sorption isotherms for the three mentioned catalysts are reported, while, in Figure 2 are reported the corresponding pore size distributions.

The specific surface area and the pores distribution of the catalyst BASF K-310 are, on the contrary, comparable with ones of the BASF Cu-1234-1/16-3F catalyst. The characteristics of another commercial Cu-Zn-Al-O catalyst have also been studied. The presence of alumina, in both BASF catalysts, is responsible of the relatively high specific surface area. Furthermore, in Table 1 are also reported the dispersion and

the specific surface area of Cu determined with the N₂O method for each catalyst.

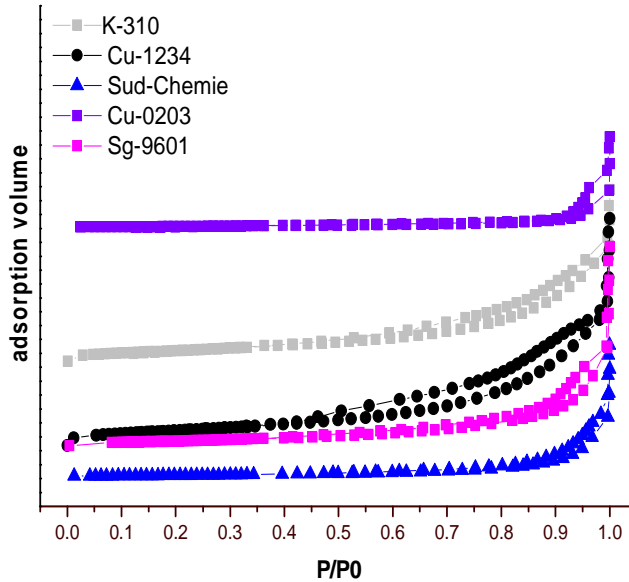


Figure 1-BET N₂ sorption isotherms for the three tested catalysts.

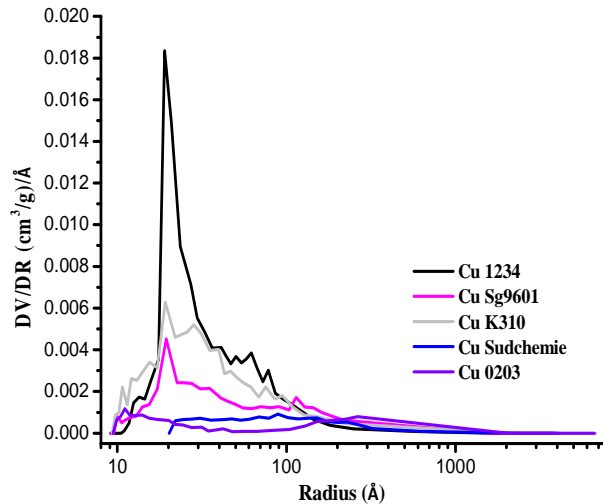


Figure 2: pore distribution curves

Table 1. Specific surface area, pores volume distribution, copper surface area and dispersion and for all the proven catalysts.

Sample	Composition given by the companies	Surface area (m ² /g)	Pores volume (cm ³ /g)	Copper dispersion %	Cu surface area (m ² /g)	Pore distribution, vol. %		
						r<20Å	20Å<r<1000Å	r>1000Å
BASF K-310	CuO-ZnO-Al ₂ O ₃ (40-40-20 % b.w.)	106	0.29	1.97	4.05	10.08	83.66	6.23
BASF Sg-9601	CuO:ZnO:Al ₂ O ₃ (37:37:26)	62	14.2	-	-	7.00	87.3	5.70
BASF Cu-1234	CuCr ₂ O ₄ -CuO-Cu-BaCrO ₄ -Al ₂ O ₃ (45-1-13-11-30 % b.w.)	127	0.41	1.22	2.05	12.27	83.84	3.90
Sud-Chemie T-4466	CuO/CuCr ₂ O ₄ (CuO/Cr ₂ O ₃ = 53/45)	21	0.11	1.48	3.71	-	89.83	10.16
BASF Cu-0203	Cu:Cr (CuO/Cr ₂ O ₃ =64:36%b.w)	13	2.90	-	-	6.60	78.00	15.4

As it can be seen in Table 1, the BASF K-310 catalyst has both the highest Cu dispersion and specific surface area. It is interesting to observe that the unsupported catalyst T-4466, despite the lowest overall specific surface area, shows a Cu dispersion and a Cu specific surface area comparable with that of the BASF K-310 catalyst. At last, the catalyst Cu-1234 shows the lowest dispersion and copper surface area, notwithstanding the presence of 30% b.w. of an alumina support. Probably, this catalyst has been calcined at relatively high temperature; this involves the grown of the Cu particles by sintering inside the promoters to obtain a stable configuration. The alumina support, in this case, has the main scope to disperse the copper chromite particles, as it can be appreciated by observing the XRD diffraction patterns, reported in Figure 3, related to the fresh copper chromite based catalysts (not pre-treated with hydrogen).

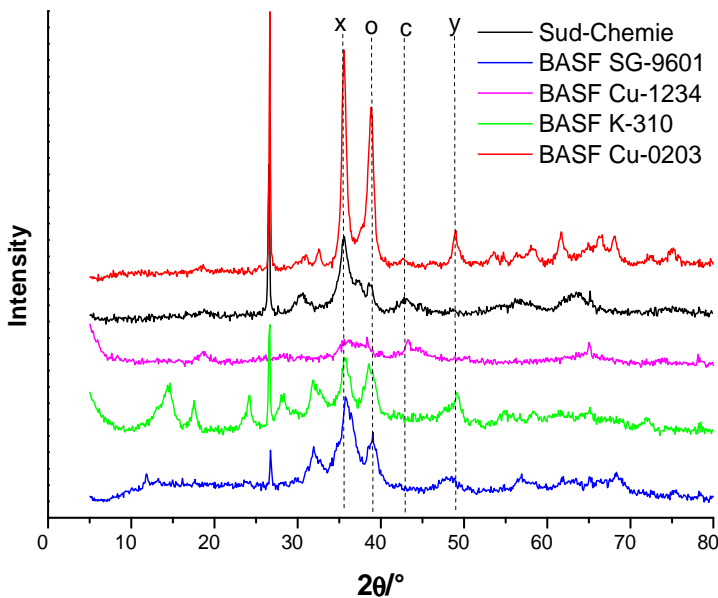


Figure 3: XRD diffraction patterns obtained for the different examined catalysts. (x) (o) cubic spinel CuCr_2O_4 . (o) CuO . (c, y) Cu (0).

As a matter of fact, the copper/copper chromite catalyst Cu-1234-1/16-3F shows different wide and weak diffraction peaks indicative of small copper chromite particles size in the 2θ range $35\text{-}37.5^\circ$, that are related to the cubic spinel CuCr_2O_4 probably with a structure stabilized by protons, as different authors have previously suggested for catalysts reduced with hydrogen (this is a catalyst pre-reduced by the supplier) [20-22].

The Sud Chemie T-4466 catalyst shows, on the contrary, more sharp diffraction peaks and even if it is well known that for the above mentioned 2θ range CuCr_2O_4 diffraction peak is overlapped with the CuO one [23], on a qualitative basis it is possible to conclude that the T-4466 catalyst is characterized by CuCr_2O_4 crystallites greater than the Cu-1234-1/16-3F one. This is also confirmed by the great difference in specific surface area of the two mentioned catalysts. The X-Ray diffraction peaks at $2\theta = 42^\circ\text{-}43^\circ$ are typical of Cu (0) phase. The analysis of the diffraction pattern, related to BASF K-310 catalyst, shows CuO phase peaks and also the presence of other different compounds like aurichalcite $((\text{Cu,Zn})_5(\text{CO}_3)_2(\text{OH})_6)$ at $15^\circ\text{-}28^\circ$ 2θ and hydrozincite $(\text{Zn}_5(\text{CO}_3)_2(\text{OH})_6)$ at $25^\circ\text{-}32^\circ$ 2θ . Alumina used as support for both the BASF catalysts resulted an amorphous phase. Moreover, three SEM images of a copper-chromite catalyst T-4466, the copper chromite alumina catalysts Cu-1234 and finally of the K-310, of $\text{CuO-ZnO-Al}_2\text{O}_3$ are depicted in Figure 4A-4B (APPENDIX A).

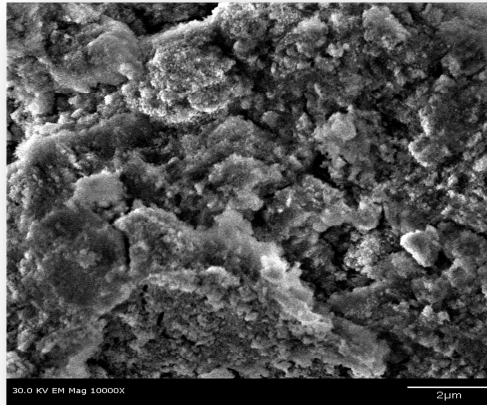


Figure 4A: SEM micrographs recorded under 30 KV, 500 nm of CuCrAl (Cu-1234).

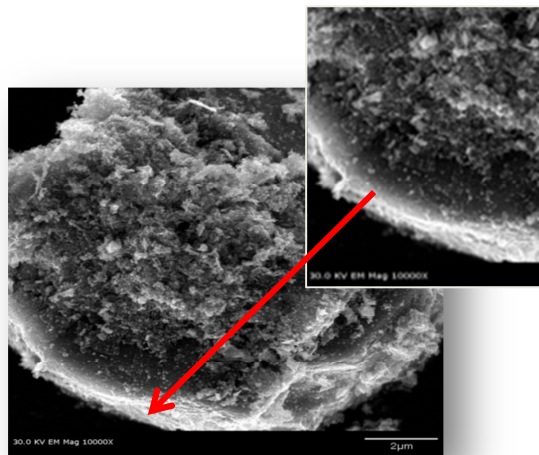


Figure 4B: SEM micrographs recorded under 30 KV, 500 nm of CuZnAl (K-310).

A Careful examination of the micrograph at a magnification of the catalyst Cu-1234, reported in Figure 4A, reveals that is not easy to identify particles of copper on a surface. These results are in agreement with both the TPO measure of low surface area and low copper surface dispersion and XRD. Well, to clarify this statement, as showed by the TPO results the copper surface of Cu-1234 are is $2.05 \text{ m}^2/\text{g}$, this value is lowest respect to the ones obtained for the other catalysts, thus, this low dispersion (1.22%) is due to the low concentration of copper on the catalyst surface. Moreover, the SEM could clarify the XRD diffraction pattern of Cu1234, in which the peaks look like weak and abroad for effect of the alumina support; more probably, this catalyst has been prepared by coprecipitation of metal salts. In the case of K-310, which SEM is reported in Figure 4B, a closer view of some of the larger particles reveals the existence of much smaller particles on the surface has been reported. These features are estimated to be $\sim 10\text{-}20 \text{ nm}$ in size and may account for some of the dispersed copper phase observed in the XRD patterns.

The surface composition of three fresh catalysts was measured by x-ray photoelectron spectroscopy (APPENDIX A). The samples were examined in oxidized form, because the XPS instrument was not equipped of a pre-reduction chamber. Moreover, a pre-reduction, not in-situ, of the sample, first of XPS measure, turns out to be needless because, as demonstrated by the phd thesis work [24] by transferring the samples, after the reduction, to the XPS sample analysis apparatus, the oxidation cannot be ruled out and consequently, the obtained results could be not easy to interpret. Surface atomic weigh percentage of each elements for the three examined catalysts, obtained by CASA elaborator, are presented in Table 2. As shown the catalyst Cu-1234 has the lowest content of copper on the catalyst surface, this result is in good agreement with the TPO measure of the copper dispersion [25].

Table 2: Concentration of each component on the catalysts surface

Catalyst	Cu 2p	O 1s	C 1s	Al 2p	Cr 2p	Ba	Zn
Cu-1234	7.3	54.7	12.7	21.1	3.7	0.4	
T-4466	11.2	44.7	28.0		11.8		
K-310	15.4	48.2	17.1	16.2			7.2

The Figure 5A shows that Cu-1234, T-4466 and K-310 exhibit binding energy signals at 932.2-932.8 eV that corresponds to Cu^{2+} in Cu_2O compound is generally attributed to Cu^{2+} located in an octahedral and tetrahedral sites of CuCr_2O_4 , in agreement with Zhang and Brooks literature works [26,27]. K-310 exhibits distinct satellite peaks suggesting Cu^{+2} as in CuO , indicating that the catalyst is in a fully oxidized state.

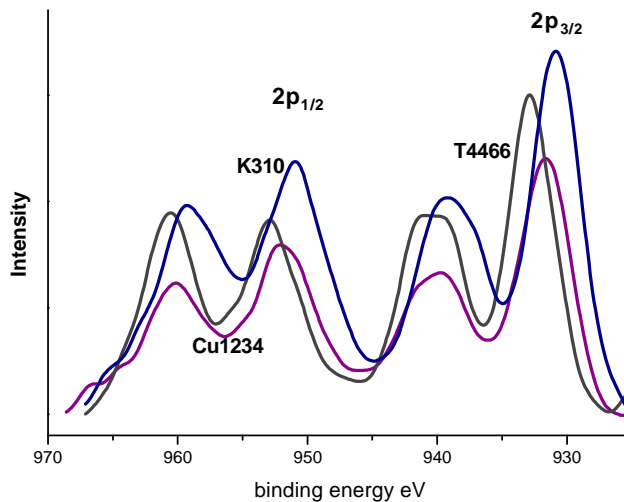


Figure 5A: XPS binding energy signals of copper

The binding energy Cr 2p_{3/2} of all the catalysts containing chromia is in the range 576.58-578.7 eV attributed to the Cr^{3+} in Cr_2O_3 compounds (Figure 5B), in good agreement with studies by Brooks et al. (577.0 eV)[27].

The spectra reported in Figure 5B shows a small variation in binding energy of Cr observed in T-4466, the shoulder peak at higher binding energy in each manifold (ca. 580 eV Cr 2p_{3/2}) is assigned to the Cr⁶⁺ present in the previously characterized CuCrO₄ phase [28].

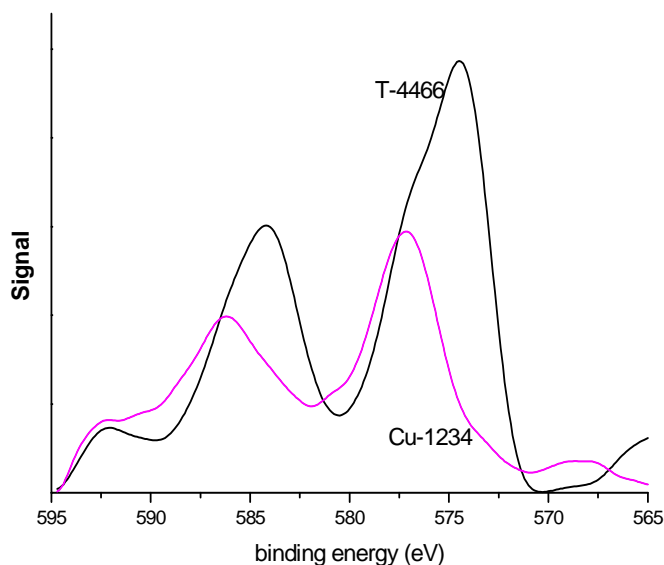


Figure 5B: XPS binding energy signals of chromium

All the mentioned catalysts have been submitted to thermal programmed reduction (TPR) with hydrogen, in order to evaluate the degree of reducibility of the copper species APPENDIX A.

Before the TPR, the catalysts were pretreated with an inert nitrogen flow by gradually increasing the temperature until 300°C. The catalysts were then cooled at room temperature and again heated from room temperature to 300°C in a flow stream of 25 cm³/min consisted of 6% of hydrogen in nitrogen, as already described in a previous section. The obtained results are reported in Figure 6. A first observation is that the reduction of the copper chromite catalysts starts in both cases at the same lower temperature of about 150°C, while, the start tem-

perature for K-310 catalyst is 180° C. In particular, in the case of copper chromite catalysts is possible to observe a shift of the starting temperature of reduction hinge on by the chromium content.

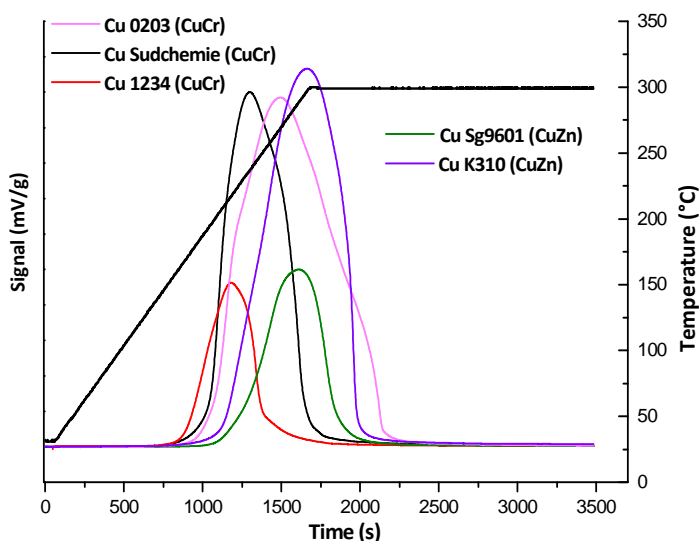


Figure 6: TPR profiles of Cu-1234, T-4466, Cu-0203, Sg-9601, K310. Temperature range: 25-300°C. Reduction realized with a stream of 25 cm³/min of 6%H₂ in N₂

At higher chromium content, as in case of the Cu-1234, the maximum temperature of reduction has been localized at about 200°C, by decreasing the chromium content (Cu-0203) the maximum temperature of reduction is observed at 270°C.

Another observation is that the peak area obtained for the BASF 1234-16-3F ($8.6 \cdot 10^6$ mV s/g) catalyst is much smaller than the others obtained for both the catalysts of copper-chromite respectively Sud Chemie T-4466 ($2.26 \cdot 10^7$ mV s/g) and Basf Cu-0203 ($3.49 \cdot 10^7$ mV s/g) and the catalysts of copper-zinc BASF K-310 ($8.60 \cdot 10^7$ mV s/g) and BASF Sg-9601 ($1.13 \cdot 10^7$ mV s/g), in agreement with the fact that this is a pre-reduced catalyst. The low reduction area of the catalyst Sg-9601, also in this case, could be ascribed to the pre-reduced nature of the

catalyst. The pre-reducing treatment is almost necessary to obtain a more stable configuration but on the other hand, this treatment could get catalyst with a lowest specific surface area. Several considerations about the copper reducibility have been found in literature. According to the literature [13, 34] Cu^{2+} can be reduced to Cu° by hydrogen through two different reactions, being the following the first one:



The reduction of copper oxide not linked to chromium oxide is a reaction occurring for all the tested catalysts. The second copper reduction path is that of copper chromite, occurring for about 50% of the total copper chromite through the following reaction [34]:



Cu° formed in this way, grows epitaxially [34] on the spinel surface, while, H^+ remains inserted into the spinel structure taking the place of Cu^{2+} for compensating the negative charges of the crystal lattice. This process could be labeled by the following equation:



The spinel $\text{Cu(II)}(1-y)\text{H} + 2y\text{Cr}_2\text{O}_4$ is an acid catalyst in which, in case of Cu-1234, some basic promoters of Barium oxide are dispersed.

By observing Figure 6, it is clear that the catalysts Cu-1234, T-4466 and Cu-0203 containing copper chromite, are more reducible than K-310 and Sg-9601. In the TPR profile of the pre-reduced catalyst Cu-1234, the low peak area at 225°C has been attributed almost exclusively to the effect of the reaction (2). As a matter of fact, by heating this catalyst under a stream of inert gas, at 300°C, as in our previously described pre-treatment, the inverse of the reaction (2) occurs as shown by Colley et al.⁴ and copper ions formed return to be reducible with hydrogen.

The amount of hydrogen consumed in the TPR, for the catalyst Cu-1234, was 1.14 mmols/(g of catalyst), while, the copper reducible with

the reaction (1), on the basis of the catalyst formulation, corresponds to 0.124 mmols/g, related to the content of 1% of CuO. 0.975 mmols/g are, on the contrary, related to 50% of the copper chromite, that is, in total 1.10 mmoles/g corresponding to a good agreement for the pre-reduced catalyst. The catalyst T-4466 has given a value for the hydrogen consumed of 3.01 mmoles/g that is less than the value obtainable by the declared composition ($\text{CuO} + 1/2 \text{CuCr}_2\text{O}_4$) corresponding to a minimum value of about 5 mmoles/g. Probably, in this case, the reduction occurring during the TPR until 300°C is not complete and higher temperature are necessary to obtain the complete reduction of the catalyst. As matter of fact the copper chromite T-4466 was reduced also at higher temperature of about 600°C. In this particular case the hydrogen consumed, of 5.99 mmoles/g, correspond exactly to the value obtainable by the declared composition of 6.00 mmoles/g. At this purpose the catalysts could be reduced at high temperature or at lower temperature but for more prolonged time in particular 16-18h are enough to reduce completely also at 200°C the copper catalyst surface. Tu et al. [2-3] has shown that the catalysts reducibility is strongly dependent by the catalytic environment. As shown by Prasad [30] and Adkins [31], the reduction of the species Cu^{2+} is withdrawn by the eventually presence of basic oxide such as chromia or zinc oxide. The chromia has been considered a good structural promoter for its ability to achieve dispersed the copper because it could not be reduced at temperature higher than 800°C [32,33]. Finally, K-310 catalyst gives place to a H_2 consumption of 4.07 mmols/g, instead of 5.02 mmols/g, corresponding to the CuO composition. In this case, only reaction (1) occurs. Maybe, less reducible complexes of copper with zinc are formed. The NH_3 -TPD measurements were carried out with the scope of determining the characteristics of the surface acidity of the different examined catalysts (APPENDIX A). In Figure 7 the NH_3 -TPD plots, obtained for respectively the K-310, T-4466 and Cu-1234, catalysts are

reported. Both K-310 and Cu-1234 catalysts show similar surface acidity in the range of 100-350°C and 350-450°C corresponding to respectively acid sites of weak and medium strength. This behaviour is in agreement with the observations made by Prasad et al. [30], that attributes these peaks mainly to the alumina acidity contribution.

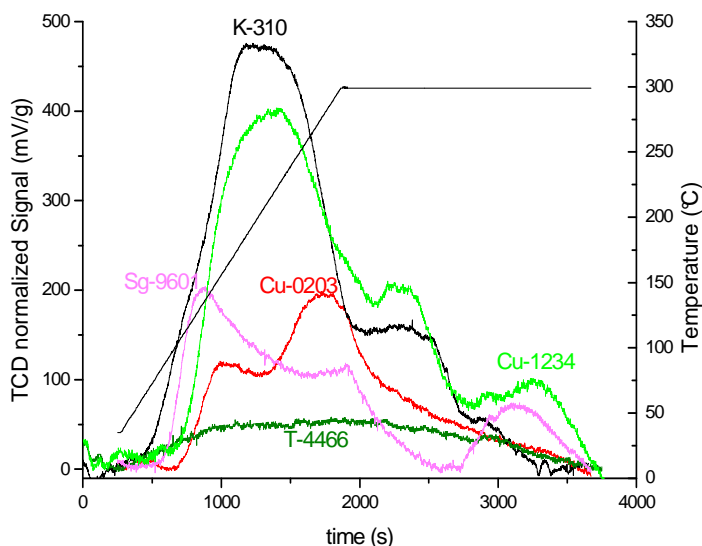


Figure 7 - A comparison of the TPD-NH₃ patterns of all the examined catalysts.

It is interesting to point out that a pronounced peak, at 500°C, has been observed for the pre-reduced catalyst Cu-1234. This peak corresponds, according to Colley et al⁴ [4], to the Bronsted acid sites formed as a consequence of reaction (2). The strong acidic sites are due to the presence also of alumina support. In fact also each catalyst of copper-zinc supported on alumina has strong acidic sites. In particular the catalyst Sg-0203, with higher content of alumina (26%_{wt}) respect to the classical Cu-Zn-Al-O formulation (20%_{wt}), have an higher concentration of strong acidic sites.

These sites are not present obviously in the copper/copper chromite fresh catalyst T-4466 and Cu-0203. Moreover, this last catalyst is less

acid because does not contains alumina support. A quantitative evaluation of the acid sites distribution is reported in Table 3.

Table 3. Surface acidities of the examined catalysts evaluated by NH_3 -TPD

Sample	Specific acidity distribution (mmol NH_3 /g)		
	$100 < T_1(^{\circ}\text{C}) < 250$	$350 < T_2(^{\circ}\text{C}) < 450$	$T_3 > 500^{\circ}\text{C}$
BASF Cu-1234	0.185	0.123	0.029
BASF K-310	0.283	0.057	0.006
Sud-Chemie T-4466	0.033	0.047	-
Sg-9601	0.143	-	0.030
Cu-0203	0.022	-	-

The CO_2 -TPD measurements were carried out with the scope of determining the characteristic of the surface basicity of the different examined catalysts (APPENDIX A). A strong surface basicity can promote the formation of ethyl acetate through the Tischenko reaction but also the acetaldehyde condensation to acetaldol and successive by products (see scheme 1). In Figure 8, the CO_2 -TPD plots obtained for respectively the copper-zinc catalysts K-310 and Sg-9601 and copper-chromia catalysts T-4466, Cu-1234 and Cu-0203 catalysts have been reported. In Table 4 are summarized the basicity distribution in four different range of temperature.

Table 4: Surface basicity of the examined catalysts evaluated by CO_2 -TPD

Sample	Specific basicity distribution (mmol CO_2 /g)			
	$100 < T_1(^{\circ}\text{C}) < 200$	$300 < T_2(^{\circ}\text{C}) < 350$	$400 < T(^{\circ}\text{C}) < 470$	$T_3 > 500^{\circ}\text{C}$
BASF Cu-1234	5.92	0.69	6.42	1.21
BASF K-310	3.32	3.91	1.23	1.69
Sud-Chemie T-4466	4.28	6.87	1.58	0.56
Sg-9601	2	-	3.47	7
Cu-0203	2.34	-	3.95	1.8

The CO₂-TPD profiles show the presence of four different basic sites with different strength respectively in the regions 100-200°C, 300-350 °C, 400-480°C and above 500°C. The obtained results are in good agreement with the ones reported in the literature [34].

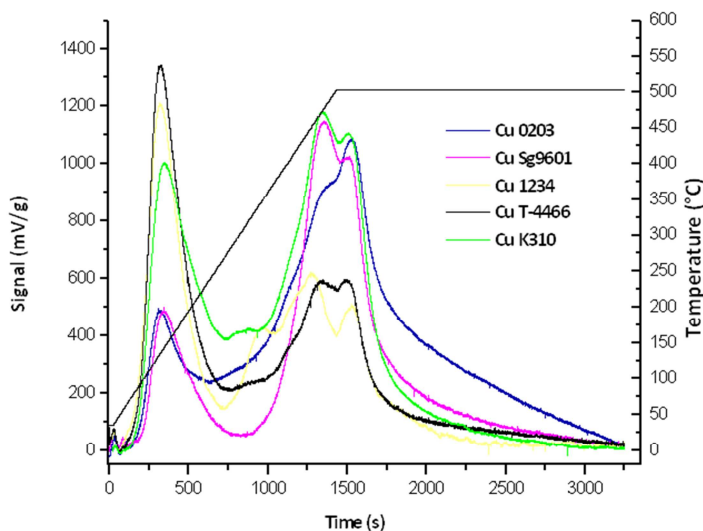


Figure 8: A comparison of the TPD- CO₂ patterns of Cu-1234, Sg-9602, T-4466, K-310, Cu-0203 examined catalysts.

Figure 8 shows that all the examined catalysts have basic sites but with a different distribution between weak, medium and high strength. K-310 is the most basic catalyst in agreement with the presence of ZnO in its composition. It is interesting to observe that the presence of BaCrO₄ reported by BASF for the catalyst Cu-1234 has a particular consequence on the surface basicity of the sample.

Probably, during the reduction pre-treatment of the catalyst, the specie BaCrO₄ is reduced to barium chromite or to a mixture of BaO and Cr₂O₃ but BaO is neutralised by the Lewis acid sites of both alumina

and chromia, because, in the TPD with CO_2 no basic sites of high strength appear.

Therefore, pre-reduced catalyst Cu-1234 shows a particular structure, if compared with the other catalysts, characterised by the presence of copper metal deposited on the chromite surface and near to Bronsted acid sites of the reduced copper chromite (reaction 9), while, BaO neutralises external acidity. The presence of Bronsted acid sites inside the reduced copper chromite have been demonstrated by Colley et al [4] attributing to these sites the good selectivities to ethyl acetate of the copper chromite based catalysts.

B-4.2.2 In-situ characterization

In-situ diffuse reflectance infrared fourier transform (DRIFT) in ethanol flow has been realized with the aim to observe the adsorbed phases produced and adsorbed on the previously reduced catalyst surface (APPENDIX A). The Figure 9A shows the DRIFT spectra for the copper chromite alumina commercial catalysts Cu-1234. Thanks to the use of such a diluent as silicon powder, the spectra of our black sample appear clear (fumed silica : catalyst= 5 : 1 wt%). The use of fumed silica is justified by the several trials that have shown the ability of black samples, characteristic of almost of the catalyst employed, to absorb the infrared radiation and to reflect weakly the radiation. The catalysts have been previously reduced in hydrogen flow at 300°C for 1h, after that a flow of inert have been fed to the chamber to clean the fitting, the tube and the chamber. After cooling the chamber, a flow of $2.2 \text{ cm}^3/\text{min}$ of ethanol diluted in $25 \text{ cm}^3/\text{min}$ of nitrogen was feed to the catalyst compartment. The spectrum for each sample has been collected at three different temperatures, 100 , 200 and 300°C and under flowing ethanol. The assignment of the bands was made by analogy

with the spectra of known compounds and by comparison with published literatures.

The figure 9A displays the DRIFT spectra of Cu-1234, showing barely distinguished features at a wavenumber of 3750 that corresponds to the -OH group of the adsorbed ethanol.

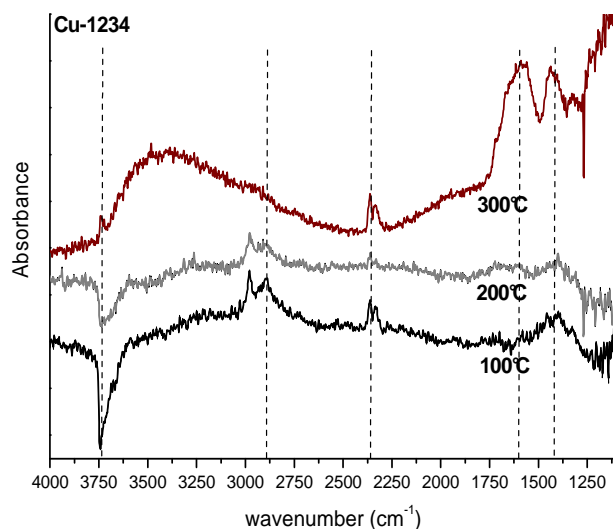


Figure 9A: DRIFT spectra of Cu-1234 at 100-200-300°C in ethanol flow of $2.2 \text{ cm}^3/\text{min}$. The catalyst was previously reduced in hydrogen flow at 300°C for 1h.

At higher temperature ($>200^\circ\text{C}$) a $1400\text{-}1600 \text{ cm}^{-1}$ a well-defined peak related to the -COO ester phase (ethylacetate) have been identified [35], where the signal at 1550 cm^{-1} corresponds to $\nu_{\text{sym}}(\text{COO})$ [36-38]. At a wavenumber of $2800\text{-}3000 \text{ cm}^{-1}$, other two not well defined features can be identified that correspond to the -CH_3 and/or $\text{-C}_2\text{H}_5$ groups. By increasing the temperature the bands of adsorbed -OH disappear, indicating the ethanol consumption in favor of the formation of the ester group in a range temperature of $200\text{-}300^\circ\text{C}$ [39,40]. More probably the ethylacetate adsorbed on copper catalyst gets a signal, re-

lated to C=O stretch, at about 1650 cm^{-1} while the signal at 1550 cm^{-1} is related to the same specie adsorbed on alumina [41]. An important aspect to take in account is the total absence of acetaldehyde adsorption signal that generally is observed at 1750 cm^{-1} . The nonappearance of adsorbed aldehyde is fundamental, because is a synonymous of a catalyst that does not deactivate because of fooling phenomenon. At this purpose, it is possible to anticipate that the promoters of chromium and zinc have the function to limits the adsorption of acetyl specie on the surface.

In Figure 9B the DRIFT spectra of a copper chromite catalyst has been represented. The spectra also in this case shows different bands corresponding to -OH at 3750 cm^{-1} , -CH_3 and $\text{-C}_2\text{H}_5$ at $2800\text{-}3000\text{ cm}^{-1}$, CO_2 adsorbed at $2300\text{-}2400\text{ cm}^{-1}$, acetaldehyde specie at 1757 cm^{-1} but the intensity of the signals related to the adsorbed esters species are relatively less intense.

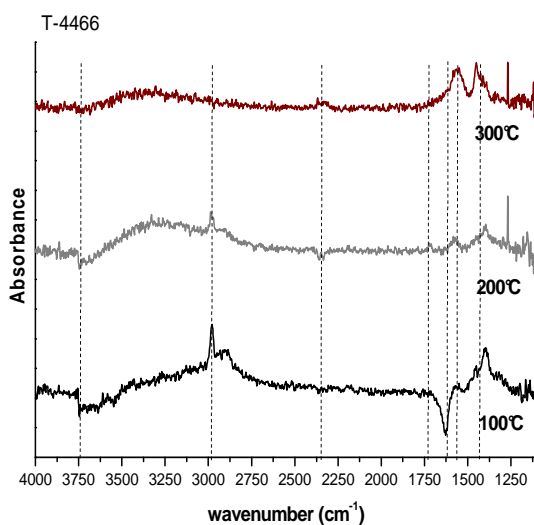


Figure 9B: DRIFT spectra of T-4466 at 100-200-300°C in ethanol flow of $2.2\text{ cm}^3/\text{min}$. The catalyst was previously reduced in hydrogen flow at 300°C for 1h.

Finally figure 9C, related to the catalyst Cu/ZnO/Al₂O₃ (K310), shows the signal related to C=O stretch of acetaldehyde group at relatively low temperature 100°C. At higher temperature, the signal of adsorbed ethanol disappears in favor of the esters. Probably the catalysts are not able to adsorb acetaldehyde that is present essentially in the gas phase. Another possibility is related to the kinetic of esters formation that is faster than the acetaldehyde formation. Once formed the acetaldehyde this reacts rapidly with the unreacted ethanol to get ethyl acetate and for this reason the acetaldehyde adsorbed is not detected or the signal is relatively low. This last aspect confirms that the acetaldehyde is an intermediate of reaction.

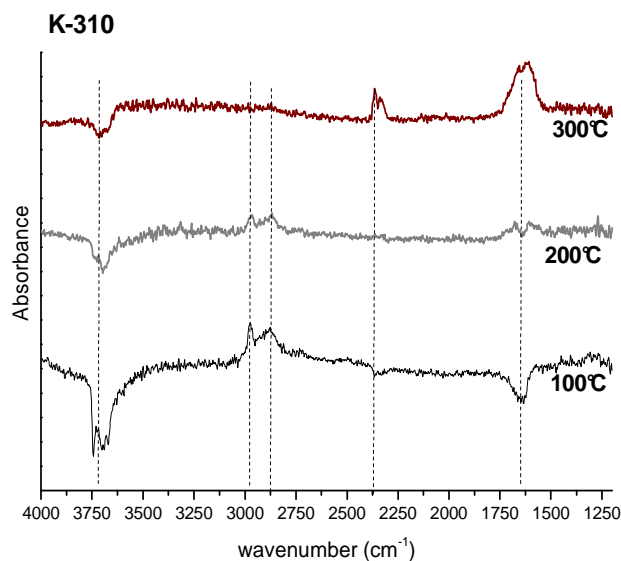


Figure 9C: DRIFT spectra of K-310 at 100-200-300°C in ethanol flow of 2.2 cm³/min. The catalyst was previously reduced in hydrogen flow at 300°C for 1h.

The more clear spectra of Cu-1234 and K-310 can be justified on the basis of the better reflectance of the catalysts provided by the alumina support. A possible scheme of the reaction, on the basis of the FTIR results can be proposed (Figure 10).

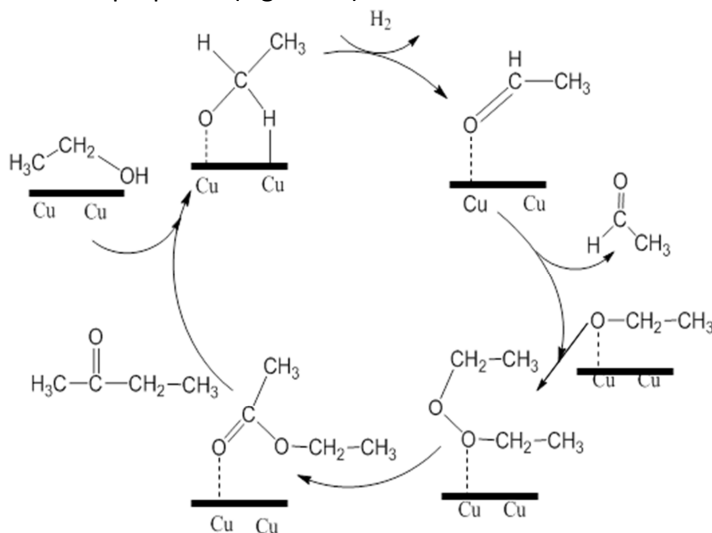


Figure 10: scheme of reaction obtained on the basis of FTIR investigation.

The hypothesized mechanism is in agreement with the ones proposed by Inui et al. A possible route toward the formation of ethyl acetate has been already discussed [6,43,44], but the several theories look like controversial. As reported by Inui the reaction proceeds via hemiacetal as an intermediate, formed by ethanol adsorption, whereas hemiacetal has not been detected in the reaction of ethanol [7-10]. The fine structure, of Cu and Cr was determined by using in-situ EXAFS/XANES. The experiments were conducted in order to determine oxidation states of Cu and Cr during different reaction conditions. The XANES and EXAFS experiments were carried out at the Advanced Photon Source (APS) of Argonne National Laboratory (ANL) (APPENDIX A). The

spectra were obtained in transmission mode at the sector 10 MRCAT (Material Research Collaborative Access Team) beam line B, equipped with a bending magnet. The experimental data obtained is fitted to the model scattering equation to get the coordination numbers; inter-atomic distances using standard the WINXAS97 and ATHENA software. Self-supported catalyst wafers were prepared by pressing the sample, diluted by silica, in a cylindrical holder with multiple channels that can contain up to six catalysts at a time. In Figure 11 the picture of the configuration of reactor and wafers employed is illustrated.

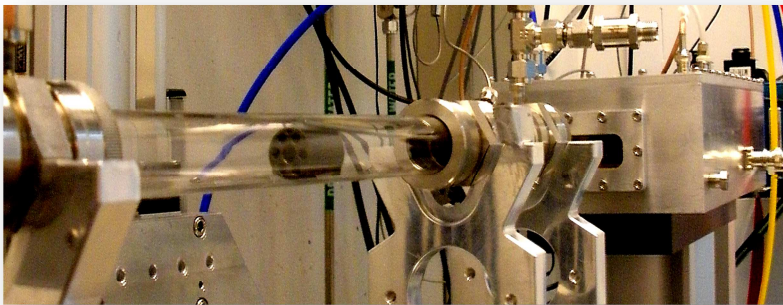


Figure 11: reactor and wafer configuration system employed to realize the Xanes measure

The dilution of a sample with silica and the amount of diluted sample to make wafers were adjusted to get the optimized absorption edge height $\chi(E)$ to about 1 unit. In Cu, Cr, Zn samples, the value of dilution ratio varied between 1:2 to 1:7 (wt sample: wt silica) and the typical amount required for wafer preparation was 7mg-15mg of the diluted sample. The 6 channel multiple sample holder was placed in the center of a quartz reaction tube of 0.75" ID. 18" long. The tube has special fitting arrangements at both ends for inlet and outlet of the re-

actant gases to flow through the reactor as well as it had an opening for a thermocouple (K-type) to measure the sample temperature. The reactor tube fittings have openings at both ends which were covered with polyimide film providing a window to allow transmission of X-ray and a seal of the tube. The reactor set-up was heated by an electrical furnace to control the reactor temperature. This complete set up allowed us to obtain measurements during reaction conditions i.e. *in operando* mode. The sample measurements were taken in the following three conditions:

- *In air at room temperature*
- *Reduced sample at room temperature*
- *In situ at 270 °C during reaction with ethanol*
- *In air after reaction*

The sample was first reduced at 300 °C for 1 h in 5% H₂ (balance He) atmosphere at a flow rate of 50cm³/min in a hood outside the x-ray beam station to optimize utilization of the beam line. After reduction, the sample was cooled down in the gas flow to room temperature then the flow was stopped and the inlet and outlets valves closed to isolate the reactor and avoid air contact. The gas lines were disconnected and the reactor was transferred to the beam line and reactant gases reconnected, purging fitting tubes and valves before flowing reactant gases into the reactor. The spectrum was first obtained at room temperature on the reduced samples then the reactor temperature was raised from room temperature to 270 °C under the continuous flow of reactants. Standards for the reduced metals were obtained from foils and for the oxides from CuO, Cu₂O, Cr₂O₃ and CrO₃ furnished by Sigma Aldrich. By the comparison with the reference XANES spectra, the Cu K-edge XANES spectra (Cu K edge – 8979 eV analysis) of the sample have been analyzed. In order to avoid the local binding structure in the catalyst the spectra in the Xanes region has been distorted thus affects the fitting. A linear combination fitting is performed with a

fitting range of 20~30 around absorption edge and a fitting space derivative. Spectra were taken at all the three catalysts, at Cu edges of 8979 eV, to study the change in oxidation states, and estimate the size of nanoparticles (NP) and the coordination state of each element. This information is helpful in determining the oxidation state of the elements which are related to the activity and selectivity of the catalyst during reaction.

In order to understand the characteristics of the Cu K-edge XANES of Cu oxides, Cu K-edge XANES spectra of typical Cu oxides with known crystal structures and valence states have been measured. At this purpose In Figure 12A the Cu edge XANES spectra of the three different Cu standards of Cu^0 , Cu^+ and Cu^{2+} are reported.

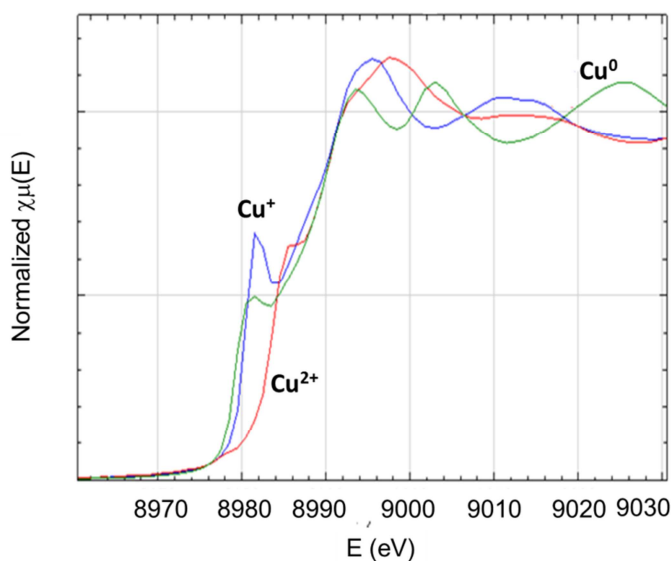


Figure12A: Cu^0 , Cu^+ , Cu^{2+} standards Xanes spectra

The XANES spectra, shown in Figure 12 (B-D), were helpful in qualitatively assessing the oxidation state of the bulk material.

As it can be seen at the Cu edge (Figure 12B) the Cu, in Cu-1234 catalyst at room temperature, is partially oxidized Cu^{2+} . After reduction, the peak edge does not match well with that of the pure Cu metal reference foil XANES. In more details after reduction of copper it is possible to identify two different oxidation states of copper: metallic Cu and Cu^{+1} species, typically presented by the spinel of copper chromite catalysts. In presence of ethanol/He only, a small change seems to take place but still mostly Cu is in reduced state.

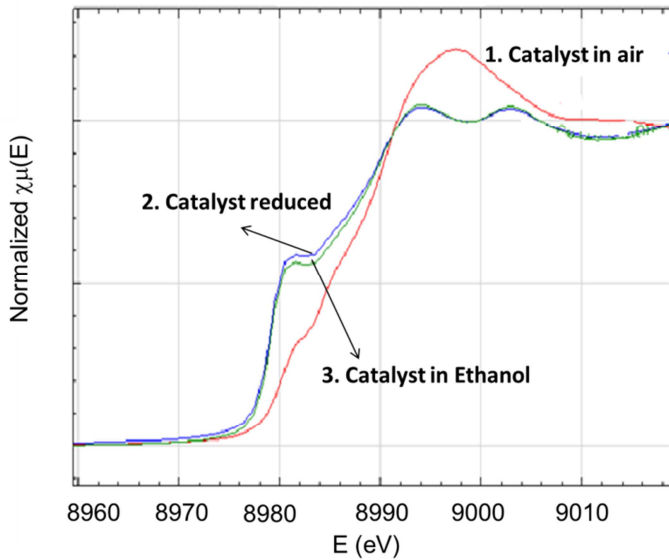


Figure 12 B: Cu Edge Xanes-Cu-1234. The measure has been done in different step. 1. Exposure to the air. 2. catalyst reduction. 3. Ethanol decomposition.

In table 5A are summarized the percentage composition of each oxidation state in the three operating mode.

Table 5A: percentage composition of each copper oxidation state

Cu oxid. state	Exposure to the Air	Catalyst Reduced	Ethanol Exposure
Cu ⁰	0.270	0.84	0.710
Cu ⁺	0.214	0.26	0.290
Cu ²⁺	0.524	-	-

The presence of two oxidation state is in agreement with the TPR measures that discriminate two different way of copper reduction. The reduction of copper oxide not linked to chromium oxide is a reaction occurring for all the tested catalysts. The second copper reduction path is that of copper chromite, occurring for about 50% of the total copper chromite. Cu⁰ formed in this way, grows epitaxially on the spinel surface, while, H⁺ remains inserted into the spinel structure taking the place of Cu²⁺ for compensating the negative charges of the crystal lattice. The spinel Cu (II)(1-y)H+2yCr₂O₄ is an acid catalyst in which, in case of Cu-1234, some basic promoters of Barium oxide are dispersed. Moreover, this behavior is demonstrated also by TPD-NH₃ measure in which the presence of strong acidic sites related to the presence of a charge H⁺ is inserted in the spinel structure. The presence of copper in two oxidation state also after reduction of the catalyst at high temperature (>300°C) could suggest that the active phase in the dehydrogenation to ethyl acetate is the spinel of copper chromite and not the reduced copper as suggested by Prasad et al. [45]. The same considerations have been done for the copper-chromia catalyst T-4466. By comparing the EXAFS spectra of the copper-chromia T4466 catalysts with the ones of the copper standard, it is possible deduce that in air the catalyst is partial oxidized form while after reduction the edge match well with that of the pure Cu metal reference foil XANES, showing a completely reduction of copper to copper foil (Figure 12 C).

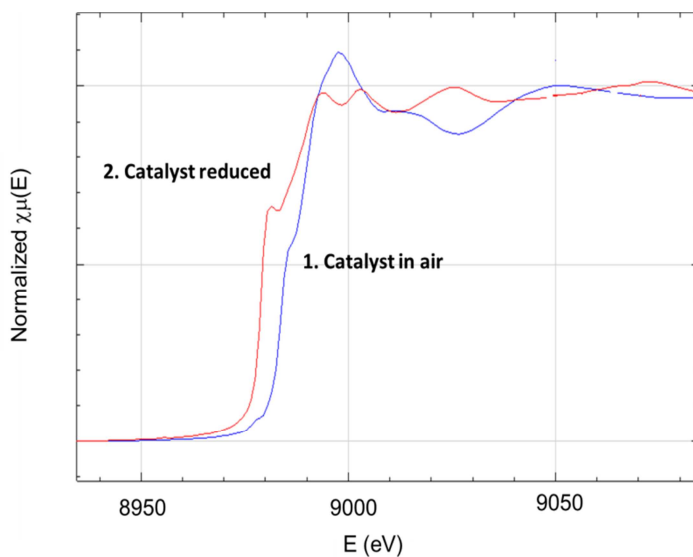


Figure 12C: Cu Edge Xanes-T-4466. The measure has been done in different step. 1. Exposure to the air. 2. catalyst reduction. 3. Ethanol decomposition.

In table 5B the composition of the different oxidation states, at two different catalyst treatments, have been reported.

Table 5B: percentage composition of each copper oxidation state for T-4466

Cu oxid. state	Exposure to the Air	Catalyst Reduced
Cu ⁰	0.085	1.00
Cu ⁺	0.018	-
Cu ²⁺	0.841	-

As it can be seen at the Cu edge (Figure 12 D) the K-310 catalyst at room temperature, is partially oxidized Cu²⁺. After reduction, the peak edge matches as well with that of the pure Cu metal reference foil XANES and on K-310 catalyst only copper foil have been individuated.

In presence of ethanol/He only, a small change seems to take place but still mostly Cu is in reduced state.

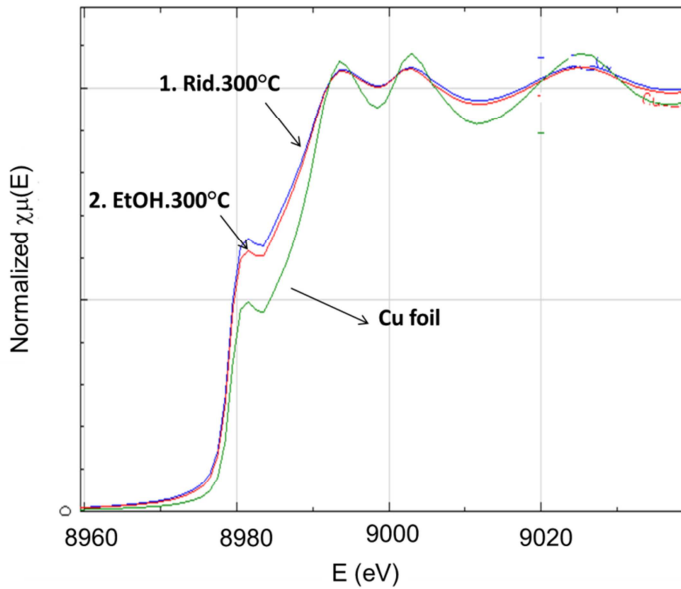


Figure 12D: Cu Edge Xanes-K310 The measure has been done in different step. 1. Exposure to the air. 2. catalyst reduction. 3. Ethanol decomposition.

In Table 5C the composition of the different oxidation states, at three different catalyst treatments, have been reported.

Table 5C: percentage composition of each copper oxidation state for K-310

Cu oxid. state	Exposure to the Air	Catalyst Reduced	Ethanol Exposure
Cu^0	-	1.000	1.000
Cu^+	-	-	-
Cu^{2+}	1.000	-	-

Spectra were taken at all the three catalysts at Cr edges of 5989 eV. At the same way in order to understand the characteristics of the Cr K-edge XANES of Cr oxides, Cr K-edge XANES spectra of typical Cr oxides with known crystal structures and valence states (standards) have been measured. One of the main drawbacks for Cr data set do not have reliable reference signal. The analysis is based on the assumption that during the measurement, there is no energy shift. Cr foil data is noisy in the xanes region. Fitting is performed in xanes region fitting range: -20 to +30 around absorption edge and fitting space energy (normalized). In Figure 13A the XANES spectra for the two chromium standard (Cr^{3+} and Cr^{6+}) have been reported.

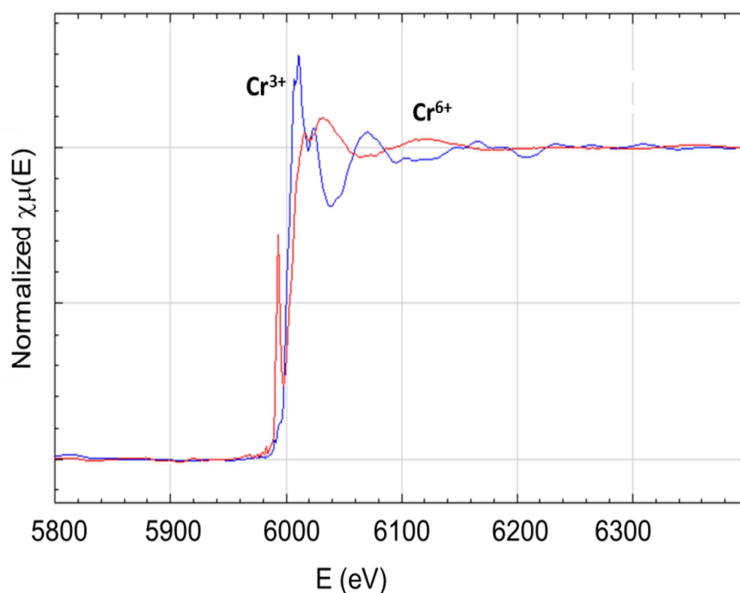


Figure 13A: Cr Edge Xanes of two standards CuCr_3 and Cu_2O_3 .

By the comparison of the chromia spectra of both the catalysts Cu-1234 and T-4466 in air with the standard Cr^{3+} (see Figure 13B) a perfect matching has been obtained.

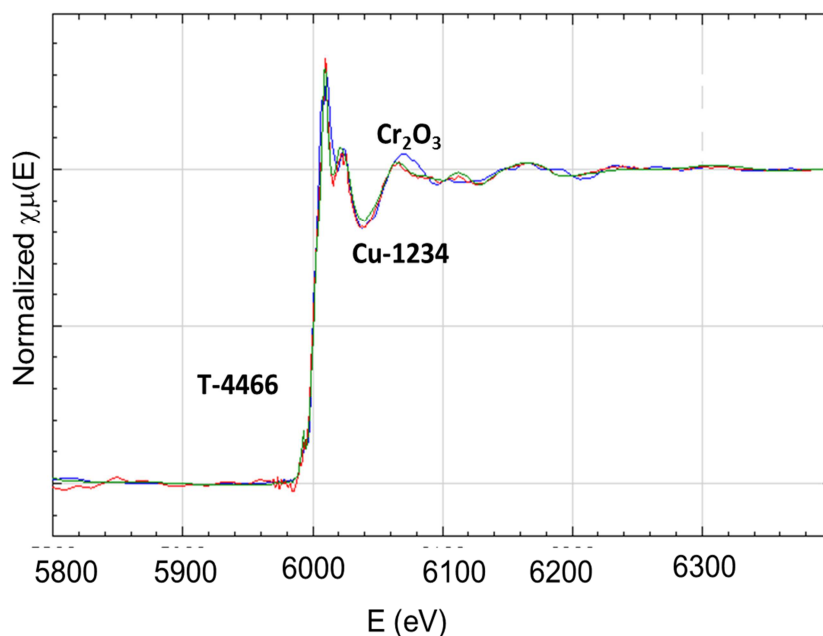


Figure 13 B: Cr Edge Xanes. Comparison of the oxidation state of two catalysts Cu-1234 and T-4466 in air.

The fresh commercial catalysts of copper chromite are Cr^{6+} free also before the pre-treatment. This is a key factor for the industrial application of these catalysts. The absence of Cr^{6+} , a possible carcinogenic element, makes this process green, safety for human healthy and at low environmental impact.

In Figure 13C are shown the EXAFS spectra for the catalysts Cu-1234 and T-4466 after reduction that are perfectly matched with the profile of the Cr^{3+} standard.

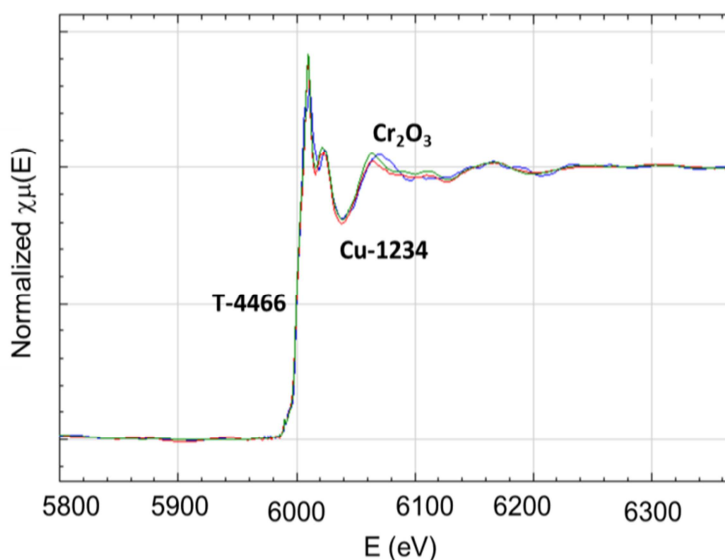


Figure 13C: Cr Edge Xanes. Comparison of the oxidation state of two catalysts Cu-1234 and T-4466 after hydrogen reduction at 300°C.

Thus, after the pre-treatment of the catalysts in hydrogen flow, no great changes in the chromium oxidation states have been detected. After a detailed description of the physical and chemical characteristic of the commercial copper catalysts promoted with chromia or zinc unsupported and supported on alumina, a depth investigation of the performances of these catalysts into ethanol dehydrogenation reaction to ethyl acetate has been realized. A discussion of the correlation of the structural and chemical properties, in terms of basicity and acidity, with their performances will be discussed into the final section of this chapter.

B-4.3 High pressure dehydrogenation

In this research, five different commercial catalysts have been studied, promoted with two different oxides such as chromia and zinc and sup-

ported or unsupported on alumina. The main aim is to evaluate the performances of these commercial catalysts to produce ethyl acetate and pure hydrogen at high pressure (10-30 bar) and temperature (200-260°C).

A first examination on the performances of two different Cu-ZnO-Al₂O₃ catalysts has been done. After that, the performances of three different copper chromite catalysts with different content of chromia, unsupported or supported on alumina have been evaluated.

Copper is, normally, present in the catalysts composition in the form of oxide and must be reduced to metal to be active. For this reason all the proven catalysts in pellets have been submitted to the already described pre-treatment with a flow stream of hydrogen mixed with nitrogen for about 18 hours at 200°C. This pre-treatment is very important for the catalysts performances, as it can be appreciated in Table 6, in which conversions and selectivities, obtained for the catalyst BASF Cu-1234-1/16-3F after respectively 2, 4, 10 and 18 hours of pre-treatment are reported. In particular in Table 6 the kinetic runs after 2, 4, 10 and 18 hours, performed at 220°C with ethanol liquid flow rate of 0.1 cm³/min diluted in a mixture of H₂ 6% in N₂ at 20 bar using 50.12 g of Cu-1234 catalyst have been reported.

Table 6: Effect of activation time performed with a gas mixture of H₂ 6% in N₂, at temperature of 200°C, pressure 1 bar.

Activation time (h)	X (%)	S _{AcOEt} (%)	S _{CH₃CHO} (%)	S _{others} (%)
2	31.59	34	49.6	16.4
4	35.4	51.7	43.5	14.8
10	44.33	96.82	1	2.17
18	57.35	97.74	-	2.26

As it can be seen, the conversion increased at more prolonged pre-treatment and after 18 hours no further change of conversion should occur. The results reported in Table 6 show that the prolonged reduction time have a significantly effects also on the ethyl acetate selectivity, this suggest that the copper in reduced oxidation state is more selective to desired product of reaction.

A so long pre-treatment with hydrogen is necessary, in particular, for the BASF-K310 catalyst that is the less reducible catalyst, as previously demonstrated by TPR profiles, in order to reduce completely the catalyst. In the present research, the behavior of five different catalysts, in the ethanol dehydrogenation, has been studied. At first, the behavior of the BASF K-310 catalyst, which composition was rich in copper oxide supported on Al_2O_3 and ZnO was studied. The main scopes were to individuate the best operative conditions (temperature, pressure and contact time) for the reaction to ethyl acetate by evaluating the related performances in term of conversion, selectivity, by products formation and catalyst stability. In Table 7 the results of ethanol conversion, ethyl acetate and acetaldehyde selectivity, obtained by changing the pressure and the ethanol residence time, have been summarized. In more details, the performances of the copper-zinc-alumina catalyst (K-310) have been studied at different temperature 170-200°C, pressure 1-15-20 bar, residence time 5.6-943.9 ghmol^{-1} . As reported in Table 7 by increasing the temperature of reaction from 170°C to 200°C a sensible increase of the ethanol conversion from 56 to 63% has been appreciated. Another aspect to take in account is the effect of the residence time of the ethanol, at this purpose in Figure 14A an histogram of the ethanol conversion, acetaldehyde and ethyl acetate selectivities at two different residence time respectively of 32.44 and 97.32 ghmol^{-1} have been reported. The experimental results have been obtained by performing the reaction at a temperature of 200°C and at a pressure of 20 bar.

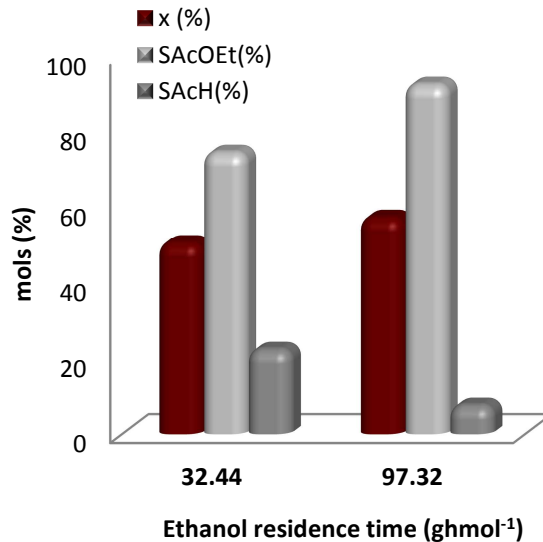


Figure 54A: catalyst K310. Ethanol conversion, acetaldehyde and ethyl acetate profiles at two different residence time 32.44-97.32 ghmol⁻¹, at 200°C, 20 bar.

As confirmed by the profile in Figure 14A the residence time have a significantly effect on the ethyl acetate selectivity that increase by 80 to 97% at high residence time of 97.32 ghmol⁻¹. The ethanol conversion is of about 50%_{mols} and was not affected by the variation of residence time because the ethanol conversion has reached the equilibrium of reaction.

More significantly is the effect of the pressure of reaction, as matter of fact at atmospheric pressure and at low residence time (5ghmol⁻¹) the main product of reaction is the acetaldehyde with a selectivity of about 84% (Figure 14B).

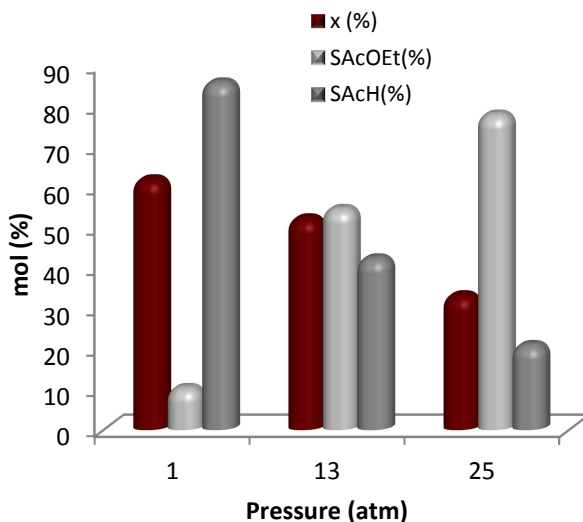


Figure 64B: catalyst K-310. Effect of the total pressure (1-13-25 atm). Temperature 200°C, residence time 5ghmol⁻¹, inert flow 4cc/min.K-310

At first, as confirmed by the profile of Figure 14B, by increasing the pressure of reaction from 1 atm to 25 atm the ethanol conversion decreases from 60% to 30%. This behavior is in agreement with our thermodynamic study reported in chapter 2 of the current section. Moreover, the pressure has a significant effect on the selectivity to acetaldehyde and ethyl acetate. At atmospheric pressure, the main product of reaction is acetaldehyde (86%) and by increasing the pressure of reaction at 13 atm a significant increase of ethyl acetate is observed (52%). At pressure higher than 20 bar the main product of reaction is the ethyl acetate with a selectivity of about 78%. The mass balance on the carbon is closed by considering the other sub-products of this reaction mainly aldehydes and ketones C₃-C₄. In particular, the formation of methyl ethyl ketone is the main inconvenient to obtain the purity target requires by industry for ethyl acetate that forms an

azeotrope with the ketone above mentioned. The obtained results are in perfect agreement with the literature [5,46-48] the performances of a copper-zinc-alumina catalyst at a temperature of 200°C and atmospheric pressure, in this condition for a conversion of about 40% a selectivity to acetaldehyde of 98% has been obtained. Another aspect to be considered is the effect of the pre-reduction of the catalyst in situ with a stream of 5cm³/min of 6% H₂ in N₂. The Figure 14C shows the comparison between two different runs performed on K-310 at a pressure of 20 bars, at a residence time of about 97ghmol⁻¹ and at a temperature of 200°C, respectively with a pre-reduced catalyst (Table7, run 7A) and a not reduced ones (Table7, run 6A).

As shown by the profiles of Figure 14C the effects of the pre-reduction treatment on both the activity and ethyl acetate selectivity are significant. The fresh catalyst shows a low activity (15%) and a poor selectivity to ethyl acetate (15%). After the reduction with a stream of 6% H₂ in N₂, the activity of the catalyst is highly promoted (55%) and the ethyl acetate selectivity rising up to a value of about the 80%.

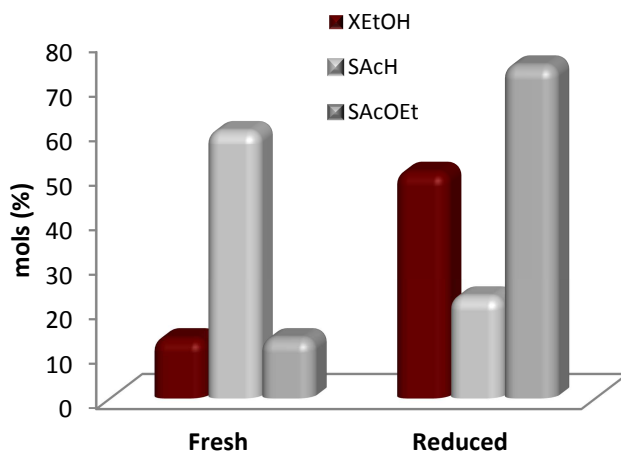


Figure 7: effects of the pre-treatment on K-310 catalyst performances

The improved selectivity to ethyl acetate is due in this case also to the effect of the residence time. At higher residence time, of about 97ghmol^{-1} , a selectivity to ethyl acetate of 80% has been obtained vs the 59% obtained at lowest residence time of 5ghmol^{-1} . This very promising results, in terms of pressure effect, have been forwarded to a more deeply investigation. The mainly aspects that should be considered to propose a catalyst, as a possible candidate for application in an industrial process, is its thermal, mechanical and chemical strength. As matter of fact the main factors to take in account to apply the catalyst in an industrial process is its durability, resistance to sintering, to poisoning effect and to thermal stress. Several studies have already shown the scarce resistance to sintering of copper-zinc-allumina at temperature of reaction higher than 200°C [47,49]. At this purpose the K-310 activity have been studied at two different pressures of 1 bar and 20 bar, at a temperature of 200°C and at constant residence time of 5.6ghmol^{-1} . The profiles of activity have been reported in Figure 14D.

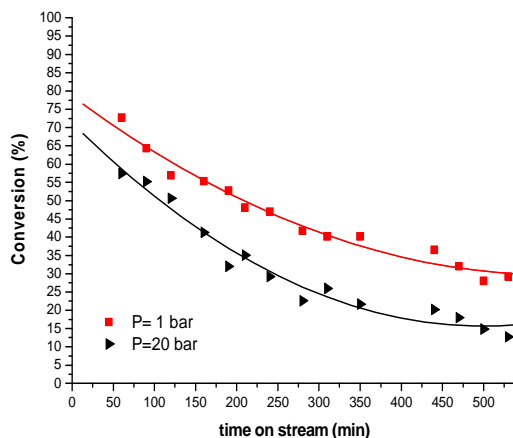


Figure 14D - Deactivation profiles for K-310 catalyst. ■ The run has been performed with 0.58g of catalyst at temperature of 200°C , at atmospheric pressure and at contact time of 5.6ghmol^{-1} , N_2 flow rate $4 \text{cm}^3/\text{min}$. ▲. The run has been performed with 10 g of catalyst at 200°C , at 20 bars and contact time of 98.7ghmol^{-1} with N_2 flow rate $25 \text{cm}^3/\text{min}$.

The rapid deactivation after about 1h of reaction is due to the effect of both sintering of copper on the catalysts surface and to the fouling of the catalysts surface by the effect of acetaldehyde adsorption. The activity faster decreases by increasing the pressure, as it can be seen in the above mentioned figure. However, we can conclude that copper deposited on ZnO-Al₂O₃ produces mainly acetaldehyde, at low pressure (1 bar), ethylacetate at higher pressure (10-20 bars) but with a maximum selectivity of 80-83%. Many by-products, deriving from the acetaldehyde condensation, are formed lowering the selectivity. Then, the catalyst is subjected to deactivation probably by sintering as suggested by the literature for this type of copper catalysts [47,49]. On the other hand as this catalyst is less selective in the studied reaction it cannot be excluded a contribution of fouling to the deactivation as a consequence of the acetaldehyde condensation reactions giving place to strongly adsorbed bulky molecules.

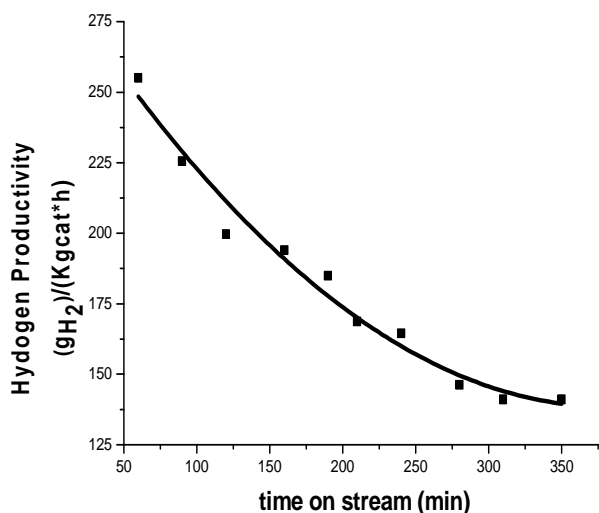


Figure 14E: K310 catalyst. Hydrogen productivity profile in dependence by the time on stream for K-310 catalyst. Temperature 200°C, Pressure 1 bar, residence time 5.6 ghmol⁻¹.

The K-310 catalyst, by operating with 0.58 g of catalyst, at temperature of 200°C, at atmospheric pressure and at contact time of 5.6 g_{mol}⁻¹ and N₂ flow rate 4 cm³/min, have shown a maximum of hydrogen productivity of about 259 g_{H2}/(Kg_{cat}*h). By increasing the time on stream, the ethanol conversion decreases by the effect of the fouling of the active sites due to the coke deposition. Consequently the hydrogen productivity slightly decreases until 135 g_{H2}/(Kg_{cat}*h) after about 350 min of time on stream (see Figure 14E).

Table 7. Some catalytic results obtained for the catalyst **K-310** by opportunely changing some significant operative conditions. *The Run 6A is related to the performances of a catalyst not pre-reduced with 6%H₂in N₂ flow. This run should be compared with Run 7A.

RUN	Cat. (g)	W/F (ghmol ⁻¹)	T (°C)	P (atm)	F _{EtOH} (cm ³ /min)	F (H ₂ 6%/N ₂) (cm ³ /min)	F _{N₂} (cm ³ /min)	X (%)	S _{AcOEt} (%)	S _{CH₃CHO} (%)	S _{others} (%)	PH ₂ (gH ₂ /Kg _{cat} h)
1A	0.58	5.6	170	1	0.1	-	4	64.3	10.7	89.0	n.d.	224.90
2A	0.58	5.6	200	1	0.1	-	4	52.7	12.5	87.5	n.d.	184.88
3A	0.58	5.6	200	15	0.1	-	4	51.6	58.9	37.1	5.0	173.78
4A	10.14	98.7	200	15	0.1	-	5	24.1	74.3	20.0	5.7	4.56
5A	10.14	98.7	200	20	0.1	-	5	28.6	80.7	10.2	9.1	5.22
6A*	10.14	98.7	200	20	0.1	5	-	13.3	13.3	59.9	26.7	1.95
7A	10.14	97.32	200	20	0.1	5	-	57.39	92.46	7.52	0.02	11.51
8A	10.14	32.44	200	20	0.3	5		50.62	74.52	22.63	2.85	29.61
9A	9.70	943.9	200	15	0.01	5	-	56.2	82.2	9.2	8.6	1.08
10A	9.70	943.9	200	15	0.01	5	-	63.5	83.1	11.0	5.8	1.25

The performances of another commercial copper zinc alumina (Sg-9601) catalyst have been studied. The catalyst supplied by BASF has an analogue composition of K-310 but is tougher to sintering, because during the preparation has been submitted to thermal treatment to stabilize the active phase. The catalytic runs have been performed at a pressure of 20 bar, at a constant residence time of 4 ghmol⁻¹ and by using a mixture of 6% H₂ in N₂ of 25 cm³/min.

The results in terms of activity and selectivity have been reported in Table 8. The profiles of conversion (Figure 15A) show that the catalysts has a relatively low activity and its behavior could be justified by the lowest specific surface area of this catalyst of about (62 m²/g) respect to the K-310 of about (120 m²/g).

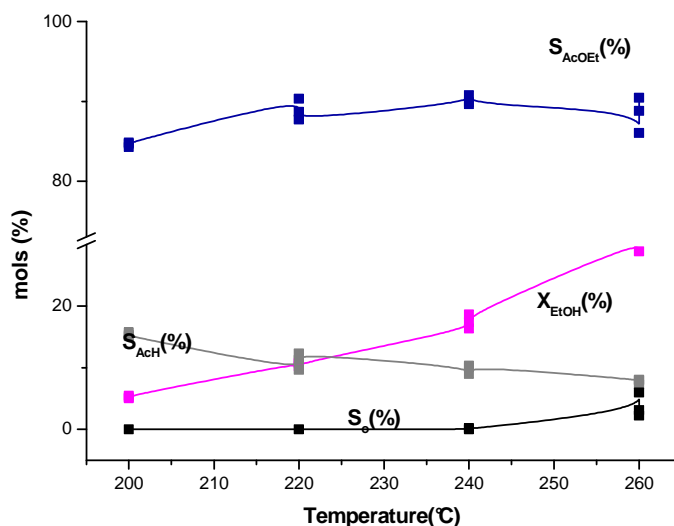


Figure 15A: catalyst Sg-9601. The runs were performed at 20 bar, at 4 ghmol⁻¹ of residence time and with a mixture of 6% H₂ in N₂ of 25 cm³/min

Despite the low activity (ethanol conversion <30%mol) the catalyst shows an high selectivity to ethyl acetate, that increases with the reaction temperature by reaching a maximum of about 90% at 240°C. At temperature higher than 260°C the selectivity decreases by the effect of the molecules decomposition to CO and H₂. The main advantage of this catalyst is the higher stability, also at higher temperature of reaction and after about 40 h of reaction, the catalyst did not deactivates for the effect of sintering of the active phase or fouling due to acetaldehyde adsorption and successive polymerization. The hydrogen productivity of Sg-9601, by operating at constant residence time of 4 ghmol⁻¹, at a pressure of 20 bar and by using a constant total flow of H₂6% in N₂ of 25 cm³/min, changes by increasing the temperature of reaction from 200 to 260°C in the range 25-130 g_{H₂}/(Kg_{cat}*h). It is evident that at higher temperature, the dehydrogenating action of the catalyst is higher and the ethanol conversion rising up to 30% (Figure 15 B).

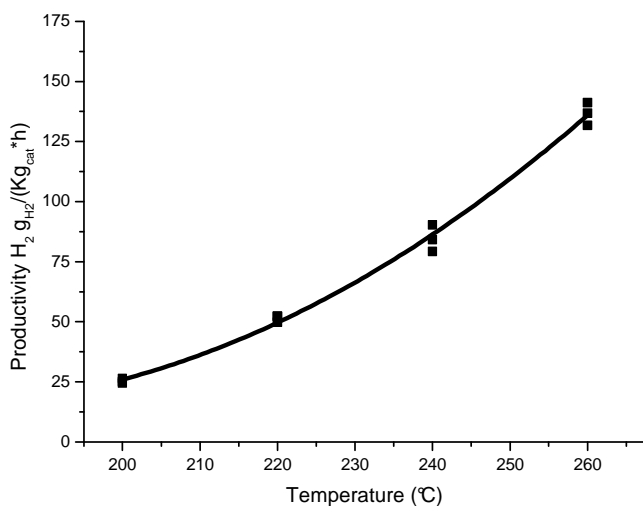


Figure 15B: Sg-9601. Hydrogen productivity profile vs temperature of reaction (200-260°C). Pressure 20 bar, residence time 4 ghmol⁻¹ and a mixture of 6% H₂ in N₂ of 25 cm³/min.

This catalyst could be considered a possible candidate for industrial application provided, thus, its performances will be investigated in more details, and this aspect will be subject of next future works.

Table 8: Sg-9601 catalytic results obtained by opportunely changing some significant operative conditions.

RUN	Cat. (g)	W/F (ghmol ⁻¹)	T (°C)	P (atm)	F _{EtOH} (cm ³ /min)	F _{H26% N2} (cm ³ /min)	X (%)	S _{AcOEt} (%)	S _{AcH} (%)	S _{ALTRI} (%)	PH ₂ (gH ₂ /Kg _{cat} h)
1A	2.10	4.25	200	20	0.5	25	5.05	84.27	15.73	0.00	24.47
2A	2.10	4.25	200	20	0.5	25	5.21	84.64	15.36	0.00	25.24
3A	2.10	4.25	200	20	0.5	25	5.45	84.84	15.15	0.00	26.40
1B	2.10	4.25	220	20	0.5	25	10.80	90.33	9.66	0.01	52.32
2B	2.10	4.25	220	20	0.5	25	10.27	88.68	11.32	0.00	49.76
3B	2.10	4.25	220	20	0.5	25	10.77	87.70	12.30	0.00	52.18
1C	2.10	4.25	240	20	0.5	25	16.36	89.88	10.11	0.01	79.25
2C	2.10	4.25	240	20	0.5	25	17.41	90.77	9.03	0.20	84.18
3C	2.10	4.25	240	20	0.5	25	18.64	89.64	10.33	0.03	90.28
1D	2.10	4.25	260	20	0.5	25	30.08	88.81	8.07	3.12	141.18
2D	2.10	4.25	260	20	0.5	25	28.89	86.05	7.98	5.97	131.61
3D	2.10	4.25	260	20	0.5	25	28.89	90.45	7.28	2.27	136.79

The performances of the copper catalysts promoted by chromium oxide have been studied. In particular the performances of two different Copper-Chromia catalysts, T-4466 and Cu-0203 supplied, respectively, by Sud-Chemie and BASF, with a different weight ratio of $\text{CuO}:\text{Cr}_2\text{O}_3$ have been investigated. In more details, the performances of a commercial copper chromite catalyst promoted with barium oxide, chromia and alumina has been examined in several operative conditions of pressure, temperature, residence time and hydrogen partial pressure. The results obtained for the Sud Chemie T-4466 copper/copper chromite catalyst are summarized in Table 9. In this case, 50 g of catalyst have been charged in the packed bed reactor. This catalyst resulted more stable to sintering and we have had the possibility to operate also at temperatures higher than 200°C.

In Figure 16 A an indication of the performances of T-4466 catalyst, at different temperature of reaction, have been observed. As already known, the operating temperature has a strong effect on the conversion but has not affect the selectivity results. In particular, at 260°C a conversion of 50% has been obtained vs 30% at 200°C.

The selectivities of this copper/copper chromite catalyst (96% for a conversion of 50%) are much higher than the ones obtained with the BASF K-310 catalyst but the best values have been obtained at higher temperatures. However, activities are relatively low, for this catalyst, in accordance with its low specific surface area. It must be pointed out that the presence of copper chromite in the catalyst composition has a positive effect on both the selectivity to ethyl acetate and stability to copper sintering and catalyst deactivation.

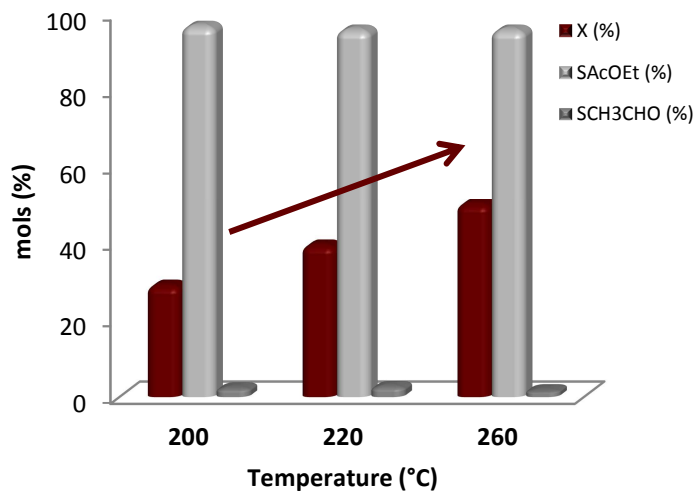


Figure 16A: T-4466. Effect of the temperature (200-220-260°C). Temperature 20°C, residence time 98.23 ghmol⁻¹, a mixture of 6% H₂ in N₂ of 25 cm³/min.

The catalyst stability has been established by controlling periodically the conversion and selectivity in the conditions of run 3B, of Table 9, during the time. Both conversion and selectivity remained unchanged for about 70 hours of reaction.

Table 9: Examples of catalytic results obtained for the Sud-Chemie T-4466 catalyst. All the dehydrogenation reactions were realized at a pressure of 20 bars.

RUN	Cat. (g)	W/F (ghmol ⁻¹)	T (°C)	F _{EtOH} (cm ³ /min)	F _{H₂ 6%/N₂} (cm ³ /min)	X (%)	S _{AcOEt} (%)	S _{CH₃CHO} (%)	Sothers (%)	P _{H₂} (g _{H₂} /Kgc _{at} h)
1B	50.47	98.23	200	0.5	25	29.18	96.8	2.2	1.0	5.82
2B	50.47	98.23	220	0.5	25	39.63	95.8	2.6	1.6	7.86
3B	50.47	98.23	260	0.5	25	50.4	95.8	1.6	2.6	9.90

The performances of Cu-0203 catalyst have also been described. This catalyst has a composition very similar to the ones of copper/chromia T-4466. The runs were performed by using only 2g of catalyst. The results of conversion and product selectivity have been presented in Table 10. In Figure 17A the results as function of the reaction temperature have been represented.

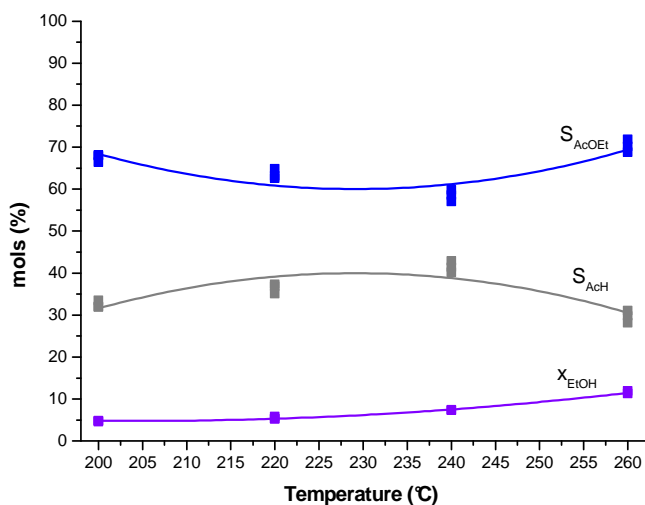


Figure17A: Cu0203, W/F=4ghmol₁, temperature 220°C, pressure 20 bar, 25cm³/min of H₂6% in N₂.

The activity of the examined catalyst is very poor, less than 15% of ethanol conversion also at relatively high temperature of reaction (260°C). In addition, the selectivity to ethyl acetate is less than 70% and one of the acetaldehyde is one of the main co-products of reaction with a selectivity of about 32-37%. The hydrogen productivity of Cu-0203 is comprised in the range 25-65 g_{H₂}/(Kg_{cat}*h) (Figure 17B). The performances of the catalyst in exam will be compared in the next paragraph with the ones, obtained by using a catalyst bed of 2g, of the other two catalysts studied Sg-9601, a copper/ZnO/Al₂O₃, and Cu-

1234, a copper chromite catalyst promoted with alumina and barium oxide.

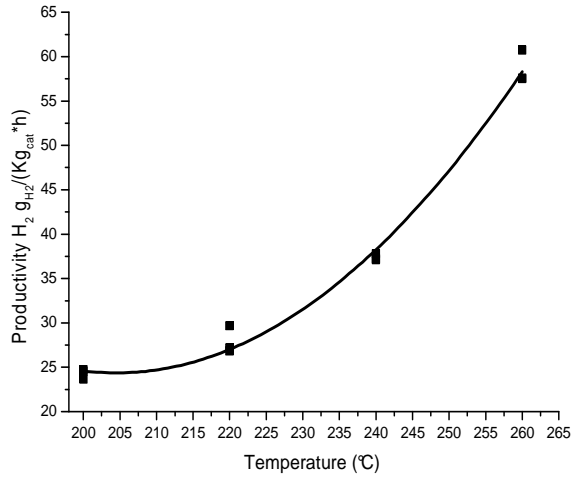


Figure 17B8: Cu-0203. Hydrogen productivity profile vs temperature of reaction (200-260°C). Pressure 20 bar, residence time 4 g_{mol}⁻¹ and a mixture of 6% H₂ in N₂ of 25 cm³/min.

Table 10: Examples of catalytic results obtained for the **Cu-0203** catalyst. All the dehydrogenation reactions were realized at a pressure of 20 bars, at $W/F=4\text{ghmol}^{-1}$ and by feeding a mixture of $25\text{cm}^3/\text{min}$ 6% H_2 in N_2 .

RUN	Cat. (g)	W/F (ghmol^{-1})	T ($^{\circ}\text{C}$)	P (atm)	F_{EtOH} (cm^3/min)	$F_{\text{H}_2\text{6\%N}_2}$ (cm^3/min)	X (%)	S_{AcOEt} (%)	S_{AcH} (%)	S_{ALTRI} (%)	PH_2 ($\text{gH}_2/\text{Kg}_{\text{cat}} \text{h}$)
1A	2.00	3.90	Sg9601	20	0.5	25	4.65	68.07	31.93	0.00	23.65
2A	2.00	3.90	200	20	0.5	25	4.82	66.48	33.51	0.01	24.52
3A	2.00	3.90	200	20	0.5	25	4.86	67.90	32.09	0.01	24.72
1B	2.00	3.90	220	20	0.5	25	5.34	64.89	35.11	0.00	27.16
2B	2.00	3.90	220	20	0.5	25	5.83	63.15	36.85	0.00	29.66
3B	2.00	3.90	220	20	0.5	25	5.28	62.61	37.38	0.01	26.86
1C	2.00	3.90	240	20	0.5	25	7.30	58.59	41.41	0.00	37.13
2C	2.00	3.90	240	20	0.5	25	7.32	57.06	42.93	0.01	37.23
3C	2.00	3.90	240	20	0.5	25	7.43	59.77	40.22	0.01	37.79
1D	2.00	3.90	260	20	0.5	25	11.32	70.22	29.78	0.00	57.58
2D	2.00	3.90	260	20	0.5	25	11.31	71.82	28.18	0.00	57.53
3D	2.00	3.90	260	20	0.5	25	11.96	68.77	31.03	0.20	60.72

Catalyst BASF Cu-1234-1/16-3F contains relatively dispersed copper chromite particles (see X-rays diffraction of Figure 3) supported on alumina. This catalyst has been studied in a more details, because provided the best performances for what concerns activity, selectivity and stability. A wide range of experimental runs were performed and in particular the catalytic reactor was charged with respectively 2-10-50g of catalyst. The runs were performed at different temperature (200-260°C), pressure (1-30 bar), residence time (1-20 g h mol^{-1}) and at three different hydrogen molar flow rate (7.31×10^{-4} – 2.19×10^{-3} - 3.66×10^{-3} mol/h) and consequently at three different mixture of H₂ 6% in N₂ of respectively 5-15-25 cm³/min.

Catalyst bed 2g - In more detail in the Tables 11A-C are reported the runs performed, by using 2g of catalyst, respectively at 10-20-30 bar, at different temperature (200-260°C) and by using a constant hydrogen flow rate (3.66×10^{-3} mol/h).

In Table 11D the results obtained, by operating at two different temperatures 200-220°C and at a constant pressure 20 bars, by using two different ethanol residence time (1-20 g h mol^{-1}) has been summarized. In Tables 11E-11F, the comparison of the performances obtained by changing the hydrogen fed to the reactor have been reported. The runs in this case have been obtained for the three residence times (1-4-20 g h mol^{-1}) at a constant pressure (20 bar), temperature (220°C), and at three different hydrogen partial pressure. The comparison of the performances has been reported in the profile of Figure 18 A-I.

In Figure 18A the ethanol conversions as function of the reaction temperature for the catalyst of copper chromite, promoted with barium chromate and alumina, at three different pressure 10-30 bars, have been reported. The runs have been performed by using 2g of catalyst, 4g h mol^{-1} of residence time, 3.66 mol/h of hydrogen and 0.057mol/h of nitrogen.

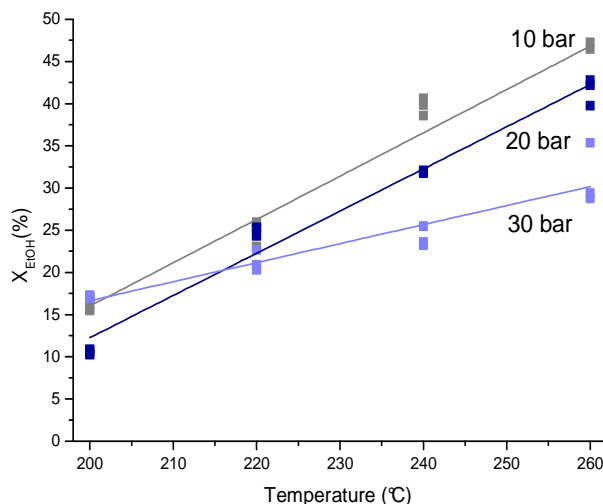


Figure 18A: catalyst Cu-1234. Ethanol conversion profiles. The runs were performed by changing the temperature (200-260°C) and at three different pressure 10-20-30 bar, at 4 ghmol⁻¹ of residence time and with a mixture of 6% H₂ in N₂ of 25 cm³/min.

At a pressure of 10 bar the catalyst shows a conversion of about 15% that increase until reach a 45% at 260°C. By increasing, the pressure from 10 to 30 bar an evident decrease of the activity has been observed. In particular, at 260°C and at a pressure of 30 bar a conversion of 27% has been obtained. This behavior is in agreement with the thermodynamic studies reported in the chapter 2 of the section B. In Figure 18B, the selectivities to ethyl acetate have also been compared. At very low residence time, as in this particular case of about 4ghmol⁻¹, the selectivity to ethyl acetate is of about 62% at a temperature reaction of 200°C and slightly increases to 67% at a temperature of 260°C. At low temperature, 200°C at a pressure of both 20-30 bar the selectivity is included in the range 80-85%. By increasing the temperature the best selectivity to ethyl acetate has been obtained by operating at a pressure of 20 bar in all the range of temperature examined.

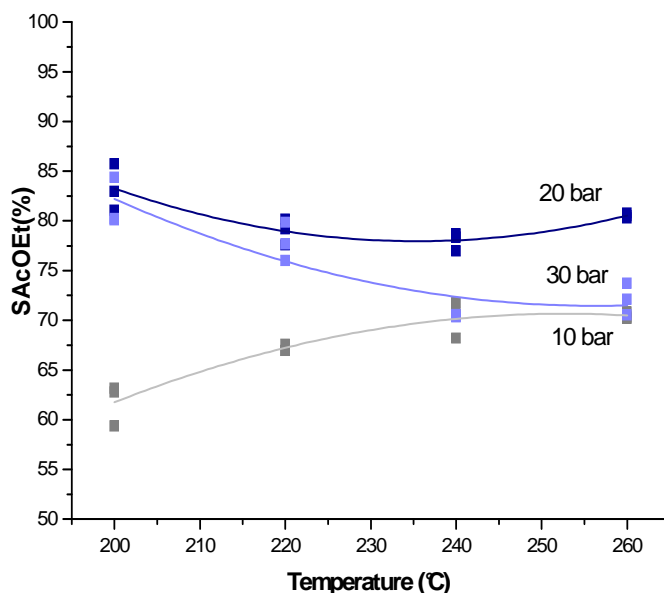


Figure 18B: catalyst Cu-1234. Ethyl acetate selectivity profiles. The runs were performed by changing the temperature (200-260°C) and at three different pressure 10-20-30 bar, at 4 g mol^{-1} of residence time and with a mixture of 6% H₂ in N₂ of 25 cm³/min.

The pressure has a great influence on the acetaldehyde formation. As demonstrated by the profiles of Figure 18C at low temperature (200°C) and at a pressure of 10 bar the acetaldehyde selectivity is around 38-40% and decrease, at parity of temperature, to 15-18%. The effect of the increased pressure is stronger at higher temperature of reaction.

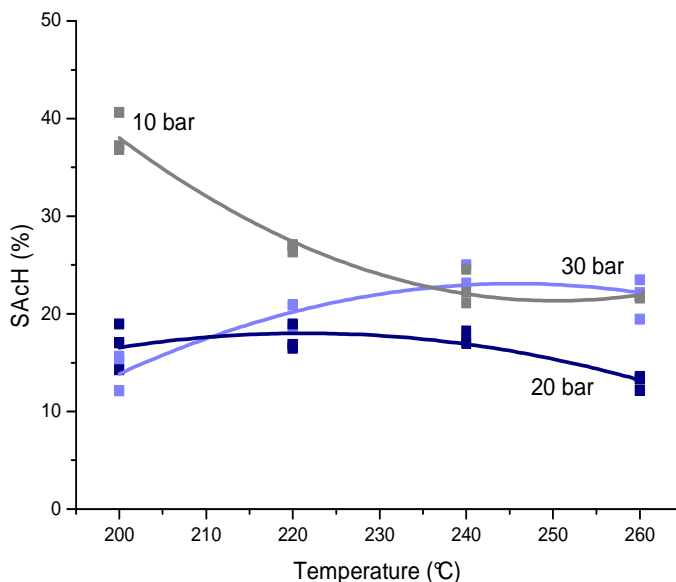


Figure 18C: catalyst Cu-1234. Acetaldehyde selectivity profiles. The runs were performed by changing the temperature (200-260°C) and at three different pressure 10-20-30 bar, at 4 ghmol^{-1} of residence time and with a mixture of 6% H_2 in N_2 of $25 \text{ cm}^3/\text{min}$.

The hydrogen productivity has been studied also for the catalysts of Cu-1234. At a constant residence time of 4 ghmol^{-1} and H_2 6% in N_2 flow of $25 \text{ cm}^3/\text{min}$, the profiles of hydrogen productivity vs the reaction temperature at three different operating pressure has been reported in Figure 18D.

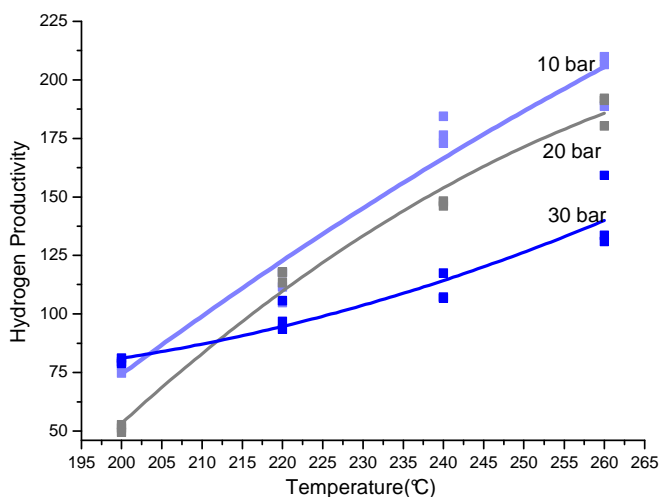


Figure 18D: catalyst Cu-1234. Hydrogen productivity profiles. The runs were performed by changing the temperature (200-260°C) and at three different pressure 10-20-30 bar, at 4 g_{mol}⁻¹ of residence time and with a mixture of 6% H₂ in N₂ of 25 cm³/min.

By increasing the reaction temperature, the hydrogen productivity increases but on the other hand the increase of the reaction pressure suppress the dehydrogenating activity of the catalyst and consequently a reduction of the ethanol conversion promotes the decrease of the hydrogen productivity. The higher hydrogen productivity of about 200 g_{H₂}/(Kg_{cat}*h) has been obtained by operating at 10 bar and 260°C of reaction. The hydrogen productivity of this catalyst Cu-1234 and the obtained results are very promising for a future application of this catalytic system an industrial process for ethyl acetate and pure hydrogen production.

The effect of how the residence time affects the ethanol conversion and the selectivities of the main products of the dehydrogenation reaction is well represented in Figure 18E.

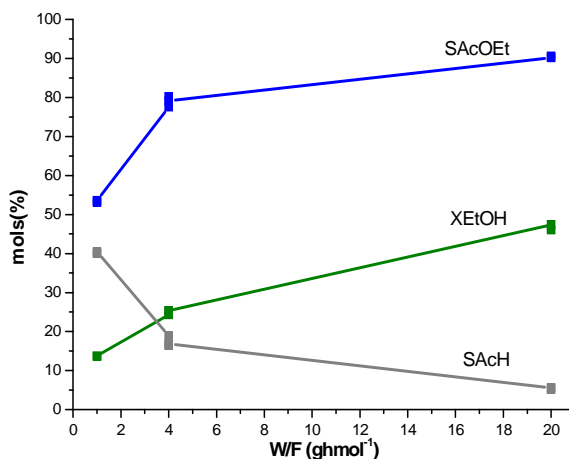


Figure 18E: catalyst Cu-1234. Ethanol residence time effect on the ethanol conversion and main products selectivity. The runs were performed by changing the residence time 1-4-20 ghmol^{-1} . The runs were performed at 20 bar and 220°C.

At low residence, time of about 1ghmol^{-1} , the ethanol conversion is of about 12% and increases to 25% at 4ghmol^{-1} . At higher residence time of 20ghmol^{-1} an ethanol conversion of 48% has been achieved. The residence time affects in significant way the selectivity to the desired product of reaction. At low residence time a selectivity to ethyl acetate of 52% vs 42% of selectivity to acetaldehyde has been obtained. At first to favor the main reaction product to reach the industrial target of purity (98.9%) is necessary to increase the ethanol residence time, as demonstrated by the profiles of Figure 18E, at 20ghmol^{-1} a selectivity to ethyl acetate of about 90% has been obtained. The acetaldehyde selectivity is less than 10%. In Figure 18F the dependence of the hydrogen productivity from the ethanol residence time has been represented. The runs have been performed at 20 bar, 220°C, at H_2 6% in N_2 flow of $25\text{cm}^3/\text{min}$ and at three different residence time of 1-4-20 ghmol^{-1} .

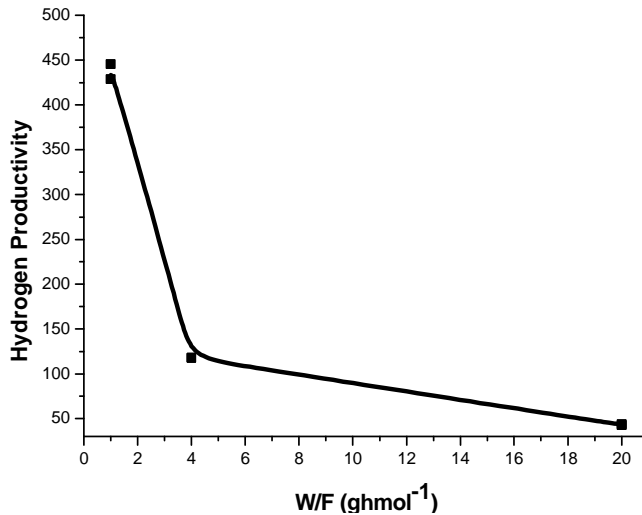


Figure 18F: catalyst Cu-1234. Ethanol residence time effect on the hydrogen productivity. The runs were performed by changing the residence time 1-4-20 ghmol⁻¹. The runs were performed at 20 bar and 220°C.

The profile of Figure 18F has shown that the higher hydrogen productivity, in the reaction condition above described, was of about 400 g_{H2}/(Kg_{cat}*h). A depth investigation of the hydrogen partial pressure effects on the catalysts activities and selectivities to ethyl acetate have been realized by fed in the reaction apparatus, three different hydrogen molar flow respectively of 7.31×10^{-4} - 2.19×10^{-3} and 3.66×10^{-3} mol/h in mixture with ethanol (see Figure 18G-I). In Figure 18G the ethanol conversion profiles vs the hydrogen molar flow rate (mol/h) at three different residence time of 1-4-20ghmol⁻¹ have been reported.

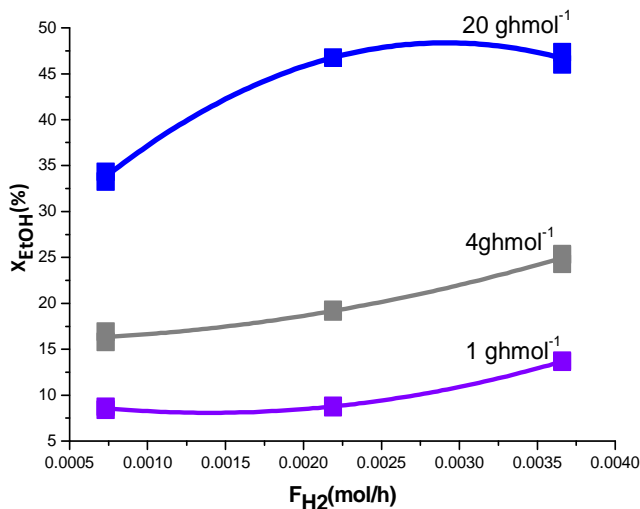


Figure 18G: catalyst Cu-1234. Variation of hydrogen molar flow rate effect on the catalyst conversion. The runs were performed by changing the hydrogen flow rate (7.31×10^{-4} - 2.19×10^{-3} and 3.66×10^{-3} mol/h). The runs were performed at 20 bar and 220°C.

The profiles of conversion show the effect of hydrogen partial pressure on the catalyst activity. It is clear that by increasing the hydrogen molar flow a significant increase of the ethanol conversion is observed and this phenomenon is more strongly evident for higher residence times. The best results have been obtained at 20 g mol^{-1} by fed hydrogen flow of 0.0037 mol/h . At these conditions, an ethanol conversion of 47% was achieved. In Figure 18H the selectivity profiles show the favorable effect of the hydrogen pressure on ethyl acetate formation.

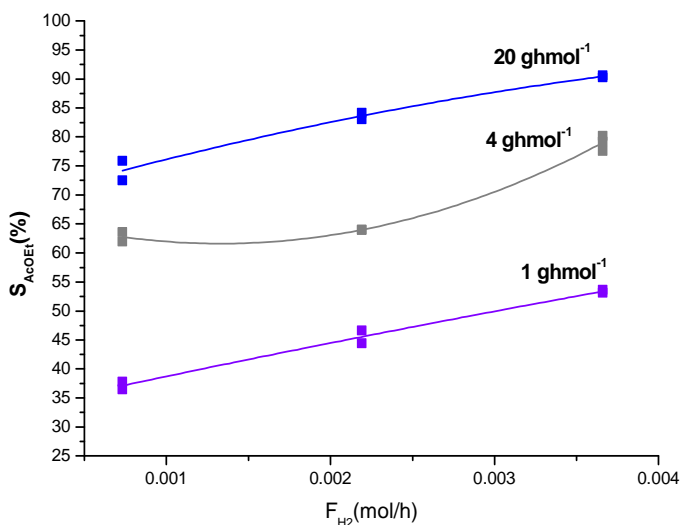


Figure 18H: catalyst Cu-1234. Variation of hydrogen molar flow rate effect on the ethyl acetate selectivity. The runs were performed by changing the hydrogen flow rate (7.31×10^{-4} - 2.19×10^{-3} and 3.66×10^{-3} mol/h). The runs were performed at 20 bar and 220°C

At low residence, time 1 $ghmol^{-1}$ the ethyl acetate selectivity increase from 37% to 53% by increasing the hydrogen flow from 7.31×10^{-4} to 3.66×10^{-3} mol/h. The residence time of 20 $ghmol^{-1}$, at low hydrogen partial pressure, gives an ethyl acetate selectivity of about 75%. The ethyl acetate selectivity achieves a maximum of 90% at 20 $ghmol^{-1}$ and hydrogen flow of 3.66×10^{-3} mol/h. In Figure 18I, the profiles of acetaldehyde selectivity by changing the hydrogen molar flow rate fed in the apparatus have been reported. Moreover, this study was performed at three different residence time 1-4-20 $ghmol^{-1}$.

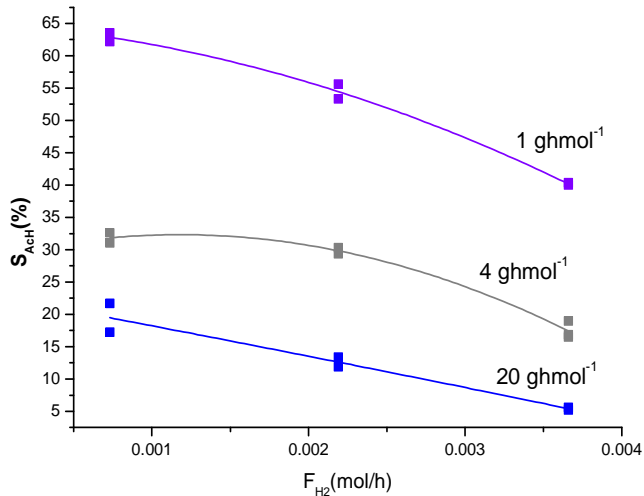


Figure 181: catalyst Cu-1234. Variation of hydrogen molar flow rate effect on the acetaldehyde selectivity. The runs were performed by changing the hydrogen flow rate (7.31×10^{-4} - 2.19×10^{-3} and 3.66×10^{-3} mol/h). The runs were performed at 20 bar and 220°C.

The acetaldehyde selectivity at low residence time ($1ghmol^{-1}$) and at low hydrogen pressure 7.31×10^{-4} is of about 63%. In this condition, the acetaldehyde is the main reaction product. Increasing the residence time and hydrogen partial pressure favors, a decrease of acetaldehyde that in this process is undesired because limits the target of ethyl acetate purity required by industry.

Table 11A: Experimental Runs of Cu-1234 catalysts. The runs have been performed in a range of 200-260°C of temperature, by using a catalytic bed of 2g, at 10 bar, at a residence time of 4ghmol^{-1} , an ethanol flow of 0.5mol/h, a total flow of 6% H_2 in N_2 of 25 cm^3/min that corresponds to $\text{FN}_2=0.057$ mol/h and to $\text{F}_{\text{H}_2}=3.66\text{E-}3$ mol/h.

N	Wcat (g)	W/F EtOH (ghmol^{-1})	T (°C)	P (atm)	FEtOH (mol/h)	FN ₂ (mol/h)	FH ₂ (mol/h)	XEtOH (%)	SACOEt (%)	SAcH (%)	Sothers (%)	P _{H₂} ($\text{g}_{\text{H}_2}/\text{Kgcat h}$)
1	2.07	4	200	10	0.5	0.057	3.66E-03	16.16	62.79	37.21	0.01	78.07
2	2.07	4	200	10	0.5	0.057	3.66E-03	15.47	59.38	40.62	0.01	74.73
3	2.07	4	200	10	0.5	0.057	3.66E-03	16.79	63.16	36.84	0.01	81.11
4	2.07	4	220	10	0.5	0.057	3.66E-03	25.94	67.6	26.35	6.05	117.73
5	2.07	4	220	10	0.5	0.057	3.66E-03	24.55	66.99	27.02	5.99	111.49
6	2.07	4	220	10	0.5	0.057	3.66E-03	23.07	66.94	27.09	5.97	104.80
7	2.07	4	240	10	0.5	0.057	3.66E-03	39.8	70.64	21.1	8.26	176.39
8	2.07	4	240	10	0.5	0.057	3.66E-03	38.59	68.21	24.55	7.24	172.93
9	2.07	4	240	10	0.5	0.057	3.66E-03	40.62	71.78	22.22	6.00	184.46
10	2.07	4	260	10	0.5	0.057	3.66E-03	46.46	70.21	21.84	7.95	206.60
11	2.07	4	260	10	0.5	0.057	3.66E-03	42.18	70.84	21.8	7.36	188.77
12	2.07	4	260	10	0.5	0.057	3.66E-03	47.26	70.33	21.61	8.06	209.91

Section B
Chapter 4
Experimental

Table 11B: Experimental Runs of Cu-1234 catalysts. The runs have been performed in a range of 200-260°C of temperature, by using a catalytic bed of 2g, at 20 bar, at a residence time of 4ghmol⁻¹, an ethanol flow of 0.5mol/h, a total flow of 6%H₂ in N₂ of 25 cm³/min that corresponds to FN₂=0.057 mol/h and to FH₂=3.66E-3 mol/h.

N	Wcat (g)	W/F EtOH (ghmol ⁻¹)	T (°C)	P (atm)	FEtOH (mol/h)	FN ₂ (mol/h)	FH ₂ (mol/h)	XEtOH (%)	SACOEt (%)	SAcH (%)	Sothers (%)	P _{H2} (gH ₂ /Kgcat h)
13	2.07	4	200	20	0.5	0.057	3.66E-03	10.6	81.07	18.93	0.01	51.21
14	2.07	4	200	20	0.5	0.057	3.66E-03	10.89	85.73	14.27	0.01	52.61
15	2.07	4	200	20	0.5	0.057	3.66E-03	10.24	82.96	17.04	0.01	49.47
16	2.07	4	220	20	0.5	0.057	3.66E-03	25.33	79.18	16.85	3.97	117.51
17	2.07	4	220	20	0.5	0.057	3.66E-03	25.27	80.19	16.46	3.35	117.99
18	2.07	4	220	20	0.5	0.057	3.66E-03	24.29	77.59	18.93	3.48	113.26
19	2.07	4	240	20	0.5	0.057	3.66E-03	32.08	78.37	17.27	4.36	148.22
20	2.07	4	240	20	0.5	0.057	3.66E-03	31.99	78.7	16.94	4.36	147.80
29	2.07	4	240	20	0.5	0.057	3.66E-03	31.74	77	18.25	4.75	146.05
30	2.07	4	260	20	0.5	0.057	3.66E-03	42.79	80.81	12.14	7.05	192.14
31	2.07	4	260	20	0.5	0.057	3.66E-03	39.76	80.29	13.59	6.12	180.32
32	2.07	4	260	20	0.5	0.057	3.66E-03	42.18	80.54	13.32	6.14	191.26

Section B
Chapter 4
Experimental

Table 11C: Experimental Runs of Cu-1234 catalysts. The runs have been performed in a range of 200-260°C of temperature, by using a catalytic bed of 2g, at 30 bar, at a residence time of 4ghmol⁻¹, an ethanol flow of 0.5mol/h, a total flow of 6%H₂ in N₂ of 25 cm³/min that corresponds to FN₂=0.057 mol/h and to F_{H₂}=3.66E-3 mol/h.

N	Wcat (g)	W/F EtOH (ghmol ⁻¹)	T (°C)	P (atm)	FEtOH (mol/h)	FN ₂ (mol/h)	FH ₂ (mol/h)	XEtOH (%)	SACOEt (%)	SAcH (%)	Sothers (%)	P _{H₂} (gH ₂ /Kgcath)
33	2.07	4	200	30	0.5	0.057	3.66E-03	17.3	76.02	20.9	3.1	81.00
34	2.07	4	200	30	0.5	0.057	3.66E-03	16.94	77.68	18.58	3.7	78.78
35	2.07	4	200	30	0.5	0.057	3.66E-03	17.03	79.85	16.85	3.3	79.56
36	2.07	4	220	30	0.5	0.057	3.66E-03	20.89	80.23	15.63	4.12	96.74
37	2.07	4	220	30	0.5	0.057	3.66E-03	20.3	80.08	15.2	4.72	93.44
38	2.07	4	220	30	0.5	0.057	3.66E-03	22.64	84.41	12.12	3.46	105.58
39	2.07	4	240	30	0.5	0.057	3.66E-03	25.47	70.36	25.02	1.38	117.36
40	2.07	4	240	30	0.5	0.057	3.66E-03	23.6	70.39	23.15	6.46	106.64
41	2.07	4	240	30	0.5	0.057	3.66E-03	23.21	70.58	24.89	4.53	107.05
42	2.07	4	260	30	0.5	0.057	3.66E-03	35.35	73.74	19.45	6.81	159.14
43	2.07	4	260	30	0.5	0.057	3.66E-03	28.76	72.14	22.17	5.69	131.03
44	2.07	4	260	30	0.5	0.057	3.66E-03	29.4	70.55	23.49	5.96	133.56

Section B
Chapter 4
Experimental

Table 11D: Experimental Runs of Cu-1234 catalysts. The runs have been performed in a range of 200-220°C of temperature, by using a catalytic bed of 2g, at 20 bar, at two different residence time of 4-20ghmol⁻¹, by using an ethanol flow of 0.1-1.5 mol/h, a total flow of 6%H₂ in N₂ of 25 cm³/min that corresponds to F_{N₂}=0.057 mol/h and to F_{H₂}=3.66E-3 mol/h.

N	Wcat (g)	W/F EtOH (ghmol ⁻¹)	T (°C)	P (atm)	FetOH (mol/h)	FN ₂ (mol/h)	FH ₂ (mol/h)	XEtOH (%)	SACOEt (%)	SAcH (%)	Sothers (%)	PH2 (gH2/Kgcat h)
45	2.07	1	200	20	1.5	0.057	3.66E-03	7.64	39.62	60.38	0.0001	110.72
46	2.07	1	200	20	1.5	0.057	3.66E-03	7.24	44.74	55.26	0.0001	104.93
47	2.07	1	200	20	1.5	0.057	3.66E-03	7.74	39.75	60.25	0.0001	112.17
48	2.07	1	220	20	1.5	0.057	3.66E-03	30.00	53.61	40.37	6.02	408.61
49	2.07	1	220	20	1.5	0.057	3.66E-03	33.00	53.13	40	6.87	445.40
54	2.07	20	220	20	0.1	0.057	3.66E-03	46.02	90.62	5.21	4.17	42.61
55	2.07	20	220	20	0.1	0.057	3.66E-03	47.35	90.25	5.59	4.16	43.85

Section B
Chapter 4
Experimental

Table 11E: Experimental Runs of Cu-1234 catalysts. The runs have been performed at 220°C of temperature, at a pressure of 20 bars, by using a catalytic bed of 2g, at a two different residence time of 1-4ghmol⁻¹, by using ethanol flow of 0.5-1.5 mol/h. The runs have been performed at three different flow rate of the mixture of 6% H2 in N2 (5-15-25 cm³/min).

N	Wcat (g)	W/F EtOH (ghmol ⁻¹)	T (°C)	P (atm)	FetOH (mol/h)	FH ₂ 6%N ₂ (cm ³ /min)	FN ₂ (mol/h)	FH ₂ (mol/h)	XEtOH (%)	SACOEt (%)	SAcH (%)	Sothers (%)	PH2 (gH2/Kgcat h)
48	2.07	1	220	20	1.5	25	0.057	3.66E-03	13.74	53.61	40.37	6.02	187.14
49	2.07	1	220	20	1.5	25	0.057	3.66E-03	13.63	53.13	40	6.87	183.97
60	2.07	1	220	20	1.5	15	0.034	2.19E-03	8.7	46.66	53.34	0	126.09
61	2.07	1	220	20	1.5	15	0.034	2.19E-03	8.85	44.41	55.59	0	128.26
62	2.07	1	220	20	1.5	5	0.011	7.31E-04	8.41	37.81	62.19	0	121.88
63	2.07	1	220	20	1.5	5	0.011	7.31E-04	8.74	36.46	63.54	0	42.22
16	2.07	4	220	20	0.5	25	0.057	3.66E-03	25.33	79.18	16.85	3.97	117.51
17	2.07	4	220	20	0.5	25	0.057	3.66E-03	25.27	80.19	16.46	3.35	117.99
18	2.07	4	220	20	0.5	25	0.057	3.66E-03	24.29	77.59	18.93	3.48	113.26
50	2.07	4	220	20	0.5	15	0.034	2.19E-03	19.09	63.96	29.38	6.66	86.08
51	2.07	4	220	20	0.5	15	0.034	2.19E-03	19.27	63.99	30.29	5.72	87.77
52	2.07	4	220	20	0.5	5	0.011	7.31E-04	16.9	61.97	32.6	5.42	77.21
53	2.07	4	220	20	0.5	5	0.011	7.31E-04	15.79	63.58	31.06	5.36	72.19

Section B
Chapter 4
Experimental

Table 11F: Experimental Runs of Cu-1234 catalysts. The runs have been performed at 220°C of temperature, at a pressure of 20 bars, by using a catalytic bed of 2g, at a residence time of 20ghmol⁻¹, by using ethanol flow of 0.1 mol/h. The runs have been performed at three different flow rate of the mixture of 6%H₂ in N₂ (5-15-25 cm³/min).

N	W _{cat} (g)	W/F _{EtOH} (ghmol ⁻¹)	T (°C)	P (atm)	F _{EtOH} (mol/h)	FH ₂ 6%N ₂ (cm ³ /min)	FN ₂ (mol/h)	FH ₂ (mol/h)	XEtOH (%)	S _{ACOEt} (%)	S _{AcH} (%)	S _{others} (%)	PH ₂ (gH ₂ /Kgc _{at} h)
54	2.07	20	220	20	0.1	25	0.057	3.66E-03	46.02	90.62	5.21	4.17	42.61
55	2.07	20	220	20	0.1	25	0.057	3.66E-03	47.35	90.25	5.59	4.16	43.85
56	2.07	20	220	20	0.1	15	0.034	2.19E-03	46.77	84.17	11.87	3.96	43.40
57	2.07	20	220	20	0.1	15	0.034	2.19E-03	46.77	83.07	13.35	3.58	43.57
58	2.07	20	220	20	0.1	5	0.011	7.31E-04	33.26	75.9	17.24	6.86	29.93
59	2.07	20	220	20	0.1	5	0.011	7.31E-04	34.33	72.5	21.69	5.81	31.24

Catalyst bed 10g- Several runs have been performed at two different residence time of respectively at 35 ghmol^{-1} and 97 ghmol^{-1} . The reactor has been charged with 10 g of catalyst Cu-1234 and fed with two different ethanol flows of respectively $0.1\text{-}0.3 \text{ cm}^3/\text{min}$.

The runs have been performed in the range of temperature of $200\text{-}260^\circ\text{C}$, at pressures of $10\text{-}20$ bars and by operating with a total flow of $6\% \text{ H}_2$ in N_2 of $5 \text{ cm}^3/\text{min}$, which correspond to the use of the lowest hydrogen flow of $7.31\text{E-}4 \text{ mol/h}$. The most significantly results have been reported in Table 12. To well understand the aim of these results, firstly, the evaluations of the catalyst behavior at the same residence times, but by using an higher quantity of catalyst (50g) and different hydrogen molar flow rate in the inlet stream has been studied.

Section B
Chapter 4
Experimental

Table 12: Experimental Runs of Cu-1234 catalysts. The runs have been performed at 200- 260°C of temperature, at a pressure of 10-20 bars, by using a catalytic bed of 10g, at a two different residence time of 34-104ghmol⁻¹, by using ethanol flow of 0.1-0.3 mol/h. The runs have been performed at a flow rate of the mixture of 6% H₂ in N₂ of 5cm³/min).

RUNS	T (°C)	P (atm)	W/F EtOH (ghmol ⁻¹)	FEtOH (cm ³ min ⁻¹)	F6%H ₂ in N ₂ (cm ³ /min)	FN ₂ (mol/h)	FH ₂ (mol/h)	X (%)	SACOEt (%)	SACH (%)	Sal. (%)	PH ₂ (gH ₂ /Kgcath)
60	220	20	34.4	0.3	5	0.011	7.31E-4	49.59	87.73	11.36	0.91	30.00
61	240	20	34.4	0.3	5	0.011	7.31E-4	58.42	86.78	9.08	4.14	34.19
62	200	10	104.13	0.1	5	0.011	7.31E-4	46.85	87.29	10.90	1.81	9.36
63	220	10	104.13	0.1	5	0.011	7.31E-4	57.62	87.68	5.05	7.27	10.87
64	240	10	104.13	0.1	5	0.011	7.31E-4	58.79	88.26	8.72	3.02	11.60
65	260	10	104.13	0.1	5	0.011	7.31E-4	62.04	86.29	17.94	6.04	13.16
66	200	30	104.13	0.1	5	0.011	7.31E-4	62.02	72.0	21.4	6.6	11.79

Catalyst bed 50g - The kinetic runs have been performed by changing the ethanol contact time from 32.48 to 97.45 g h mol⁻¹, the temperature from 200 to 260°C, and the pressure from 10 to 30 atm. The best results have been obtained at 220-240 °C, 20 atm and 97.45 g h mol⁻¹ of ethanol contact time with a conversion of 55-61% and a selectivity to ethyl acetate of 98-99%. It is important to point out that all the runs of Table 13 have been made on the same catalyst and that the catalyst worked for different months without showing deactivation. In Figure 19, the effect of temperature on, respectively, the conversion and selectivity for three different values of the pressure, at a constant ethanol contact time of 32.48 g h mol⁻¹ can be appreciated.

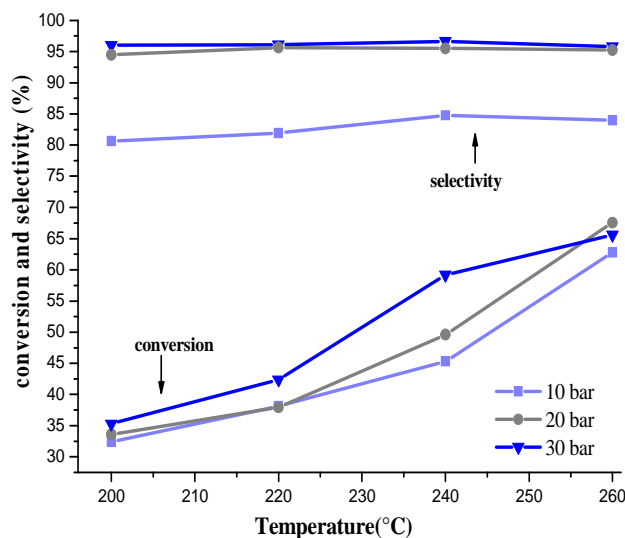


Figure 19: Effect of temperature and pressure on catalytic activity and selectivity of the copper chromite based catalyst Cu-1234. The catalytic tests have been conducted at residence time of $W/F=32.48 \text{ ghmol}^{-1}$.

As it can be seen, the conversion increases with the temperature, while, the selectivity is not affected by the temperature change, but is

dramatically affected by the pressure from 10 to 20 bars. A further increase of the pressure from 20 to 30 bars has a lower effect. Therefore, it can be concluded that 20 bar is the optimal pressure for this set of runs. In Figure 20, the effect of the temperature on, respectively, the conversion and the selectivity for three different values of the pressure, at the ethanol contact time of $97.45 \text{ g h mol}^{-1}$, is reported. Once again, the conversion increases with the temperature at the different pressures of 10, 20 and 30 bar, although the slope of the increase is lower for the runs performed at the highest pressure.

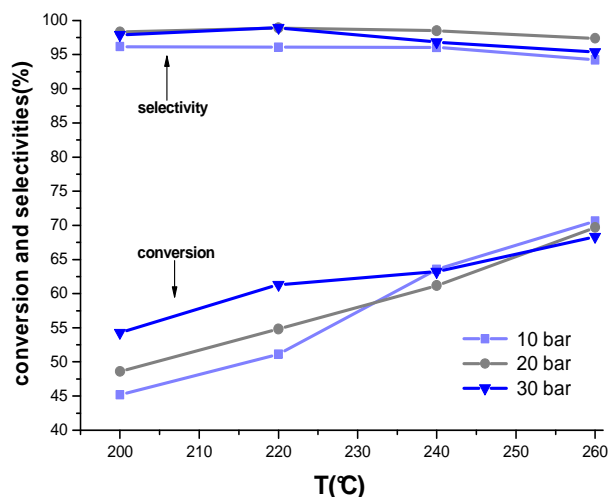


Figure 20 - Effect of temperature and pressure on catalytic activity and selectivity of the copper chromite based catalyst Cu-1234. The catalytic tests have been conducted at residence time of $W/F=97.45 \text{ ghmol}^{-1}$.

Table 13. Catalytic results over copper based catalyst. The dehydrogenation reaction were conducted at different pressure (10-30 bar), temperature (200-260°C) and at different contact time.

RUN	Cat. (g)	W/F (ghmol ⁻¹)	T (°C)	P (atm)	F _{EIOH} (cm ³ /min)	F _{H₂-6% N₂} (cm ³ /min)	F _{N₂} (mol/h)	F _{H₂} (mol/h)	X (%)	S _{AcOEt} (%)	S _{AcH} (%)	S _{others} (%)	P _{H₂} (g _{H₂} /h Kg _{cat})
1 C	50.70	97.45	200	10	0.5	25	0.057	3.66E-3	45.3	96.2	3.2	0.6	9.04
2 C	50.70	97.45	220	10	0.5	25	0.057	3.66E-3	51.1	96.1	2.9	1.0	10.15
3 C	50.70	97.45	240	10	0.5	25	0.057	3.66E-3	61.8	96.5	1.1	2.4	12.10
4 C	50.70	97.45	260	10	0.5	25	0.057	3.66E-3	69.7	93.4	1.5	5.1	13.27
5 C	50.70	97.45	200	20	0.5	25	0.057	3.66E-3	48.6	98.3	1.3	0.4	9.71
6 C	50.70	97.45	220	20	0.5	25	0.057	3.66E-3	54.8	98.9	0.8	0.3	10.96
7 C	50.70	97.45	240	20	0.5	25	0.057	3.66E-3	61.16	98.5	0.9	0.6	12.20
8 C	50.70	97.45	260	20	0.5	25	0.057	3.66E-3	70.6	94.2	0.5	5.3	13.42
9 C	50.70	97.45	200	30	0.5	25	0.057	3.66E-3	54.3	97.9	1.3	0.8	10.81
10 C	50.70	97.45	220	30	0.5	25	0.057	3.66E-3	63.2	96.8	0.6	2.6	12.35
11 C	50.70	97.45	240	30	0.5	25	0.057	3.66E-3	63.2	96.8	0.6	2.6	12.35
12 C	50.70	97.45	260	30	0.5	25	0.057	3.66E-3	67.2	96.0	0.8	3.2	13.05
	50.70	97.45	200	30	0.5	15	0.057	3.66E-3	58.4	87.7	9.1	3.2	11.34
13 C	50.70	32.48	200	10	1.5	25	0.057	3.66E-3	34.8	78.2	10.6	11.2	18.60
14 C	50.70	32.48	220	10	1.5	25	0.057	3.66E-3	40.5	86.9	6.3	6.8	22.72
15 C	50.70	32.48	240	10	1.5	25	0.057	3.66E-3	59.9	84.0	6.3	9.6	32.56
16 C	50.70	32.48	260	10	1.5	25	0.057	3.66E-3	60.4	84.2	4.9	10.9	32.40
17 C	50.70	32.48	200	20	1.5	25	0.057	3.66E-3	35.3	93.5	5.2	1.3	20.97
18 C	50.70	32.48	220	20	1.5	25	0.057	3.66E-3	47.2	96.9	1.9	1.2	28.07
19 C	50.70	32.48	240	20	1.5	25	0.057	3.66E-3	61.2	96.1	1.8	2.1	36.07
20 C	50.70	32.48	260	20	1.5	25	0.057	3.66E-3	67.5	95.2	1.7	3.0	39.38
21 C	50.70	32.48	200	30	1.5	25	0.057	3.66E-3	35.9	94.8	3.7	1.5	21.29
22 C	50.70	32.48	220	30	1.5	25	0.057	3.66E-3	42.4	96.1	2.0	1.9	25.04
23 C	50.70	32.48	240	30	1.5	25	0.057	3.66E-3	60.9	95.8	2.1	2.1	35.89
24 C	50.70	32.48	260	30	1.5	25	0.057	3.66E-3	65.6	93.8	2.6	3.6	38.07

The selectivities, as it has been appreciated also at low ethanol residence time, are poorly affected by the temperature but, in this case, are less sensible to the increase of the pressure from 10 to 20 bars. At last, it is interesting to observe by comparing Figure 8 and 9 that the increase of ethanol contact time is beneficial to the reaction selectivity reaching in this case, the top value. By concluding, according to the described results the best operative conditions for the dehydrogenation of ethanol to ethyl acetate on the BASF Cu-1234-1/16-3F catalyst are: 220°C, 20 bars and about 100 g h mol⁻¹ of ethanol contact time. The hydrogen productivity in the condition of reaction reported in Table 13 is included in the range 9-40 g_{H₂}/(Kg_{cat}*h).

Another important aspect is related to the presence of a hydrogen stream fed to the reactor with the reactant during the runs. In this case the effect of the partial pressure at high residence time (30-100 ghmol⁻¹) have been studied. The results obtained performing runs, in which the molar flow rate of hydrogen in the system was changed, by maintaining constant the flow rate of ethanol have been reported in Figure 21-22. In Figure 21, the comparison was between runs performed at 200°C, 30 bar, residence time of 97ghmol⁻¹ and at three different partial pressures of hydrogen fed. In Figure 22, the comparison was between runs performed in range of temperature 200-260°C, 10 bar, residence time of 97ghmol⁻¹ and at two different total flow of H₂6% in N₂ respectively of 5cm³/min and 25 cm³/min.

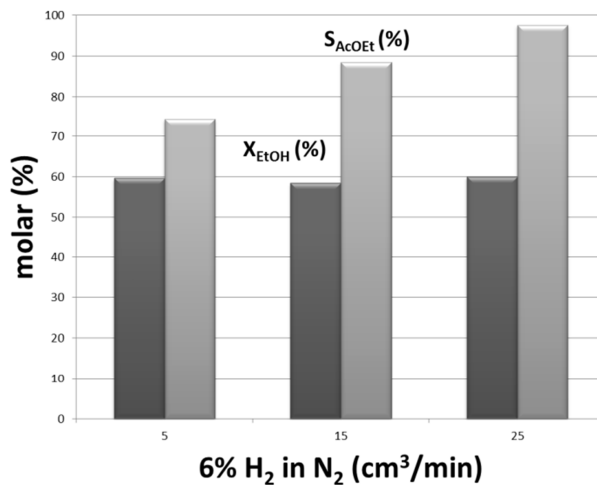


Figure 21: Hydrogen partial pressure effect on catalytic performance of copper chromite based catalyst Cu-1234. The reaction has been conducted at temperature of 200°C, total pressure of 30 bar and at residence time of 97.45 ghmol⁻¹.

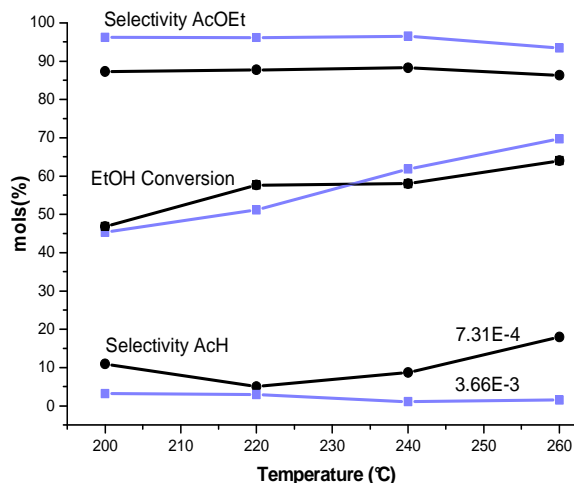


Figure 22: Comparison of Cu-1234 performances at two different Hydrogen flow respectively of $7.31E-4$ and $3.66E-3$ mol/h. The runs have been performed at 200°C , 10 bar, 100 ghmol^{-1} .

As it can be seen, the ethanol conversion is poorly affected by the hydrogen partial pressure but the selectivity to ethyl acetate strongly increases, by increasing the hydrogen molar flow rate. This means that, in an industrial plant, recycled pure hydrogen, produced during the dehydrogenation reaction, could be useful as carrier gas, respect to inert diluents like nitrogen, to promote the ethyl acetate selectivity.

To summarize the several obtained results, a comparison between the performances of the catalysts studied have been reported.

In Figure 23 A-D the comparison of the catalytic performances in terms of hydrogen productivity, ethanol conversion, ethyl acetate and acetaldehyde selectivity have been reported for the catalysts Cu-1234 (Cu-Cr-Al), Sg-9601 (Cu-Zn-Al), Cu-0203 (Cu-Cr). The runs have been performed for each system at a pressure of 20 bar, at a residence time of about 4 ghmol^{-1} , by fed a mixture of $6\%\text{H}_2$ in N_2 of $25\text{ cm}^3/\text{min}$. The behavior of the examined system has been studied in a range of temperature of $200\text{-}260^{\circ}\text{C}$.

The conversion profiles (Figure 23A) have shown the higher activity of CuCrAl (Cu-1234) catalyst, at 260°C and at a residence time of 4 ghmol⁻¹ is of about 40%. The activity of Cu-0203, in the same operative conditions, is very low and of about 10%. The ethyl acetate selectivity's profiles have shown the higher performances, with 85-90% of ethyl acetate selectivity, of Cu-1234 and Sg-9601 respect to Cu-0203 (65-70%) at a temperature of reaction higher than 220°C. In these case the selectivity is included in the range 85-90%.

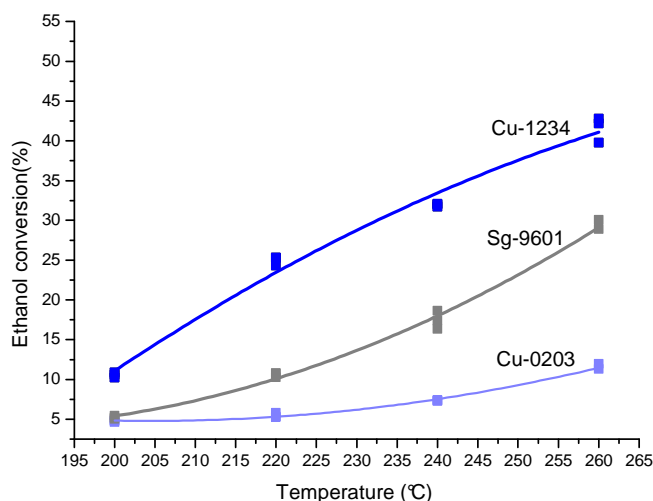


Figure 23A: Conversion profiles of Cu-1234, Sg-9601, Cu-0203. The runs were performed at 20 bar and 4ghmol⁻¹ of residence time.

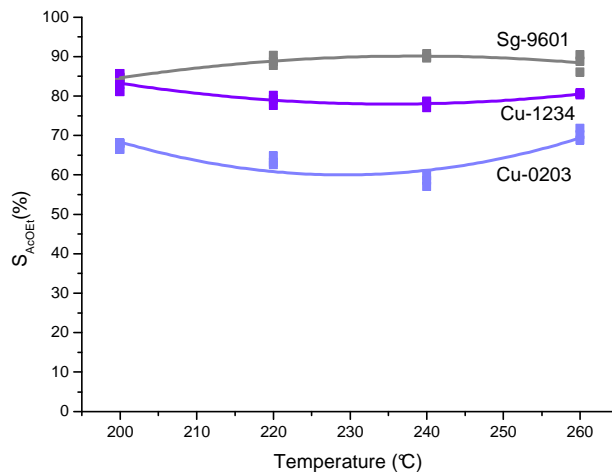


Figure 23B: ethyl acetate selectivity profiles of Cu-1234, Sg-9601, Cu-0203. The runs were performed at 20 bar and 4ghmol^{-1} of residence time.

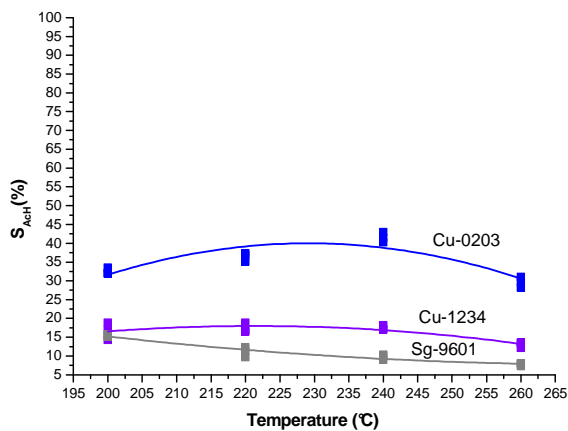


Figure 23C: acetaldehyde selectivity profiles of Cu-1234, Sg-9601, Cu-0203. The runs were performed at 20 bar and 4ghmol^{-1} of residence time.

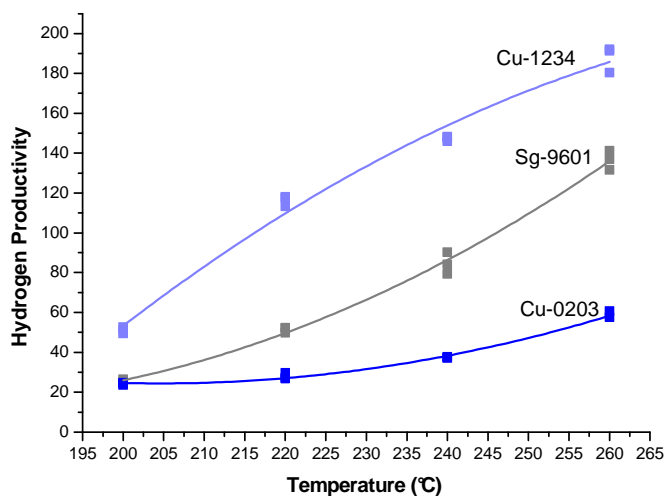


Figure 23D: hydrogen productivity profiles of Cu-1234, Sg-9601, Cu-0203. The runs were performed at 20 bar and 4ghmol^{-1} of residence time.

The catalyst CuCr (Cu-0203) favor the acetaldehyde production that in the range of temperature 200-260°C is of about 35-40%.

To well understanding the evolution of the ethanol conversion, ethyl acetate and acetaldehyde selectivity, at three different residence times the Figure 24 should be considered in this discussion. In particular, the experimental profiles of ethanol conversion, acetaldehyde and ethyl acetate selectivities obtained for the catalyst Cu-1234 at different residence time, by operating at 220°C, at 20 bar, with a flow of hydrogen 6% in N_2 of $25\text{ cm}^3/\text{min}$ have been reported.

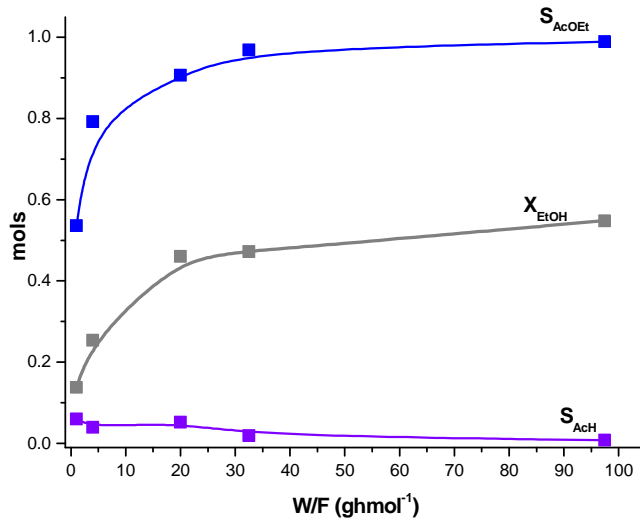


Figure 24: Cu-1234 catalyst. Effect of the ethanol residence time on the catalyst performances. The runs were performed at 220°C, 20 bar and by feeding 25 cm³/min of H₂ in N₂.

At relatively low residence time of about 1 ghmol⁻¹ the ethanol conversion is less than 10% whilst the ethyl acetate is less than 50%. As demonstrated in chapter 3 of this section, at temperature lowest than 300°C no acetaldehyde should be detected. This consideration is valid in the case of a Gibbs reactor in which an infinite residence time is considered. The experimental result have been collected at finite and very low residence time (<100 ghmol⁻¹) and in this conditions high acetaldehyde selectivity's have been obtained and moreover, a wide range of by-products, directly derived by acetaldehyde condensations, have been detected. By increasing the residence time the ethyl acetate selectivity and the ethanol conversion reaches the equilibrium.

B-4.4 Discussion and Mechanism of reaction

On the basis of the several obtained results some conclusion can be reached. The catalyst of CuCrAl (Cu-1234) have shown, together with the K-310 and Sg-9601 the best performances in terms of activity and ethyl acetate selectivity. The poor activity of T-4466 and Cu-0203 could be attributed mainly to the low specific surface area that characterize the catalyst examined. But as demonstrate the catalyst K-310 (CuZn-Al-O) is more susceptible to sintering and after about 10 h of reaction deactivate for effect of both sintering of copper and fouling of the catalyst surface due to acetaldehyde adsorption.

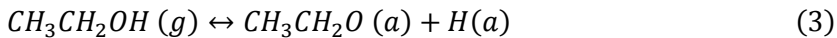
The Cu-1234 is characterized by very small copper crystallites, as demonstrated by XRD and SEM, inserted in alumina support. This characteristic is very promising to obtain highly active catalysts system. The most relevant aspects, arising from the results obtained with BASF Cu-1234-1/16-3F catalyst, are the positive effect on the selectivity to ethyl acetate of increasing: the partial pressure of hydrogen, the temperature from 200 to 220°C, the pressure up to 20 bars and the ethanol contact time from 32.5 to 97.5 g h mol⁻¹. All the mentioned aspects cooperate to increase the selectivity to ethyl acetate. The most surprising is the effect of pressure, because, dehydrogenations normally occur with an increase of moles, therefore, would be favored by the low pressure. In order to deepen this aspect, it could be useful to consider one of the most accredited reaction scheme for ethanol dehydrogenation proposed by Inui et al. [8] and reported in the introduction of this chapter. This reaction scheme does not consider the surface intermediates interactions, and although is reasonable, because, justify all the observed reaction products, both the main intermediates hemiacetal and acetaldol have not been experimentally observed by the authors. Maybe, these species are present only as precursors adsorbed on the copper surface. However, according to this

scheme the reaction occurs in two chemical steps. The first one is the dehydrogenation of ethanol to acetaldehyde favored, as expected, by the low pressure and short ethanol residence time and the second step characterized by two competitive acetaldehyde condensation reactions, one involving two acetaldehyde molecules for giving acetaldol and another one giving hemiacetal by condensing one molecule of ethanol and one of acetaldehyde. The in-situ DFTIR characterization results obtained in ethanol flow, confirm this hypothesis. In fact at low temperature of reaction ($<100^{\circ}\text{C}$) mainly it is individuate adsorbed ethanol that gradually disappear to favor the formation of acetaldehyde and esters, like ethyl acetate. As it can be seen in the reaction scheme, several by products can be obtained from acetaldol by further condensation and dehydrogenation (aldehydes and ketones), while, from hemiacetal only ethyl acetate can be obtained by dehydrogenation.

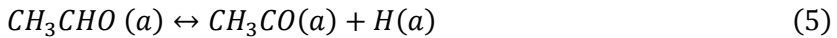
The condensation reactions are clearly favored by the pressure in contrast to the successive dehydrogenations. Therefore, the use of a moderate pressure (20 bars) should be a good compromise between these two contrasting demands.

Another important aspect to be considered is the acetaldehyde accumulation in the system, favoring the auto-condensation reaction so giving undesired by products. Therefore, in order to obtain a high selectivity to ethyl acetate, it is necessary to minimize the partial pressure of acetaldehyde in the system. Different factors would contribute in maintaining low the acetaldehyde concentration in the system favoring the pathway to ethyl acetate. The increase of temperature, for example, favors the reaction with the highest activation energy the increase of pressure corresponds to an increase of ethanol concentration in the system the increase of ethanol residence time gives time to the second reaction step to occur. At last, the presence of hydrogen in

the feeding stream could slow down the ethanol dehydrogenation rate to acetaldehyde concurring to maintain low the partial pressure of acetaldehyde. However, a very high selectivity to ethyl acetate can be achieved only with a catalyst surface favoring exclusively the condensation route to ethyl acetate. At this purpose, it is important to deepen the reaction mechanism. According to Colley et al.[4], which studied the mechanism of the ethyl acetate formation on a copper chromite catalyst, the reaction mechanism would be characterized by a first step, in which ethanol is dissociatively adsorbed on the catalyst surface as it follows:



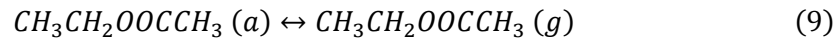
As the hydrogen collected by the authors for the ethanol adsorption was more than the amount foreseen for this reaction, other successive dehydrogenations steps have been proposed to occur such as:



Then the reactions forming the main observed products should be:

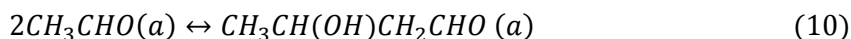


Finally, the reaction of adsorbed ethoxy species with adsorbed acetyl groups gives place to adsorbed ethyl acetate that slowly desorbs:

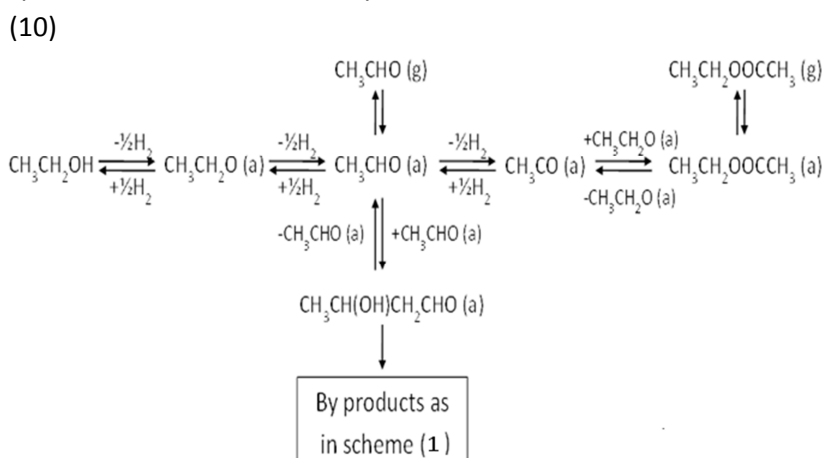


According to Colley et al.[4], ethyl acetate desorption (9) would be the rate determining step, being this compound strongly adsorbed on the Bronsted acid sites present on the surface of the copper chromite catalyst as a consequence of the reaction (2). As seen, this mechanism does not consider the possibility of the formation of the adsorbed hemiacetal intermediate as postulated in the scheme (1) by Inui et al. [8] but suggests a direct formation of ethyl acetate. This mechanism well explains the ethyl acetate formation but does not explain the al-

ternative pathway passing through the condensation of two acetaldehyde molecules. Probably, as suggested by the scheme (1), strongly adsorbed acetaldol is formed, that is then easily involved in many further reactions giving several by-products instead of desorbing:



A more reliable reaction scheme, taking into account the intermediate species adsorbed on the catalytic surface, would be:



According to this mechanism, the selectivity will be strongly affected also by the peculiarity of the copper catalytic sites, retaining the different adsorbed species as previously described. At low pressure, it has been experimentally observed that reactions (4) and (6) mainly occur. On the contrary, at moderate pressure condensation reactions are generally favored but with a large predominance of reactions (8) and (9) on reaction (6). The selectivity between the condensation reactions (8) and (9) is then determined by two main factors: the partial pressure of acetaldehyde, as already mentioned, and the structure of the surface of the catalyst. As a matter of fact White et al. [50] has shown, for example, that isolated Cu atoms are more selective in producing

acetaldehyde, while, the formation of ethyl acetate is promoted by poorly dispersed catalysts, so the catalysts rich of multi-sites assemblies are able to favor the condensation reactions.

Therefore, this type of selectivity will strongly be affected by: the nature of the catalyst, the preparation method, the catalyst pre-treatment, the acid-base properties of the catalytic environment and the type of used support [38] and promoters. By concluding, for increasing the selectivity to ethyl acetate, it is imperative both to keep low the acetaldehyde concentration, to reduce the probability of the occurrence of reaction (18), requiring two vicinal acetaldehyde adsorbed molecules, and to avoid the presence of sites favoring this coupling reaction. As a matter of fact, in this work we observed, by comparing the results obtained with the catalysts K-310 and T-4466, that the presence of copper chromite increases the selectivity to ethyl acetate. The catalyst Cu-1234 has reached a very satisfactory activity and selectivity this last never obtained before.

We attribute the obtained results to the particular structure of this catalyst having Cu^0 epitaxially grown on the surface of the chromite during the reduction with hydrogen [5] and to the acid environment near this Cu^0 , always formed during the reduction as a consequence of reaction (10). On the basis of EXAFS spectra of Cu-1234 copper chromite alumina catalyst, the oxidation state change of copper changed drastically during the reduction and a mixture of Cu^0/Cu^+ could be individuate. The spinel of CuCr_2O_4 is difficult to reduce and as suggested by Plyasova et al [12] only 50% of the total copper could be reduce.

Cu^0 promotes the dehydrogenation reactions and the acid environment hinders the acetaldehyde auto-condensation. Al_2O_3 support [51,52] has an important dispersion effect on copper chromite crystallites, while, $\text{BaO-Cr}_2\text{O}_3$ has probably a positive effect in avoiding the catalyst deactivation by sintering. BaO in particular has also the effect

of neutralizing the Lewis acid sites of both chromia and alumina [2,3], creating a more efficient barrier to sintering and limiting, as a consequence of the neutralization, the strength of both acid and basic sites, that could modify the selectivity. Another important aspect is to verify the eventually presence of Cr^{6+} . As confirmed by the XPS binding energy of Cr, the fresh catalyst Cu-1234 is exempt by Cr^{6+} , unlike of T-4466, and this represent an important factor that make this process green and sustainable.

On the basis of the obtained results, the best catalyst BASF Cu-1234-1/16-3F has been considered for a possible process development. Many other kinetic runs have been performed on this catalyst in both differential and integral reactors with the aim to achieve kinetic laws and related parameters of the involved reactions, in agreement with the proposed mechanism. The detailed kinetic approach will be reported in the next chapter of this thesis. However, considering the best results obtained (Table 13), it seems possible to obtain pure ethyl acetate and hydrogen without a post-treatment of hydrogenation on acetaldehyde and by-products, as described in a previous technology [53-55]. Obviously, this aspect must be further deepened; being crucial for the economy of the process, but the very high selectivity achieved is the basis for reaching this goal. In this process, unreacted ethanol, after dehydration, must be recycled together with the small amount of produced acetaldehyde. Correspondingly, hydrogen must be partially recycled because its use, as carrier gas, is beneficial for the promotion of ethyl acetate selectivity (see Figure 21). The ethyl acetate separation from ethanol requires at least two distillation columns for breaking the azeotrope. On the basis of all the mentioned aspects, a simplified process scheme like the one reported in Figure 25 can be drawn [56,57].

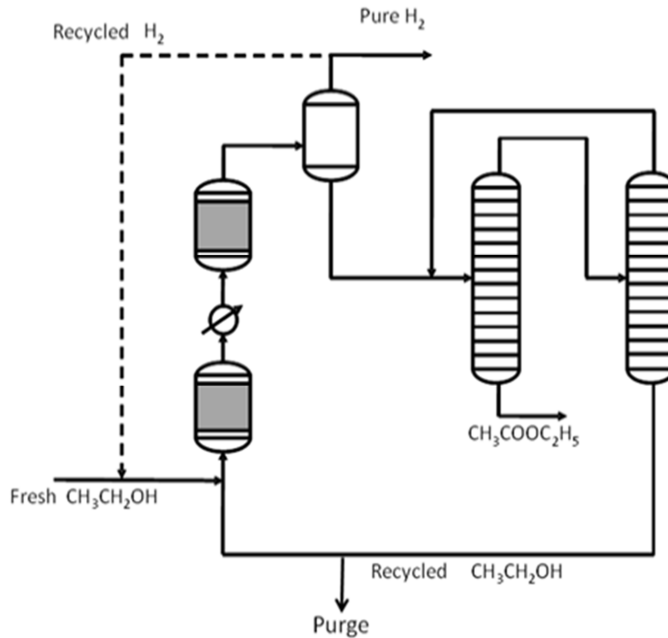


Figure 25 - A simplified scheme of the process based on the use of a new copper/copper chromite commercial catalyst.

The interesting obtained results will be interpreted in the next chapter of this section by using essentially three kinetics models: an empirical power law, a dual site adsorption based mechanism, and a Langmuir-Hinshelwood-Hougen-Watson. The power law kinetic was then used to realize a plant hypothesis illustrated in the final chapter of this section.

B-4.5 References

- [1] B.N.Dolgov, M.M. Koton, N.V.Siderov *J.Gen.Chem.USSR* 6, 1456 (1936).
- [2] Tu,Y.J., Chen,Y.W. & Li,C. *Journal of Molecular Catalysis* 89, 179-189 (1994a).
- [3]Tu,Y.-J., Li,C. & Chen,Y.-W. *Journal of Chemical Technology and Bio-technology* 59 , 141-147 (1994b).
- [4] Colley,S.W., Tabatabaei,J., Waugh,K.C. & Wood,M.A. *Journal of Catalysis* 236, 21-33 (2005).
- [5]Iwasa,N. & Takezawa,N. *Bulletin of the Chemical Society of Japan* 64, 2619-2623 (1991).
- [6] D.J. Elliot and F.Pennella Phillips Petroleum Company, Bartlesville, Oklahoma 359-367 (1989).
- [7]K.Inui, T.Kurabayashi, S.Sato *Applied Catalysis A: General* 237 (2002) 53-61.
- [8] K.Inui, T.Kurabayashi, S.Sato, N.Ichikawa *Journal of Molecular Catalysis A: General* 216 (2004) 147-156.
- [9] K.Inui, T.Kurabayashi, S.Sato *Journal of Catalysis* 212, 207-215 (2002).
- [10] Alexandre B. Gaspar, Flavia G. Barbosa, Sonia Letichevsky, Lucia G. Appel, *Applied Catalysis A: General* 380 (2010) 113–117.
- [11] Aparecida M. Kawamoto, Luiz Claudio Pardini and Luis Claudio Rezende, *Aerospace Science and technology* 8, (2004), 591-598.
- [12] L. M. Plyasova, V. F. Anufrienko, A. I. Beskrovnyi, I. Yu. Molina, T. A. Krieger, V. N. Ikorskii, T. V. Larina and L. P. Davydova, *Journal of structural chemistry* vol.43, n.2, pp.252-256, 2002.
- [13] Plyasova L.M.1; Molina I.Y.1; Kriger T.A.1; Davydova L.P.1; Malakhov V.V.1; Dovlitova L.S.1; Yur'eva T.M. *Kinetics and catalysis* vol.42, n.1, pp.126-131, 2001.

- [14] R. Rao, A. Dandekar, R. T. K. Baker, and M. A. Vannice *Journal of catalysis* 171, 406-419 (1997).
- [15] Wei Li, Hua Cheng, *Solid State Iterscience* 9 (2007) 750-755.
- [16] I.I. Simentsova, A.V.Khasin, L.P. Davydova and T.M. Yurieva *React.Kinet.Catal.Lett.vol.82, n.2*, 355-361 (2004).
- [17] LL. Jalowiecki, G.Wrobel, M.Daage, J.P.Bonnelle *Journal of catalysis* 107, 375-392 (1987).
- [18] T.P. Minyukova , I.I. Simentsova, A.V. Khasin, N.V. Shtertser, N.A. Baronskaya, A.A. Khassin, T.M. Yurieva *Applied Catalysis A: General* 237 (2002) 171-180.
- [19] G. Carotenuto, M. Di Serio, E. Santacesaria, R. Tesser, *Italian Patent NA2010A000009*, 2010. PCT-WO 2011/104738 A2.
- [20] A. A. Khasin, T. M. Yur'eva, L. M. Plyasova, G. N. Kustova, H. Jobic, A. Ivanov, Yu. A. Chesalov, V. I. Zaikovskii, A. V. Khasin, L. P. Davydova, and V. N. Parmon *Russian Journal of general Chemistry*, 2008, vol.78, No.11, pp.2203-2213.
- [21] R.B.C Pillai *Catalysis Letters* 26 (1994) 365-371.
- [22]R. Rao, A. Dandekar, R. T. K. Baker,1 and M. A. Vannice *Journal of catalysis* 171, 406-419 (1997).
- [23] A. Gervasini, S. Bennici *Applied catalysis A: general* 281 (2005) 199-205.
- [24] S.Guerriero *phD thesis, University of Notre Dame*, 2011
- [25]JF, Moulder, Stickle WF, Sobol PE, and Bomben KD. *Handbook of x-Ray Photoelectron Spectroscopy : A Reference Book of Standard Spectra for Identification and Interpretation of XPS Data*, edited by Chastain J. Vol. 1. Eden Prairie, MN: Physical Electronics Division, Perkin-Elmer Corp, 1992.
- [26] M. Zhang, G.Li, H. Jiang *Catal.Lett.*(2011) 141:1104-1110.
- [27]Brooks, A. R.; Clayton, C. R.; Doss, K.; Lu, Y. C. J. *Electrochem.Soc.* 1986, 133, 2459

- [28] Philip G. Harrison et al , Chem. Mater. 2000, 12, 3113-3122
- [29] A. A. Khasin, T. M. Yur'eva, L. M. Plyasova, G. N. Kustova, H. Jobic, A. Ivanov, Yu. A. Chesalov, V. I. Zaikovskii, A. V. Khasin, L. P. Davydova, and V. N. Parmon Russian Journal of general Chemistry, 2008, vol.78, No.11, pp.2203-2213.
- [30] P. G. MENON AND J. PRASAD JOURNAL OF CATALYSIS 17, 23&244 (1970)
- [31] Adkins, H.; Connor, R. 1931. The catalytic hydrogenation of organic compounds over copper chromite. J. Am. Chem. Soc. 53: 1091-1095.
- [32] O.V. Makarova, T.M. Yurieva, G.N. Kustova, A.V. Ziborov, L.M. Plyasova, T.P. Minyukova, L.P. Davydova, V.I. Zaikovskii: Kinet. Katal., 34, 681 (1993)
- [33] T.M. Yurieva, L.M. Plyasova, O.V. Makarova, T.A. Krieger: J. Mol. Catal. A: Chemical, 113, 455 (1996)
- [34] Fujita, S.I., Iwasa, N., Tani, H., Nomura, W., Arai, M. & Takezawa, N. Reaction Kinetics and Catalysis Letters 73, 367-372 (2001).
- [35] J. Llorca et al. / Journal of Catalysis 227 (2004) 556–560
- [36] A. Yee, S.J. Morrison, H. Idriss, J. Catal. 186 (1999) 279.
- [37] G.B. Deacon, R.J. Phillips, J. Coord. Chem. Rev. 33 (1980) 227.
- [38] H. Idriss, C. Diagne, J.P. Hindermann, A. Kiennemann, M.A. Bar-teau, J. Catal. 155 (1995) 219.
- [39] Millar GJ et al. J.Chem.Soc.Faraday Trans 1 1991; 87:2785]
- [40] Borrello E., J.Phys Chem. 1967; 71 2938]
- [41] D. M. MONTI, N. W. CANT, D. L. TRIMM, AND M. S. WAINWRIGHT JOURNAL OF CATALYSIS 100, 17-27 (1986)
- [42] K. Inui et al. / Journal of Molecular Catalysis A: Chemical 216 (2004) 147–156
- [43] K. Takeshita, J. Sci. Hiroshima Univ., Ser. A 54 (1990) 99

- [44] K. Takeshita, S. Nakamura, K. Kawamoto, *Bull. Chem. Soc. Jpn.* 51 (1978) 2622¹ [45] Prasad *Bulletin of Chemical Reaction Engineering & Catalysis*, x (x), 2011, p.1 - p.51.
- [46] Raich, B.A. & Foley, H.C. *Industrial and Engineering Chemistry Research* 37, 3888-3895 (1998).
- [47] Kanoun, N., Astier, M.P. & Pajonk, G.M. *Reaction Kinetics and Catalysis Letters* 44, 51-56 (1991a)
- [48] P.C. Zonetti et al. / *Journal of Molecular Catalysis A: Chemical* 334 (2011) 29–34]
- [49] C.P. Thurgood; J.C. Amphlett; R.F. Mann and B.A. Peppley *Topics in Catalysis* vol.22, 2003.
- [50] Kenvin, J.C. & White, M.G. Supported catalysts prepared from mononuclear copper complexes: Catalytic properties. *Journal of Catalysis* **135**, 81-91 (1992).
- [51] R.S. Rao, R.T.K. Baker, M.A. Vannice, *Catal. Lett.* 60 (1999)]
- [52] Kanoun, N., Astier, M.P. & Pajonk, G.M. Dehydrogenation of ethanol and CO₂-H₂ conversion on new coprecipitated Cu/Cr-Al catalysts. *Journal of Molecular Catalysis* **79**, 217-228 (1993).
- [53] S.W. Colley, C.R. Fawcett, M. Sharich, M. Tuck, D.J. Watson, M.A. Wood, EP 1 117 758
631 B1, 2004 process for the preparation of ethyl acetate. 759
- [54] S.W. Colley, C.R. Fawcett, M. Sharich, M. Tuck, D.J. Watson, M.A. Wood, et al. 760 United States Patent US 7,553,397, B1 June 30, 2009 process. 761
- [55] S.W. Colley, C.R. Fawcett, M. Sharich, M. Tuck, D.J. Watson, M.A. Wood, Davy 762 Process Tech., Republic of South Africa (1978)
2004/9535-18,7,05.
- [56] PCT-WO 2011/104738 A2.

[57] E. Santacesaria, G.Carotenuto, R.Tesser, M.Di Serio, Chemical Engineering Journal in press 10.1016/j.cej.2011.10.043.

SECTION B

Chapter 5 A kinetic Study

B-5.1 Introduction

A *catalyst* was defined by J. J. Berzelius in 1836 as a compound, which increases the rate of a chemical reaction, but which is not consumed by the reaction [1]. This definition allows for the possibility that small amounts of the catalyst are lost in the reaction or that the catalytic activity is slowly lost. However, the catalyst affects only the reaction rate, it changes neither the thermodynamics of the reaction nor the equilibrium composition. Catalysis is of crucial importance for the chemical industry, the number of catalysts applied in industry is very large, and catalysts come in many different forms, from heterogeneous catalysts in the form of porous solids over homogeneous catalysts dissolved in the liquid reaction mixture to biological catalysts in the form of enzymes. The thermodynamics frequently limits the concentration of a desired product. As the catalyst does not affect the thermodynamics of the reaction, it is vain to search for a catalyst to improve the conversion of the reagents and the selectivity to the desired products. Instead, the reaction conditions (temperature, pressure and reactant composition) must be optimized to maximize the equilibrium concentration of the desired product. Once suitable reaction conditions have been identified, generally the reaction rate is found to be too low, frequently by orders of magnitude and consequently the search for a suitable catalyst begins.

The study of the kinetics of heterogeneous catalyzed reactions consists of at least three rather different aspects.

Kinetics studies for design purposes. In this field, results of experimental studies are summarized in the form of an empirical kinetic expression. Empirical kinetic expressions are useful for design of chemical reactors, quality control in catalyst production, comparison of different brands of catalysts, studies of deactivation and of poisoning of catalysts.

Kinetics studies of mechanistic details. If a reasonable and not too detailed reaction mechanism is available, an experimental kinetic study may be used to determine details in the mechanism. Mechanistic considerations may be very valuable as guidance for kinetic studies.

Kinetics as a consequence of a reaction mechanism. The deduction of the kinetics expression from a proposed reaction mechanism generally consists in a reasonably straightforward transformation, where all the mechanistic details are eliminated until only the net gas-phase reaction and its rate remains. This approach may be used to investigate if a proposed mechanism is consistent, what the reaction rate is and if it is consistent with available experimental data. For the three aspects of the kinetics study, the optimal experimental and theoretical approach is quite different. By following this approach, the main goal of this chapter was the development of a kinetic model that can be used to predict the conversion and selectivity of ethanol dehydrogenation to ethyl acetate.

Our kinetic investigation starts from the reaction mechanisms (Scheme 1, Chapter 5-Section B) proposed in the literature [2] with the aim to find the most reliable kinetic laws. According to a previous ethanol dehydrogenation to acetaldehyde kinetic study, made by Tu et al. [3], on unsupported Cu and Cr promoted Cu, this reaction is of first order

with respect to ethanol and has an apparent activation energy of 12.2 Kcal/mol. To our knowledge, only one paper has been published concerning the kinetics of the ethyl acetate formation on Cu based catalysts, in particular on Cu/copper chromite catalyst [4]. Colley et al. [4] have demonstrated that in a first step ethanol adsorbs on to the Cu component of Cu/Cr₂O₃ catalysts as an ethoxy species with an activation energy of 7.41 Kcal/mol and, successively, the ethoxy species adsorbed is dehydrogenated to an acetyl species with an activation energy of 22.50 Kcal/mol. Finally the ethoxy and acetyl species adsorbed on Cu, react to form adsorbed ethyl ethanoate and, assuming a first-order desorption, this has a desorption activation energy of 43.06 Kcal/mol.

Cause of the limited literature information in this research work, we have studied the kinetics of this reaction on the already mentioned commercial copper/copper chromite catalyst supported on alumina and promoted with barium chromite BASF Cu-1234 (CuCrO₄/CuO/Cu/BaCrO₄/Al₂O₃ (45:1:13:11:30% b.w.)). The kinetic runs were carried out in packed bed tubular reactor, alternatively filled with 2 or 50 g of catalyst, approximately isothermal, by feeding pure ethanol together with a mixture of nitrogen and hydrogen as carrier gas. The runs have been made by changing the temperature in the range of 200-260°C, the pressure between 10 and 30 bars and the residence time from 1 to 20 g·mol⁻¹. The parameters obtained by regression analysis of the experimental data obtained by using 2g of catalysts were, thus used in to simulate the experimental profiles obtained by runs performed with 50 g of catalys.

The first step to realize an intrinsic kinetic investigation is to evaluate the transport limitations. The absence of transport limitations provides kinetic parameters as expression of the chemical nature of the reaction. At first purpose, an evaluation of the inter-phase and intra-particles mass transfer limitation, by using respectively Mears [5]

Model 1: different empirical models based on a power law kinetic have been hypothesized.

Model 2: starting from the Scheme 1, each reaction step has been described by different elementary steps of adsorption/desorption. Several dual sites adsorption models have been realized in which for the reaction (1), related to the acetaldehyde formation, among the four different steps of adsorption/desorption, different rate determining step (RDS) have been considered.

Model 3: Langmuir-Hinshelwood-Hougen-Watson (LHHW) kinetic model has been used for interpreting all the experimental data collected. This model corresponds to a mechanism in which the first step is the dissociative adsorption of ethanol on the surface, giving an adsorbed ethoxy group that gives place with two consecutive steps to acetaldehyde and ethyl acetate. The rate determining step is the surface reaction.

The several models have been briefly described on the basis of the simulation curves trends with the experimental results. The good or bad fitting of experimental vs calculated has been evaluated by calculating the overall average error.

As computing language, Matlab has been used with the aim to simulate all the experimental runs by regression of the kinetics, adsorptions and equilibrium parameters.

In Table 1 a summary of the models developed, of their typology, of the main details and of the total number of the parameters has been reported. All the mentioned models, as it will be illustrated in the next paragraph, have given good results for what concerns the correlation index and the average per cent error, but only the *Langmuir-*

Hinshelwood-Hougen-Watson model (LHHW model 3) gives place to kinetic parameters with physical mean.

Table 1: Kinetic models developed

Model	Typology	Description	N°Parameters	Paragraph
1.1	power law	simplified	11	B.5.4.1.1
1.2	power law	simplified	13	B.5.4.1.2
1.3	power law	$K_{ei} = f(T)$	13	B.5.4.1.3
2.1	dual site	RDS: AcH desorption	18	B.5.4.2.1
2.1A	dual site	RDS: AcH desorption $K_{ei} = f(T)$	18	B.5.4.2.2
2.2	dual site	RDS: ethoxy adsorbed formation	18	B.5.4.2.3
2.3	dual site	RDS: acetaldehyde adsorbed formation	18	B.5.4.2.4
3	LHHW	$K_{ei} = f(T)$	14	B.5.4.3

This kinetic model allows a satisfactory fitting of all the performed experimental runs with a standard error below 15%. The obtained kinetic parameters of the best model, has a physical mean. A list and the meaning of each symbols is reported at the end of this chapter.

B-5.2 Diffusion limitation

In experimental studies of heterogeneously catalyzed reactions, the first study should be focused on the determination of the interactions between the kinetics and transport phenomena.

To ensure that the kinetic data obtained in an experimental reactor reflect only chemical events, gradients must be virtually eliminated from two domains:

- a. intraparticle gradient within individual catalysts particles

b. interphase gradient between the external surface of the particles and fluid adjacent to them.

Figure 1 depicts porous adsorbent particles in a catalysts bed with sufficiently generality to illustrate the nature and location of individual transport and dispersion mechanisms. Each mechanism involves a different driving force.

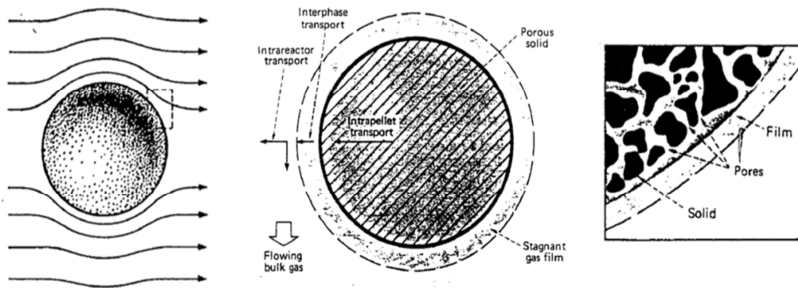


Figure 1. Mass transfer in a reactor results of interphase and intra-pellets transport.

The intraparticles transport may be limited mainly by pore diffusion and solid diffusion. The interphases or extraparticle mechanisms are affected by the design of the contact device and depend on the hydrodynamic conditions outside the particles. The external mass reflects the transfer between the external surfaces of the adsorbent particles and surrounding liquid phase. Moreover, the transport limitations are directly dependent by the operative condition adopted to perform the reaction such as the temperature and the pressure.

It is desirable to have some means to ascertain the effects of transport on reaction rates, a priori, both from the experimental measurement of catalytic reaction kinetics and for the design of catalytic reactors too. Such criteria must be based upon what can be measured or directly observed. The approach to this problem can ensue two different ways: (1) the development of means for the determination of catalytic effectiveness on the basis of observable quantities in a given

situation. (2) Development of a priori criteria to ensure the absence of significant concentration/temperature gradients. In our case, the second way was followed and a substantial number of a priori criteria for the estimation of transport effects on catalytic reaction rates have been individuated in the literature. Thus, to ensure that the kinetic experiments, taking place in the reactor, are kinetically controlled and not influenced by mass or heat transfer, reaction conditions were selected such that the Mears criterions for external diffusion and the Weisz and Prater criterion for intra-particles diffusion limitations are satisfied [9,10]. In Table 2 the main properties required, to apply both the criteria mentioned, has been summarized.

Table 2: Summary of the properties, parameters, bed characteristics needed to apply the criteria.

Properties	Acronyms/units	value
Bed porosity	ϵ_B	0.4
Bulk density catalyst	ρ_B (g/cm ³)	0.955
Tortuosity	τ	0.4
Constriction factor	σ	0.8
Molecular diffusivity EtOH in N ₂	D_i (cm ² /min)	6.12
Pellets diameter	d_p (cm)	0.1
Cross sectional area of the tube	A_c (cm ²)	2.54
Kinematic viscosity	ν (cm ² /min)	0.0092
Reaction order	n	2

B-5.2.1 Intra-particles transport

Intra-particles transport has been analyzed for ethanol dehydrogenation at high pressure (10-30 bar) and high temperature (200-260°C) to produce ethyl acetate. In particular, the *Weisz and Prater criterion* for the absence of concentration gradients, in an isothermal spherical particle was applied. It's assumed that the Fick's

first law governs diffusion in the porous media, that the effective diffusivity, D_e , remains independent of the nature of reaction and that the intrinsic catalytic activity is distributed uniformly throughout the catalytic bed. To ensure $\eta > 0.95$ in an isothermal spherical particle with a first-order reaction, the criterion requires (Eq.1):

$$\frac{r_A R_p^2}{C_0 D_{eff}} < 1 \quad (1)$$

The ways to calculate the reaction velocity r_A (2), radius R_p (3), the concentration C_0 (4) and diffusivity (5) have been described in the following equations 2-5.

$$r_A = \frac{F_E^0}{(1 - \varepsilon_B) \frac{W_{cat}}{\rho_B}} = \left[\frac{mol}{min \ cm^3} \right] \quad (2)$$

$$R_p = \frac{V}{S} = [cm] \quad (3)$$

$$C^0 = (C_{EtOH}^{in} - C_{EtOH}^{out})/2 \quad (4)$$

$$D_{eff} = D_i \left(\frac{\varepsilon^* \sigma}{\tau} \right) \quad (5)$$

As it can be seen, in Figure 2 the intra-particles criterion as function of the temperature, at three different reaction pressures has been evaluated.

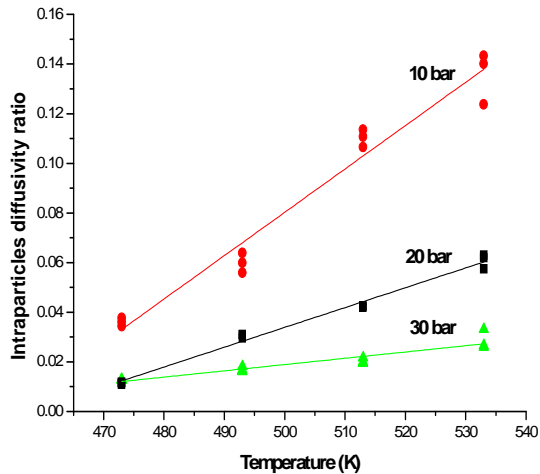


Figure 2: Weisz and Prater criterion

By the profiles reported in Figure 2, by increasing the temperature the increase of intra-particles ratio is higher than the ones obtained at lowest temperature of reaction. The increase of temperature implies an increase of the reaction rate and consequently, as the criterion suggests a raise of the intra-particles transport limitations. On the other hand, also the pressure effect on the diffusion can be appreciated by the profiles of Figure 2. By increasing the operating pressure, the transport phenomena limitations could be decrease. Nevertheless the highest temperature and lowest pressure of reaction, the diffusion coefficient is less than 1 and consequently it is possible conclude that the reaction is not limited by intra-particles transport phenomena.

B-5.2.2 Inter-phase transport

Assuming an isothermal system the resistance to the bulk mass transport across the film around the particles can be described by the Mears criteria:

$$\frac{r_A \rho_b R_p n}{K_c C_0} < 0.15 \quad (6)$$

The mass transfer coefficient has been defined as function of the bed porosity, diameter of the particles, diffusivity, and Sherwood number as reported into the Eq.7.

$$K_c = \frac{1 - \varepsilon_b}{\varepsilon_b} \left(\frac{D_i}{d_p} \right) Sh' \quad (7)$$

In order to obtain the Sherwood number it's possible to choose the Thoenes-Kramers equation, flow conditions through a catalyst bed, in which Sh' (Eq.8) is correlated respectively to Re' (Reynolds) (Eq.9) and Sc' (Schmidt) numbers (Eq.10):

$$Sh' = (Re')^{1/2} (Sc')^{1/3} \quad (8)$$

$$Re' = \frac{U d_p}{(1 - \varepsilon_b) \mu} \quad (9)$$

$$Sc' = \frac{\mu_i}{D_i} \quad (10)$$

In Figure 3 the profiles of interphase criterion at different temperature and pressure of reaction have been reported. As it can be appreciated from Figure 3 the intra-phase transport limitation is higher at high temperature while the pressure increase have a favorable effect. Anyway the intra-phase diffusivity ratio is always lower than 0.15 and we can conclude that the kinetic of reaction is not affected by intra-phase transport phenomena.

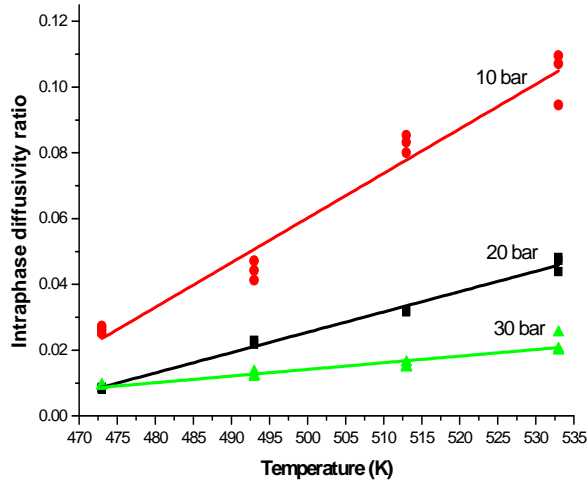


Figure 3: Mears Criterion

B-5.3 Kinetic study of ethanol dehydrogenation

B-5.3.1 Reaction mechanism pathway

The different and main reaction steps, by which ethyl acetate starting from ethanol has been obtained, have been reported (Eq.a-c).

The first step is an ethanol dehydrogenation to acetaldehyde and hydrogen.



The subsequent step is another dehydrogenation reaction of ethanol and acetaldehyde to ethyl acetate and hydrogen.



And finally a secondary reaction of aldol condensation of two acetaldehyde molecules favors the formation of several sub-products C_3 - C_4 aldehydes and chetones such as methylethylchetone, acetone, crotonaldehyde, that will be indicate, as lumped by-products, with the acronym "others".



The collected kinetic data, at different pressure, temperature and residence time, were interpreted by a mono-dimensional plug flow reactor model for which an isothermal condition was assumed. This assumption is justified by the relatively low ethanol conversion obtained with 2 grams of catalyst and by the high thermal capacity of the reactor body. On the basis of the reaction pathway, for each components of the reacting system it has been considered ordinary differential equation (ODE) and by integration of each ones, the concentration profiles of both the reagents and the products inside the reactor, assuming that the reactor is isothermal, were evaluated. The general ODE equation (11) has been reported:

$$\frac{dF_i}{dW} = \sum_{j=1}^3 \alpha_{ij} (r_j) \quad (11)$$

where $i=1-6$ representing the components, reactants and products, while $j=1-3$ representing the reactions in the assumed scheme. α_{ij} represents the corresponding stoichiometric coefficients for component i in reaction j . More explicitly, the ODE's expressions are :

$$\frac{dF_{EtOH}}{dW} = -r_1 - r_2 \quad (12)$$

$$\frac{dF_{AcH}}{dW} = r_1 - r_2 - 2r_3 \quad (13)$$

$$\frac{dF_{H_2}}{dW} = r_1 + r_2 \quad (14)$$

$$\frac{dF_{AcOEt}}{dW} = r_2 \quad (15)$$

$$\frac{dF_{Other}}{dW} = r_3 \quad (16)$$

$$\frac{dF_{Inert}}{dW} = 0 \quad (17)$$

By introducing the dimensionless length of the bed, z , defined as $z=L/L_{bed}$ [0,1], the mass balances for each component, can be advantageously written in dimensionless form as it follows (18):

$$\frac{dF_i}{dz} = w_{cat} \sum_{j=1}^3 \alpha_{ij} (r_j) \quad (18)$$

Introducing the dimensionless catalyst weight w (catalyst weight)= $L^*(w_{cat}/L_{bed})$, the differential rate equations 19-24 have been obtained:

$$\frac{dF_{EtOH}}{dz} = w_{cat}(-r_1 - r_2) \quad (19)$$

$$\frac{dF_{AcH}}{dz} = w_{cat}(r_1 - r_2 - 2r_3) \quad (20)$$

$$\frac{dF_{H_2}}{dz} = w_{cat}(r_1 + r_2) \quad (21)$$

$$\frac{dF_{AcOEt}}{dz} = w_{cat} * r_2 \quad (22)$$

$$\frac{dF_{Other}}{dz} = w_{cat} * r_3 \quad (23)$$

$$\frac{dF_{Inert}}{dz} = 0 \quad (24)$$

The system of differential equations was numerically integrated using ode45 function, in MATLAB. All kinetic parameters were subject to a mathematical regression analysis involving minimization of the objective function, represented by a nonlinear least squares fitting for the determination of the adjustable models parameters, by using the following objective function that was minimized by mathematical regression analysis:

$$RMS = \frac{1}{N} \sum_{i=1}^N (\alpha_i^{exp} - \alpha_i^{cal})^2 \quad (25)$$

In this relation a^{exp} and a^{calc} are respectively related to both experimental and calculated conversions and selectivities. The overall average error has been calculated by using the following expression:

$$\text{err} = \sum_{j=1}^4 \left[\frac{1}{N} \left| \sum_{i=1}^N \left(\frac{\alpha_{ji}^{\text{exp}} - \alpha_{ji}^{\text{calc}}}{\alpha_{ji}^{\text{exp}}} \right) \right| 100 \right] \quad (26)$$

Where j is an index for, respectively, ethanol conversion, acetaldehyde selectivity, ethylacetate selectivity and other by-products selectivity. The full program code used for the parameter fitting and the differential equation solver can be found in Appendix B. Moreover, to discriminate the several models studied the Pearson correlation index R^2 , was used and calculated as following:

$$R^2 = 1 - \frac{(SSE)/(Nsp - np - 1)}{SST/(Nsp - 1)} \quad (27)$$

Where, Nsp are the total experimental runs, np are the total number of the parameters employed and SSE represents the differences between the experimental and calculated data, as expressed by equation 28.

$$SSE = \sum_{i=1}^N (\alpha_{ie} - \alpha_{ic})^2 \quad (28)$$

The value of SST is the quadratic sum of all the experimental data as expressed by the relation 29.

$$SST = \sum_{i=1}^N \alpha_{ie}^2 \quad (29)$$

The Pearson coefficient must be a number included between zero and 1. As demonstrated in the next paragraphs, a good correlation between the model and experimental data ($R^2 > 0.88$) has been obtained. In some of the examined models, the dependence of the equilibrium constants by the reaction temperature was considered. In particular, as already described in Section B- Chapter 3, where a

detailed thermodynamic study was reported, the specifics related to the determination of the equilibrium constants were reported. Our kinetic runs have been performed in a narrow range of temperature, thus, we have applied the Van't Hoff equation for evaluating the dependence of the equilibrium constants by the temperature (30).

$$K_{ei} = K_{erif} * \exp \left[\left(\frac{\Delta H_i}{R} \right) \left(\frac{1}{T_{ref}} - \frac{1}{T} \right) \right] \quad (30)$$

The dependence of the equilibrium constants on the temperature has been expressed by the following equation (31):

$$\ln(K_{e_i}) = A + \frac{B}{T} \quad (31)$$

The values of the constants A and B are the following: reaction 1 A=16.5, B=-9136.4, reaction 2 A=-4.79, B=4386.0. As already mentioned, these expressions have directly been used in some of the developed kinetic model.

B-5.4 Kinetic models

Different kinetic models have been reported, based on different adsorption mechanisms. The real mechanism of ethanol dehydrogenation to ethyl acetate is not well defined yet. Nevertheless, most authors agree that the first elementary step is the molecular adsorption of ethanol on the active site to give ethoxide and adsorbed hydrogen. The ethoxide species are, in order, dehydrogenated to acetaldehyde, adsorbed on the catalyst surface, which reacts with an adsorbed ethoxy group to give ethyl acetate. The wide range of by-products could be obtained by aldol condensation of two adsorbed acetaldehyde molecules that must be controlled using optimal operating conditions to favor the ethyl acetate production. In more detail, the expressions of the rates of reaction for three different

models have been deduced on the basis of mechanistic considerations.

The kinetic constants (k_i) and consequently reaction rates can be expressed as function of the temperature of reaction (T) and by considering a reference temperature (T_{ref}) of 220°C, according to the Arrhenius equations, by using the following equation (32).

$$k_i = k_i^{ref} \exp \left[\frac{E_{Ai}}{R} \left(\frac{1}{T_{ref}} - \frac{1}{T} \right) \right] \quad (32)$$

In the next paragraphs the details of each models have been described.

B-5.4.1 Power law

B-5.4.1.1 Model 1.1

The kinetic expressions for the model in exam are reported (33 a-c). In particular it has been assumed a simply power law model in which the equilibrium has been neglected.

$$r_1 = k_1 p_{EtOH}^\alpha p_{H_2}^\beta \quad (33 a)$$

$$r_2 = k_2 p_{EtOH}^\gamma p_{ACH}^\delta p_{H_2}^\omega \quad (33 b)$$

$$r_3 = k_3 p_{ACH}^2 \quad (33 c)$$

Where k_1 , k_2 , k_3 are the kinetic constants. In the model in exam the parameters value: the reference kinetic constants K_1^{ref} , K_2^{ref} , K_3^{ref} , the activation energies and the reaction orders ($\alpha, \beta, \delta, \gamma, \omega$), have been estimated on runs performed by using two grams of catalysts (see Chapter 4-Section B). The kinetic constants at a temperature of reference of 220°C, the corresponding activation energy parameters and the exponential parameters of the power law have been reported in Table 3.

Table 3: Model 1.1. Kinetic parameters of the power law model determined by regression analysis on all the experimental runs performed by using the reactor loaded with 2 g of catalyst (see chapter 4).

Average Error 14.65			
Average Correlation Index 0.82			
Kinetic constants	(mol/cm³ h)	Activation Energy	(Kcal/mol)
k_1^{ref}	1.59E-2	Ea_1	19.27
k_2^{ref}	0.11	Ea_2	2.41E-3
k_3^{ref}	1.28E-3	Ea_3	5.69
Reaction orders			
α	0.50		
β	-0.50		
γ	1.67		
δ	-1.37		
ω	-0.24		

In Figure 4A and 4B are reported the parity plot diagrams obtained respectively for the ethanol conversion and selectivities to the main products of reaction such as ethyl acetate and acetaldehyde, where the validity of the adopted kinetic model can be better appreciated.

The Figure 4C shows the fitting of conversion experimental data with the calculated ones, obtained by operating in a range of temperature of 180-300°C, at three different pressure (10-30 bar) and by using an ethanol flow rate of 0.5 cm³/min that correspond to a residence time of 4 ghmol⁻¹ (see chapter 4-Section B). In Figure 4D the fitting of ethyl acetate selectivity experimental data with the calculated ones, obtained by operating in a range of temperature of 180-300°C, at three different pressure (10-30 bar) and by using an ethanol flow rate of 0.5 cm³/min that correspond to a residence time of 4 ghmol⁻¹ (see chapter 4-Section B) have been reported.

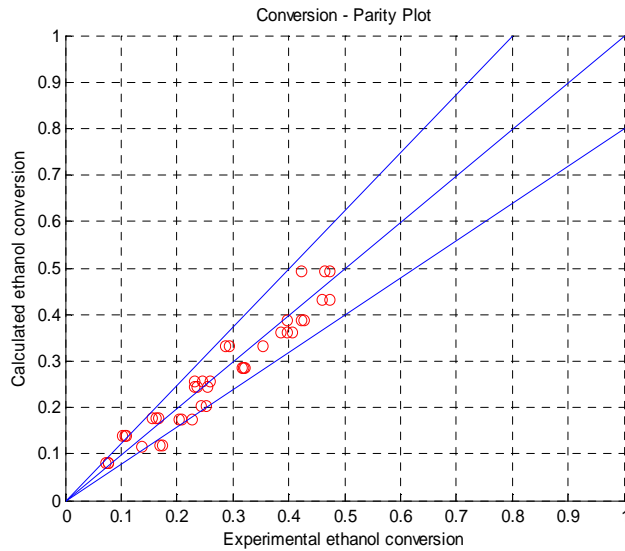


Figure 4A: Parity plot for ethanol conversion calculated vs experimental (2 g catalyst).

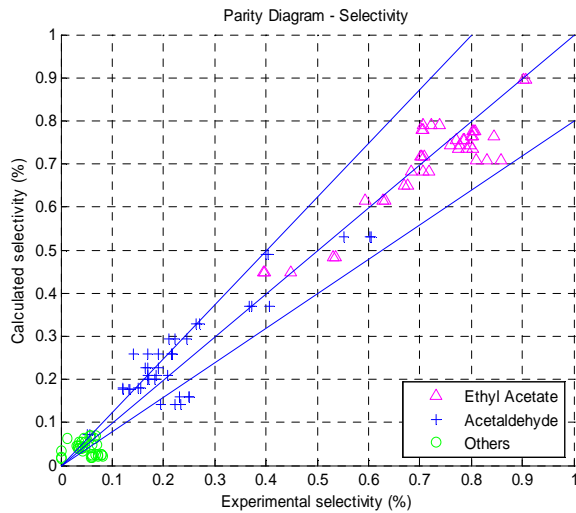


Figure 4B: Parity plot of acetaldehyde, ethyl acetate, others selectivity calculated vs experimental (2 g catalyst).

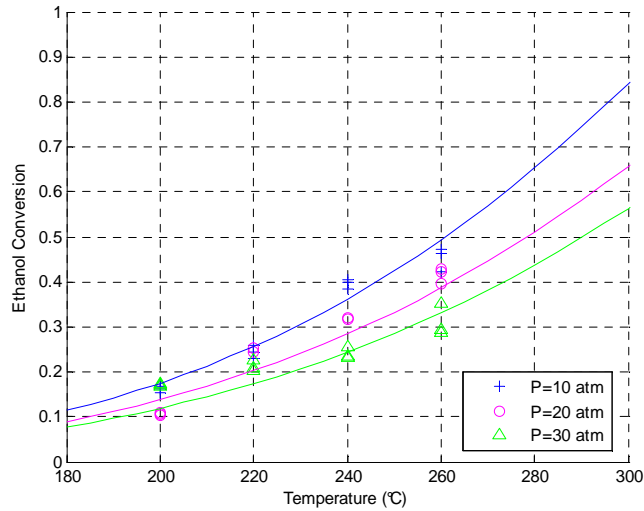


Figure 4C: ethanol conversion as a function of temperature reaction. The runs were performed at three different pressures (10-20 bars), at a residence time of 4ghmol^{-1} , by fed a constant flow of $\text{H}_26\%\text{N}_2$ $25\text{ cm}^3/\text{min}$.

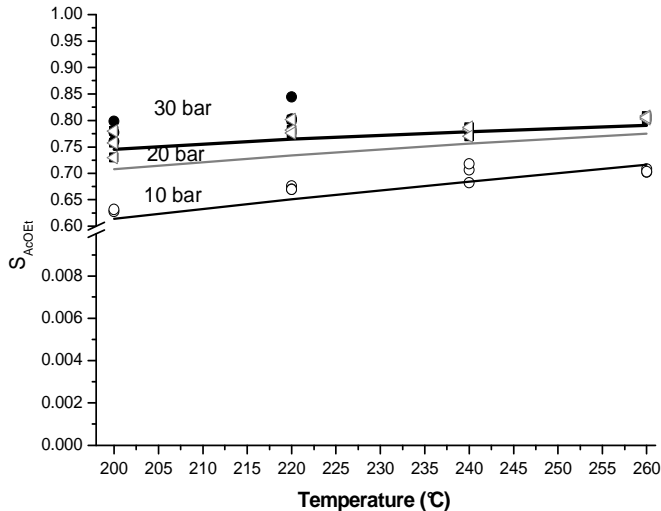


Figure 4D: ethyl acetate selectivities as a function of temperature reaction. The runs were performed at three different pressures (10-20 bars), at a residence time of 4ghmol^{-1} , by fed a constant flow of $\text{H}_26\%\text{N}_2$ $25\text{ cm}^3/\text{min}$.

As shown in Figure 4C the calculated conversion profiles by using a power law model are able to well interpret the experimental data obtained in the above-mentioned conditions. On the other hand, the model was not able to give a reasonable interpretation of the experimental selectivity data of ethyl acetate, this aspect is more clearly evident at higher pressure (20-30) bar as shown in Figure 4D. In Figure 4E the experimental and calculated profiles of ethanol conversion as function of the reaction temperature obtained by operating at three different residence time $1-20 \text{ ghmol}^{-1}$, at constant pressure of 20 bar and by feeding into the apparatus system respectively $1.5-0.5-0.1 \text{ cm}^3/\text{min}$ have been reported. In this case, the calculated profiles are able to simulate the dependence of the ethanol conversion by the residence time adopted. As it can be seen at higher residence time of 20 ghmol^{-1} the ethanol conversion is at a temperature of 220°C of about 43%.

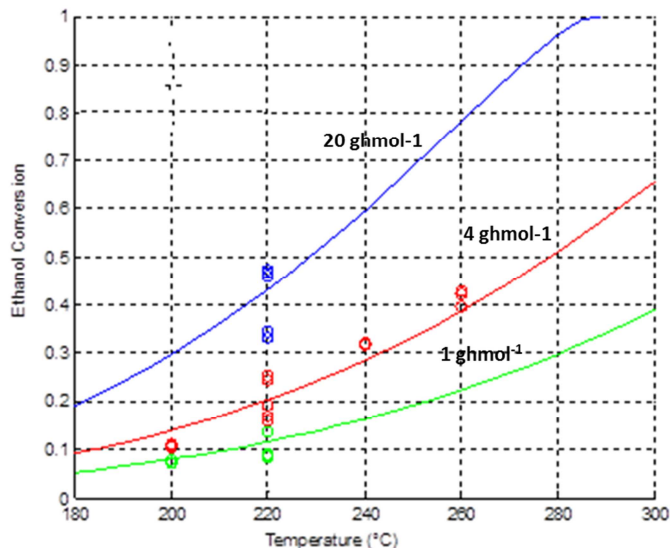


Figure 4E: ethanol conversion as a function of temperature reaction. The runs were performed at three different residence time of 1.30-

3.89-19.46 g mol^{-1} , by fed a constant flow of H₂ 6% N₂ 25 cm³/min and at constant pressure of 20 bar.

This behavior is in agreement with the experimental results in which the ethanol conversion, at the same mentioned temperature and residence time, is in the range 35-43%. At lowest residence time the calculated profiles by power law kinetic model are able to well describe the experimental data.

The model 1.1 was used also in simulation to individuate also the best parameter fitting of the experimental data obtained for the all the experimental runs performed by using 50 g of catalyst. Thus, the empirical kinetic expressions obtained could be useful for design purpose and in particular, as it will be described in Chapter 6 of this section, a plant hypothesis for the dehydrogenating reactor to produce ethyl acetate has been proposed. The Table 4 describes the parameters, the kinetic constants at a temperature of reference of 220°C, the corresponding activation energy parameters and the exponential parameters of the power law, obtained for experimental runs performed at 50 g.

Table 4: Kinetic parameters of the power law model 1.1 determined by regression analysis on all the experimental runs performed by using the reactor loaded with 50 g of catalyst (see chapter 4).

Average Error 12.21			
R²=0.88			
Kinetic constants	(mol/cm ³ h)	Activation Energy	(Kcal/mol)
K ₁ ^{ret}	3.54	Ea ₁	7.71
K ₂ ^{ret}	0.41	Ea ₂	4.52
K ₃ ^{ret}	29.22	Ea ₃	10.30
Exponential Parameters power law			
α	1.010		
β	0.063		
γ	1.095		
δ	-0.953		
ω	0.997		

The average standard error resulted less than 13% as it can be appreciated by Figures 5A and 5B, in which are reported the parity plots for, respectively, the ethanol conversion and the selectivity to acetaldehyde, ethyl acetate and others.

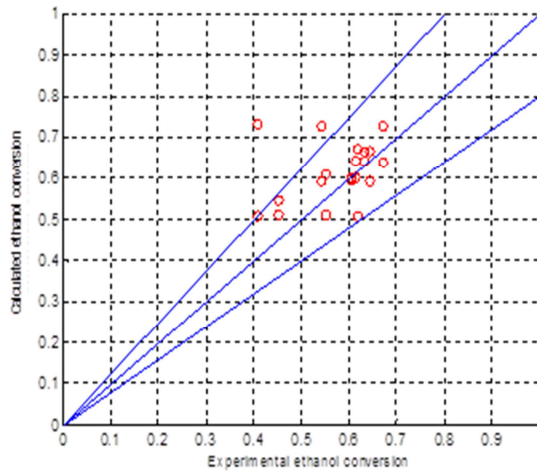


Figure 5A: Parity plot for ethanol conversion calculated vs experimental (50 g catalyst).

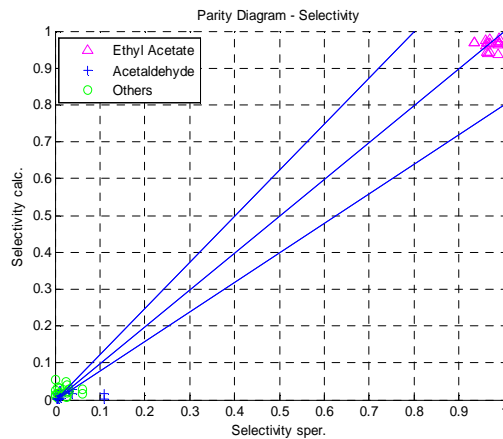


Figure 5B: Parity plot for selectivity's calculated vs experimental (50 g catalyst).

B-5.4.1.2 Power law model 1.2

By increasing the number of parameters, another expression of the power law was derived and the rate laws are reported on following.

$$r_1 = k_1 * p_{EtOH}^\alpha * p_{H_2}^\omega * p_{AcH}^\theta \quad (34 a)$$

$$r_2 = k_2 * p_{EtOH}^\beta * p_{AcH}^\gamma * p_{H_2}^\delta * p_{AcOEt}^\phi \quad (34 b)$$

$$r_3 = k_3 * p_{AcH}^2 \quad (34 c)$$

The values of the obtained kinetic parameter are reported in Table 5.

Although the higher number of parameters, the value of the average error is still non enough low. The obtained parameters are not able to well describe the experimental results. Moreover, the average error on the data at 50 g is very high and of about 25%.

Table 5: Kinetic parameters of the power law model 1.2 determined by regression analysis on all the experimental runs performed by using the reactor loaded with 2 g of catalyst.

Average Error- Parameter adjustment 14.62			
R²=0.89			
Kinetic constants	(mol/cm³ h)	Activation Energy	(Kcal/mol)
K ₁ ^{rif}	1.64E-2	Ea ₁	17.98
K ₂ ^{rif}	8.68E-2	Ea ₂	5.91
K ₃ ^{rif}	1.20E-3	Ea ₃	15.67
Exponential Parameters power law			
α	0.49		
β	-0.38		
γ	1.37		
δ	-1.32		
ε	-4.27		
ω	-1E-2		
φ	1.01		

The obtained parameters have physical meaning and can be used to interpret as well the obtained experimental data.

B-5.4.1.3 Power law model 1.3

The model 1.3 consists of a power law expression in which the overall reaction rate expressions are dependent by the corresponding equilibrium constants. Power law rate expressions used in the reaction pathway for dehydrogenation of ethanol to acetaldehyde, dehydrogenation of ethanol to ethyl acetate, aldol condensation of acetaldehyde to other sub-products are shown in the equations 35a-c.

$$r_1 = k_1 P_{EtOH}^\alpha \left(1 - \frac{1}{K_{e1}} \frac{P_{ACH}^\beta P_{H2}^\gamma}{P_E^\alpha} \right) \quad (35 a)$$

$$r_2 = k_2 P_{EtOH}^\delta P_{ACH}^\varepsilon \left(1 - \frac{1}{K_{e2}} \frac{P_{ACH}^\varphi P_{H2}^\omega}{P_{EtOH}^\delta P_A^\varepsilon} \right) \quad (35 b)$$

$$r_3 = k_3 P_{ACH}^2 \quad (35 c)$$

In order to respect congruence, two of the 7 order of reaction have been evaluated to respect the congruence as reported in the equations 36 a-b.

$$\alpha = \beta + \gamma - 1 \quad (36 a)$$

$$\varphi = \delta + \varepsilon - \omega \quad (36 b)$$

The equilibrium constants K_{e1} and K_{e2} have been calculated, as already described in the previous section B-5.3.2. In Figure 6A-B the parity plots of conversion and selectivity were reported. The obtained parameters have been used in simulation to describe the experimental runs obtained by using high residence time (30-100 ghmol⁻¹) on 50 g of catalysts, at temperature of 200-260°C and in the pressure range 10-30 bar. As it can be seen by the values of Table 6 and Figure 7A-B, also in this case have not obtained a satisfactory agreement.

Table 6: Model 1.3. Kinetic parameters of the power law with equilibrium models determined by regression analysis on all the experimental runs performed by using the reactor loaded with 2 g of catalyst.

Average Error 21.30			
$R^2=0.94$			
Kinetic constants	(mol/g_{cat} h)	Activation Energy	(Kcal/mol)
Kr1	3.51×10^{-3}	Ea1	16.50
Kr2	5×10^{-2}	Ea2	9.80
Kr3	8×10^{-3}	Ea3	5.00
Exponential Parameters			
α (by eq.36a)	1.17		
β	1.01		
γ	1.16		
δ	$7. \times 10^{-2}$		
ε	1.40		
ω	1.43		
φ (by eq.36b)	0.040		

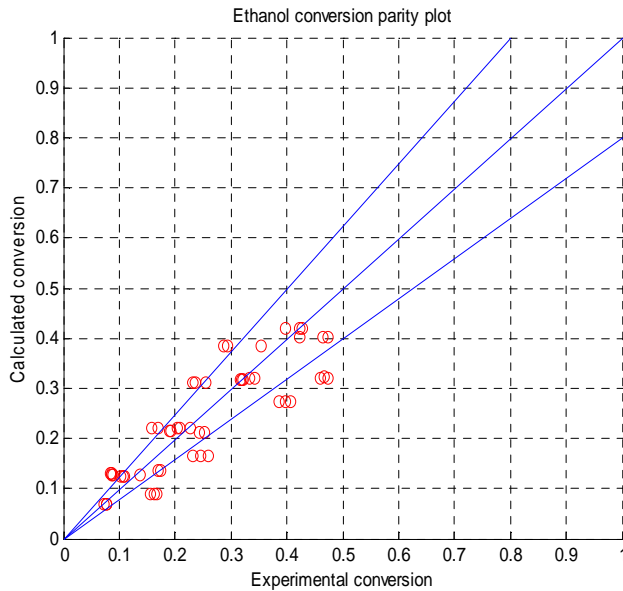


Figure 6A: Parity plot for ethanol conversion calculated vs experimental (2 g catalyst).

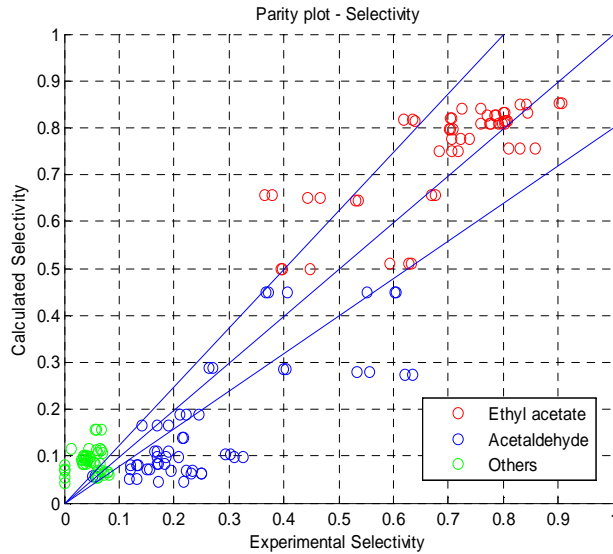


Figure 6B: Parity plot for selectivity calculated vs experimental (2 g catalyst).

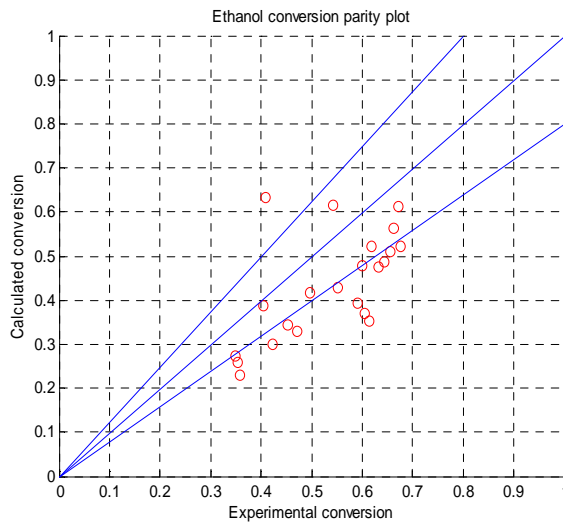


Figure 7A: Parity plot for ethanol conversion calculated vs experimental (50 g catalyst).

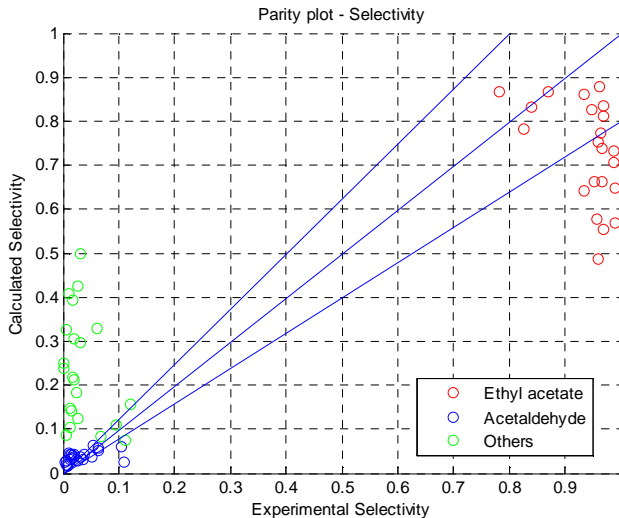


Figure 7B Parity plot for selectivity calculated vs experimental (50 g catalyst).

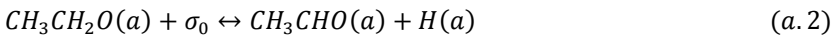
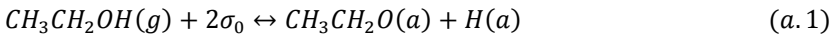
This empiric model 1.3 shows not satisfactory performances (Average Correlation Index $R^2=0.92$, Average error= 21.30%). However, by observing the obtained values for the apparent reaction orders, it is possible to conclude that some orders (δ and φ) are near to zero, this probably means that more reliable kinetic equations would contain adsorption terms appearing at the denominator. At this scope, we have tested many different kinetic models derived from different hypothesis of reaction mechanism as reported in the next paragraph.

B-5.4.2 Adsorption dual-site

Another approach to kinetics studies is based on the hypothesis of reliable mechanistic consideration. At this purpose, in this model a dual site adsorption mechanism was proposed. In particular, σ_0 and Θ_0 was assuming as, respectively, the free sites and the fraction of the free active sites present on the catalyst surface. Whilst, with σ_i and

$\Theta_i = \sigma_i / \sigma_{\text{tot}}$ were indicated the sites and the fraction of active sites occupied by the reactant (i). Assuming that the number of sites consumed in the adsorption and dissociation steps must be equal to the number of sites liberated in the formation and desorption steps, each reaction (a-c) consists of different adsorption steps. Thus, it is possible to split up each reaction in a series of elementary adsorption step, where the symbol (a) is related to adsorbed species while (g) the components in gas phase.

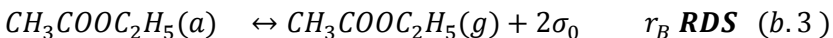
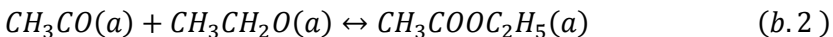
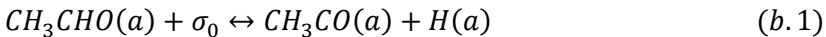
A. The model was structured assuming for the **reaction a**, related to the acetaldehyde production, four different adsorptions/desorption steps (a.1-4),



The reaction rate expression is therefore (Eq.37).

$$r_A = r_{a.3} = K_A * \theta_{AcH} - K_{-A} * P_{AcH} * \theta_0 \quad (37)$$

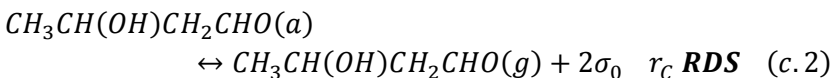
B. The **reaction b**, related to the ethyl acetate formation, was been well described by three different adsorption steps, as reported (b.1-3):



The reaction rate expression is therefore (Eq.40):

$$r_B = r_{b.3} = K_B * \theta_{AcOEt} - K_{-B} * P_{AcOEt} * \theta_0^2 \quad (38)$$

C. Finally, the **reaction c** related to the formation of by-products was been well described by two adsorption step, as reported (c.1-2):



The desorption of the acetaldol intermediate specie to by-products (others) was been assumed the rate determining step for the reaction 39.

$$r_C = r_{c.2} = K_C * \theta_{A0} - K_{-C} * P_{Others} * \theta_0^2 \quad (39)$$

The partial pressure of acetaldehyde, ethyl acetate and "others" are respectively indicated as P_A , P_{Ac} and P_0 while the sites occupied respectively by acetaldehyde, ethyl acetate, hydrogen, ethoxide, acetaldol and others are respectively reported as θ_{ACH} , θ_{AcOEt} , θ_H , θ_{EX} , θ_{A0} and θ_{others} .

Finally, the adsorption/kinetics parameters for each reaction Kr_a , Kr_{-a} , Kr_b , Kr_{-b} and Kr_c , Kr_{-c} have been reported. The dependence of the adsorption constants by the reaction temperature can be expressed by using the Van't Hoff equation.

B-5.4.2.1 Model 2.1

In the model 2.1 it has been assumed for the reaction a as RDS r_A (rate determining step) the acetaldehyde desorption to the gas phase (reaction a.3). For the reaction b and for the reaction c the RDS are respectively the expressed by the equations *b.3* and *c.2*.

Thus, it should be possible derive the adsorption equilibrium constants K_i and successively the occupied sites fractions.

Reaction a

$$k_{a.1} = k_1 = \frac{\theta_{EtOH}\theta_H}{\theta_0^2 P_{EtOH}}$$

$$k_{a.2} = k_2 = \frac{\theta_{ACH}\theta_H}{\theta_0 \theta_{EtOH}}$$

$$k_{a.4} = k_4 = \frac{P_{H2}\theta_0}{\theta_H^2}$$

$$\theta_{EtOH} = k_1 p_{EtOH} \sqrt{\frac{k_4}{p_{H2}}} \theta_0$$

$$\theta_{ACH} = k_1 k_2 p_{EtOH} \frac{k_4}{p_{H2}} \theta_0$$

$$\theta_H = \sqrt{\frac{p_{H2}}{k_4}} \theta_0$$

Reaction b

$$k_{b.1} = k_5 = \frac{\theta_{Ax}\theta_H}{\theta_0 \theta_{AcH}}$$

$$k_{b.2} = k_6 = \frac{\theta_{AcOEt}}{\theta_{Ax}\theta_{EtOH}}$$

$$\theta_{EtOH} = k_1 k_2 k_5 p_{EtOH} \frac{k_4^{1.5}}{p_{H2}} \theta_0$$

$$\theta_{EtOH} = k_1^2 k_2 k_5 k_6 p_{EtOH} \left(\frac{k_4}{p_{H2}}\right)^2 \theta_0^2$$

Reaction c

$$k_{c.2} = k_8 = \frac{\theta_{Ao}}{\theta_{AcH}^2}$$

$$\theta_{Ao} = k_8 \left(k_1 k_2 k_4 \frac{p_{EtOH}}{p_{H2}}\right)^2 \theta_0^2$$

By the reported expressions, it should be possible to calculate the site fractions as function of free sites fraction θ_0 ($\theta_{EtOH}, \theta_{AcH}, \theta_{Ax}, \theta_H, \theta_{AcOEt}, \theta_{Ao}$) and an overall balance on the free and adsorbed sites must be equal to 1 as the in following expression is indicated.

$$\theta_0 + \theta_{EtOH}\theta_{AcH} + \theta_{Ax} + \theta_H + 2 * \theta_{AcOEt} + 2 * \theta_{Ao} = 1 \quad (39)$$

By the resolution of the reported equation it is possible obtain an equation of the second order respect to θ_0 (40).

$$A\theta_0^2 + B\theta_0 + C = 0 \quad (40)$$

Where A, B and C have the following expressions:

$$A = 2k_1^2 k_2 k_5 k_6 p_E^2 \frac{k_4^2}{p_H^2} + 2k_8 k_1^2 k_2^2 k_4^2 \frac{p_{EtOH}^2}{p_{H2}^2}$$

$$B = 1 + k_1 p_{EtOH} \sqrt{\frac{k_4}{p_H}} + k_1 k_2 k_4 \frac{p_{EtOH}}{p_{H2}} + k_1 k_2 k_5 p_{EtOH} \left(\frac{k_4}{p_H}\right)^{1.5} + \sqrt{\frac{p_H}{k_4}}$$

$$C = 1$$

The model in exam has 18 parameters: K_i represents the adsorption constants, $K_{r_i} - k_{r_i}$ the kinetics constants of the direct/inverse reactions, whilst $E_{a_i} - E_{a_i}$ the corresponding activation energies. The dependence of the kinetic constants by the reaction temperature has been expressed, as already said, by the Arrhenius equation (26). The obtained parameters are thus reported in Table 7.

Table 7: kinetics parameters obtained by hypnotizing as rate determining step the acetaldehyde desorption to gas phase (a.3) for the *reaction a*.

Adsorption Parameters			Kinetics constant (mol/hg _{cat})		Activation Energies (Kcal/mol)	
k_1 [atm ⁻¹]	6.31	r_1	k_{rA}	32.32	Ea_A	14.8
k_2 [-]	1.38E-3		k_{r-A}	46.65	Ea_{-A}	0.00619
k_4 [atm]	39.74	r_2	K_{rB}	37.49	Ea_B	10.86
k_5 [-]	23.51		k_{r-B}	189	Ea_{-B}	0.0015
k_6 [-]	2.62e-3	r_3	K_{rC}	33.98	Ea_C	22.62
k_8 [-]	2.56		K_{r-c}	59.02	Ea_{-c}	33.63
Average error: 16.52						
Correlation Index $R^2=0.98$						

The parity plots of Figure 8 A-B show the not enough satisfactory correlation between the experimental data and calculated ones.

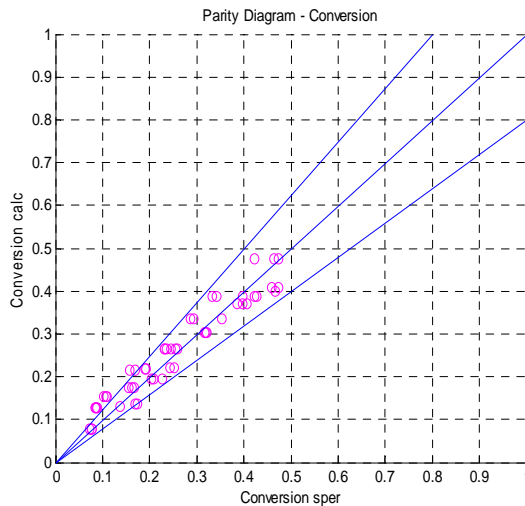


Figure 8A: Parity plot for ethanol conversion calculated vs experimental (2 g catalyst).

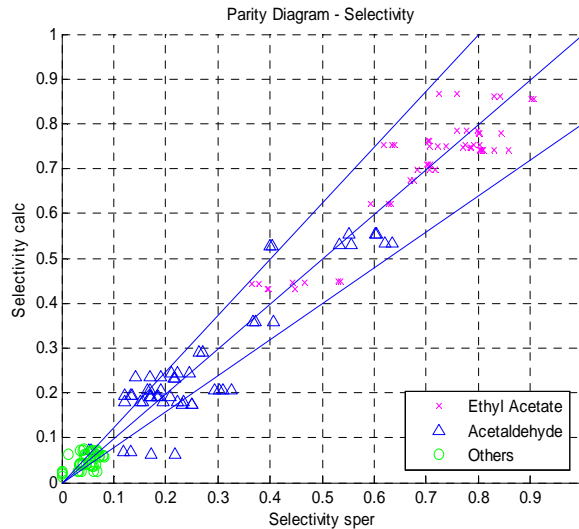


Figure 8B: Parity plot for selectivities calculated vs experimental (2 g catalyst).

In Figure 8C the profile of ethanol conversion as function of the reaction temperature at three different pressure 10-30 bar have been reported. The experimental runs have been performed in this case at a constant residence time of 4 ghmol^{-1} . The symbols are the experimental data, whereas lines the calculated data. At lowest temperature of reaction, a deviation is observed probably due to the default of controlling temperature. At higher temperature the agreement would seem better but still not enough satisfactory. In Figure 8D, the selectivity's profiles of the main reaction product, ethyl acetate, obtained in the same mentioned conditions are also reported. In this case it should be possible identify a good agreement between the experimental (symbols) and calculated data only at low pressure, were the ethyl acetate selectivity is relatively low, less than 70%, and the sensibility if the models is higher.

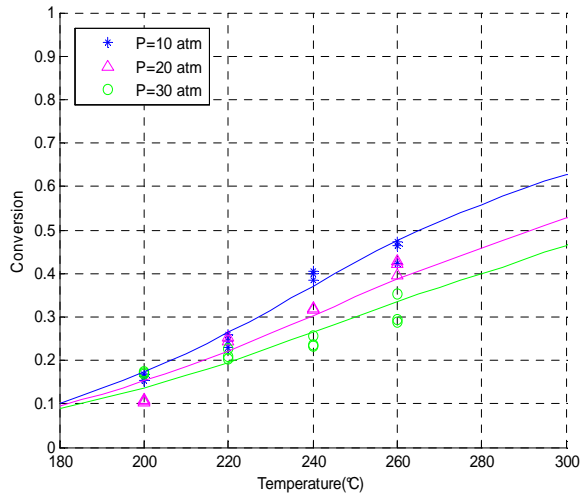


Figure 8C: ethanol conversion as a function of temperature reaction. The runs were performed at three different pressures (10-20 bars), at a residence time of 4ghmol^{-1} , by fed a constant flow of $\text{H}_26\%\text{N}_2$ $25\text{ cm}^3/\text{min}$.

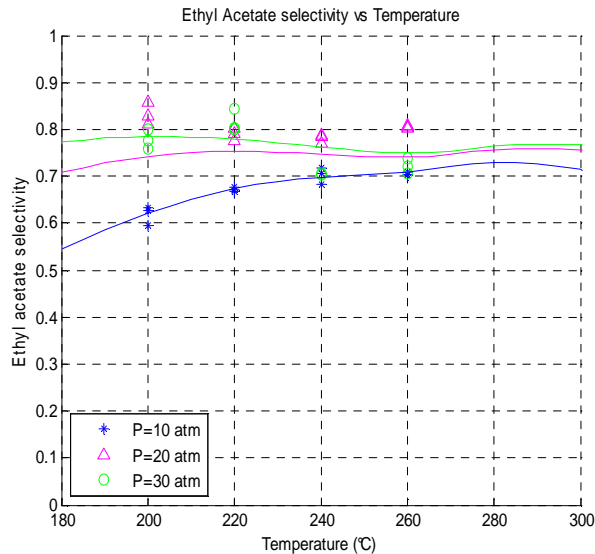


Figure 8D: ethyl acetate selectivity as a function of temperature reaction. The runs were performed at three different pressures (10-20 bars), at a residence time of 4ghmol^{-1} , by fed a constant flow of $\text{H}_26\%\text{N}_2$ $25\text{ cm}^3/\text{min}$.

In Figures 8E the conversion and in Figures 8F ethyl acetate selectivities profiles have been reported by operating at a constant pressure of 20 bar and at three different residence time of 1.3-3.89-19.46 ghmol^{-1} that correspond to an ethanol feeding of respectively 1.5-0.5-0.1 cm^3/min . The calculated profiles of conversion are able to fit quite well the conversion results whilst it is not the same for selectivity to ethyl acetate. The kinetics parameters determined by regression analysis of the experimental data with 2 g of catalyst have been used to simulate the behavior of experimental data at 50 g. In this case an average error of 26.50 and $R^2=0.95$ has been obtained. The parity plots of Figure 9 A-B show the not satisfactory agreement obtained.

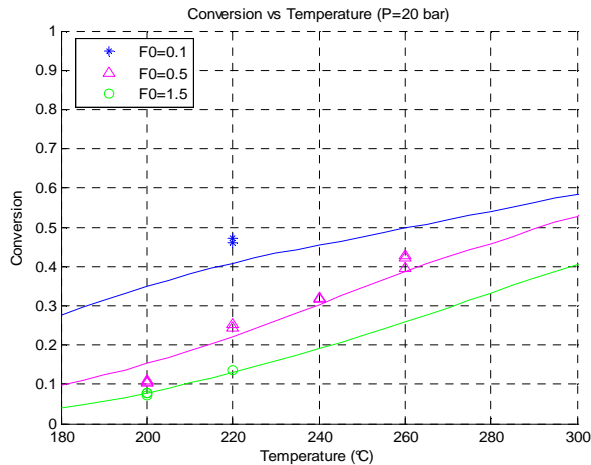


Figure 8E: ethyl acetate conversion as a function of temperature reaction. The runs were performed at constant pressures of 20 bars, at three different residence time of 1-4-20 ghmol^{-1} , by fed a constant flow of $\text{H}_26\%\text{N}_2$ 25 cm^3/min .

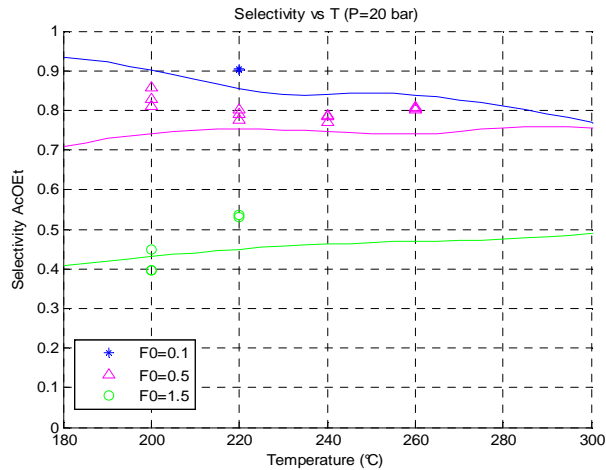


Figure 8F: ethyl acetate selectivities as a function of temperature reaction. The runs were performed at constant pressures of 20 bars, at three different residence time of 1-4-20ghmol⁻¹, by fed a constant flow of H₂6%N₂ 25 cm³/min.

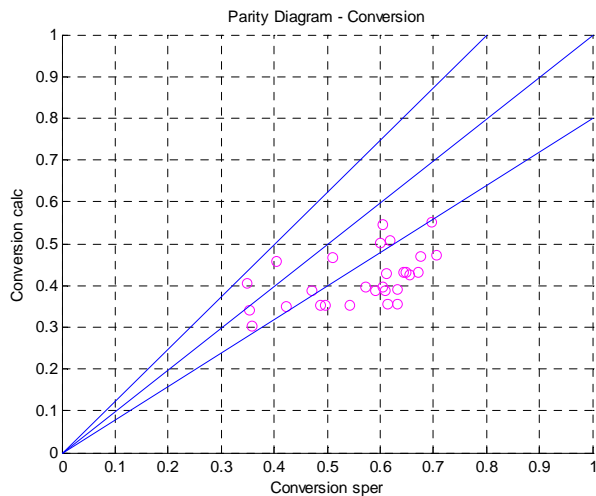


Figure 9A: Parity plot for ethanol conversion calculated vs experimental (50 g catalyst).

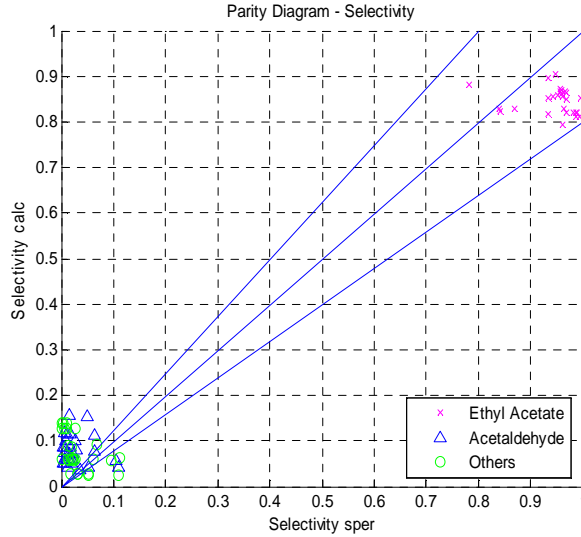


Figure 9B: Parity plot for ethyl acetate selectivity calculated vs experimental (50 g catalyst).

B-5.4.2.1.1 Model 2.1A

In this case, the same hypothesis of RDS, of the model 2.1.A has been assumed, but, within, the dependence of the equilibrium constants by the reaction temperature was considered by using the Van't Hoff expression. The rate expression for each different step has been represented by equation 1-3. In particular has been reported the ethanol dehydrogenation reaction to acetaldehyde:

$$r_A = r_1 = K_A * \left(\theta_A - \frac{1}{Kea} * P_A * \theta_0 \right) \quad (41a)$$

The rate expression for ethanol dehydrogenation reaction to ethylacetate:

$$r_B = r_2 = K_B * \left(\theta_{AE} - \frac{1}{Keb} * P_{AC} * \theta_0^2 \right) \quad (41b)$$

Finally, the desorption of the acetaldol intermediate specie to subproducts (others) was been assumed the rate determining step for the reaction 3.

$$r_C = r_3 = K_C * \left(\theta_{AA} - \frac{1}{K_{ec}} * P_0 * \theta_0^2 \right) \quad (41c)$$

The partial pressure of acetaldehyde, ethyl acetate and other are respectively indicate as P_A , P_{Ac} and P_0 while the fraction of sites occupied respectively by acetaldehyde, ethyl acetate, hydrogen, acetaldol and others are respectively reported as θ_{AcH} , θ_{AcOEt} , θ_H , θ_{Ax} and θ_{A0} . The k_A , k_B , and k_C represent the adsorption/kinetics parameters. The obtained values of each parameter are reported in Table 8.

In figure 10 A-B are shown the parity diagrams respectively for the ethanol conversion and for the products selectivities. Although the model takes in account the dependence of the equilibrium constant by the reaction temperature, no significant improvements have been obtained.

Table 8: dual site kinetic model parameters, determined by regression analysis on all the experimental runs performed by using the reactor loaded with 2 g of catalyst.

Adsorption Parameters		Kinetics constant (mol/hg _{cat})		Activation Energies (Kcal/mol)	
k_1 [atm ⁻¹]	40.11	k_{rA}	20.27	E_{aA}	20.87
k_2 [-]	3.51×10^{-3}	k_{r-A}	0.34	ΔH_a	-9.8×10^{-3} (VL)
k_4 [atm]	10.50	K_{rB}	31.30	E_{aB}	11.16
k_5 [-]	89.90	k_{r-B}	5.66×10^{-3}	ΔH_b	-7.32×10^3 (VL)
k_6 [-]	3.66×10^{-3}	K_{rC}	106.56	E_{aC}	28.62
k_8 [-]	1.52	K_{r-c}	1.74×10^{-2}	ΔH_c	-1.49×10^3 (VL)
Conversion Average error: 21.74					
Correlation Index $R^2=0.94$					

This behavior could be find explanation in the low sensibility of the model to fitting experimental value of selectivity's to acetaldehyde and others, present in the withdrawn in concentration less than 1%. Moreover, in Figure 10C the ethanol conversion as a function of temperature reaction, for runs performed at three different pressures (10-20 bars), at a residence time of 4ghmol⁻¹, by fed a constant flow of H₂6%N₂ 25 cm³/min has been represented. The Figure 10D represents the ethyl acetate selectivities profiles. The calculated profiles of conversion and selectivity to ethyl acetate are difficult to interpret. As It can be seen, at low pressure (10 bar) and low temperature the ethanol conversion should be higher than the once obtained at 20-30 bar and at temperature of 220-260°C.

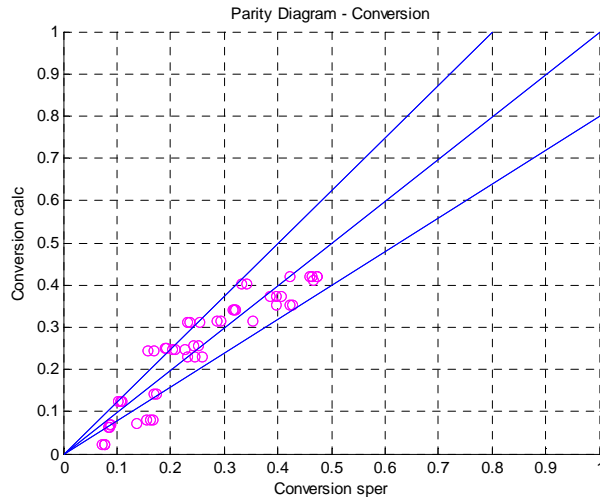


Figure 10A: Parity plot for ethanol conversion calculated vs experimental (2 g catalyst).

The model is not able to interpret this aspect, whilst at higher temperature a reasonable fitting of the experimental data has been obtained. The model is able to well interpret the experimental data of conversion obtained at 30 bar. In Figure 10E, the profiles, at three different residence time $1-20 \text{ ghmo}^{-1}$, have been obtained. The model is able to well interpret the experimental data obtained by using a residence time of 4 ghmol^{-1} that correspond to the ethanol fed of 0.5 mol/h . The calculated data on a system charged with 50 g, obtained by using this same model and the kinetic parameters reported in Table 8 show unsatisfactory results, as it can be seen by parity plot of Figure 11 A-B.

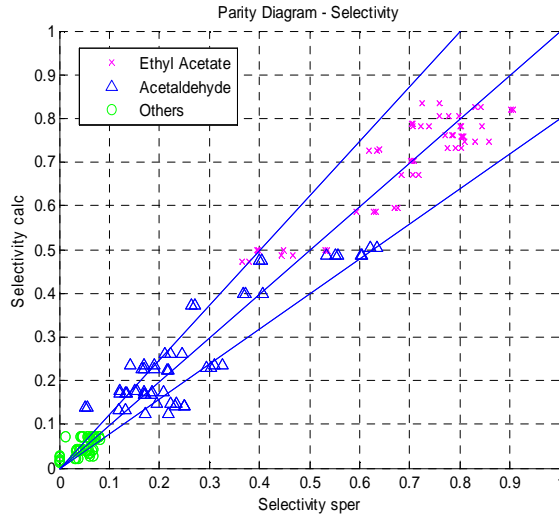


Figure 10B: Parity plot for selectivities calculated vs experimental (2 g catalyst).

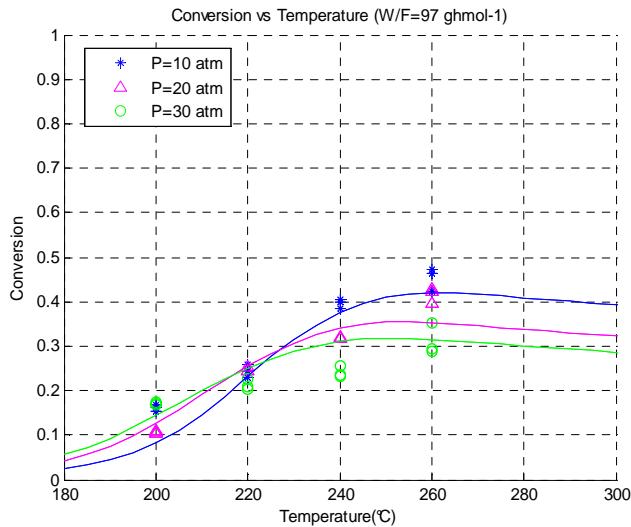


Figure 10C: ethanol conversion as a function of temperature reaction. The runs were performed at three different pressures (10-20 bars), at a

residence time of 4ghmol^{-1} , by fed a constant flow of $\text{H}_26\%\text{N}_2$ $25\text{ cm}^3/\text{min}$.

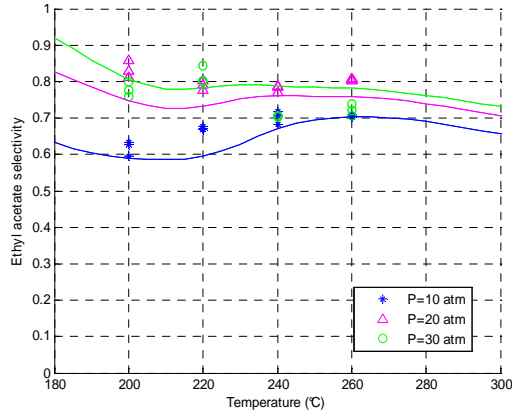


Figure 10D: ethyl acetate selectivity as a function of temperature reaction. The runs were performed at three different pressures (10-20 bars), at a residence time of 4ghmol^{-1} , by fed a constant flow of $\text{H}_26\%\text{N}_2$ $25\text{ cm}^3/\text{min}$.

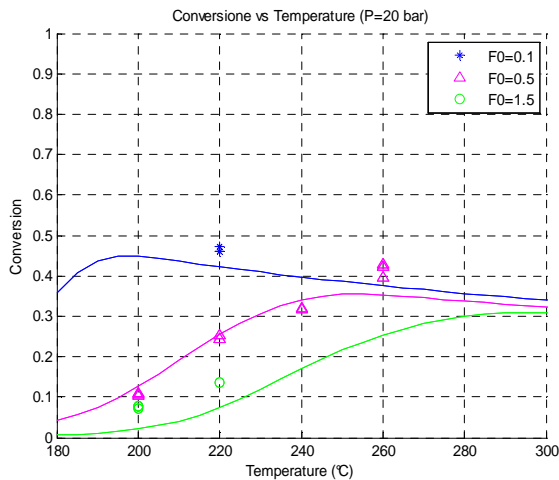


Figure 10E: ethyl acetate conversion as a function of temperature reaction. The runs were performed at constant pressures of 20 bars, at three different residence time of $1\text{-}4\text{-}20\text{ghmol}^{-1}$, by fed a constant flow of $\text{H}_26\%\text{N}_2$ $25\text{ cm}^3/\text{min}$.

Moreover the average error is of about 31.11 and the value of $R^2=88.7$. This model could not satisfy our requirement and for this reasons the investigation was depth by considering as rate determining step the reaction of ethoxy adsorbed formation by gas phase ethanol.

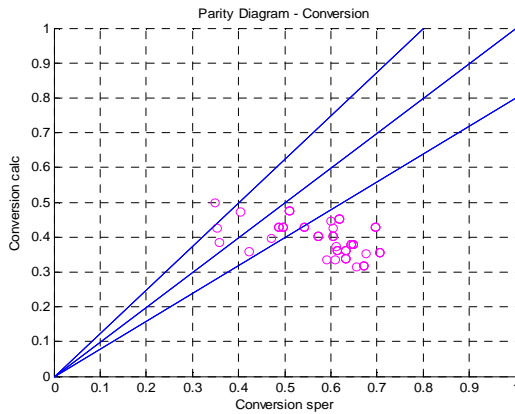


Figure 11A: Parity plot for ethanol conversion calculated vs experimental (50 g catalyst).

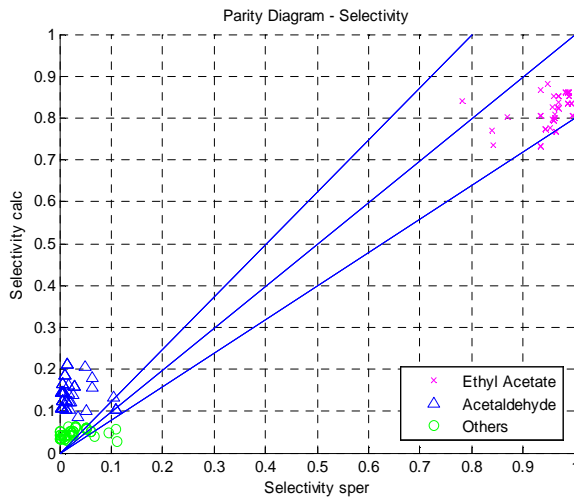


Figure 11B: Parity plot for selectivities calculated vs experimental (50 g catalyst).

B-5.4.2.2 Model 2.2

In the model 2.2 it has been assumed for the reaction a as RDS r_A (rate determining step) the ethoxy adsorbed formation by gas phase ethanol (reaction 1a). In Table 9 the parameters results have been summarized. Nevertheless the low average error and the good agreement between the experimental and calculate data, this model cannot consider acceptable because of the absence of physical meaning for the obtained parameters ($E_a > 50$ Kcal/mol).

Table 9: dual site kinetic model parameters, determined by regression analysis on all the experimental runs performed by using the reactor loaded with 2 g of catalyst.

Adsorption Parameters		Kinetics constant (mol/hg _{cat})		Activation Energies (Kcal/mol)	
K_2	0.97	K_{rA}	2.77	E_{aA}	53.69
K_3 [atm]	0.10	K_{r-A}	1.26	E_{a-A}	41.51
K_4 [atm]	1.32	K_{rB}	0.34	E_{aB}	15.04
K_5	6.87	K_{r-B}	1.09	E_{a-B}	37.28
K_6	0.57	K_{rC}	0.85	E_{aC}	26.16
K_8	0.85	K_{r-c}	0.63	E_{a-c}	53.96
Conversion Average error: 15.26					
Correlation Index $R^2=0.98$					

B-5.4.2.3 Model 2.3

In the model 2.3 it was assumed as rate determining step of the reaction a, the acetaldehyde adsorbed formation by adsorbed ethoxy group (reaction a.2). The details of the model have been not considered because, although all the parameters, as shown in Table 10, obtained have a physical meaning the overall average error is too

high (20.74) to consider this model effective for the description of experimental results.

Table 10: dual site kinetic model parameters, determined by regression analysis on all the experimental runs performed by using the reactor loaded with 2 g of catalyst.

Adsorption Parameters		Kinetics constant (mol/hg _{cat})		Activation Energies (Kcal/mol)	
K _E	0.71	K _{rA}	88.41	E _{aA}	14.20
K _A	0.57	K _{r-A}	112.1	E _{a-A}	0.57
K _H	0.76	K _{rB}	0.11	E _{aB}	11.30
K _C	0.41	K _{r-B}	0.4	E _{a-B}	11.90
K _{AE}	31.51	K _{rC}	0.26	E _{aC}	14.90
K _{AA}	0.36	K _{r-C}	0.27	E _{a-C}	41.10
<i>Average error: 20.74</i>					
<i>Correlation Index R²=0.95</i>					

Moreover, the parameters have been used to obtain in simulation the curves to fit the experimental data obtained by using 50 g of catalysts. The average error on this model is of about 30.97 and the coefficient of linear correlation is of about 0.89.

By concluding, many kinetic models have been developed on empirical laws or mechanism hypothesis and most of them have given parameters with no physical meaning. At this purpose our investigation have developed, as the last paragraph of this chapter will show, a Langmuir-Hinshelwood-Hougen-Watson (LHHW) model to interpretation the experimental data on both 2g and 50 g of catalyst. It should be useful to anticipate that this model have shown a good coherence between the experimental and calculated data.

B-5.4.3 Model 3

When a catalytic reaction was considered, it is possible image the reaction mechanism as consisting in different steps. Each of these steps may be of different types, and the adsorbed species react with each other, that surface species may migrate into the bulk, that reactive radicals desorb and then react in the gas-phase etc. The Langmuir–Hinshelwood-Hougen-Watson mechanisms form an important class of reactions. These mechanisms consist of the following types of steps:

- Adsorption from the gas-phase
- Desorption to the gas-phase
- Dissociation of molecules at the surface
- Reactions between adsorbed molecules

At this purpose, by assuming with σ_0 and Θ_0 respectively the free sites and the fraction of the free the active sites present on the catalyst surface and with σ_i and $\Theta_i = \sigma_i / \sigma_0$ respectively the sites and the fraction of the active sites occupied by reactant (i), the following reaction scheme can be assumed for the dehydrogenation reaction of ethanol. For the reaction a the mechanism hypothesis should be so represented:



For this reaction, the rate determining step should be the surface reaction between chemisorbed ethanol and a catalyst free site to form adsorbed acetaldehyde. For the reaction b (44) we suggest the following mechanism:





In this case, the rate determining step should be the dual sites reaction between two adsorbed molecules of respectively ethanol and acetaldehyde to give adsorbed ethyl acetate and hydrogen.

The reaction 3, occurring in a very small amount between two molecules of adsorbed acetaldehyde to give other by-products have been described in an approximated way by a second order irreversible reaction. The kinetic laws are, thus expressed:

$$r_1 = k_1\theta_E\theta_0 - k_{-1}\theta_A\theta_H \quad (45)$$

$$r_2 = k_2\theta_E\theta_A - k_{-2}\theta_{Ac}\theta_H \quad (46)$$

Applying a balance on the free sites and the adsorbed ones it possible to write:

$$\begin{aligned} \theta_0(k_{EtOH}p_{EtOH} + k_{ACH}p_{ACH} + k_{AcOEt}p_{AcOEt} + k_Hp_H) \\ = \theta_{ACH} + \theta_{EtOH} + \theta_{AcOEt} + \theta_H \end{aligned} \quad (47)$$

$$\theta_0 = \frac{1}{1 + \sum ki pi} \quad (48)$$

$$\theta_i = \frac{k_i p_i}{1 + \sum ki pi} \quad (49)$$

Generally, the mathematical expressions for the rate equations may be expressed by a combination of three terms, the kinetics term, the potential term and the adsorption term (eq.50) [10]:

$$r = \frac{(Kinetic\ term)(potential\ term)}{(adsorption\ term)^n} \quad (50)$$

Therefore, on the basis of the described mechanisms the following kinetic rate laws can be derived (50 a-c):

$$r_1 = \frac{k_1 P_{EtOH} \left(1 - \frac{1}{K_{e1}} \frac{P_{ACH} P_{H_2}}{P_{EtOH}}\right)}{(1 + b_{EtOH} P_{EtOH} + b_{ACH} P_{ACH} + b_H P_H + b_{AcOEt} P_{AcOEt})^2} \quad (50a)$$

$$r_2 = \frac{k_1 P_{EtOH} \left(1 - \frac{1}{K_{e2}} \frac{P_{AcOEt} P_{H_2}}{P_{EtOH} P_{ACH}}\right)}{(1 + b_{EtOH} P_{EtOH} + b_{ACH} P_{ACH} + b_H P_H + b_{AcOEt} P_{AcOEt})^2} \quad (50b)$$

$$r_3 = k_3 P_{AcH}^2 \quad (50c)$$

Where, the dependence of the equilibrium constant by the reaction temperature was already described in the paragraph B-5.3.2.

In Table 11, all the kinetic parameters determined by regression analysis are reported. The equilibrium constants Ke_1 and Ke_2 have been calculated, as described in the previous Chapter 3.

From the kinetic parameters reported in Table 11 it is possible to observe that k_3 has a very low value and a negligible value of the activation energy. This is the consequence of: (i) the approximation introduced by considering a pseudo-second order rate law; (ii) the fact that reaction c corresponds to an ensemble of different reactions considered as acetaldehyde that gives "others"; (iii) the very low amount of by-products found corresponds to a low precision in the analytical determination. The kinetic effect of the hydrogen adsorption is negligible with respect to the other values. The other values have a reasonable physical mean. The average standard error resulted less than 14% ($R^2=0.98$) and the validity of the developed model can be appreciated in Figures 12A and 12B in which are reported the parity plots for, respectively, the ethanol conversion and the selectivity to acetaldehyde, ethyl acetate and others.

Table 11 – Kinetic parameters of the LHHW dual site model determined by regression analysis on all the experimental runs performed by using the reactor loaded with 2 g of catalyst.

Kinetic constants		Activation Energy (Kcal/mol)
k_1^{ref}	97.1 (mol/(g _{cat} h atm))	36.25
k_2^{ref}	0.089 (mol/(g _{cat} h atm ²))	12.95
k_3^{ref}	0.0011 (mol/(g _{cat} h atm ²))	1.6E-4
Adsorption parameters		Adsorption enthalpy (Kcal/mol)
b_{EtOH}^{ref}	10.4 (atm ⁻¹)	-25.53
b_{AcH}^{ref}	98.4 (atm ⁻¹)	-7.02
b_{EA}^{ref}	41.2 (atm ⁻¹)	-13.91
b_H^{ref}	2.5×10^{-4} (atm ⁻¹)	-13.34

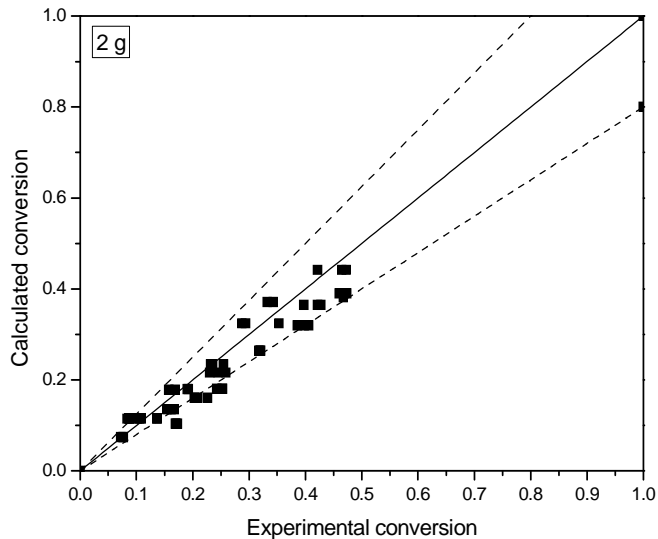


Figure 12A: Parity plots related to the ethanol conversion by considering a catalyst bed of 2g.

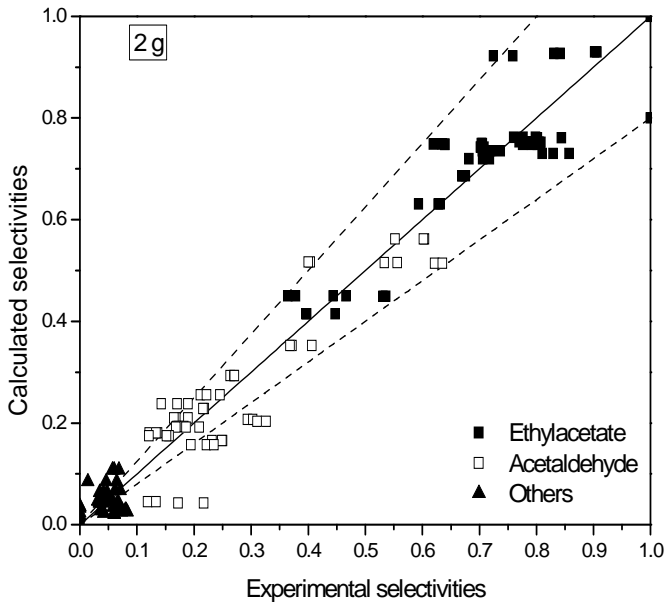


Figure 12B: Parity plots related to selectivities by considering a catalyst bed of 2g.

In Figure 12 C the conversion profiles of conversion in dependence of the reaction temperature have been reported at three different pressure respectively of 10, 20, 30 bar. The calculated profiles of conversions with the LHHW are able to fitting experimental data of ethanol conversion. The same is true for the ethyl acetate selectivity's (see Figure 12D). In Figure 12E the experimental and calculated profiles of ethanol conversion as function of the reaction temperature obtained by operating at three different residence time $1\text{-}20\text{ ghmol}^{-1}$, at constant pressure of 20 bar and by feeding into the apparatus system respectively $1.5\text{-}0.5\text{-}0.1\text{ cm}^3/\text{min}$ have been reported. In this case, the calculated profiles are able to simulate the dependence of the ethanol conversion by the residence time adopted. In Figure 12F, as well, the calculated profiles of ethyl acetate selectivity were able to fit the experimental date.

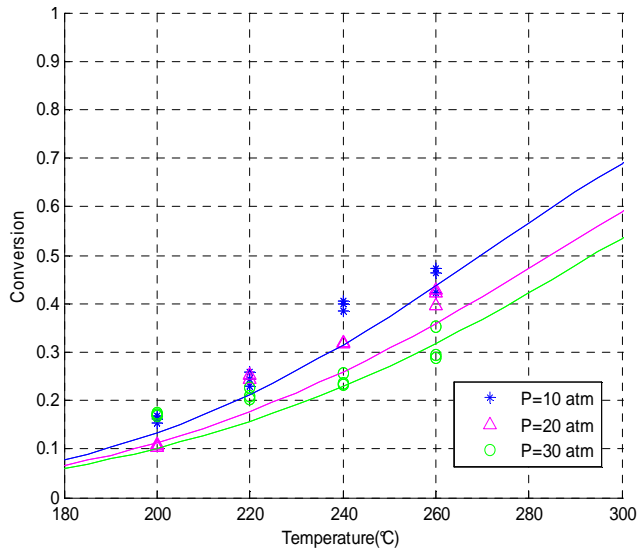


Figure 12 C: ethanol conversion as a function of temperature reaction. The runs were performed at three different pressures (10-20 bars), at a residence time of 4ghmol^{-1} , by fed a constant flow of $\text{H}_26\%\text{N}_2$ $25\text{ cm}^3/\text{min}$.

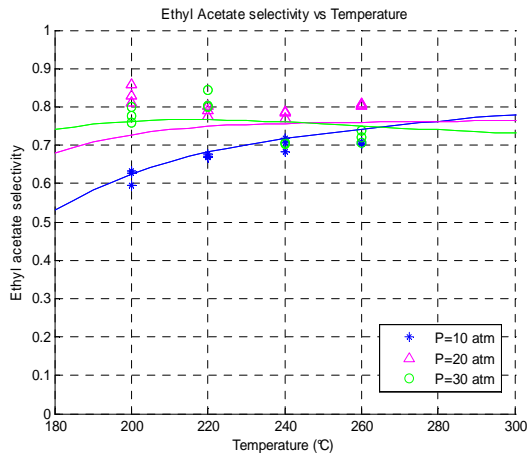


Figure 12 D: ethyl acetate profile as a function of temperature reaction. The runs were performed at three different pressures (10-20 bars), at a residence time of 4ghmol^{-1} , by fed a constant flow of $\text{H}_26\%\text{N}_2$ $25\text{ cm}^3/\text{min}$.

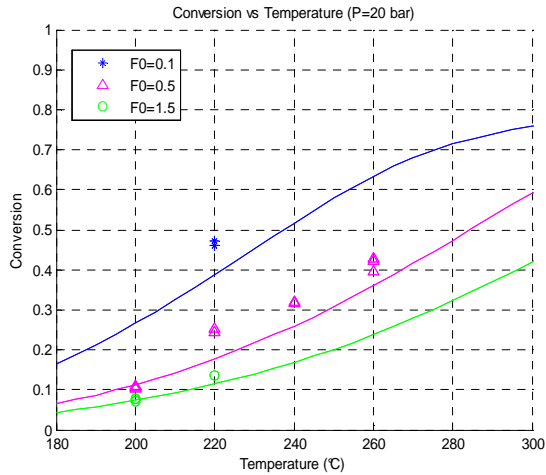


Figure 13E: ethanol conversion as a function of temperature reaction. The runs were performed at constant pressures of 20 bars, at three different residence time of $1\text{-}4\text{-}20\text{ghmol}^{-1}$, by fed a constant flow of $\text{H}_2\text{6}\%\text{N}_2\ 25\ \text{cm}^3/\text{min}$.

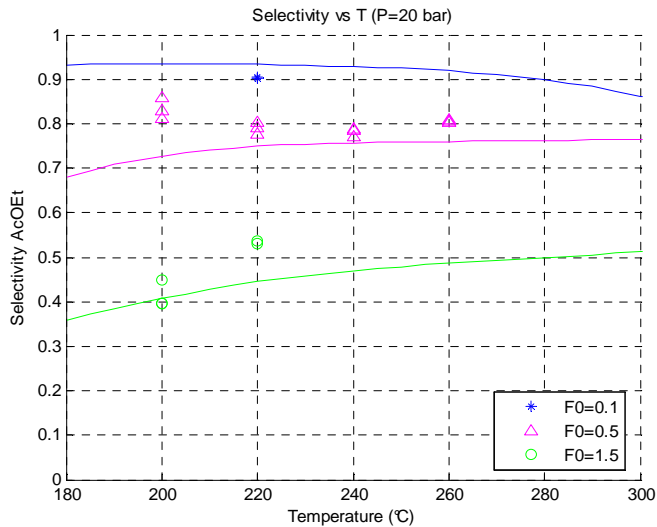


Figure 14F: ethyl acetate selectivity as a function of temperature reaction. The runs were performed at constant pressures of 20 bars, at three different residence time of $1\text{-}4\text{-}20\text{ghmol}^{-1}$, by fed a constant flow of $\text{H}_2\text{6}\%\text{N}_2\ 25\ \text{cm}^3/\text{min}$.

Some kinetic runs have been performed by charging the same tubular reactor with 50 g of catalyst instead of 2 g. Two different consecutive ovens have been used for heating the reactor with the aim to obtain as much as possible an isothermal profile along the catalytic bed. This has been experimentally verified and a variation of not more than $\pm 5^{\circ}\text{C}$ has been observed along the reactor. In Table 12 some of the performed runs are reported together with the adopted experimental conditions. In the same Table are also reported for comparison experimental and calculated values of ethanol conversions and selectivities of respectively ethyl acetate, acetaldehyde and other by-products. Calculations have been made with the LHHW described model using the kinetic parameters reported in Table 11 and the agreement obtained is very satisfactory (see Table 12 and Figure 13A-F).

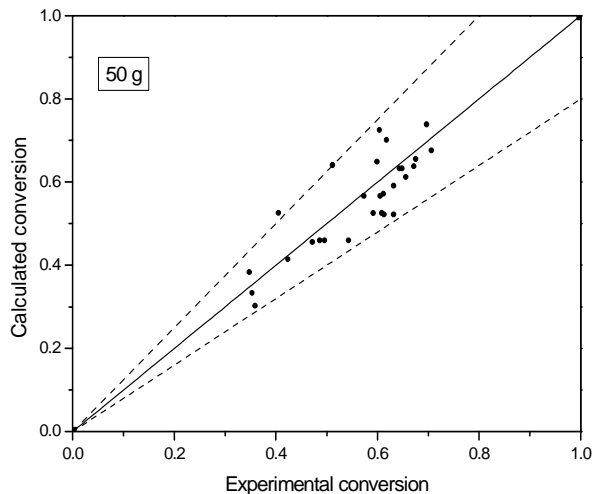


Figure13 A: Parity plots related respectively to the ethanol conversion and selectivities by considering a catalyst bed of 50g.

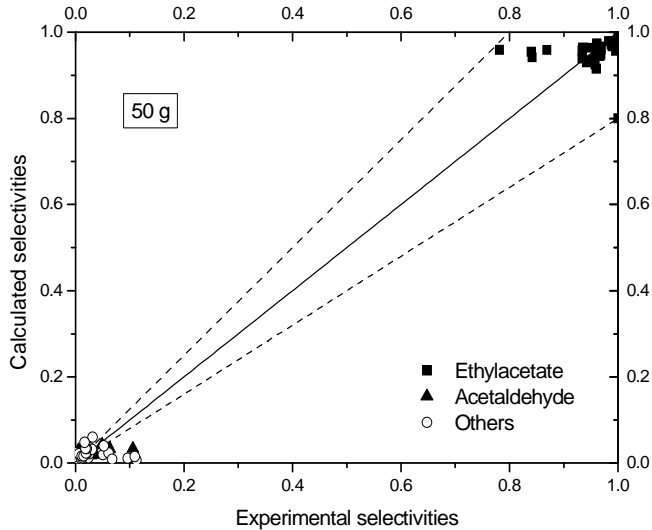


Figure 13B: Parity plots related respectively to the ethanol conversion and selectivities by considering a catalyst bed of 50g.

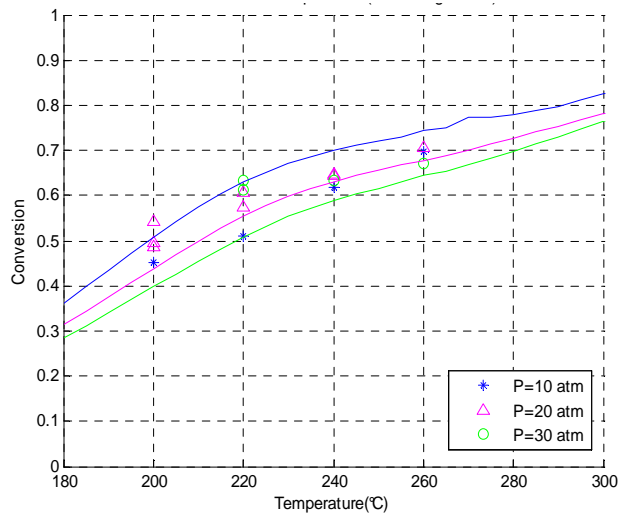


Figure 13C: ethanol conversion as a function of temperature reaction. The runs were performed at three different pressures (10-20 bars), at a residence time of 97 ghmol^{-1} , by fed a constant flow of $\text{H}_2\text{:6}\text{N}_2$ $25 \text{ cm}^3/\text{min}$.

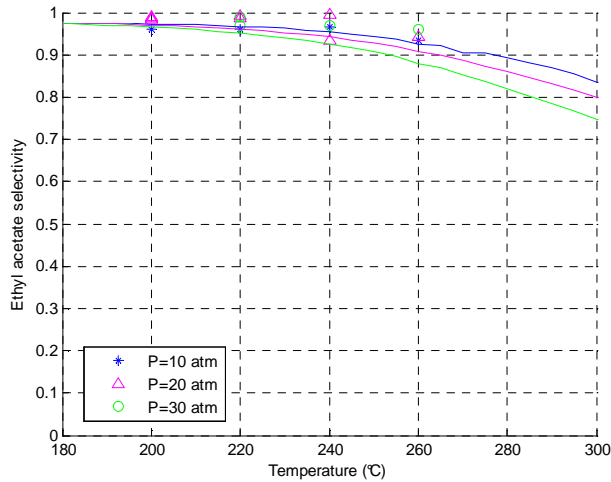


Figure 13D: ethyl acetate selectivity's profiles as a function of temperature reaction. The runs were performed at three different pressures (10-20 bars), at a residence time of 97 ghmol^{-1} , by fed a constant flow of $\text{H}_2 6\% \text{N}_2$ $25 \text{ cm}^3/\text{min}$.

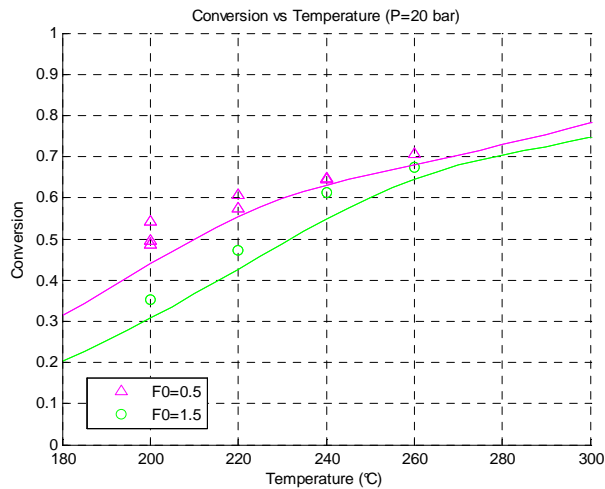


Figure 12E: ethanol conversion as a function of temperature reaction. The runs were performed at constant pressures of

20 bars, at three different residence time of 30-97 ghmol⁻¹, by fed a constant flow of H₂6%N₂ 25 cm³/min.

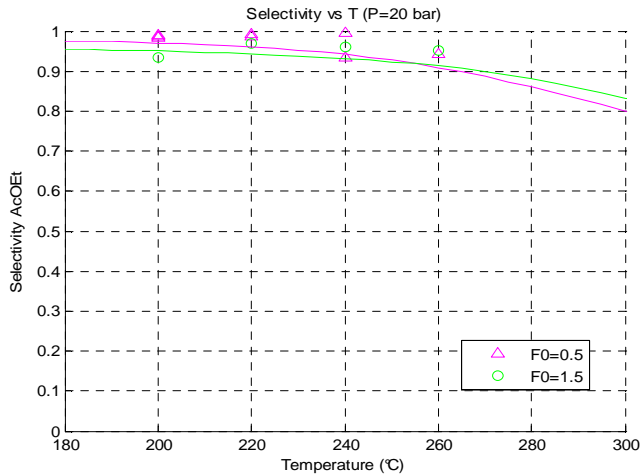


Figure 12F: ethyl acetate selectivity as a function of temperature reaction. The runs were performed at constant pressures of 20 bars, at three different residence time of 30-97 ghmol⁻¹, by fed a constant flow of H₂6%N₂ 25 cm³/min.

The calculated profiles fit with a good agreement the experimental data obtained at different temperature, pressure and residence time as shown in the profile of conversion and selectivity get in the wide range of operative conditions explored, as demonstrated by the Figure 12C-F. However, the results obtained in these runs correspond, very probably, to equilibrium conditions. This can be appreciated in Figure 13, in which the profiles of respectively conversions and selectivities are reported as a function of the residence time.

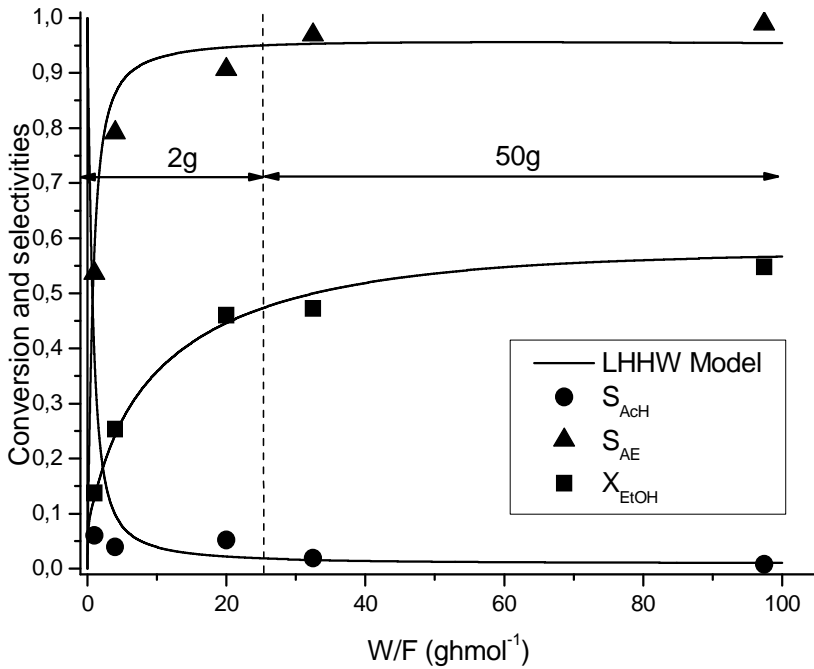


Figure 13 – Conversion and selectivities obtained for different residence times. This plot has been obtained by considering all data collected in both the reactors containing respectively 2 and 50 g of catalyst working at 220°C, 20 bars with a constant flow of a mixture of 6% H₂ in N₂ of 25 cm³/min that correspond to an hydrogen flow of 3.77x10⁻³ mol/h and nitrogen flow of 0.057mol/h.

As it can be seen, the runs made with 50 g of catalyst show the approaching to a plateau for both conversion and selectivities. For this reason these runs have not been considered together with the ones performed with 2 g of catalyst in the regression analysis but are used here to verify the model. The average standard error in simulating these runs is of 11% and R²=97.30.

Table 12: Comparison of experimental and calculated data by using LHHW model. The runs have been performed by using 50g of catalyst, temperature range: 200°-260°C, pressure range: 10-30 bar, at two different residence time of 34.4-97.32 ghmol⁻¹, keeping constant the nitrogen (5.7x10⁻² mol/h) and hydrogen (4x10⁻³ mol/h) flow rates.

Operative conditions				Experimental data				Calculated data with the LHHW model			
T(°C)	P(bar)	F _{EtOH} (cm ³ /min)	W/F (ghmol ⁻¹)	X _{EtOH}	S _{AcOEt}	S _{Ach}	S _{Others}	X _{EtOH}	S _{AcOEt}	S _{Ach}	S _{Others}
200	10	0.5	97.32	0.51	0.96	0.03	0.01	0.63	0.97	0.02	0.01
220	10	0.5	97.32	0.62	0.97	0.01	0.02	0.70	0.95	0.03	0.02
240	10	0.5	97.32	0.70	0.93	0.02	0.05	0.74	0.93	0.04	0.05
260	10	0.5	97.32	0.50	0.99	0.01	0.00	0.43	0.97	0.01	0.00
200	20	0.5	97.32	0.49	0.98	0.01	0.00	0.43	0.97	0.01	0.00
200	20	0.5	97.32	0.57	0.99	0.01	0.00	0.55	0.96	0.01	0.00
220	20	0.5	97.32	0.61	0.99	0.01	0.00	0.55	0.96	0.01	0.00
220	20	0.5	97.32	0.65	1.00	0.00	0.00	0.63	0.94	0.02	0.00
240	20	0.5	97.32	0.64	0.93	0.00	0.06	0.63	0.94	0.02	0.06
240	20	0.5	97.32	0.71	0.94	0.01	0.05	0.68	0.91	0.03	0.05
260	20	0.5	97.32	0.54	0.99	0.11	0.01	0.43	0.97	0.01	0.01
200	20	0.5	97.32	0.61	0.99	0.00	0.01	0.51	0.95	0.01	0.01
220	30	0.5	97.32	0.63	0.97	0.01	0.03	0.51	0.95	0.01	0.03
220	30	0.5	97.32	0.63	0.97	0.01	0.03	0.59	0.93	0.02	0.03
240	30	0.5	97.32	0.67	0.96	0.01	0.03	0.64	0.88	0.02	0.03
260	30	0.5	97.32	0.35	0.78	0.11	0.11	0.35	0.95	0.04	0.11
200	10	1.5	34.40	0.41	0.87	0.06	0.07	0.50	0.95	0.04	0.07
220	10	1.5	34.40	0.60	0.84	0.06	0.10	0.63	0.94	0.04	0.10
240	10	1.5	34.40	0.60	0.84	0.05	0.11	0.72	0.93	0.04	0.11
260	10	1.5	34.40	0.35	0.94	0.05	0.01	0.30	0.95	0.03	0.01
200	20	1.5	34.40	0.47	0.97	0.02	0.01	0.43	0.94	0.03	0.01
220	20	1.5	34.40	0.61	0.96	0.02	0.02	0.55	0.93	0.03	0.02
240	20	1.5	34.40	0.68	0.95	0.02	0.03	0.65	0.92	0.03	0.03
260	20	1.5	34.40	0.36	0.95	0.04	0.02	0.27	0.94	0.02	0.02
200	30	1.5	34.40	0.42	0.96	0.02	0.02	0.39	0.93	0.02	0.02
220	30	1.5	34.40	0.61	0.96	0.02	0.02	0.51	0.92	0.02	0.02
240	30	1.5	34.40	0.59	0.97	0.01	0.02	0.51	0.92	0.02	0.02
240	30	1.5	34.40	0.66	0.96	0.03	0.02	0.61	0.89	0.03	0.02

List of symbols

r	observed reaction rate per unit particle volume	[mol/(min cm ³)]
r_j	reaction rate	[mol/(min g _{cat})]
C_0	reactant concentration at the external surface of the particle	[mol/cm ³]
R_p	radius of the particle	[cm]
D_{eff}	effective diffusivity coefficient	[cm ² /min]
F_i	molar flow rate of component i	[mol/min]
F_E°	inlet ethanol flow rate	[mol/min]
X_E, X_{EtOH}	ethanol conversion	[-]
S_i	Selectivity to component i	[-]
D_i	molecular diffusivity of ethanol in nitrogen	[cm ² /min]
ϵ_B	porosity of the bed	[-]
ρ_B	bulk density of the catalyst bed	[g/cm ³]
τ	tortuosity factor	[-]
σ	constriction factor	[-]
k_c	mass transfer coefficient	[cm/min]
n	reaction order	[-]
d_p	pellets diameter	[cm]
v_0	volumetric flow rate	[cm ³ /min]
A_c	cross sectional area of the reactor tube	[cm ²]
U	superficial velocity= v_0/A_c	[cm/min]
μ	kinematic viscosity	[cm ² /min]
n_{Ci}	number of carbon atoms in component i	[-]
A_{Ci}	Chromatographic area of component i	[-]
z	dimensionless bed length	[-]
W, w_{cat}	catalyst weight	[g]
α_{ij}	stoichiometric coefficient of component i in reaction J	[-]
N_R	number of reactions	[-]
L	axial coordinate	[cm]
L_{BED}	length of the catalytic bed	[cm]
a_i	conversion or selectivities	[-]
N	number of experimental measurements	[-]
Sh'	Sherwood number	[-]

σ_i catalytic site occupied by component i	[-]
k_j kinetic constant of reaction j [mol/(g h atm)] (k_1)	
[mol/(g h atm ²)] (k_2, k_3)	
b_i adsorption parameters	[atm ⁻¹]
K_{ej} equilibrium constant of reaction j	[-]
P_i partial pressure of component i	[atm]

Subscripts

EtOH ethanol

AcH acetaldehyde

EA ethylacetate

H₂ hydrogen

Others subproducts derived by aldol condensation (esters, aldehyde, alcohols and chetones C3-C4).

B-5.5 References

- [1] Per Stoltze, Introduction to heterogeneous catalysis.
- [2] K. Inui et al. / Journal of Molecular Catalysis A: Chemical 216 (2004) 147–156
- [3] Tu, Y.-J., Li, C. & Chen, Y.-W. Journal of Chemical Technology and Biotechnology 59, 141-147 (1994b).
- [4] Colley, S.W., Tabatabaei, J., Waugh, K.C. & Wood, M.A. Journal of Catalysis 236, 21-33 (2005).
- [5] D.E. Mears Ind. Eng. Chem. Process Des. Develop., Vol. 10, No. 4, 1971 541
- [6] Weisz, P. B.; Prater, C. B., Advan. catal., 6, 143 (1954).
- [7] J. B. Butt, Reaction Kinetics and reactors design, 2001
- [8] H.S. Fogler, Elements of chemical reaction engineering 4th edition.
- [9] H. Weisz, Z. Physik. Chem., N.F., 11, 1 (1957)
- [10] John B. Butt, Reaction Kinetics and reactors design, second edition, 2000

SECTION B

Chapter 6

Plant Design

C-6.1 Introduction

An overall process simulation, made in ChemCAD, was used as a base for the sizing of the different characteristic units of the hypotized plant for the ethyl acetate production. The study shows the possibility to realize a plant to produce ethyl acetate and pure hydrogen by ethanol dehydrogenation. The plant capacity is of about 160 kton/year and by assuming an activity of 8000 hours/years. The hourly productivity is for ethylacetate of about 21 t/h and for hydrogen of 1 t/hour. An ethanol fed of 23 t/h is assumed.

C-6.1.1 Introduction to the scale-up

Scaling up is a major task for chemical engineers and is the fundamental step in the realization and optimization of an industrial plant [1]. The scale up activity represents the synthesis of the know-how accumulated in the various phase of the process development from the design of laboratory experiments and the derivation of kinetic correlations, to fluid dynamic experiments, mathematical modeling, design and operation of pilot and industrial plants. The term "scale up" has been usually explained as "how to design a pilot or industrial reactor able to replicate though a standard methodology the results obtained in laboratory". This is a limiting definition, since experiments has shown that it does not really exist a standard way through process innovation.

Scale up is the ability of finding out the quantitative rules that describes the operation of a chemical reactor at different scales, operating conditions and with different reaction technologies.

The scale up is realized on the basis of a mathematical model that is the synthesis of ideas and experimental data and is the main tool to be used for scaling up or improving the performance of an industrial unit. The mathematical model may be simple or a complex one within available data, knowledge, ideas and objectives.

Most novel chemical processes present chemical engineering challenges. The following section describes some of the challenges that were addressed during the development of the ethyl acetate process. Resolution of these problems required a combination of fundamental chemical engineering research and application of state-of-the-art software tools for steady state and dynamic simulation and computational fluid dynamics.

C-6.1.2 Ethanol dehydrogenation to Ethyl acetate: process design

The development deals with process engineering trends for improving biotechnological production of ethanol. The future availability of ethanol in the next future will require its use in process to produce chemicals such as ethylene, acetaldehyde, ethyl acetate, still now produced by fossil sources. In particular, the ethyl acetate is increasing its share of the oxygenated solvents market. As demand rises, producers are seeking more economic, environmentally compatible and reliable process routes. Actually, the Davy Process Technology is the only developed and commercialized process technology that addresses all these issues. This technology adds value to ethanol and, in a fully integrated fermentation facility, can provide a process that is

carbon neutral. The process consists of several parts that can be summarized in four steps: ethanol drying, dehydrogenation, selective hydrogenation and refining (see Figure 1). The product is cooled in an integrated heat exchanger system, hydrogen being separated from the crude product. The hydrogen is mainly exported.

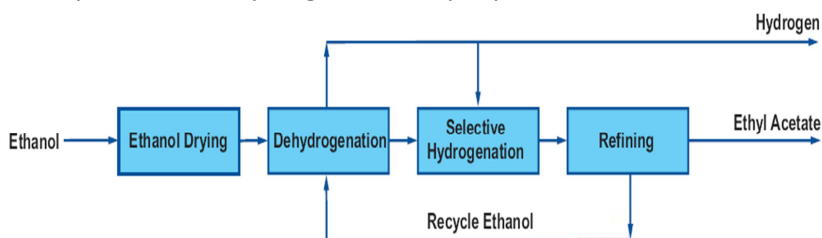


Figure 1: simplified scheme of the Davy process

Crude product is passed through a second catalytic reactor to allow selective 'polishing' to remove minor by-products such as carbonyls. Polished product is passed to a distillation train where a novel distillation system allows the ethanol/ ethyl acetate/water azeotrope to be broken. The products from this distillation scheme are unreacted ethanol, which is recycled, and ethyl acetate product. The main advantage of this process is the use of a single renewable feedstock that allows significant production cost benefits over other technologies. This process is proven to be safe, efficient and reliable and the resulting product has been readily accepted by end-users. The elimination of acetic acid as a feedstock allows for lower grade materials of construction thereby reducing investment and maintenance costs. With conventional process routes to ethyl acetate, hydrocarbon molecules are broken down and reformed. The major benefit of the Davy Process Technology is that it relies only upon the availability of ethanol, the majority of which is produced by fermentation. As fermentation, ethanol is derived from biomass and this relies on atmospheric carbon dioxide there is no depletion of a

non-renewable feedstock. The major application of ethyl acetate is as a solvent in coatings and inks. In the atmosphere it is readily oxidized to carbon dioxide and water. Davy Process Technology has made a break-through so that ethyl acetate is produced in two process stages (fermentation to bioethanol and catalytic dehydrogenation) from natural resources rather than petrochemicals. This route is far less likely to suffer cost fluctuations; production economics are therefore more stable. As the Davy Process Technology route is almost 100% carbon efficient there is no net carbon dioxide contribution. Moreover, the only by-product is hydrogen which is the ultimate clean fuel.

The main drawback of the Davy process is the needs of an hydrogenating reactor to convert the several co-products of reaction, such as C₃-C₄ aldehydes and ketones to the corresponding alcohols. On the basis of the surprising results obtained in our research, as demonstrated by the experimental runs reported in chapter 4 of the current section, a new simplified process in which a catalyst of copper/copper chromite/alumina/barium chromate was used to obtain by the dehydrogenation ethyl acetate with high purity and pure hydrogen. The main peculiarities of this process is the use of a very selective commercial catalyst Cu-1234 that gives during the dehydrogenation step an ethyl acetate selectivity of about 98.8% vs an ethanol conversion of 65% [2].

In this chapter, the key role is an evaluation of the equipment that should be employed for a future realization of the scale up of the dehydrogenation reactor through the analysis of major trends in process synthesis, modeling, simulation and optimization related to ethyl acetate and pure hydrogen production. Main ways of process intensification through reaction– reaction, reaction–separation and separation–separation processes are analyzed in the case of ethyl acetate production. Finally, some concluding considerations on

current and future research tendencies in ethyl acetate production regarding process design and integration are presented.

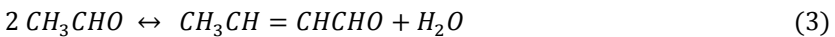
C-6.2 Main aspect of the project

C-6.2.1 Necessary Information and Simulation Hints

The main step of the process is the ethanol dehydrogenation to ethyl acetate represented by the two reactions:



The co-products of the reaction, mainly C₃-C₄ aldehydes and ketones, derive by the aldol condensation of the acetaldehyde produced during the ethanol dehydrogenation step. To take in account the secondary reactions, an approximate way is by considering the aldohol condensation to crotonaldehyde and water according to the reaction (3).



The kinetics of this reaction was previously studied and was derived by a laboratory experimentation in a fixed bed tubular reactor (section 200). For the main steps of reaction (1)-(3), the kinetic expressions have been reported below (4)-(6)

$$r_1 = k_1 P_{EtOH}^\alpha P_{H_2}^\delta \quad (4)$$

$$r_2 = k_2 P_{EtOH}^\beta P_{AcH}^\gamma P_{H_2}^\omega \quad (5)$$

$$r_3 = k_3 P_{AcH}^2 \quad (6)$$

The dependence of the kinetic constant k_1 , k_2 e k_3 from the reaction temperature was expressed by using the Arrhenius law, for more details see chapter 5. In Table 1 the values of the activation energies, of the pre-exponential factors and of the enthalpies of reactions have been reported. In Table 2 the have been summarized the values of the exponents of the power law have been reported. On the basis of a simplified kinetic consisting of a power law empirical model, a process for ethyl acetate production has been designed.

Table 1:power law parameters

Reaction	Activation energies (cal/mols)	kinetic constant (mols/(h cm ³))	Entalphy (cal/mole)
1	7715	3.545	16350
2	4519	0.416	-9970
3	10284	29.922	-

Table 2:esponential power law parameters

Parameters	Values
α	1.001
β	0.063
γ	1.095
δ	-0.953
ω	0.997

C-6.2.2 Process description

The overall process can be divided into three sections, for each of them approximate evaluations has been done. In more detail, the sections have been designated as ethanol dehydration (100), reaction (200) and respectively, acetaldehyde and ethyl acetate purification

and recovery (300) (400). The figure 1 represents a global scheme of all the apparatus employed in each section. The reaction was performed in four adiabatic reactors in series that could be considered as consisting of four catalytic beds of the same reactor, with intermediate heating. All the calculations were realized by using the PSRK (predictive Soave-Redlich-Kwong) thermodynamics for K-values, as suggested by the Chemcad expert system.

The process consists of four sections:

1. Section "100" – fresh ethanol purification and recycle.

In this section, the ethanol was dehydrated because an excess of water could be dangerous firstly for the ethyl acetate selectivity, in fact the presence of water could favor the acetic acid formation, and moreover could promote a drastic increase of the recycle flows. The dehydration is realized by using a system of double distillation columns, at atmosphere pressure, where the ethylene glycol was used to broken the azeotrope ethanol/water[3].

Furthermore, the formation of reaction by-product produce a small amount of water too. The produced water must be removed before the unreacted ethanol can be recycled to the reaction section. Water removal can either be integrated within the ethyl acetate unit or can be part of a larger external ethanol refining facility. If the ethanol feed has a high water content, an integrated water removal unit can be designed to dry both the recycle and feed ethanol before it is fed to the reactors. Studies indicate that molecular sieve based processes are generally the most economic, although conventional entrainer base distillation systems or pervaporation based processes could also be used [4].

2. Section "200" – Catalitic reactors

In the reaction section, dry ethanol is first heated in a feed/product and then vaporized before entering the dehydrogenation reactor. Here the ethanol is dehydrogenated to ethyl acetate. The reaction is

endothermic and the vapour is reheated several times in the reactor to maintain the reaction temperature. The apparatus of reaction is composed by four adiabatic catalytic beds with an inter-beds heating to offset the global endothermicity of the reaction. The reactors work in the best conditions of temperature and pressure identified in the experimental section (see chapter 4) respectively of 220°C and 20 bar.

3. Section “300” – Hydrogen purification and acetaldehyde separation
The stream leaving the reactors contains mainly acetaldehyde, unreacted ethanol and hydrogen. In this section, the hydrogen recovery is necessary to obtain it in highly purity degree. The separation was realized in two flash operating at two different temperatures and pressures. In this section the modality of separation of the acetaldehyde and hydrogen should be better defined, as matter of fact this two components should not feed in the next section. At present, in the calculation, this separation is implemented as an ideal separation.

4. Section “400” – Ethyl acetate and others recovery

In this last section the unreacted ethanol is separated by ethyl acetate and recycled to the section “100”. This separation is realized with Pressure Swing Distillation (PSD) by using two distillation columns working at two different pressures respectively of 20 and 1 bar. Successively a separation of other by-products, all lumped as crotonaldehyde, should be realized but actually, this is considered as an ideal separation and should be defined in future study.

In the next paragraph all the sections will be described in more detail.

C-6.2.2.1 Section "100"

The ethylene glycol was used as entrainer to realize the ethanol dehydration. As shown in Figure 3A, the fresh ethanol (1) and the recycled one (11) was heated at 80°C by using an heat exchanger E-101. In Table 3, the compositions of each stream (Kg/h) are summarized.

Table 3: Flow 1-11 summaries

Stream No.	1	2	3	4	5	7	8	11
Name	FRESH ETOH				BY-PASS		FEED-0	RECY-ETOH
-- Overall --								
Molar flow kmol/h	507.0262	507.0262	1303.5646	1303.5646	0.0130	1280.9406	1293.0969	796.5384
Mass flow kg/h	23000.0018	23000.0018	59631.5989	59631.5989	0.5963	59192.0000	59771.1494	36631.6060
Temp C	20.0000	20.0000	55.4957	80.0000	80.0000	249.6300	243.8839	77.0000
Pres bar	1.0000	1.0000	1.0000	1.0000	1.0000	20.0000	20.0000	1.0000
Vapor mole fraction	0.0000	0.0000	0.0000	1.000	1.000	1.000	1.000	0.0000
Flowrates in kg/h								
Ethanol	22770.0003	22770.0003	58864.6273	58864.6273	0.5886	58805.7808	59329.2087	36094.6306
Ethyl Acetate	0.0000	0.0000	377.4401	377.4401	0.0038	377.4399	428.7271	377.4401
Hydrogen	0.0010	0.0010	0.0010	0.0010	0.0000	0.0010	0.2393	0.0000
Acetaldehyde	0.0000	0.0000	0.0000	0.0000	0.0000	0.0000	3.6373	0.0000
Nitrogen	0.0000	0.0000	0.0000	0.0000	0.0000	0.0000	0.0000	0.0000
Water	230.0000	230.0000	387.3099	387.3099	0.0039	1.1687	1.2536	157.3100
Cis-Crotonaldehy	0.0000	0.0000	2.2237	2.2237	0.0000	1.5996	2.0689	2.2237
Ethylene Glycol	0.0000	0.0000	0.0000	0.0000	0.0000	6.0094	6.0094	0.0000

The outlet was fed directly in the by-pass current by passing the ethanol purification section. As shown in Figure 3B, the separation was realized by fed a make-up current of ethylene glycol (45) that was sent with the ethylene glycol recycles (51) to a first distillation column T-101 operating at atmospheric pressure. The overhead products contains mainly ethanol and traces of ethyl acetate whilst the bottom was fed to a second distillation column T-102 able to separate the water, from the overhead, and the ethylene glycol from the bottom section, thus recycled to T-101. In Table 4, the composition of each current is so summarized.

Table 4: Flow 25-53 summaries

Stream No.	35	42	43	44	45	46	47	48
Name		EG MAKEUP						
-- Overall --								
Molar flow kmol/h	12.1562	1303.6518	1281.0388	1281.0258	0.8056	701.4273	724.1156	700.6919
Mass flow kg/h	579.1498	59635.5182	59196.4302	59195.8313	50.0000	43535.2464	43978.7853	43489.5966
Temp C	-20.0000	80.0000	79.9997	77.0731	80.0000	80.0003	182.2720	195.5586
Pres bar	50.0000	1.0000	1.0000	1.0000	1.0000	1.0000	1.0000	1.0000
Vapor mole fraction	0.0000	1.000	1.000	0.0000	0.0000	0.0000	0.0000	0.0000
Flowrates in kg/h								
Ethanol	523.4316	58868.7097	58810.3982	58809.8100	0.0000	0.0000	58.8901	0.0000
Ethyl Acetate	51.2879	377.2564	377.2600	377.2562	0.0000	0.0000	0.0000	0.0000
Hydrogen	0.2383	0.0010	0.0010	0.0010	0.0000	0.0000	0.0000	0.0000
Acetaldehyde	3.6377	0.0000	0.0000	0.0000	0.0000	0.0000	0.0000	0.0000
Nitrogen	0.0000	0.0000	0.0000	0.0000	0.0000	0.0000	0.0000	0.0000
Water	0.0849	387.3234	1.1664	1.1626	0.0000	0.3864	386.5464	0.3864
Cis-Crotonaldehy	0.4693	2.2223	1.5981	1.5981	0.0000	0.0008	0.6250	0.0008
Ethylene Glycol	0.0000	0.0000	6.0047	6.0047	50.0000	43534.8601	43532.7233	43489.2103
Stream No.	49	50	51	52	53			
Name		WATER	PURGE-EG	RECY-EG				
-- Overall --								
Molar flow kmol/h	23.4239	0.0701	700.6218	700.6919	1281.0258			
Mass flow kg/h	489.1947	4.3490	43485.2449	43489.5966	59195.8313			
Temp C	90.9666	80.0000	80.0000	80.0000	80.0000			
Pres bar	1.0000	1.0000	1.0000	1.0000	1.0000			
Vapor mole fraction	0.0000	0.0000	0.0000	0.0000	1.000			
Flowrates in kg/h								
Ethanol	58.8901	0.0000	0.0000	0.0000	58809.8100			
Ethyl Acetate	0.0000	0.0000	0.0000	0.0000	377.2562			
Hydrogen	0.0000	0.0000	0.0000	0.0000	0.0010			
Acetaldehyde	0.0000	0.0000	0.0000	0.0000	0.0000			
Nitrogen	0.0000	0.0000	0.0000	0.0000	0.0000			
Water	386.1601	0.0000	0.3864	0.3864	1.1626			
Cis-Crotonaldehy	0.6242	0.0000	0.0008	0.0008	1.5981			
Ethylene Glycol	43.5202	4.3489	43484.8587	43489.2103	6.0047			

Optionally, a purge of the ethylene glycol could be useful to keep under control the impurities concentration that could gather into the recycle loop. In this section the heat exchanger E-102, warm up the ethanol from 77°C to 80°C whilst the E-103 cool down the ethylene glycol from 195°C to 85°C. The heat exchangers could be connected to optimize the thermal recovery between the two above mentioned streams.

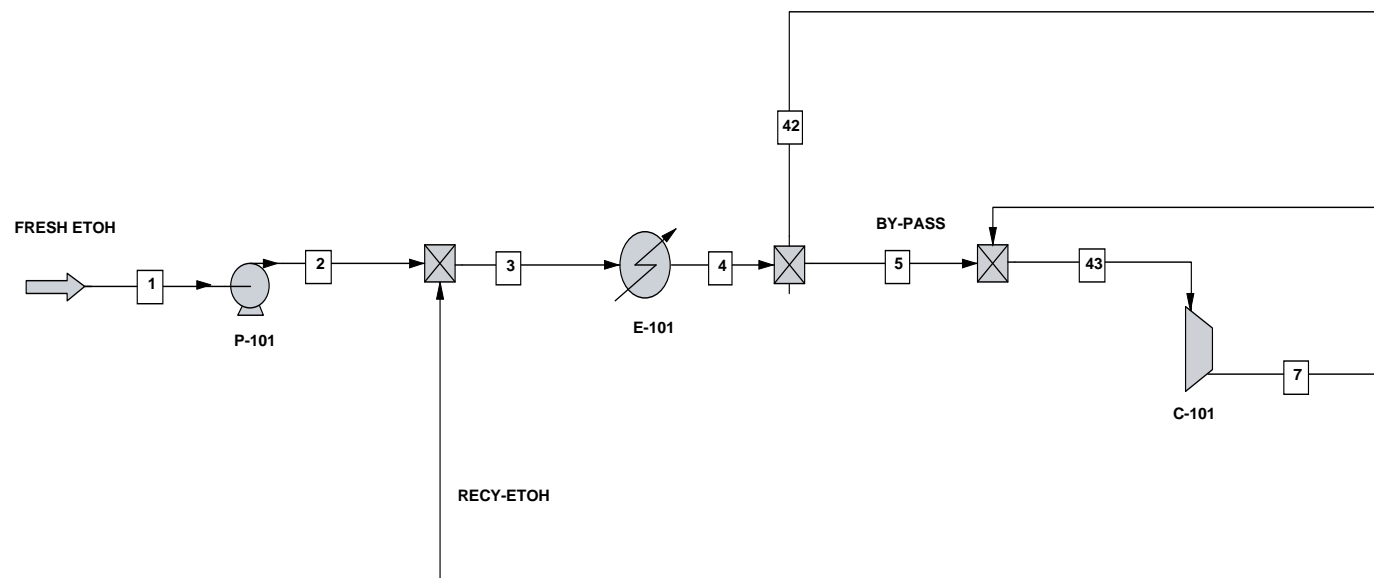


Figure 3A: section "100"

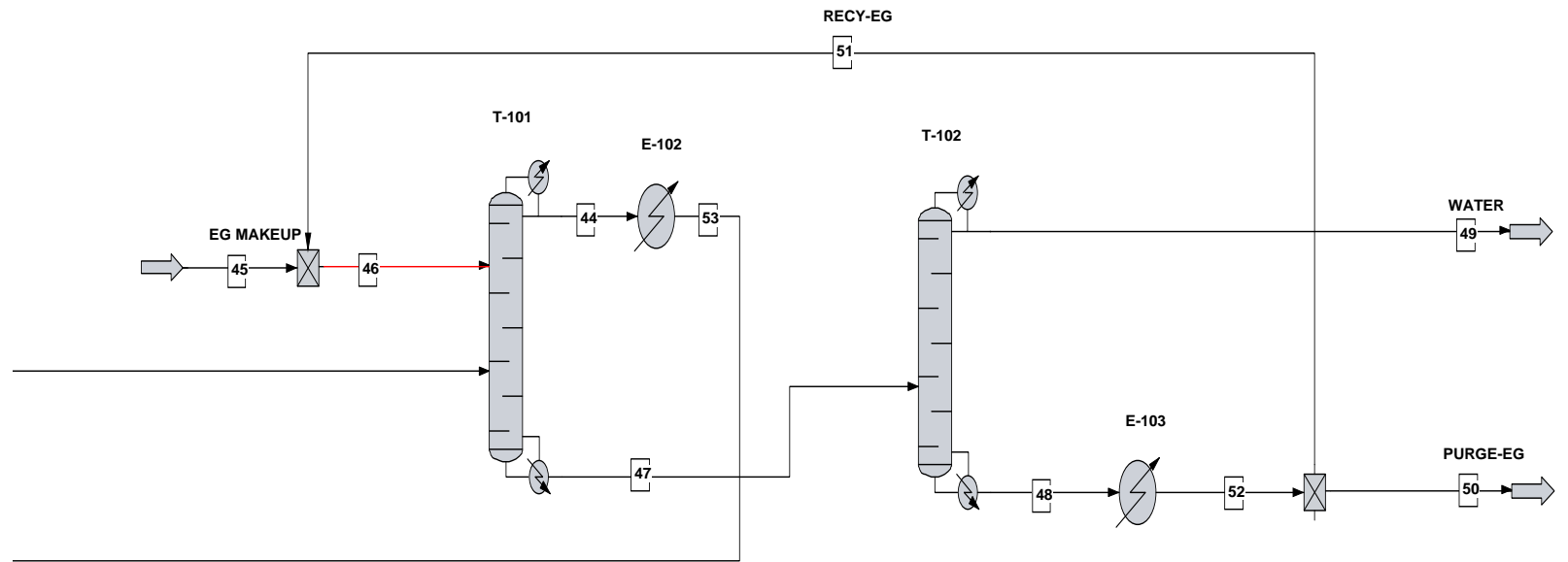


Figure 3B: : section "100"

C-6.2.2.2 Section "200"

The reaction section was composed by four adiabatic catalysts bed of 10 m³ for each and with an inlet temperature of 220°C for the first two ones and 230°C for the third and fourth reactor (see Figure 4). The presence of heat exchangers (E-202, E-203 and E-204) between the reactors is necessary to offset the endothermicity of the examined reaction. The operating pressure of each reactor is of 20 bar. The ethanol global conversion is of about 40% and the in more detail the fractional conversion obtained in each of four reactors is reported in Table 5.

Table 5: fractional conversions

Catalytic bed	Ethanol conversion
1	0.185
2	0.278
3	0.341
4	0.389

In table 6 the streams composition is reported.

Stream No.	8	9	38	16	36	15	17	18
Name	FEED-0	FEED-1	OUT-1	FEED-2	OUT-2	FEED-3	OUT-3	FEED-4
-- Overall --								
Molar flow kmol/h	1293.2897	1293.2897	1445.3220	1445.3220	1490.4344	1490.4344	1527.3062	1527.3062
Mass flow kg/h	59779.0544	59779.0544	59775.5082	59775.5082	59775.5365	59775.5365	59775.5223	59775.5223
Temp C	243.8851	220.0000	209.2989	220.0000	214.9440	230.0000	226.6004	230.0000
Pres. bar	20.0000	20.0000	20.0000	20.0000	20.0000	20.0000	20.0000	20.0000
Vapor mole fraction	1.000	1.000	1.000	1.000	1.000	1.000	1.000	1.000
Flowrates in kg/h								
Ethanol	59337.1182	59337.1182	48348.9033	48348.9033	42788.0418	42788.0418	38067.8967	38067.8967
Ethyl Acetate	428.7706	428.7706	8209.3888	8209.3888	14694.2435	14694.2435	18560.3371	18560.3371
Hydrogen	0.2393	0.2393	481.0280	481.0280	724.2210	724.2210	887.0007	887.0007
Acetaldehyde	3.6377	3.6377	2326.5096	2326.5096	841.8034	841.8034	500.7122	500.7122
Nitrogen	0.0000	0.0000	0.0000	0.0000	0.0000	0.0000	0.0000	0.0000
Water	1.2510	1.2510	118.4864	118.4864	148.0433	148.0433	154.6579	154.6579
Cis-Crotonaldehy	2.0680	2.0680	458.1865	458.1865	573.1819	573.1819	598.9170	598.9170
Ethylene Glycol	6.0047	6.0047	6.0047	6.0047	6.0047	6.0047	6.0047	6.0047
Stream No.								
	33	21						
Name								
	OUT-4							
-- Overall --								
Molar flow kmol/h	1556.5880	1556.5880						
Mass flow kg/h	59775.5011	59775.5011						
Temp C	227.6554	5.0000						
Pres. bar	20.0000	20.0000						
Vapor mole fraction	1.000	0.3194						
Flowrates in kg/h								
Ethanol	36249.8832	36249.8832						
Ethyl Acetate	21369.7908	21369.7908						
Hydrogen	1010.3055	1010.3055						
Acetaldehyde	372.0951	372.0951						
Nitrogen	0.0000	0.0000						
Water	157.4894	157.4894						
Cis-Crotonaldehy	609.9333	609.9333						
Ethylene Glycol	6.0047	6.0047						

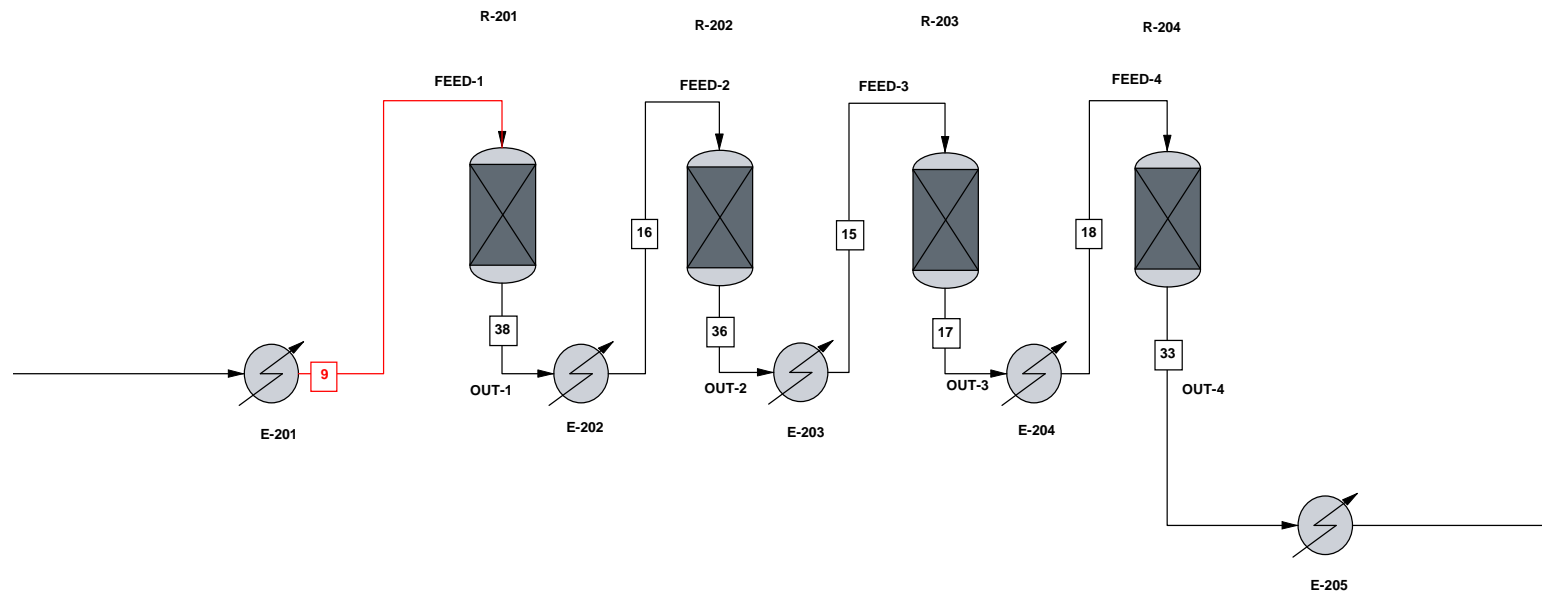


Figure 4: section 200

C-6.2.2.3 Section "300"

In Figure 5 was represented the section 300. The stream in the outlet of the fourth reaction step (section 200) was cooled to 5°C in E-205 and sent to a flash unit (V-301) that works at 5°C and 20 bar. The liquid stream (10) passed through the next step of purification of the ethyl acetate, whilst, the gaseous phase was purified to obtain hydrogen with a high grade of purity. At this purpose an auxiliary current of fresh ethanol was added (41) and sent to the compressor to obtain a pressure of 50 bar, after that the outlet was cooled down to -20°C in the heat exchanger E-301. The flash unit V-302, operating at -20°C and 50 bar, produced in the bottom a recycling current of ethyl acetate and ethanol, decompressed at 20 bar and sent, as feeding, at the first reactor. By the same unit (V-302) was recovered 1000 kg/h of hydrogen at 99.98% vol. The bottom of the section V-301 went through the ethyl acetate purification section among the heat exchangers E-303 that was fed to the separator T-302. In this unit the residual acetaldehyde and hydrogen should be removed to promote the next step of purification (section 400). This unit is an ideal separator where the gas phase containing acetaldehyde and hydrogen were separated by all the other components. In table 7 all the composition streams were summarized.

Table 7: stream composition for the section 300.

Stream No.	21	19	10	41	54	6	40	20
Name	RAW H2			AUX ETOH			PURE H2	
-- Overall --								
Molar flow kmol/h	1556.5948	497.2069	1059.3877	10.8533	508.0602	508.0603	508.0603	495.9041
Mass flow kg/h	59775.8413	1083.9023	58692.0000	500.0000	1583.9016	1583.9005	1583.9005	1004.7536
Temp C	5.0000	5.0000	5.0000	-20.0000	3.3576	73.5434	-20.0000	-20.0000
Pres bar	20.0000	20.0000	20.0000	20.0000	20.0000	50.0000	50.0000	50.0000
Vapor mole fraction	0.3194	1.000	0.0000	0.0000	0.9776	0.9998	0.9761	1.000
Flowrates in kg/h								
Ethanol	36250.0958	25.7275	36224.3686	500.0000	525.7270	525.7258	525.7258	2.2969
Ethyl Acetate	21369.9733	53.5481	21316.4228	0.0000	53.5480	53.5480	53.5480	2.2601
Hydrogen	1010.3077	999.6957	10.6120	0.0000	999.6957	999.6958	999.6958	999.4576
Acetaldehyde	372.0985	4.3726	367.7258	0.0000	4.3726	4.3726	4.3726	0.7349
Nitrogen	0.0000	0.0000	0.0000	0.0000	0.0000	0.0000	0.0000	0.0000
Water	157.4883	0.0851	157.4031	0.0000	0.0851	0.0851	0.0851	0.0002
Cis-Crotonaldehy	609.9335	0.4732	609.4602	0.0000	0.4732	0.4732	0.4732	0.0039
Ethylene Glycol	5.9453	0.0000	5.9453	0.0000	0.0000	0.0000	0.0000	0.0000
Stream No.	37	39	35	55	12	13	29	
Name	RECYET+EA				ACETALD+H2			
-- Overall --								
Molar flow kmol/h	495.9041	495.9041	12.1562	12.1562	1059.3877	13.6116	1045.7760	
Mass flow kg/h	1004.7536	1004.7536	579.1471	579.1471	58692.0000	378.3340	58313.6083	
Temp C	20.0000	20.0000	-20.0000	-19.5884	200.0000	200.0000	200.0000	
Pres bar	50.0000	50.0000	50.0000	20.0000	20.0000	20.0000	20.0000	
Vapor mole fraction	1.000	1.000	0.0000	0.005808	1.000	1.000	1.000	
Flowrates in kg/h								
Ethanol	2.2969	2.2969	523.4291	523.4291	36224.3686	0.0000	36224.3686	
Ethyl Acetate	2.2601	2.2601	51.2878	51.2878	21316.4228	0.0000	21316.4228	
Hydrogen	999.4576	999.4576	0.2383	0.2383	10.6120	10.6119	0.0001	
Acetaldehyde	0.7349	0.7349	3.6377	3.6377	367.7258	367.7221	0.0037	
Nitrogen	0.0000	0.0000	0.0000	0.0000	0.0000	0.0000	0.0000	
Water	0.0002	0.0002	0.0849	0.0849	157.4031	0.0000	157.4031	
Cis-Crotonaldehy	0.0039	0.0039	0.4693	0.4693	609.4602	0.0000	609.4602	
Ethylene Glycol	0.0000	0.0000	0.0000	0.0000	5.9453	0.0000	5.9453	

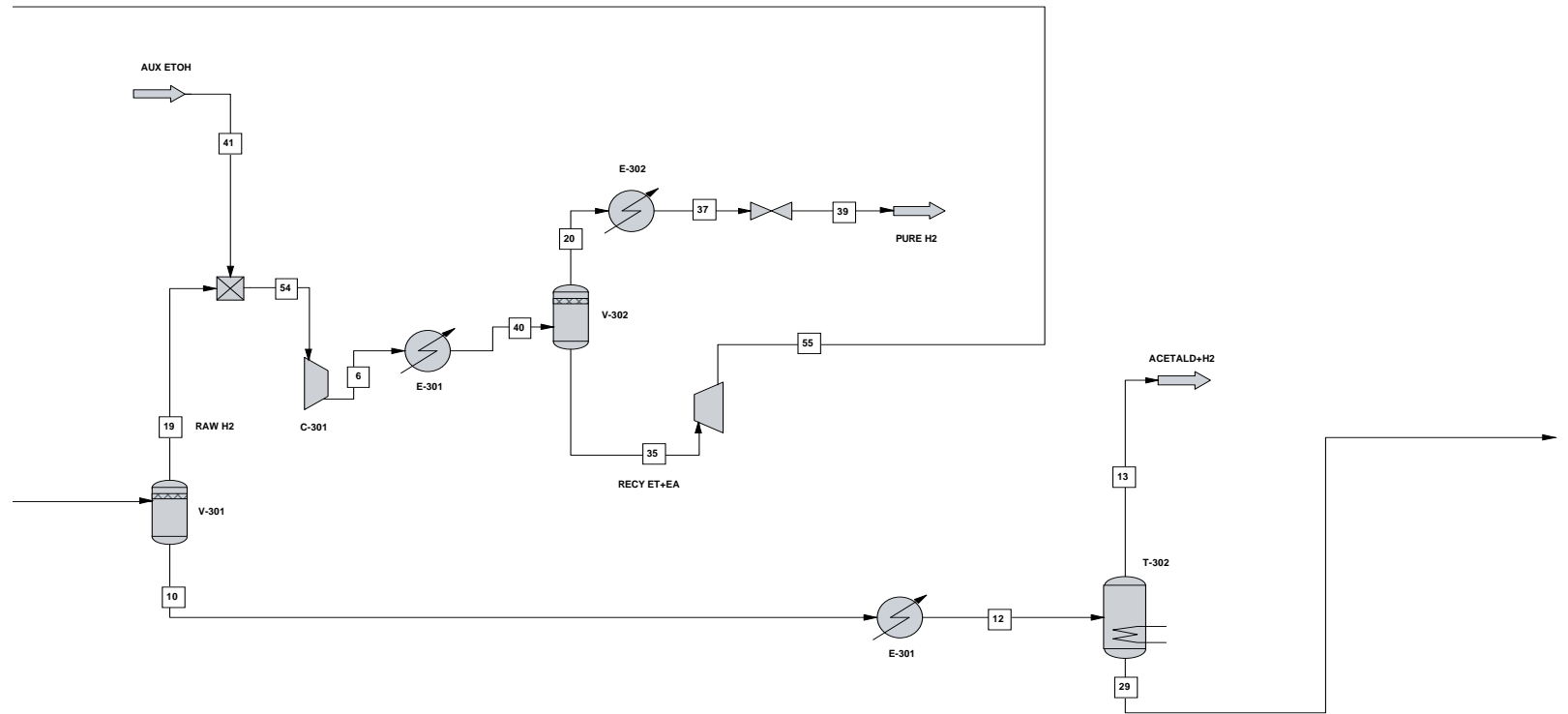


Figure 5: section 300

C-6.2.2.3 Section "400"

The separation of ethyl acetate product from unreacted ethanol and byproducts is complicated by low boiling, binary and ternary azeotropes of ethanol, ethyl acetate and water. It was found that the composition of these azeotropes varies significantly with pressure and so a pressure swing distillation scheme was adopted to separate the products. In pressure swing distillation systems, there is an optimum between the column refluxes and the recycle stream, which gives minimum heat input to the system. In the ethyl acetate system, extensive optimization studies showed that minimum heat input could be achieved by limiting the accumulation of water in the column overhead system. The separation of the ethyl acetate by ethanol would be realized in the current section (see figure 6). The azeotropic composition is sensible to the pressure variation and as matter of fact it changed significantly by varying the pressure from 1 bar to 20 bar, pressure of reaction. In particular, the azeotropic compositions changed as represented in Table 8.

Table 8: variation of azeotropic composition with the pressure

Pressure (bar)	Temperature (°C)	Ethanol molar fraction
1	70.7	0.47
20	179.0	0.85

The separation scheme consists of a first column (T-401), working at 20 bar, in which on the overhead the azeotrope ethyl acetate/ethanol was separated by the crude ethyl acetate. The overhead of T-401 was sent to T-402 that worked at 1 bar, able to separate the azeotrop ethanol/ethylacetate whilst on the bottom (11) the obtained ethanol was sent to rectification section (section 100). After that the overhead outlet of T-401 was compressed at 20 bar with C-401 and heated at 200°C in E-401.

The bottom of the column contained crude ethyl acetate with about 100 kg/h of ethanol and 600 kg/h of crotonaldehyde.

The mass balance on the current 34 have the following compositions (Table 9):

Table 9: current 34-outlet stream composition

	weight (%)
Ethanol	0.6
Ethyl acetate	96.6
Acetaldehyde	6.9×10^{-6}
Others	2.80

This current (34) was sent to an ideal separation unit (T-403) able to separate the pure ethyl acetate by the other components (bottom). The separation is ideal and dictated by the vincol of purity imposed in the above mentioned separation section (T-403). In table 10 the composition of each current is summarized.

Table 10: section 400 stream compositions

Stream No.	29	24	27	28	14	30	22	23
Name								PURGE
-- Overall --								
Molar flow kmol/h	1045.7760	2545.2689	1499.5591	249.0538	2296.2117	2296.2117	1499.5742	0.0150
Mass flow kg/h	58313.6083	146195.3014	87888.0505	21670.0583	124525.0252	124525.0252	87889.0000	0.8789
Temp C	200.0000	199.9962	200.0000	206.0000	178.7069	73.2980	61.1286	61.1286
Pres bar	20.0000	20.0000	20.0000	20.0000	20.0000	1.0000	1.0000	1.0000
Vapor mole fraction	1.000	1.000	1.000	0.0000	0.0000	0.5167	0.0000	0.0000
Flowrates in kg/h								
Ethanol	36224.3686	83727.1768	47502.2448	125.1452	83602.0000	83602.0000	47502.7196	0.4750
Ethyl Acetate	21316.4228	61458.7611	40149.2538	20931.6525	40527.0000	40527.0000	40149.6578	0.4015
Hydrogen	0.0001	0.3694	0.3694	0.0000	0.3694	0.3694	0.3694	0.0000
Acetaldehyde	0.0037	14.9665	14.9648	0.0015	14.9650	14.9650	14.9650	0.0001
Nitrogen	0.0000	0.0000	0.0000	0.0000	0.0000	0.0000	0.0000	0.0000
Water	157.4031	377.4866	220.0789	0.0779	377.4088	377.4088	220.0811	0.0022
Cs-Crotonaldehy	609.4602	610.6042	1.1443	607.2359	3.3681	3.3681	1.1443	0.0000
Ethylene Glycol	5.9453	5.9453	0.0000	5.9453	0.0000	0.0000	0.0000	0.0000
Stream No.	25	26	34	31	32			
Name				ETHYLAC	BY-PROD			
-- Overall --								
Molar flow kmol/h	1499.5591	1499.5591	249.0538	236.3857	12.6682			
Mass flow kg/h	87888.0505	87888.0505	21670.0583	20827.0000	843.0630			
Temp C	61.1286	61.9798	76.7607	76.7607	76.7607			
Pres bar	1.0000	20.0000	1.0000	1.0000	1.0000			
Vapor mole fraction	0.0000	0.0000	0.8521	1.000	0.0000			
Flowrates in kg/h								
Ethanol	47502.2448	47502.2448	125.1452	0.0000	125.1452			
Ethyl Acetate	40149.2538	40149.2538	20931.6525	20827.0000	104.6573			
Hydrogen	0.3694	0.3694	0.0000	0.0000	0.0000			
Acetaldehyde	14.9648	14.9648	0.0015	0.0000	0.0015			
Nitrogen	0.0000	0.0000	0.0000	0.0000	0.0000			
Water	220.0789	220.0789	0.0779	0.0000	0.0779			
Cs-Crotonaldehy	1.1443	1.1443	607.2359	0.0000	607.2359			
Ethylene Glycol	0.0000	0.0000	5.9453	0.0000	5.9453			

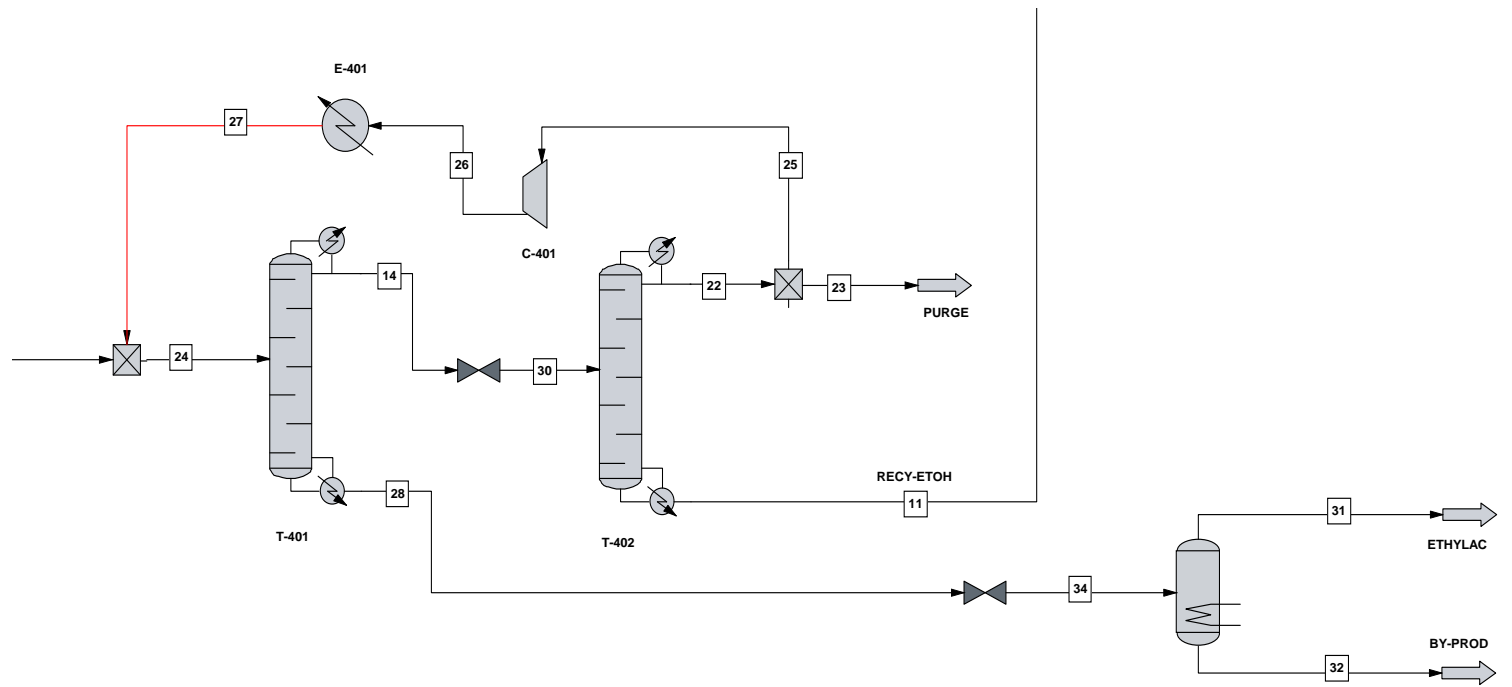


Figure 6: Section 400

C-6.3 Summary

In this paragraph, a summary of the mass and energy balance was reported. In particular in table 11 is represented the overall mass balance expressed respectively in Kmol/h and Kg/h on the inlet and outlet global mixture.

Table 11: Overall mass balance

Overall Mass Balance	kmol/h		kg/h	
	Input	Output	Input	Output
Ethanol	505.11	4.05	23270.00	186.80
Ethyl Acetate		237.76	-	20948.10
Hydrogen		501.06	0.001	1010.03
Acetaldehyde		8.36		368.41
Nitrogen				
Water	12.767	21.44	230.000	386.23
Cis-Crotonaldehy		8.67		607.83
Ethylene Glycol	0.806	0.86	50.000	53.63
Total	518.685	782.21	23550.00	23561.039

The process should be improved, as it can be seen by the results reported in Table 9, the weigh percentage of the sub-products is too high. In Table 12 the overall energy balance was reported. In Appendix C a summary of the all equipment for each sections is reported.

Table 12: Overall energy balance

Overall Energy Balance	kcal/h	
	Input	Output
Feed Stre	-3.48185e+007	
Product Streams		-2.72971e+007
Total Heating	1.2739e+008	
Total Cooling	-1.26139e+008	
Power Added	4.42322e+006	
Power Generated	-505.656	
Hrxn correction	1.86227e+006	
Total	-2.72824e+007	-2.72971e+007

A possibility could be the use of a kinetic law able to well interpret the experimental data. The simplified power law is not able to describe the experimental data as the model LHHW as demonstrate in chapter 5 of the current section. At this purpose, a future development should be the use of LHHW in chemcad to scale up of the process. Moreover, the Davy process have realized the scale up by using a kinetic model of Langmuir-Hinchelwood to fit the experimental data. The final kinetic model was then used to develop tubular and multiple adiabatic bed reactor models and a four bed adiabatic reactor with inter-bed reheating was the economic choice for this application.

C-6.4 References

- [1] G.Donati, R.Paludetto / Catalysis Today 34 (1997) 483-533
- [2] E.Santacesaria, M.Di Serio, R.Tesser, G.,Carotenuto WO 2011/104738 A2
- [3] Colley et al, US PATENT 7,553,397 B1 Jun 30,2009
- [4] Davy process technology brochure www.davy.com Novel Technology for an Industrial Solvent by Mike Ashley

SECTION B

Conclusions

The investigation of several literature researches, as shown in chapter 1, have displayed the performances of different phase into ethanol dehydrogenation. The results of ethyl acetate are not higher than the 94%. As repeatedly pointed, the main problem of this reaction is strictly related to the individuation of optimal operative conditions in terms of temperature, pressure, residence times, and inlet hydrogen flow. Actually, the individuation and the choice of an active, selective and stable catalytic system remains still a great challenge. The foregoing technologies, however, have not satisfied the economical requirements for industrial application, especially regarding the space-time yield (STY) of ethyl acetate, selectivity to ethyl acetate, and production of by-products such as methyl ethyl ketone (MEK). In the practical plant operation, MEK in the products causes a serious problem in the purification of ethyl acetate because MEK and ethyl acetate forms an azeotropic mixture. It is very difficult to separate MEK from the mixture under ordinary distillation. Therefore, on the basis of such these considerations, in this research, the attention has been paid on the study of the ethanol dehydrogenation at high pressure with the aim to produce ethyl acetate as well as hydrogen, as second main reaction product, of this reaction, after acetaldehyde. The hydrogen produced in our innovative proposed process, is completely exempt of CO_x and easily separated by the condensable by-products of reaction. As demonstrate by using a relatively high

pressure (10-30 bar), temperature of 200-260°C, ethanol residence time of 1-100 g_{cat}h mol⁻¹, a productivity to hydrogen in the range of 20-300 g_{cat}h mol⁻¹ has been obtained. The key factor of our invention is the develop of innovative process, simplified respect to the Davy, able to convert ethanol 65% to ethyl acetate, with a selectivity of 97.8%, and pure hydrogen in only one step without the use of hydrogenating reactor to convert the several by-product to ethanol.

The individuation of the best operative conditions was done on the basis of a preliminary thermodynamic study of ethanol dehydrogenation reaction at high temperature and pressure, reported in chapter 3. By this theoretical study was demonstrated the necessity to operate in a low range of temperature of 200-260°C and at a moderate pressure 20-30 bars to favor the ethyl acetate formation rather than acetaldehyde. Moreover, was demonstrate the strong dependence of the ethanol conversion by the pressure, in fact by increasing the reaction pressure an evident decrease of the ethanol conversion was observed. On the other hand, the increase of pressure favors the ethyl acetate selectivity with respect to acetaldehyde. The last product is favored at low pressure and high temperature of reaction (>300°C). The experimental runs, performed in the range of temperature and pressure suggested by the thermodynamic study, were realized by using several copper based catalysts promoted with chromium or zinc. By the obtained results, as shown in chapter 4, we can conclude that it is possible to obtain ethyl acetate with a satisfactory conversion and very high selectivity by using a copper/copper chromite catalyst, containing an opportune support, like alumina, and different promoters, having the main scopes of preventing the sintering of the metal and the subsequent catalyst deactivation and create an acid-base environment favorable to the desired reaction. We have seen, in agreement with the current literature, that the operative conditions are very important for

obtaining high activities and selectivities. In particular, at low pressure (1-5 bars) acetaldehyde is the main reaction product but moderately increasing the pressure up to 20-30 bars the selectivity is shifted toward the formation of ethyl acetate as main product. Afterward, by operating in the conditions favorable to ethyl acetate formation, the selectivity could be lowered by the presence of a competitive reaction pathway originated by the acetaldehyde self-condensation. This pathway gives place to many possible by-products, as seen in scheme (1) reported in chapter 4. As, very probably, the two possible condensation reactions occur on two different multi-sites assemblies, on the copper surface, a further increase of the selectivity depends on: the type of catalyst used the preparation method, the catalyst pre-treatment, the acid-base properties of the catalytic environment and the type of used support and promoters. Our experimental observation, for example, is that copper/copper chromite catalysts (T-4466 and Cu-1234) are more stable to sintering and more selective than copper catalysts (K-310) supported on a mixture of oxides with basic character ($\text{Al}_2\text{O}_3/\text{ZnO}$). Moreover, supported copper chromite catalyst (Cu-1234), in which copper chromite is more dispersed, resulted more active and more selective. Surprisingly, the presence of $\text{BaO-Cr}_2\text{O}_3$ in this catalyst formulation has a favorable effect. Our proposal is that, probably, this promoter increases the thermal stability of the catalyst and improves the selectivity optimizing the acid-base properties of the surface. With this catalyst a maximum of 98-99% of selectivity has been obtained for 60-65% of ethanol conversion. This performance, never obtained before, has been achieved by operating at 220-240°C, 20 bars and an ethanol residence time of 97.5 g h mol⁻¹. At last, it is important to point out that activity and selectivity are also promoted by the hydrogen partial pressure. Hydrogen keep the catalyst in the reduced form and limit the acetaldehyde formation maintaining low its concentration so

disfavoring the auto-condensation. This last observation opens the possibility in an industrial plant to use a stream of recycled hydrogen as carrier gas. Finally, in this process pure hydrogen (exempt of CO) is produced in mild conditions as by products. With the aim to sizing the reactor modeling and optimization a kinetic study of the high pressure ethanol dehydrogenation was realized. By the many proposed model, the Langmuir-Hinshelwood-Hougen-Watson kinetic model has been used for interpreting all the kinetic runs performed, that is, 62 runs performed in different operative conditions by using a tubular reactor filled with 2 g of catalyst and 28 runs made by using 50 g of catalyst. It has been shown that the runs with the lowest amount of catalyst have been performed in chemical regime and have been used to identify the best kinetic model, while, the runs performed with 50 g of catalyst give data that are near the equilibrium conditions and allow to verify both the model goodness and the validity of the equilibrium constants. The obtained agreements are satisfactory, considering the approximations introduced as the assumption of isothermal conditions and the use of the equilibrium constants directly derived from theoretical calculations. At last, the model is based on a reliable mechanism and the kinetic parameters show physical mean. Nevertheless, in a first phase of this work a simplified power law was used at first to realize the sizing of the plant equipments. Traditionally, ethyl acetate is produced by esterification of acetic acid or by oxidation of ethylene – more recent process developments are based upon ethylene addition to acetic acid. All these routes are dependent on petrochemical based feedstock and certainly, the development of the ethanol to ethyl acetate process, described here, was driven by the availability of relatively low value, fossil fuel derived ethanol. However, this novel technology offers a wider choice of feedstock and future projects may be based on fermentation ethanol derived from renewable resources.

So, the major benefit of this new process is that it relies only upon the availability of ethanol, the majority of which is produced by fermentation. As fermentation ethanol is derived from biomass and this relies on atmospheric carbon dioxide, there is no net carbon dioxide contribution. Logically, plants based upon this process would be located close to sources of low cost ethanol. Additional benefits can be realized by integration of cane sugar, ethanol and ethyl acetate units in one location. Of particular benefit in this respect is the use of waste bagasse as a fuel to support the units. The proposed new ethyl acetate process produces a high quality ethyl acetate product without, in spite of the already commercialized Davy process, the use of hydrogenation unit. Thus, the proposed process is more simple and able to produce high quality ethyl acetate in only one step of reaction. Furthermore, the use of pressure changes to break the ethyl acetate/ethanol / water azeotrope leads to an inherently cleaner product than processes such as esterification or direct addition that operate separation systems in water rich regions of the phase diagram. The key benefits of this ethanol dehydrogenation route to ethyl acetate includes:

1. **Feedstock Flexibility:** Poor quality ethanol from many sources is acceptable as feedstock to the process. The pressure swing distillation system, ensure high quality product despite the presence of impurities in the feed.
2. **High Atom Efficiency:** co-production of a hydrogen by-product stream results in a very high atom efficiency compared with the traditional esterification or acetaldehyde routes. **High Product Quality:** the novel selective hydrogenation and product distillation schemes produce product of unprecedented quality suitable in premium value applications.
3. **Environmental Compatibility:** Ethyl acetate is biodegradable and so when it is used as a solvent its vapors are rapidly rendered to carbon dioxide without imposing a toxic hazard.

The scale up of this process, on the basis of the obtained results, should be improved and refined, possibly by using kinetic laws able to describe as well the experimental data and devoting a greater attention to the purification sections that should be analyzed and evaluated in all their peculiarities in more detail. The development and use, of an adequate kinetic expression, is necessary, fundamental to develop tubular, and multiple adiabatic bed reactor models. As demonstrated in the chapter 5, of this section, the kinetic model power law is a very simplified model and is not able to well interpret the experimental data. On the other hand, as demonstrated, the Langmuir-Hichelwood-Hugen-Watson is the model able to fit the experimental data with an error of less than 12%, when the reactor was charged wth 50g. At this purpose, the LHHW could be considered as an adequate kinetic law that should be use, as future perspective, to define the process scale-up.

SECTION C

Abstract **Partial Oxidative** **Reforming (OPR)**

The aim of this section is to provide the research motivation, the background of ethanol reforming reactions, the catalyst selection, the research methodology, and objectives. The catalytic generation of hydrogen by ethanol decomposition and oxidative reforming over copper-chromite and copper-zinc catalyst supported on alumina has been investigated. The catalysts have been prepared by the innovative method of combustion synthesis, characterized by a fast heating rate and a short reaction time, leading to increase catalyst porosity. The catalytic activity and selectivity have been investigated without O₂ and under various O₂ and C₂H₅OH molar ratio in the temperature range up to 500°C. It was found that copper chromite supported on alumina shows the best activity and hydrogen selectivity during ethanol decomposition. The selectivity decreased during oxidative reforming but with a low O₂/EtOH=0.6 molar ratio at 300°C, a hydrogen rich mixture (35-40%) was obtained. The use of relatively low amount of oxygen is necessary to reduce the coke formation, which causes catalyst deactivation. The catalysts were characterized by ex-situ methods such as XRD, BET, XPS, and in-situ EXAFS and FTIR with the aim to evaluate their physic-chemical properties and to correlate the obtained results with the catalysts performance.

SECTION C

Chapter 1

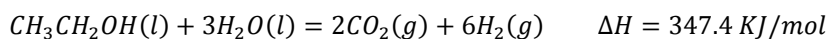
Background info

Literature Review

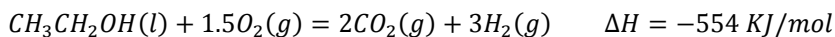
C-1.1 Introduction

Energy is one of the main factors that must be taken in account when sustainable development of our society is envisioned because there is an intimate connection between energy, the environment and development. In response to the need for cleaner and more efficient energy technologies, a number of alternatives to the current energy network have emerged. In recent years, hydrogen production from hydrogen bearing molecules has been a topic of growing research interest for its potential application in fuel cells. Hydrogen can be produced by electrolysis of water using Hoffman's apparatus, steam reforming of natural gas and other fossil fuels, as off-gases from petroleum refinery operations, and by steam reforming of methanol or ethanol. Ethanol is the only renewable source of hydrogen since it can be produced from biomass by fermentation process. This is a promising advance in the production of electrical energy from chemical energy, since the efficiency of a fuel cell is much higher than that of a combustion engine. The main technologies, devoted to the efficiently production of hydrogen from ethanol, are:

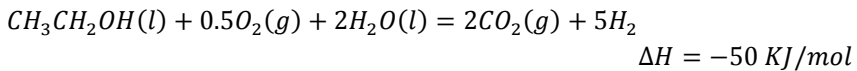
1. steam-reforming (SR)



2. oxidative steam reforming (OSR)



3. partial oxidation (PO)



While SR has been extensively studied [1-8], there are few studies in the open literature that focus on the POX [9-12] and OSR [13-16] reactions. All these technologies face one common drawback: several reaction pathways may occur depending on the reaction conditions and catalyst used. Commonly, some of these reactions lead to the formation of coke, which can in turn induce catalyst deactivation.

The choosing of an optimal phase, support with specific characteristics and of the best operative condition is fundamental to optimize the hydrogen productivity. In the next paragraph the main peculiarities and the commonly active phases used for each of the mentioned processes have been reported.

C-1.2 Ethanol steam reforming

The main research effort on hydrogen production from bio-ethanol was focused, in the last decade, on SR reaction giving the highest yield in hydrogen. This reaction was studied in details and many information can be achieved by the literature [17].

The reaction pathways and thermodynamics of this reaction were studied by several authors [6, 18-21]. The possible reaction pathways proposed of ethanol steam reforming are summarized in Table 1. It can be seen that hydrogen production differs significantly with different reaction pathways. In order to maximize hydrogen production, it is crucial to ensure sufficient supply of steam and to minimize ethanol dehydration and decomposition.

Table 1: Reaction pathways of ethanol steam reforming

Reaction	Equation	Remarks
Sufficient steam supply	$C_2H_5OH + 3H_2O \rightarrow 2CO_2 + 6H_2$	Ideal pathway, the highest hydrogen production
Insufficient steam supply	$C_2H_5OH + H_2O \rightarrow 2CO + 4H_2$ $C_2H_5OH + 2H_2 \rightarrow 2CH_4 + H_2O$	Undesirable products, lower hydrogen production
Dehydrogenation	$C_2H_5OH \rightarrow C_2H_4O + H_2$	Reaction pathways for hydrogen production in practice
Acetaldehyde decomposition	$C_2H_4O \rightarrow CH_4 + CO$	
Acetaldehyde steam reforming	$C_2H_4O + H_2O \rightarrow 3H_2 + 2CO$	Undesired pathway, main source of coke formation
Dehydration	$C_2H_5OH \rightarrow C_2H_4 + H_2O$	
Coke formation	$C_2H_4 \rightarrow \text{polymeric deposits (coke)}$	Coke formation, low hydrogen production
Decomposition	$C_2H_5OH \rightarrow CO + CH_4 + H_2$ $2C_2H_5OH \rightarrow C_3H_6O + CO + 3H_2$ $C_2H_5OH \rightarrow 0.5CO_2 + 1.5CH_4$	
Reaction of decomposition products		
Methanation	$CO + 3H_2 \rightarrow CH_4 + H_2O$ $CO_2 + 4H_2 \rightarrow CH_4 + 2H_2O$	
Methane decomposition	$CH_4 \rightarrow 2H_2 + C$	
Boudouard reaction	$2CO \rightarrow CO_2 + C$	
Water gas shift reaction (WGSR)	$CO + H_2O \rightarrow CO_2 + H_2$	Reduce coke formation, enhance hydrogen production

The literature surveys presented above reveal that the ethanol conversion and selectivity to hydrogen highly depend by the type of metal catalyst used, type of precursors, preparation methods, type of catalyst support, presence of additives, and operating conditions, i.e. water/ethanol molar ratio and temperature. In particular, the catalysts play a crucial role in the reactivity toward complete conversion of ethanol. However, each catalyst induces different pathways and, therefore, the selection of a suitable catalyst plays active role in ethanol steam reforming for hydrogen production. The catalysts should maximize hydrogen selectivity and inhibit coke formation as well as CO production. For ethanol steam reforming, different metals (Ni [22], Co [23,24], Ni–Cu [25], Pt, Pd, Rh [26–28]) deposited on oxide support (Al_2O_3 , La_2O_3 , ZnO, MgO) have been investigated. Noble metal catalysts are well known for their high catalytic activities.

C-1.2.1 Noble metal catalysts

For ethanol steam reforming, Rh, Ru, Pd, and Pt have been extensively investigated. Liguras et al. [28] compared the catalytic performance of

Rh, Ru, Pt, and Pd catalysts at 873–1123K with metal loading of 0–5 wt%. Rh showed the best catalytic performance in terms of ethanol conversion and hydrogen production. Although inactive at low loading, Ru showed comparable catalytic activity with Rh at high loading. The Ru/Al₂O₃ with 5 wt% loading could completely convert ethanol into syngas with hydrogen selectivity above 95%. High dispersion of catalyst atom at the support surface was found to enhance the activity of catalysts. The selection of support played an important role in long-term catalyst operation. Acidic supports, i.e. Al₂O₃, induced ethanol dehydration to produce ethylene, which was a source of coke formation (see Table 1). Dehydration can be depressed by adding K to neutralize the acidic support, or by using basic supports, i.e. La₂O₃ and MgO. About 15% degradation in ethanol conversion was detected for Ru/Al₂O₃ with 5wt% after operation for 100 h. For comparison, Rh/Al₂O₃ with 5 wt% loading was found to degrade considerably after operation for 100 h [29].

Another study conducted by Cavallaro [29] showed that coke formation could be greatly inhibited by operating ethanol steam reforming at high temperature (923 K) with sufficiently high Rh loading (5 wt%) and high steam/ethanol molar ratio (8.4:1). Frusteri et al. [30] evaluated catalytic performance of MgO supported Pd, Rh, Ni, and Co for hydrogen production by ethanol steam reforming. Rh/MgO showed the best performance in terms of ethanol conversion and stability, while Ni/MgO exhibited the highest hydrogen selectivity (>95%). Coke formation rate on Rh/MgO was very low as MgO was basic. It was also found that the deactivation was mainly due to metal sintering. In a recent study by Erdohelyi et al. [7], ethanol steam reforming effects on Al₂O₃ and CeO₂-supported noble metal catalysts, i.e. Pt, Ir, Pd, Rh, and Ru, were compared. By analyzing the surface species in ethanol adsorption on the supported catalysts, it was found that water enhanced the stability of ethoxide surface species, which were formed

during the dissociation process of ethanol. Consistent with previous studies, ethylene produced by dehydration of ethanol was observed on Al_2O_3 -supported noble metal catalysts. For comparison, acetaldehyde derived by dehydrogenation of ethanol was detected on CeO_2 -supported catalysts. In addition, hydrogen formation was found to decrease with time on CeO_2 -supported noble metal catalysts due to the inhibiting effect of surface acetate species formed on the support. This study was very useful as detailed analysis of surface species formed during the adsorption and reaction of ethanol was conducted, providing a better understanding on how chemical reaction proceeded on catalyst surfaces. Depositing Rh on MgAl-based spinel oxide supports exhibited higher basicity, compared with alumina-supported Rh, whereas the surface acidity was strongly reduced, resulting in improved stability [31]. In Ni–Rh bimetallic catalyst supported on CeO_2 , the addition of Ni was found to improve dispersion of Rh particles, leading to higher catalytic activity. In addition, smaller crystals of CeO_2 support could enhance Rh– CeO_2 interaction [32]. Unlike Rh, co-deposition of Pd and Zn on ZnO support led to formation of PdZn alloy, which favored dehydrogenation and hydrogen production [33].

It can be seen that Rh is generally more effective than other noble metals, such as Pt, Pd, and Au, for hydrogen production by ethanol steam reforming. At high temperature and high catalyst loading, Ru shows comparable performance with that of Rh. CeO_2 , MgO, and La_2O_3 are suitable supports for efficient ethanol reforming on Rh. The use of Al_2O_3 as support shows significant deactivation of catalyst after long-term operation. In terms of long-term stability, MgO exhibits the best performance. It is also expected that La_2O_3 may be a suitable support for Rh for stable ethanol steam reforming. So far, the development of catalyst for ethanol reforming is basically a trial-and-error approach. Detailed analyses of reactant species, intermediate product species, and final product species are lacking. Therefore, the working mecha-

nisms have not been fully understood yet. In addition, comparative long-term tests are required for practical applications.

C-1.2.2 Non Noble metal catalysts

Apart from noble metal catalysts, non-noble metal catalysts have also been used for ethanol steam reforming. Some selected studies on ethanol steam reforming over non-noble metal catalysts are summarized reported in literature [34,35]. Nickel is widely used as a low-cost non-noble metal catalyst in industry for a number of chemical reaction processes. For ethanol reforming, Ni also works well as it favors C–C rupture. Sun et al. [36] compared the catalytic activity of Ni/Y₂O₃, Ni/La₂O₃, and Ni/Al₂O₃ for hydrogen production by ethanol steam reforming. The catalysts were prepared using nickel oxalate as precursor and by impregnation–decomposition–reduced method. Operating at ambient pressure and at 593 K, conversion of ethanol using Ni/Y₂O₃ and Ni/La₂O₃ was 93.1% and 99.5%, respectively, while the selectivity of hydrogen was 53.2% and 48.5%, respectively. The high activity and stability of Ni/La₂O₃ were due to formation of a lanthanum oxycarbonate species (La₂O₂CO₃), which could react with surface carbon deposited during reaction to prevent deactivation of catalyst. For comparison, selectivity of hydrogen for Ni/Al₂O₃ catalyst reached the maximum of 47.7% at 573 K. The reported selectivity of hydrogen was relatively low, probably due to the low water/ethanol molar ratio used (3:1). It was demonstrated that increasing water/ethanol molar ratio could significantly increase selectivity of hydrogen [37]. Besides La₂O₃ and Al₂O₃, other oxides have also been studied as alternative supports for Ni catalyst. Yang et al. [38] evaluated the effect of support on ethanol steam reforming over Ni-based catalyst. At 923 K and with Ni loading of 10 wt%, almost 100% conversion of ethanol was attained for all catalyst. Selectivity to hydrogen was found in the following decreasing order: Ni/ZnO ≈ Ni/La₂O₃ > Ni/MgO > Ni/Al₂O₃. Frusteri et al.

[39] evaluated the effects of alkali addition (Li, Na, and K) on catalytic performance of Ni/MgO. The addition of Li and K was found to enhance the catalyst stability by depressing Ni sintering. The coke formation at Ni/CeO₂ was much faster than that on Ni/MgO [40]. This observation could be explained by strong interaction of the CeO₂ support with the adsorbed reaction intermediate species. Their tests also demonstrated that the basic nature of MgO favored ethanol reforming and inhibited coke formation. Akande et al. [34] investigated the effects of catalyst synthesis method, Ni loading, and temperature on the catalytic activity of Ni/Al₂O₃ catalysts for ethanol reforming. In their study, water/ethanol molar ratio of 13:1 was used, representing the actual composition of bio-ethanol produced by fermentation of biomass. Three types of preparation methods, namely, coprecipitation, precipitation, and impregnation, were evaluated. Optimal Ni loading of 15% was found for maximum ethanol conversion using Ni/Al₂O₃ catalyst prepared by coprecipitation and precipitation methods. For comparison, Ni loading did not show noticeable effect on Ni/Al₂O₃ activity when impregnation method was used. Regarding hydrogen production, the catalyst prepared by coprecipitation with Ni loading of 15% showed the best performance. In addition, Ni/Al₂O₃ prepared by coprecipitation also showed the highest selectivity of hydrogen.

In addition also the copper contributes in the reaction in exam was matter of investigation. Marino et al. [41] studied catalytic activity of CuNiK/Al₂O₃ catalysts. Ethanol dehydrogenation and C–C bond rupture were favored by Cu and Ni, respectively. In addition, K neutralized acidic sites of Al₂O₃, reducing the possibility of coke formation. A series of Cu–Ni–Zn–Al mixed oxide catalysts were prepared by the thermal decomposition of Cu_{1-x}Ni_xZnAl hydrotalcite-like precursors for ethanol steam reforming [42]. The use of a bi-metallic catalyst can have two concomitant effects. In fact, the addition of Cu species facilitated dehydrogenation of ethanol to acetaldehyde, while the presence of Ni

led to C–C bond rupture. Cobalt (Co) is another non-noble metal catalyst under extensive investigation as supported Co could break C–C bond [43]. The selectivity of H₂ decreased in the order: Co/Al₂O₃ > Co/ZrO₂ > Co/MgO > Co/SiO₂ > Co/C. Due to the basic characteristics of MgO, Co/MgO was more resistant to coke formation than that of Co/Al₂O₃ at 923 K [44]. The use of Co₂(CO)₈ as precursor produced a catalyst that was highly active (100% ethanol conversion) and selective (about 73%) toward CO-free hydrogen production by ethanol steam reforming at 623 K. Long term tests (75 h) demonstrated the stability and applicability of Co/ZnO as an active catalyst for ethanol steam reforming. In a study conducted by Batista et al. [45], Co/Al₂O₃ (8.6 wt%), Co/SiO₂ (7.8 wt%), and Co/MgO (18.0 wt%), prepared by impregnation method, all showed high catalytic activity (>90% ethanol conversion) and selectivity to hydrogen (about 70%). However, after 9 h of steam reforming at 673 K, coke formation on the catalysts were detected in the following decreasing order: Co/Al₂O₃ (24.6 wt% coke) > Co/MgO (17.0 wt% coke) > Co/SiO₂ (14.2 wt% coke). The highest coke formation on alumina was ascribed to the acidic character of alumina, which favored ethanol dehydration to ethylene. Their subsequent study showed that CO in the outlet gas stream could be reduced by increasing the cobalt content [24].

Jordi et al. [46] performed their investigation on Co/ZnO catalyst using a water to ethanol molar ratio of 13:1 (20% v/v ethanol), whereas Leclerc et al. [47] reported that water to ethanol ratios in the range of 20:1 (14%v/v ethanol) to 30:1 (10%v/v ethanol) enhanced hydrogen selectivity and inhibited the production of undesirable product such as methane (CH₄), carbon monoxide (CO), acetaldehyde, ethylene and carbon. By this examination emerges that among all catalysts tested, Rh and Ni exhibited the best activity of ethanol conversion and selectivity to hydrogen. Studies have shown that ethanol is adsorbed on Rh and Ni metals surface as ethoxide species, which forms an oxametal-

lacycle intermediate and favors C–C bond rupture [48,49]. Compared with other noble catalysts, such as Pt, Pd, and Ru, Rh is more active and selective toward hydrogen. For comparison, Pt promotes water gas shift reaction, but its activity for C–C rupture is limited. It is therefore anticipated that hydrogen production could be enhanced by using Rh–Pt bi-metallic catalysts or by passing the reactants with excessive water content through supported Rh catalyst and Pt catalyst, respectively. In addition, at high metal loading, the performance of Ru-based catalyst is comparable to Rh for hydrogen production by ethanol steam reforming. However, Ru also induces dehydration of ethanol to form ethylene, leading to coke formation via polymerization. Suitable promoters/additives should be added to prevent coke formation for effective and stable operation. Aside from noble metals, Ni is so far the best choice for hydrogen production by catalytic steam reforming of ethanol. Ni has high activity for C–C bond and O–H bond breaking and also has high activity for hydrogenation, facilitating H atoms to form molecular H₂. Addition of alkali species could modify the interaction between adsorbed species and the metal Ni, further enhancing its steam reforming activity. However, like Rh, Ni is less active for WGSR. Since Cu favors dehydrogenation and WGSR, the combination of Ni and Cu shows high steam reforming activity and high selectivity to hydrogen [44]. In addition, mixing Cu with noble metal, such as Rh may also improve hydrogen production due to enhanced WGSR by Cu. Like other catalysts, Ni-based catalysts also suffer from coke formation as well as metal sintering, leading to considerable performance degradation during long-term operation. As Ni is more economical than noble metal catalyst, research on Ni catalyst development will be fruitful. Supports also play important roles in steam reforming of ethanol, as supports help in the dispersion of metal catalyst and may enhance metal catalyst activity via metal-support interactions. Supports may promote migration of OH group toward the metal catalyst in the pres-

ence of water at high temperature, facilitating steam reforming reactions [12]. Al_2O_3 is widely used as a support in methanol steam reforming and has also been tested for steam reforming of ethanol. However, due to its acidic nature, Al_2O_3 induces dehydration of ethanol, leading to coke formation. Addition of alkali species can improve catalyst stability as its acidity can be partly neutralized. For comparison, MgO , ZnO , and CeO_2 are basic. Thus, their use as support can significantly inhibit ethanol dehydration, greatly reducing coke formation. Catalyst supports not only can affect reaction pathways, but also can affect metal dispersion and inhibit metal sintering. La_2O_3 is also a good support as La_2O_3 promotes dehydrogenation and does not induce coke formation. Therefore, MgO , ZnO , CeO_2 , and La_2O_3 are suitable support materials for ethanol steam reforming. As have been mentioned, catalyst precursors and preparation methods also affect the catalytic performance of catalyst. Use of different precursors and under different preparation conditions can result in variance of catalyst phase, surface area, particle size, surface dispersion, purity, and catalyst-support interaction [50]. As research on the comparison of precursors and preparation methods are limited, it is worthy of future research for the optimization of catalyst preparation procedures. The obstacles for stable operation of ethanol steam reforming are mainly coke formation and metal sintering. From previous reaction path analysis, coke formation is mainly caused by Boudouard reaction, polymerization of ethylene, or by decomposition of methane formed during ethanol steam reforming. Coke can destroy catalyst structure and occupy catalyst surface, thus considerably reduce catalyst activity. Coke formation is faster on acidic support as dehydration occurs. This adverse effect can be reduced by using basic oxide as support or adding alkali species onto the acidic support. Recently, novel concept of double bed reactor was proposed to improve catalyst stability [51]. In this proposed system, bio-ethanol passes through the first layer (Cu catalyst) at 573–673K to

perform dehydrogenation to acetaldehyde and hydrogen, followed by acetaldehyde steam reforming or decomposition. Ethylene formation can be prevented at 573–673 K, thus reduce the possibility of coke formation. The intermediate species are then passed through the second layer (Ni-based catalyst) to enhance hydrogen production. Although this concept remains to be demonstrated, it offers an economical method to enhance hydrogen production and catalyst stability. Besides, bi-metallic catalysts or alloy catalysts can also improve catalyst stability and enhance hydrogen production due to the interaction of the metals. Besides the rapid catalyst deactivation, another significantly drawback of the steam reforming reaction is the need of external energy supply for balancing reaction endothermicity [30,52]. In fact the steam reforming is an endothermic process in the absence of oxygen gas and requires energy input to initiate reactions.

C-1.3 Ethanol reforming and partial oxidation

The catalytic decompositions/reforming of alcohols have gained particular interest due to growing environmental, economic, and political concerns regarding energy production. Safe and efficient in situ hydrogen generation from alcohols (i.e. methanol, ethanol, propanol, butanol) can promote the use of fuel cells and other clean technologies as a source of energy for mobile applications. Alcohols can serve as H₂ carriers that are compatible with current infrastructures for liquid fuels and can be catalytically converted on-site in order to minimize energy input requirements and operating temperatures. Cavallaro and Freni [53] studied the ethanol reforming with mixed oxide catalyst CuO/ZnO/Al₂O₃, showing that the main products CO, CO₂ and H₂ are formed above 350 °C. Copper supported on alumina was studied in the ethanol reforming, showing that copper promoted a rapid dehydrogenation of ethanol to acetic aldehyde, while nickel favored the rup-

ture of carbon-carbon bonds of ethanol, with formation of methane and carbon monoxide [54].

Ethanol decomposition by reaction 1 and 2 is another reaction pathway for hydrogen generation from ethanol.



Relatively less literature is available for this reaction as compared to ethanol steam reforming and partial oxidation. Xu et al. [55] reports that decomposition of ethanol over Ni(1 1 1) proceeds by O–H bond cleavage and formation of ethoxy species on the catalytic surface.

Ethanol desorption and decomposition studies on a Rh (1 1 1) surface shows that ethanol decomposition occurs simultaneously with ethanol desorption. The decomposed ethanol leaves H and CO on the surface which desorbs at higher temperature to produce H₂ and CO. Catalytic decomposition of ethanol on a Cu/Al layered double hydroxide (LDH) catalyst was investigated at temperatures between 150–400 °C and atmospheric pressure [56]. Catalytic generation of H₂ starts at 200–300 °C along with the formation of aldehyde. Ethanol conversion of 60% was observed at 400 °C. These authors also reported that Cu/Al LDH undergoes some physical modification and produce highly dispersed metallic Cu, which could be the active phase in this catalyst. Ir(1 1 1) [57] has also been reported to be active for ethanol decomposition. The activity of supported Pd catalysts such as: Pd/ZnO, Pd/Ga₂O₃, Pd/In₂O₃, Pd/MgO, Pd/SiO₂, Pd/Al₂O₃, Pd-black along with Cu/Zn [58], were studied for the decomposition reaction. The activities of such supported Pd catalysts were greatly modified upon the formation of Pd alloy phases. Over Pd–Zn, Pd–Ga and Pd–In alloys, acetaldehyde was selectively produced at lower conversion levels. As conversion increased, ethyl acetate was produced at the expense of acetaldehyde. The selectivity for the ethyl acetate formation exceeded that of acetaldehyde over a Cu/ZnO catalyst. On metallic Pd, the de-

composition of ethanol occurred to a considerable extent. The main problem associated with the ethanol decomposition reaction on this catalyst, however, was the formation of coke at high temperatures. Based on the above literature survey it is clear that, excluding noble metals, Ni, Fe and Cu are the most frequently studied. Kumar et al. have shown the performances of Ni, Fe, and Cu based catalysts synthesized in different molar ratios using solution combustion synthesis technique. In particular among the catalysts studied $\text{Ni}_1\text{Fe}_{0.5}\text{Cu}_1$ was selected based on its activity and hydrogen selectivity for detailed studies. It was found that these catalysts are active and hydrogen selective for the ethanol decomposition reaction. Carbon formation was observed at high temperature, which slightly affects the catalyst performance. Adding oxygen to the feed reduces carbon content but it also decreases the hydrogen selectivity. Ni was found to be most active at lower temperature and selective for hydrogen and methane, Cu was selective for acetaldehyde and Fe was selective for CO_2 and ethane. Hydrogen selectivity was found to be highest for Fe at high temperature. The ethanol decomposition reaction appears to proceed through the formation of alkoxy species that decompose at higher temperatures. Further work is underway – to understand the mechanism of ethanol decomposition and partial oxidation as well as the role of different metals used in this work. The main drawback is the low hydrogen selectivity of ethanol partial oxidation. In order to enhance hydrogen production, auto-thermal reforming can be applied.

C-1.4 Ethanol oxidative steam reforming

Auto-thermal reforming, also called oxidative steam reforming, is a combination of ethanol oxidation and steam reforming [19]. Under auto-thermal steam reforming conditions, which are produced by introducing oxygen in the reaction mixture, is possible to operate with a more favorable energetic balance. In fact, the reaction is more effec-

tive and energy efficient, despite a slightly lower hydrogen yield [32]. The research is now under way to develop catalysts that control the oxidation process through the combining of catalytic partial oxidation and steam reforming of ethanol. The auto-thermal reforming not only attains thermally sustained operation, but also maximizes hydrogen production. As well known, the oxidizing environment reduces the carbon poisoning of the catalyst and could promote the decomposition of intermediate molecules such as ethylene and acetaldehyde. On the other hand, an excess of oxygen leads to a strong reduction of hydrogen as reaction product. In this respect, studies under partial oxidation conditions could contribute to a better knowledge of auto-thermal ethanol steam reforming. Generally, the ethanol conversion and hydrogen selectivity by auto-thermal reforming of ethanol vary greatly with the type of catalyst, support and oxygen/steam/ethanol molar ratios. Auto-thermal reforming is advantageous as coke formation is greatly inhibited by oxidation. Thus, long-term stable operation can be achieved. As reported by Raminet al [60], some studies on catalytic behavior of Ni, Pt- and Ru-based catalysts have recently been reported. In autothermal conditions, reports concerned the use of Ni and Cu catalysts and promoted noble metals supported on highly stable carriers, i.e., Pt-CeO₂-La₂O₃/Al₂O₃, Rh/CeO₂, Rh/Al₂O₃. As demonstrated by Adkim et al. [61] various catalysts based on noble (Rh) and not noble (Ni–Cu) metal supported over neutral (SiO₂) and amphoteric (Al₂O₃) supports, respectively, lead to stable and highly performing systems [62].

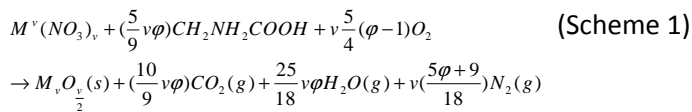
Deluga et al [63] shown the performances of several noble metals (Ni, Ru, Rh, Pt, and Pd) and metals with additives as cerium oxide, lanthanum oxide, and magnesium oxide as catalysts for this reaction. All were deposited from salt solutions on low-area alumina foams or alumina spheres. As demonstrated by the mentioned work only Rh-ceria was more stable and gave greater WGS activity than noble metals

alone. The main role of promoters is associated, in this case to metal-promoter interactions [27], which affect the adsorption-decomposition of ethanol to CH_4 and CO and their subsequent reforming with steam to produce H_2 .

C-1.5 Catalysts preparation

Combustion synthesis (CS) is an attractive technique for materials synthesis on account of being simple, economical, fast and energy efficient process. This simplicity and flexibility to synthesize a wide range of materials has led to an increase interest in using it in diverse areas as indicated by the increase in the publications on CS [64,65]. The conventional solid-solid CS can be broadly classified into two groups based on the way combustion reaction takes place. Combustion reaction can proceed as a self sustained wave front upon local ignition of the reactive pellet or it can be combusted simultaneously all over the volume by a uniform heating. The former method is known as Self-Propagating High-Temperature Synthesis (SHS) and the later as Volume Combustion Synthesis (VCS). Recent innovations have led to the use of CS in other phases as well, namely, flame synthesis (gas phase synthesis) and solution combustion synthesis. Among the above-mentioned methods, combustion synthesis in solution or SCS, due to its ability to produce nano-materials, recently gained research attention and it is being applied to diverse areas such as pigments, catalysis, electronic and magnetic materials, drug delivery etc [66]. SCS is considered as a redox reaction consisting of oxidizing agents (e.g. metal nitrates) and reducing agents (e.g. glycine, urea, hydrazine etc), also known as fuel. The exothermic reaction between metal nitrates and the fuel provide the energy required for sustaining the combustion synthesis reaction without adding external energy. Furthermore, the energy released is high enough to evaporate volatile compounds and calcine the products formed leading to the formation of crystalline phases. Because

the combustion reaction rate is very high, the crystallites formed do not have sufficient time to sinter, leading to the formation of nanopowders with higher surface areas compared to conventional synthesis. Thus SCS yields highly pure and crystalline material synthesized in a single step without requiring any further thermal treatments. The CS reaction between metal nitrates and glycine, used as fuel, can be represented by the following widely accepted scheme 1:



where M^v is a v -valent metal. The parameter ϕ , fuel to oxidizer ratio, is defined such that $\phi = 1$ corresponds to a stoichiometric oxygen concentration, meaning that the initial mixture does not require atmospheric oxygen for complete oxidation of the fuel, while $\phi > 1$ (<1) implies fuel-rich (or lean) conditions.

According to the above scheme, (Eq. 1), SCS can be used for the synthesis of metal oxides. Recent publications from our group [67-70] demonstrated the capability of using SCS to synthesize reduced metals nano-powders (e.g. Ni, Cu rather than their oxides NiO, CuO) as well. A reaction pathway was proposed to describe the controlled synthesis of different phases using impregnated layer combustion synthesis (ILCS). In the latter case, the active solution containing metal nitrate and glycine was impregnated on a thin media (e.g. cellulose paper, carbon nano-tubes or graphite sheet etc.) before combustion to facilitate the cooling of the products obtained after CS [71-73]. This faster cooling and unique microstructure of the products result in finer particles with high surface area particularly suitable for catalytic applications as indicated by experiments and model studies [9, 10]. This study complements our previous work on the synthesis and activity studies of multicomponent Ni/Fe/Cu based catalyst for hydrogen production from ethanol using SCS [74] which showed, $Ni_1Fe_{0.5}Cu_1$ to be the optimum

catalyst composition for hydrogen production from ethanol partial oxidation and decomposition reactions. As stated earlier, SCS has numerous advantages over other catalyst preparation methods such as co-precipitation, which require separation of the products after precipitation and then their calcination which may lead to sintering thus influencing the total surface area adversely. As indicated by scheme (1), except for the metal oxide product, all other products are gas phase products, which can be controlled by varying the parameter ϕ . The released gases form micro-channels on the solid as they are released during reaction thus contributing towards the porosity of the material synthesized potentially leading to high surface area.

1.3 References

- [1] P.D. Vaidya, A.E. Rodrigues, *Ind. Eng. Chem. Res.* 45 (2006) 6614.
- [2] A. Haryanto, S. Fernando, N. Murali, S. Adhikari, *Energy Fuels* 19 (2005) 2098.
- [3] H. Song, L. Zhang, R.B. Watson, D. Braden, U.S. Ozkan, *Catal. Today* 129 (2007)346.
- [4] R.M. Navarro, M.C. Alvarez-Galvan, M.C. Sanchez-Sanchez, F. Rosa, J.L.G. Fierro, *Appl. Catal. B* 55 (2004) 223.
- [5] M. Veronica, B. Graciela, A. Norma, L. Miguel, *Chem. Eng. J.* 138 (2008) 602.
- [6] A.N. Fatsikostas, X.E. Verykios, *J. Catal.* 225 (2004) 439.
- [7] A. Erdohelyi, J. Raskó, T. Kecskés, M. Tóth, M. Dömök, K. Baán, *Catal. Today* 116 (2006) 367.
- [8] V. Fierro, V. Klouz, O. Akdim, C. Mirodatos, *Catal. Today* 75 (2002) 141.
- [9] L.V. Mattos, F.B. Noronha, *J. Power Sources* 145 (2005) 10.
- [10] L.V. Mattos, F.B. Noronha, *J. Power Sources* 152 (2005) 50.
- [11] L.V. Mattos, F.B. Noronha, *J. Catal.* 233 (2005) 453.
- [12] J.L. Bi, S.N. Hsu, C.T. Yeh, C.B. Wang, *Catal. Today* 129 (2007) 330.
- [13] J. Kugai, S. Velu, C. Song, *Catal. Lett.* 101 (2005) 255.

- [14] V. Fierro, O. Akidim, C. Mirodatos, *Green Chem.* 5 (2003) 20.
- [15] S.M. de Lima, I.O. da Cruz, G. Jacobs, B.H. Davis, L.V. Mattos, F.B. Noronha, *J.Catal.* 257 (2008) 356.
- [16] E.B. Pereira, N. Homs, S. Marti, J.L.G. Fierro, P.R. de la Piscina, *J. Catal.* 257(2008) 206
- [17] M. Ni et al. / *International Journal of Hydrogen Energy* 32 (2007) 3238–3247]
- [18] Freni S, Maggio G, Cavallaro S. Ethanol steam reforming in a molten carbonate fuel cell: a thermodynamic approach. *J Power Sources* 1996; 62:67–73.
- [19] Ioannides T. Thermodynamic analysis of ethanol processes for fuel cell applications. *J Power Sources* 2001;92:17–25.
- [20] Benito M, Sanz JL, Isabel R, Padilla R, Arjona R, Daza L. Bio-ethanol steam reforming: insights on the mechanism for hydrogen production. *J Power Sources* 2005; 151:11–7.
- [21] Vaidya PD, Rodrigues AE. Insights into steam reforming of ethanol to produce hydrogen for fuel cells. *Chem Eng J* 2006;117:39–49.
- [22] Fatsikostas AN, Kondarides DI, Verykios XE (2002) *Catal Today* 75:145
- [23] Llorca J, Homs N, Sales J (2002) *J Catal* 209:306
- [24] Batista MS, Santos RKS, Assaf EM, Assaf JM, Ticianelli EA (2004) *J Power Sources* 134:27
- [25] Marino F, Boveri M, Baronetti G, Laborde M (2001) *Int J Hydrogen Energy* 26:665
- [26] Breen JP, Burch R, Coleman HM (2002) *Appl Catal B* 39:65
- [27] Navarro RM, Álvarez-Galván MC, Cruz Sánchez-Sánchez M, Rosa F, Fierro JLG (2005) *Appl Catal B* 55:229
- [28] Liguras DK, Kondarides DI, Verykios XE (2003) *Appl Catal B* 43:34512.
- [29] 16] Cavallaro S. Ethanol steam reforming on Rh/Al₂O₃ catalysts. *Energy Fuels* 2000;14:1195–9.
- [30] Frusteri F, Freni S, Spadaro L, Chiodo V, Bonura G, Donato S. et al. H₂ production for MC fuel cell by steam reforming of ethanol over MgO supported Pd, Rh, Ni and Co catalysts. *Catal Commun* 2004;5:611–5.
- [31] Aupretre F, Descorme C, Duprez D, Casanave D, Uzio D. Ethanol steam reforming over Mg_xNi_{1-x}Al₂O₃ spinel oxide-supported Rh catalysts.

J Catal 2005;233:464–77.

[31] Kugai J, Subramani V, Song C, Engelhard MH, Chin YH. Effects of nano-crystalline CeO₂ supports on the properties and performance of Ni–Rh bimetallic catalyst for oxidative steam reforming of ethanol. J Catal 2006;238:430–40.

[32] Casanovas A, Llorca J, Homs N, Fierro JL, de la Piscina PR. Ethanol reforming processes over ZnO-supported palladium catalysts: effect of alloy formation. J Mol Catal A Chem 2006;250:44–9.

[33] Akande AJ, Idem RO, Dalai AK. Appl Cat A Gen 2005;287:159–75.

[34] Aboudheir A, Akande AJ, Idem RO, Dalai AK. Int J Hydrogen Energy 2006;31:752–61.

[35] Sun J, Qiu XP, Wu F, Zhu WT. Int J Hydrogen Energy 2005;30:437–45.

[36] Comas J, Marino F, Laborde M, Amadeo N. Chem Eng J 2004;98:61–8.

[37] Yang Y, Ma JX, Wu F. Int J Hydrogen Energy 2006;31:877–82.

[38] Frusteri F, Freni S, Chiodo V, Spadaro L, Blasi OD, Bonura G, Cavallaro S. Appl Catal A Gen 2004;270:1–7.

[39] Frusteri F, Freni S, Chiodo V, Donato S, Bonura S, Cavallaro S. Int J Hydrogen Energy 2006;31:2193–99.

[40] Marino F, Baronetti G, Jobbagy M, Laborde M. Appl Catal A Gen 2003;238:41–54.

[41] Velu S, Suzuki K, Vijayaraj M, Barman S, Gopinath CS. Appl Catal B Environ 2005;55:287–99

[42] Llorca J, Homs N, Piscina PR. J Catal 2004;227:556–60.

[43] Cavallaro S, Mondello N, Freni S. J Power Sources 2001;102:198–204.

[44] Batista MS, Santos RKS, Assaf EM, Assaf JM, Ticianelli EA. J Power Sources 2003;124:99–103.

[45] Jordi, L., N. Homs, J. Sales and P. Ramirez de la Piscina, Journal of catalysis, 209,306-317 (2002).

[46] Leclerc, S., R.F. Mann and B.A. Peppley, Prepared for the CANMET Energy Technology Centre (CETC), (1998).

[47] Kugai J, Velu S, Song CS. Low-temperature reforming of ethanol over CeO₂-supported Ni–Rh bimetallic catalysts for hydrogen production.

Catal Lett 2005;101:255–64.

[48] Rasko J, Hancz A, Erdohelyi A. Surface species and gas phase products in steam reforming of ethanol on TiO₂ and Rh/TiO₂. Appl Catal A Gen 2004;269:13–25.

[49] Kaddouri A, Mazzocchia C. Catal Commun 2004;5:339–45

[50] Batista MS, Assaf EM, Assaf JM, Ticianelli EA.. Int J Hydrogen Energy 2006;31:1204–9.

[51] M.V. Twigg, M.S. Spencer/ Topics in Catalysis Vol. 22, Nos. 3–4, April 2003.

[52] S. Cavallaro, S. Freni, Int. J. Hydrogen Energy 21 (1996) 465.

[53] F.B. Noronha, M.C. Duraõ, M.S. Batista, L.G. Appel, Catal. Today 85 (2003) 13.

[54] J. Xu, X. Zhang, R. Zenobi, J. Yoshinobu, Z. Xu, J.T. Yates, Surface Science 256 (1991) 288–300.

[55] S.R. Segal, K.A. Carrado, C.L. Marshall, K.B. Anderson, Applied Catalysis A: General 248 (2003) 33–45.

[56] C.J. Weststrate, W. Ludwig, J.W. Bakker, A.C. Gluhoi, B.E. Nieuwenhuys, A European Journal of Chemical Physics and Physical Chemistry 8 (2007) 932–937.

[57] N. Iwasa, O. Yamamoto, R. Tamura, M. Nishikubo, N. Takezawa, Catalysis Letters 62 (1999) 179–184.

[58] Fierro V, Akdim O, Provendier H, Mirodatos C (2005) J Power Sources 145:659

[59] P.Ramirez de la Piscina and Narcis Homs, 2006 by Taylor & Francis Group, LLC

[60] O.Akdim et al.Top Catal (2008) 51:22–38

[61] Fierro V, Akdim O, Mirodatos C (2003) Green Chem 5:20

[62] G. A. Deluga, J. R. Salge, L. D. Schmidt, X. E. Verykios, SCIENCE VOL 303 13 FEBRUARY 2004

[63] S.T. Aruna, A.S. Mukasyan, Current opinion in solid state materials science 12 (2008) 44. A

- [64] K.C. Patil, M.S. Hegde, R. Tanu, S.T. Aruna, Chemistry of Nanocrystalline Oxide Materials: Combustion Synthesis, Properties and Applications, World Scientific Publishing Co. Pte. Ltd, Singapore, 2008.
- [65].G. Merzhanov, I.P. Borovinskaya, A.E. Sytchev, in: J.F. Baumard (Ed.), Lessons in Nanotechnology from Traditional Materials to Advanced Ceramics, Techna Group Srl, Dijon, France, 2005, pp. 1–27.
- [66] C.H. Jung, Journal of nanoparticle research 5 (2003) 383.
- [67] C.H. Jung, Mater Lett 59 (2005) 2426.
- [68] Kumar A., E.E. Wolf, Mukasyan A. S., AIChE Journal (2010 in press).
- [69] A. Kumar, E. Wolf, A. Mukasyan, AIChE J. (2011 in press) .
- [70] A. S. Mukasyan, P. Dinka, Advanced engineering materials 9 (2007) 653.
- [71] KumarA., Mukasyan A. S., Wolf E. E, Applied catalysis.A, General 372 (2010) 175.
- [72]] A. Kumar A.S. Mukasyan, E.E. Wolf, Industrial engineering chemistry research 49 (2010) 11001.
- [73] A. Kumar, A. Mukasyan, E. Wolf, Applied Catalysis A: General (2011) .

SECTION C

Chapter 2

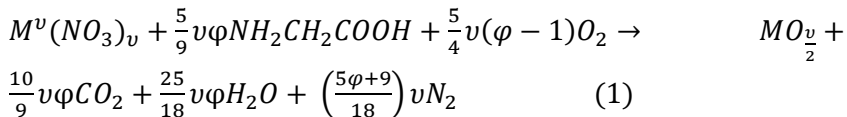
Techniques and equipment

C-2.1 Introduction

This chapter introduces some general aspects related to the catalyst preparation technique, their characterization and to the reaction apparatus of employed to perform the partial oxidative reforming reaction. In this chapter, the innovative combustion synthesis way employed to prepare catalysts composed mainly by copper chromite, unsupported and supported on alumina, and copper-zinc-alumina was proposed. Moreover, a list of the characterization techniques used to describe in details the chemical and textural properties of the examined catalysts have been described. The configuration of the reaction apparatus and of the analytical methodology was also described. Four different catalysts of copper chromite have been prepared. Each catalyst distinguishes itself by other for the compositions, the presence of a support and by the ratio phi, between glycine and oxygen, employed during the preparation. By using the same technique, a catalyst of $\text{Cu/ZnO/Al}_2\text{O}_3$ has been prepared and, its performances, compared with the performances of CuCr series. The copper chromites, prepared by combustion, have been characterized deeply and their performances in ethanol reforming and partial oxidation reforming were studied. At the end of this chapter a comparison of the catalytic performances of the above mentioned system with three different commercial catalysts has been done.

C-2.2 Catalysts Preparation: *the combustion synthesis*

The technique used in this study to prepare the catalysts is the glycine/nitrate powder synthesis, well known as combustion consisted of the following steps. Exothermic mixtures of metal nitrates (Alfa Aesar) $Me(NO_3)_x \cdot yH_2O$ (where $Me = Cu, Zr, Zn, \text{ or } Pd$) and glycine ($C_2H_5NO_2$), the fuel of the reaction, were used to synthesize catalysts by using the volume combustion synthesis (VCS) approach. More specifically, for the VCS method, reactants in desired amounts are dissolved in water and the obtained solution is thoroughly mixed to reach homogenization on the molecular level. After preheating to the 373 K, water evaporates, followed by temperature increase until the self-ignition point $T_{ig} \sim 525$ K. More precisely the solution prepared in a beaker was placed in a hot plate under a hood and then heated slowly to evaporate excess water, which resulted in a viscous liquid layer. At a certain temperature, the viscous layer ignited and underwent self-sustaining combustion, producing an ash composed of the oxide product. In fact after ignition, the temperature rises rapidly ($\sim 103 \text{ K} \cdot \text{s}^{-1}$) up to 1300 K. High temperature, accompanied by intensive gasification ($CO_2, N_2, \text{ steam}$) during a short time period (0.1-1s), converts the initial solution to a fine highly crystallized powder. In general, under equilibrium conditions, the combustion reaction in such systems can be represented in equation 1.



Where Me - is a metal with valence v , ϕ is a fuel to oxidizer ratio where $\phi = 1$ means that the initial mixture does not require atmospheric oxygen for complete oxidation of the fuel, while $\phi > 1$ represents fuel-rich conditions and $\phi < 1$ represents fuel lean

conditions. At first, three different copper chromite catalysts with the same composition, $\text{CuO-Cr}_2\text{O}_3=50:50_{\text{wt}\%}$, were prepared by combustion synthesis of a mixture of copper and chromium nitrates in presence of glycine, using three different fuel oxidizer ratios of $\phi=0.5$ (CuCr-0.5), $\phi=0.8$ (CuCr-0.8) and $\phi=3$ (CuCr-3) and the details about the composition of the mentioned catalysts have been reported in Table 1. The aim of this study is to individuate the best value of ϕ to obtain crystalline phases active and selective in the reaction examined. Once identified the best way to design the catalyst, a copper chromite supported on alumina ($\text{CuCr}_2\text{O}_4: \text{Al}_2\text{O}_3=60:20_{\text{wt}\%}$), indicated with the acronym CuCr/Al, was prepared in two different steps: a support of activated alumina (Sigma-Aldrich Brockmann I, standard grade-150 mesh) was at first impregnated with an aqueous mixture of copper nitrate, chromia nitrate and glycine as fuel ($\phi=0.8$) (see Table 1). The catalyst prepared by impregnation was then heated to realize the combustion reaction. The reaction occurred vigorously and it was undertaken with extreme caution to produce a high yield of catalysts. The performances of all these systems, all characterized by the presence of chromia as promoter, have been compared with the performances of Cu-ZnO- Al_2O_3 ($40:40:20_{\text{wt}\%}$) catalyst, denoted as CuZnAl, prepared in this case by combustion of a mixture of the nitrates of copper, zinc, and aluminum in presence of glycine by using the optimized ratio ϕ of 0.8. The prepared catalysts were sieved to 0.6- 1mm particle size and were previously pre-reduced for 2h in pure hydrogen flow of $50 \text{ cm}^3/\text{min}$, keeping constant the temperature at 300°C . Table 1 summarizes the composition and the preparation ratio of the catalysts studied in this work. In the experimental chapter of this section (chapter 3-section C) the performances of catalysts prepared by combustion synthesis have been compared with the commercial catalytic systems, which the textural and chemical properties and the performances in high pressure dehydrogenation

reaction, has been already studied in deepen in a previously section of this thesis (see Chp.2 section B). In order to facilitate the reading, a summary table (Table 2) of the features of such systems is provided below.

Table 1: catalysts compositions and acronyms

Catalyst	Acronym	Phi	Composition
Cu-ZnO-Al ₂ O ₃	CuZnAl	0.8	CuO-ZnO-Al ₂ O ₃ (40:40:20 b.w.)
CuO-Cr ₂ O ₃	CuCr-0.5	0.5	CuO-Cr ₂ O ₃ (50:50 b.w.)
CuO-Cr ₂ O ₃	CuCr-0.8	0.8	CuO-Cr ₂ O ₃ (50:50 b.w.)
CuO-Cr ₂ O ₃	CuCr-3.0	3.0	CuO-Cr ₂ O ₃ (50:50 b.w.)
CuCr ₂ O ₄ / Al ₂ O ₃	CuCr/Al	0.8	CuCr ₂ O ₄ /Al ₂ O ₃ (60:20 b.w.)

Table 2: characteristics of composition of commercial catalysts supplied by companies BASF and Sud-Chemie.

Catalyst Acronym	Composition given by the companies
BASF K-310	CuO-ZnO-Al ₂ O ₃ (40-40-20 % b.w.)
BASF Cu-1234	CuCr ₂ O ₄ -CuO-Cu-BaCrO ₄ -Al ₂ O ₃ (45-1-13-11-30 % b.w.)
Sud-Chemie T-4466	CuO/CuCr ₂ O ₄ (CuO/Cr ₂ O ₃ = 53/45)

The properties, the performances and the drawbacks of these three different catalysts have been evaluated, compared and discussed in the chapter 3 of this section.

C-2.3 Catalysts characterization

The following chapter contains all techniques and the details of the experimental operative conditions employed in this work. The textural properties of the catalysts prepared by combustion have been studied in detail and the techniques employed to characterize the mentioned materials could be classified in two different categories: ex-situ characterization such as BET, X-ray diffraction (XRD), scanning electron microscopy (SEM) and X-ray Photoelectron Spectroscopy (XPS) and in-situ ones, such as diffuse reflectance infrared fourier transform (DRIFT) in presence of ethanol and X-ray adsorption near edge spectroscopy (XANES).

BET measurements. Surface area measurements were carried out on a Quantachrome Autosorb-1 Instrument using nitrogen as the adsorbent gas. Catalyst particles were first outgassed at 473 K until the differential pressure fell below 20 mmHg/min. The weight of the outgassed sample was precisely measured before calculating the specific surface area. No other pretreatments were carried out prior to BET area measurements.

X-ray diffraction (XRD). A Bruker powders diffractometer was used to obtain XRD patterns were obtained. The scans were collected in the range 5-80° (2θ) at a rate of 0.01° (2θ)/s, using Cu K α radiation. The X-ray tube operated at 10 KV and 50 mA (Appendix A).

X-ray photoelectron spectroscopy (XPS). A Kratos XSAM-800 with an Al-K α X-ray source operating at 1486.6 eV and a 90-degree take-off angle was used for XPS analysis of O 1s, Al 2p, Cr 3d and Cu 2p electronic transitions using a multi-channel detector. Fresh ground in powder catalyst samples were adhered to brass mounts with double-sided carbon tape, prior to loading them into the analysis chamber. Samples were left to degas overnight while the vacuum system maintained a pressure less than $1 \cdot 10^{-8}$ torr. During data processing of the XPS

spectra, binding energy values were referenced to the C 1s peak (284.8 eV) from the adventitious contamination layer. At the end the obtained spectra have been analysed by using the CasaXPS software package with relative sensitivity factors obtained by Kratos library. This technique is useful to estimate the surface concentration of the several elements and their oxidation states using carbon as standard for calibrating the peaks locations (Appendix A).

X-ray adsorption near edge spectroscopy (XANES). Measurements using extended x-ray absorption spectroscopy including x-ray absorption near edge spectroscopy were carried out at the Advanced Photon Source (APS) at Argonne National Laboratory (ANL). The measurements were made in transmission mode with ionization chambers optimized for the maximum current with linear response. The measurements were made in transmission mode with ionization chambers optimized for the maximum current with linear response (~ 1010 photons detected/sec). A cryogenically cooled double-crystal Si (111) monochromator with resolution (ΔE) better than 2.5 eV at 8.979 keV (Cu K edge) was used in conjunction with a Rh-coated mirror to minimize the presence of harmonics. The integration time per data point was 1-3 sec, and three scans were obtained for each processing condition. Standard procedures based on WINXAS97 software were used to extract the XANES spectra. Phase shifts and backscattering amplitudes were obtained from XANES data obtained for the following reference compounds: CuO and Cu₂O for Cu-O and Cu foil for Cu-Cu while Cr₂O₃ and CrO₃ for Cr-O and Cr foil for Cr-Cr.

The sample was pressed into a cylindrical holder with a thickness chosen to give an absorbance ($\Delta\mu x$) of about 1.0 in the Cu edge region. Due to the high density of the Cu based catalysts, the fresh powder was diluted by a factor of 10 with fumed silica prior to being pressed into a wafer. The sample holder was centered in a continuous-flow EXAFS reactor tube 18 inches long and 0.75 inches diameter. The tube

was fitted at both ends with polyimide windows to allow transmission of the x-ray beam with gas valves fitted perpendicular to the tube. The reactor was fitted into a clamshell style electrical furnace, which was controlled and monitored with three type K thermocouples located inside the reactor tube and furnace assembly. This furnace, window, and valve configuration allowed isolation of the reactor from the atmosphere and the ability to flow various reducing, reactant, and oxidizing gas mixtures at elevated temperatures, all while being probed by the x-ray beam, meaning the catalyst under operando reaction conditions could be monitored. The catalysts were studied via XAS spectroscopy under reaction and reducing conditions. Spectrum was first recorded with the catalyst in its untreated state at room temperature (in air). All samples were previously reduced by heating in a reducing atmosphere of pure H₂ to a temperature of 300°C, then scanned after cooling to room temperature. For reaction studies under ethanol decomposition reaction conditions the temperature was changed to the desired set point and a reaction mixture of 2.2 cm³/min of CH₃CH₂OH in He was flowed over the catalyst for 30 minutes. After that the Xanes spectrum was recorded with the aim of evaluating the variation of the oxidation state during the reaction (Appendix A).

Diffuse reflectance infrared Fourier transform spectroscopy (DRIFT)

The DRIFT spectra of ethanol on copper based catalysts were obtained in a Bruker Equinox 55 spectrometer equipped with a DTSG detector and a moving interferometer with a scanner velocity of 2-30 KHz, a Mid-IR source and a beam splitter. For ethanol adsorption experiments, a weighted quantity of catalyst in powder mixed with fumed silica, necessary to prevent the adsorption of radiation by the black powder that characterize our samples, was charged in IR-Cell reactor (Harrick) equipped with a CaF₂ window, with thermostated heaters and heated at inlets and outlet to allow reactants flow into the

cell. The samples were pre-treated in-situ by heating under Helium flow ($25 \text{ cm}^3 \text{ min}^{-1}$), then reduced at 300°C in a flow of 20% H_2 in He for about 1h. The system was rapidly cooled and ethanol flow was introduced in the cell and contacted with the pre-treated sample at three different temperature $100\text{-}200\text{-}300^\circ\text{C}$ and at atmospheric pressure. For each spectrum 128 scans in the range $4000\text{--}370 \text{ cm}^{-1}$ were recorded with a resolution of 4 cm^{-1} (Appendix A). Finally, the powder microstructures of used catalysts were imaged and analyzed using a Bruker Field-Emission SEM (Appendix A).

C-2.4 Catalytic activity

C-2.4.1 Apparatus

The oxidative reforming reaction was conducted in continuous packed bed quartz tubular reactor of 50 cm length, and 10.5 mm ID (see figure 1).

A diagram of the reactor feed system is presented in Figure 1.

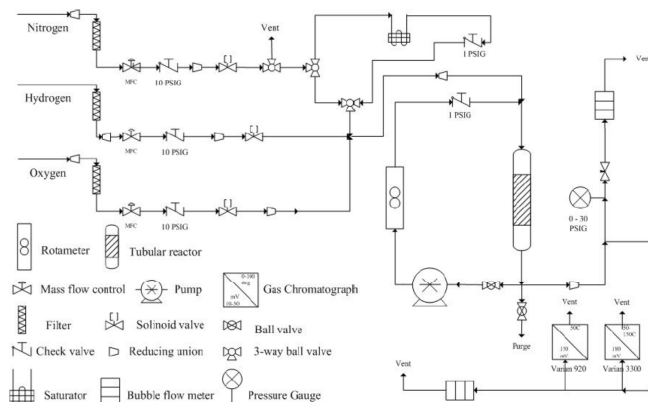


Figure 1: Diagram of the reactor setup used for kinetic evaluations and activity experiments.

Indentations approximately 10 cm from the bottom held a loose plug of fine quartz wool, on top of which the catalytic bed rested. The reactor was thermally heated with a custom made Amptek heating jacket. Reactor temperature was monitored and controlled using a K-type thermocouple placed in the center of the catalyst bed connected to an Omega CN-2100 temperature controller. A low system pressure of less than 0.5 psi was carefully maintained using a bypass and needle valve inside the reactor system to provide constant pressure in the GC sampling system. A picture of the reactor employed is represented in Figure 2.

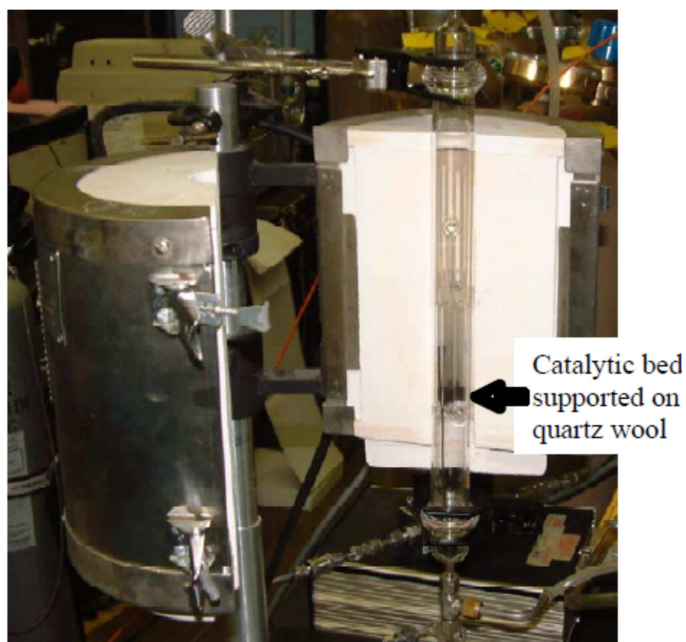


Figure 2: reactor configuration

The reactor was charged with 0.4 g of agglomerated powders of fresh catalyst. Precisely, the catalysts were first pressed at 5000 psi for 4

minutes. The resulting pellet was then broken and sieved to obtain a particle size between 0.6 and 1 mm. A mass of 400 mg sieved catalyst was used in activity experiments supported by quartz wool inside the reactor. The charged catalyst was pre-reduced in situ with a pure hydrogen flow of about $50 \text{ cm}^3 \text{ min}^{-1}$ by heating the catalytic bed from room temperature to 300°C at a rate of $4.5^\circ\text{C}/\text{min}$, the hold time at the final temperature is of about 1h.

The feed system was comprised of four calibrated Brooks 5850 series mass flow controllers, which precisely metered and mixed nitrogen, oxygen, hydrogen, and eventually an auxiliary gas (such as CO_2) if needed to form the reactor feed stream. Gas lines and fittings were (1/8") Swagelok stainless steel. Ethanol was added to the nitrogen stream via an in-line saturator, which saturated the flow to a concentration of 3.7% by volume of ethanol. By-pass valves allowed the saturator to be bypassed for situations when pure nitrogen or mixture of hydrogen in nitrogen was needed.

Then, the hydrogen flow was switched to a nitrogen flow, of about $38 \text{ cm}^3/\text{min}$, to purge the system from traces of hydrogen. The nitrogen passed through a bubbler containing ethanol resulting in a total ethanol flow of about $2.2 \text{ cm}^3 \text{ min}^{-1}$. Oxygen was then added to the ethanol reactant stream to obtain ratios of ($\text{CH}_3\text{CH}_2\text{OH}:\text{O}_2$) 0.6 and 1.5. The reaction was conducted by heating the catalytic bed from room temperature to 500°C in about 4 hours.

C-2.4.2 Gas-chromatographic method

The reaction products were analyzed on line by a gas-cromatograph (HP-5890) equipped with a six ways sampling valve. The separation and identification of the effluent products was realized employing two different gas-chromatographic packed columns connected in series: a 3.7 m Hayesep Q connected to a FID detector for the detection of ethanol, acetaldehyde, methane, carbon dioxide, methane, and a 5 m

Hayesep DB column connected to a thermo-conductivity detector (TCD) to separate nitrogen, hydrogen, oxygen, carbon monoxide. The carrier gas employed is argon at an inlet pressure of about 60 psi. The oven temperature of the gas-chromatograph is kept at 40°C for about 5 min, after that time was increased with a rate of 8°C/min to 120°C for an holding time of 5 min.

Peak positions and detector responses were calibrated using flowing mixtures of gases, such as acetaldehyde, CH₄, CO, CO₂ in nitrogen, at concentrations in the same range as those expected when monitoring reactions. Flow rates of each gas were carefully checked with the use of a bubble flow meter and a stopwatch. Repeated measurements ensured that the flow rate was correct with errors between measurements typically < 1%. Peak areas and retention times were measured at least three times for each gas concentration and at least three different gas concentrations were used to generate a response curve as peak area vs. volume percent gas. Identical procedures were used to calibrate all the reaction products of interest. After an accurate calibration for each system a measure of conversion and selectivity was realized. The ethanol conversion, hydrogen selectivity, carbon dioxide selectivity, and CO byproduct formation were calculated based on the peak area measured with the integrator and peak area response calibration as already described. Ethanol conversion was defined using equation 2 and the hydrogen selectivity by using equation 3.

$$X_{EtOH} = \frac{F_{EtOH\ in} - F_{EtOH\ out}}{F_{EtOH\ in}} \quad (2)$$

$$S_{H_2} = \frac{F_{H_2\ produced}}{3(F_{EtOH\ in} - F_{EtOH\ out})} \quad (3)$$

While, the selectivities to acetaldehyde, methane, ethylene, CO and CO₂ determined on the basis of a carbon balance for each component, are determined as (equation 4):

$$S_i = \frac{\text{mols product}_i \text{ formed}}{n_{\text{EtOH reacted}}} * \frac{nC_i}{nC_{\text{EtOH}}} = \frac{nC_i}{nC_{\text{EtOH}}} \frac{Ac_i}{Ac_{\text{EtOH}}} \left(\frac{1 - x_{\text{EtOH}}}{x_{\text{EtOH}}} \right) \quad (4)$$

X_{EtOH} represents the conversion while S_{H_2} represents the hydrogen selectivity. F_{EtOHin} and F_{EtOHout} represent the molar flow rate of the ethanol at the inlet and at the outlet of the reactor, respectively. The other main co-products observed during the gas-chromatographic analysis are: water, acetaldehyde, ethylene, CH_4 , CO and CO_2 and the composition analysis was realized on the basis of a carbon mass balance (equation 4). Where nC_i and nC_{EtOH} represent respectively the numbers of carbon atoms in the component i and in the ethanol fed, while Ac_i and Ac_{EtOH} are the normalized chromatographic peaks areas.

SECTION C

Chapter 3

Experimental Results

C-3.1 Introduction

Nowadays the catalytic generation of hydrogen by alcohols reformation is a topic of great interest. The use of ethanol is well known and in the last few years, the use of ethanol, that can be produced by second generation raw materials, has encouraged the interest of the academic and industry world. Actually, the most employed process to produce hydrogen is the catalytic steam reforming but, on the other hand, due to the strong endothermicity the requirement of the overall process external energy supply to sustain the reaction, along with the difficulties of development of a long-term stable coke resistant catalysts have led to search for other processes. At this purpose, the exothermic nature of the ethanol partial oxidation reaction looks as a reasonable alternative process for hydrogen production. In this chapter, the investigation of catalysts for processing bio-ethanol under oxidative reforming conditions has been reported. The main aim of this research is to investigate the use of ZnO and Chromia promoters to reduce coke formation and to improve the catalyst activity and hydrogen selectivity.

In particular, in this thesis the catalytic generation of hydrogen by partial oxidation of ethanol over a series of copper-zinc and Cu-chromite catalysts unsupported or supported on alumina, prepared by combustion synthesis has been realized. Combustion synthesis has been used to prepare metal oxide powders, including substituted chromite powders of high quality. The catalysts preparation and the

peculiarities of the combustion technique have been already retrieved in chapter 2 of the current section.

In a first part of this chapter, the textural properties, by using in-situ and ex-situ characterization, of the prepared catalysts were investigated. The individuation of the optimal fuel to oxidizer ratio (ϕ), as already mentioned in the chapter 2 of this section, during the preparation of the catalysts, is fundamental to obtain system with desired final textural properties. At this purpose, three different catalysts of Cu-Cr₂O₃ have been prepared by using the same composition but three different ratio $\phi=0.5-0.8-3.0$.

Once identified the best phi ratio, other two different systems, a catalysts of copper chromite supported on alumina CuCr/Al and a catalyst of copper-zinc oxide-alumina Cu-Zn-Al, have been prepared by using $\phi=0.8$. The catalysts behavior was studied in ethanol reforming and partial oxidative reforming reaction with the scope to investigate both the effect of the preparation methodology and of the presence of two different promoters such as chromia/chromium and zinc-oxide. In more detail, the partial oxidative reforming was studied under various O₂/C₂H₅OH ratios. At the end, the comparison of the performances of prepared catalysts and commercial catalysts was done. The commercial catalysts peculiarities, chemical and textural properties have been already described, in details, in the chapter 2 of the section B of this thesis. The chapter has been concluded with a discussion of the obtained results.

C-3.2 Catalysts characterization

The catalysts prepared by combustion have been submitted to a depth characterization studies. The techniques employed to characterize the prepared catalysts could be classified in two different categories: ex-situ characterization such as BET, X-ray diffraction (XRD), scanning

electron microscopy (SEM) and X-ray Photoelectron Spectroscopy (XPS) and in-situ characterizations such as diffuse reflectance infrared Fourier Transform (DRIFT) in presence of ethanol and X-ray adsorption near edge spectroscopy (XANES). A detailed description, of the equipment employed to characterize these materials and of the operative conditions used to pretreat the materials and to analyze them, has been reported in APPENDIX A. To well understanding the peculiarities of the catalysts is, thus, necessary to have both textural information of the fresh catalysts (EX-situ), to have an idea of their eventually changing during/after the reaction (In-situ) and finally to correlate their characteristics to the results of activity and selectivity in reforming and oxidative reforming reactions.

C-3.2.1 Ex-Situ Characterizations

The ex-situ techniques are able to give some information on the specific surface area (BET), on the crystalline structure (XRD), about the morphology (SEM) and the surface oxidation state of the catalysts components (XPS). These investigations give qualitatively types information only on the textural characteristics of fresh, not reduced, catalysts. The name, composition, glycine/O₂ ratio and the BET area of the synthesized catalysts prepared by combustion are summarized in Table 1.

In a first phase of this research, different copper-chromia catalysts were prepared by using different glycine/oxygen ratios. As the activity results will show, the best catalytic system was prepared by using a ratio between glycine/oxidizer of 0.8. The results reported in Table 1 show that the copper chromite supported on alumina CuCr/Al, prepared by impregnation of copper chromite on alumina and combusted, has the highest surface area of about 127 m²/g. Copper-chromite (Cu-Cr) catalysts prepared with a different ϕ ratio exhibited a

lower surface area, perhaps, due to sintering occurring at high temperature during the combustion synthesis process. Interestingly, the surface area of the CuZnAl catalyst, of about 31 m²/g, is low maybe because all the phases, included alumina, were combusted together instead of impregnating the Cu-ZnO phases on the alumina, as in the case of the CuZn/Al catalyst.

Table 1: Copper based catalysts surface area

Catalyst	Acronym	Φ	Composition	Surface area (m ² /g)
Cu-ZnO-Al ₂ O ₃	CuZnAl	0.8	CuO-ZnO-Al ₂ O ₃ (40:40:20 b.w.)	31
CuO-Cr ₂ O ₃	CuCr-0.5	0.5	CuO-Cr ₂ O ₃ (50:50 b.w.)	84
CuO-Cr ₂ O ₃	CuCr-0.8	0.8	CuO-Cr ₂ O ₃ (50:50 b.w.)	46
CuO-Cr ₂ O ₃	CuCr-3.0	3.0	CuO-Cr ₂ O ₃ (50:50 b.w.)	34
CuCr ₂ O ₄ / Al ₂ O ₃	CuCr/Al	0.8	CuCr ₂ O ₄ /Al ₂ O ₃ (60:20 b.w.)	127

Figure 1 shows the XRD diffraction patterns for all the fresh catalysts in oxidized form. The copper/copper chromite catalyst CuCr/Al, CuCr-0.5 and CuCr-0.8 shows several broad diffraction peaks indicative of small copper chromite particles size that in the case of CuCr/Al are well dispersed on the alumina support. The main phases at $2\theta = 33^\circ, 36.5^\circ, 41.1^\circ, 63^\circ$ are related to the cubic spinel CuCr₂O₄. The X-Ray diffraction peaks at $2\theta = 35^\circ - 38^\circ$ are typical of Cu (+2). The copper Cu(0) peaks are located at $2\theta = 50^\circ$, and 42.8° . Chromia diffraction peaks are located at $2\theta = 25^\circ, 34^\circ, 38^\circ, 55^\circ$ [1,2]. The CuCr-0.5 catalyst shows broad peaks due to the low dimension of copper oxide crystallites at 35° . The diffraction peaks of CuCr-0.8 have been assigned to a spinel of copper chromite, also in this case characterized by very small crystallite size.

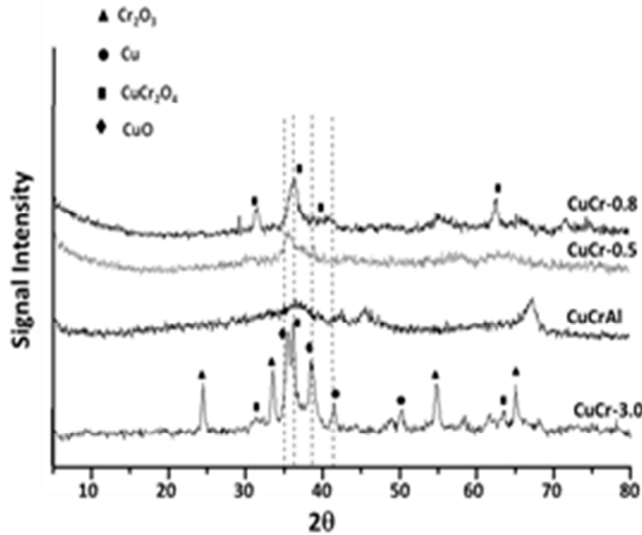


Figure 1- comparison of XRD diffraction patterns of the copper-chromite catalysts CuCr-0.5, CuCr-0.8, CuCr-3, CuCr/Al .

Finally, CuCr-3.0 has shown very well defined diffraction peaks that correspond to the several phases formed after the combustion synthesis at high temperature such as CuO, Cu, Cr₂O₃, CuCr₂O₄ assigned at 2θ value as mentioned above. The catalyst CuCr-3.0 prepared by using the higher φ ratio shows the presence of the diffraction peaks attributed to metallic copper, indicating that the catalyst in part is reduced, by the effect of large value of φ used (φ = 3), which results in a reduced metal nanoparticles [3]. The well high defined peaks are due to the larger size of the particles due to sintering occurring during the combustion synthesis in excess fuel [4]. To simplify the diffraction pattern reported above the XRD of the CuZn/Al catalyst has not been reported. In this case, ZnO phase at 2θ = 37° and a spinel of ZnAlO₄ at 2θ = 32° have been identified. The amorphous alumina support exhibits only weak and broad peaks.

SEM micrographs of the CuCr-0.8, CuCr/Al and CuZn/Al are catalysts represented in Figures 2A-C.

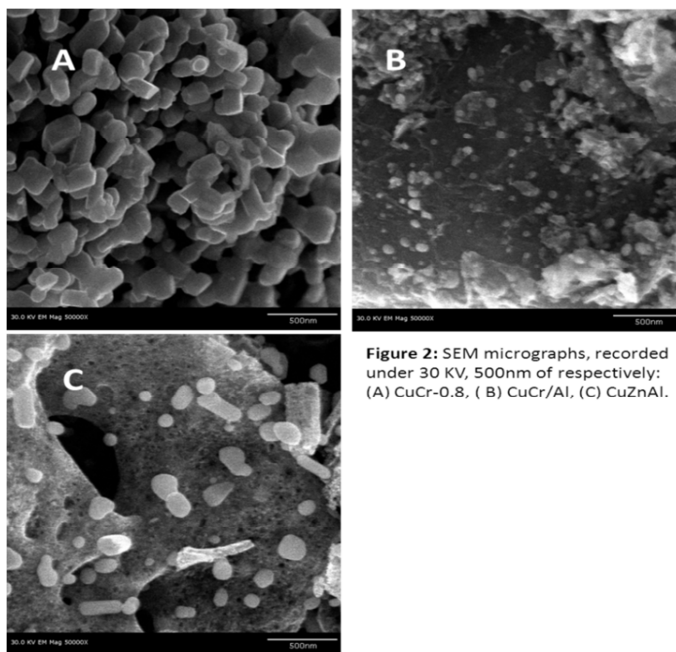


Figure 2: SEM micrographs, recorded under 30 KV, 500nm of respectively: (A) CuCr-0.8, (B) CuCr/Al, (C) CuZnAl.

The Figure 2A, corresponding to unsupported CuCr-0.8, shows individual particles of copper chromite of about 200 nm. The supported CuCr/Al catalyst shown in Figure 2B show small particles, presumably of copper chromite, of varying sizes and shapes dispersed on the alumina support in agreement with the XRD and BET results. Similarly, Figure 2C shows well defined particles supported on the alumina although we did not identified the various phases present in this case.

The surface composition, of CuCr-0.5, CuCr-0.8, CuCr-3 and CuZn/Al and CuCr/Al catalysts, was studied by XPS. The spectra are shown in Figures 3A and 3B respectively for Cu and Cr 2p 3/2 photoelectrons

with the surface composition of the selected fresh catalysts listed in Table 2 in terms of the relative % of the various elements present.

Table 2: XPS relative surface composition

	Cu 2p (%)	Zn (%)	Cr 2p (%)	Al 2p (%)	C 1s (%)	O 1s (%)
CuZn/Al	7.85	5.86	-	28.69	30.83	26.77
CuCr/Al	9.1	-	6.9	23.9	7.3	52.8
CuCr-0.5	15.9	-	15.5	-	16.8	51.8
CuCr-0.8	12.81	-	12.54	-	23.71	50.93
CuCr-3.0	11.31	-	16.85	-	16.95	54.88

Figure 3A shows that CuCr-0.5 and CuCr/Al exhibit a copper binding energy signal at 932.2-932.8 eV that corresponds to Cu^+ in Cu_2O , attributed to Cu^+ located in an octahedral and tetrahedral sites of CuCr_2O_4 [5].

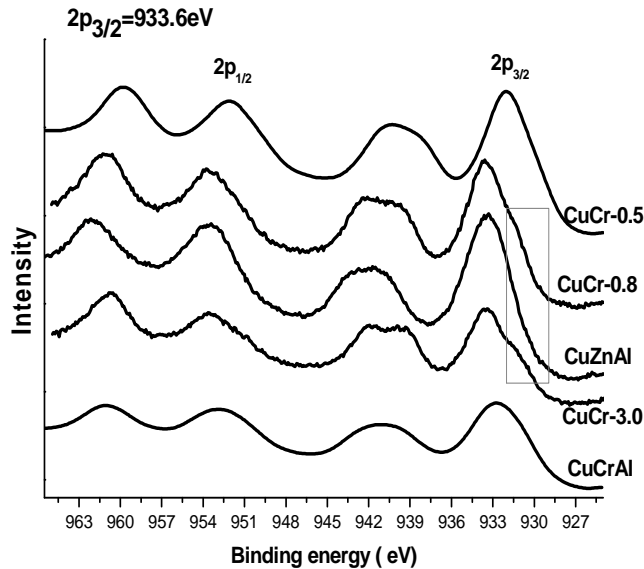


Figure 3A: copper binding energy signals.

As it can be seen CuZn/Al, CuCr-0.8 and CuCr-3.0 exhibit distinct satellite peaks at 933.6 eV that correspond to the Cu^{+2} as in CuO , indicating that the catalyst is in a fully oxidized state. Moreover the catalysts CuCr-0.8 and CuCr-3.0 show also small variation in binding energy of Cu with shoulder peaks at 932.2-932.8 eV, that correspond as above mentioned to Cu^{+} . On the fresh catalytic systems CuCr-0.8 and CuCr-3.0 a mixture of two oxidation states has been individuated. In Figure 3B, the chromium binding energy has been represented for each catalysts studied.

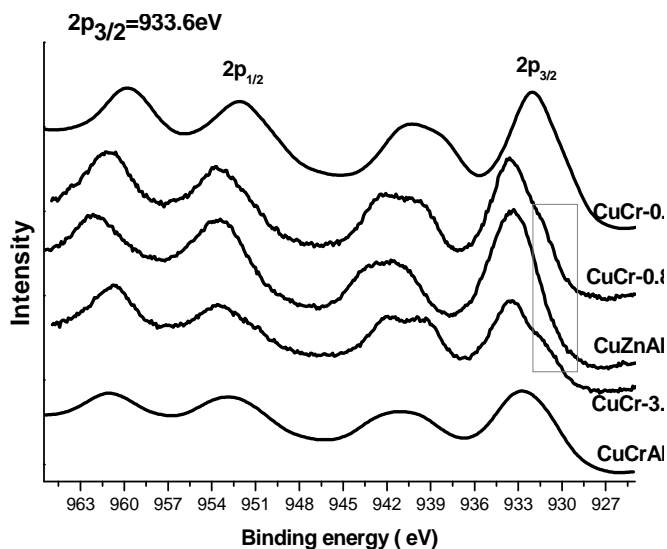


Figure 3B: chromium binding energy

The binding energy of Cr 2p_{3/2} of all the catalysts containing chromia is in the range 576.58-578.7 eV attributed to the Cr³⁺ in Cr₂O₃ compounds (Figure 3B), in good agreement with studies by Brooks et al. (577.0 eV)⁵. Moreover, the spectra reported in Figure 3B shows a small variation in binding energy of Cr observed in CuCr-0.5 and CuCr-0.8, the shoulder peaks at higher binding energy in each peak (ca. 580 eV Cr 2p_{3/2},) is assigned to the Cr⁶⁺ present in the previously characterized CuCr₂O₄ phase [6]. The accepted Zn 2p_{3/2} electron binding energy for oxidized zinc Zn⁰ reported near 1021.4 eV.

C-3.2.2 In-Situ Characterizations

The use of in-situ characterizations gives indications about the nature of adsorbed species on the catalysts surface during the ethanol

reforming reaction and about the variation of oxidation states during after respectively reduction, reaction and air exposure.

Several adsorbed species on the catalysts surface have been detected by using in-situ DRIFT in ethanol flow of $2.2 \text{ cm}^3/\text{min}$ diluted in nitrogen flow of about $25 \text{ cm}^3/\text{min}$ at 100, 200 and 300°C . In Figure 4 A-C DRIFT spectra respectively of CuCr-3, CuZn/Al and CuCr/Al catalysts have been represented. The spectra of CuCr-0.5A and CuCr-0.8B, even though diluted with fumed silica, show very weak bands difficult to identify due to the low reflectance and high absorption of infrared radiation by the black catalyst powder and hence are not shown. Figure 4A displays the DRIFT spectra of CuCr-3, showing barely distinguished features at 3750 and 1400 cm^{-1} that attributed to the $-\text{OH}$ group of the adsorbed ethanol and $-\text{COO}$ of an ester phase (ethylacetate). These DRIFT experiments enabled identification of surface ethoxy species [7]. At $2800\text{-}3000 \text{ cm}^{-1}$ another feature can be identified corresponding to the $-\text{CH}_3$ and/or $-\text{C}_2\text{H}_5$ groups. By increasing the temperature the bands of adsorbed $-\text{OH}$ disappear favoring the formation of the ester group. In particular, the spectrum 4A shows a different band, at a wavenumber of about 1750 cm^{-1} related to the formation of acetaldehyde species. Figures 4B and 4C shows the spectra for CuZn/Al and CuCr/Al supported catalysts which although obtained at the same dilution ratio catalyst/fumed silica=1:5 as in Figure 4A, the spectra is clearer due to the better reflectance provided by the alumina support. The spectra show different bands corresponding to $-\text{OH}$ at 3750 cm^{-1} , $-\text{CH}_3$ and $-\text{C}_2\text{H}_5$ at $2800\text{-}3000 \text{ cm}^{-1}$, CO_2 at $2300\text{-}2400 \text{ cm}^{-1}$, acetaldehyde specie at 1757 cm^{-1} . Figure 4C, for CuCr/Al, shows at 300°C the formation of surface acetate species $\nu_{\text{sym}}(\text{COO})$ at 1550 cm^{-1} and characteristic $\nu(\text{C}-\text{O})$ bands corresponding to mono- ($\nu(\text{CO}) = 1096 \text{ cm}^{-1}$) and bidentate ($\nu(\text{CO}) = 1055 \text{ cm}^{-1}$) ethoxy species [8-10].

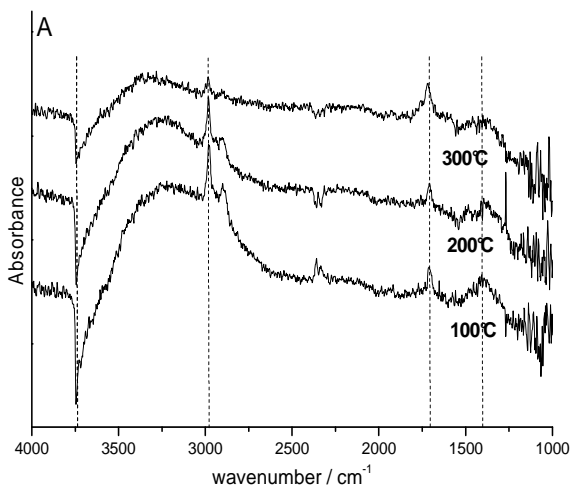


Figure 4A: (A) CuCr-3 DRIFT spectra

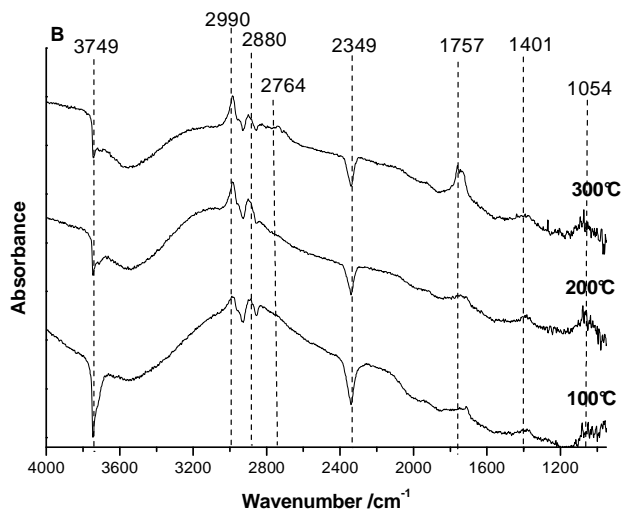


Figure 4B. CuZn/Al DRIFT spectra

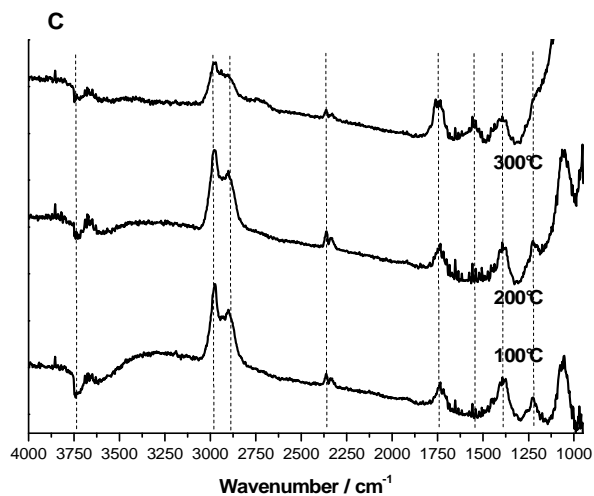


Figure 4C: CuCr/Al DRIFT spectra

Further investigation of the oxidation state under reaction conditions was carried out by in-site XANES. Figure 5A shows the Cu edge XANES spectra of the three different Cu standards: Cu^0 , Cu^+ and Cu^{2+} .

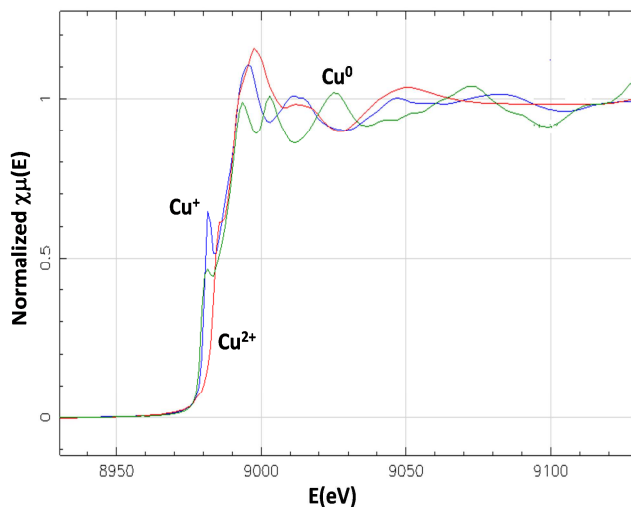


Figure 5A: Xanes spectra of Copper Standards.

By comparing the Cu edge XANES spectra of the CuCr-0.5 catalyst, reported in Figure 5B, and the standard ones, it is possible to observe a variation of oxidation state of the copper during reduction and ethanol decomposition. As it can be seen, in the CuCr-0.5 catalyst, Cu has initially an oxidation state of Cu⁺² in the fresh catalyst exposed to air. After reduction, ethanol decomposition and subsequent exposure to air after reaction the oxidation state of CuCr-0.5 is mainly Cu⁰.

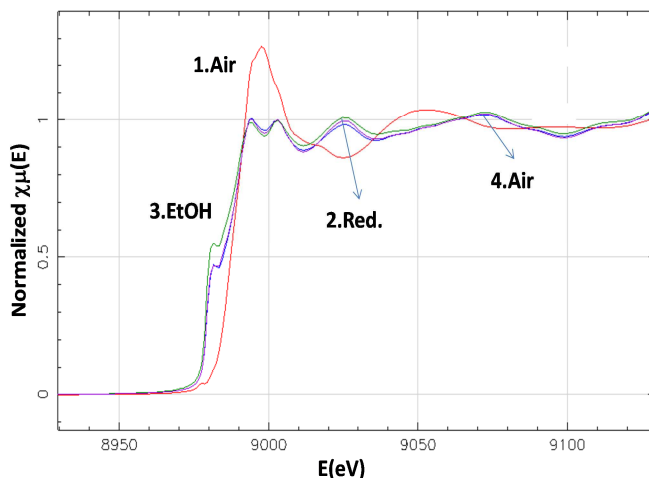


Figure 5B: Xanes spectra of CuCr-0.5 catalyst. The measure has been done in different step. 1. Exposure to the air. 2. catalyst reduction. 3. Ethanol decomposition. 4. Exposure to air after reaction.

In Figure 5C the XANES spectra of a CuCr-0.8 catalyst after the reduction and successively exposure to air are shown. In this case it can be seen that after reduction and catalyst exposure to air the curves do not fit neither the reduced or oxidized standards indicating that the oxidation state of copper is a mixture of $\text{Cu}^0/\text{Cu}^{+1}$. As previously demonstrated CuCr-0.8 catalyst has shown the best performances in the ethanol decomposition. The mixture of two oxidation state is typically present in the active copper-chromite catalyst and could represent the active phase in the ethanol decomposition reaction.

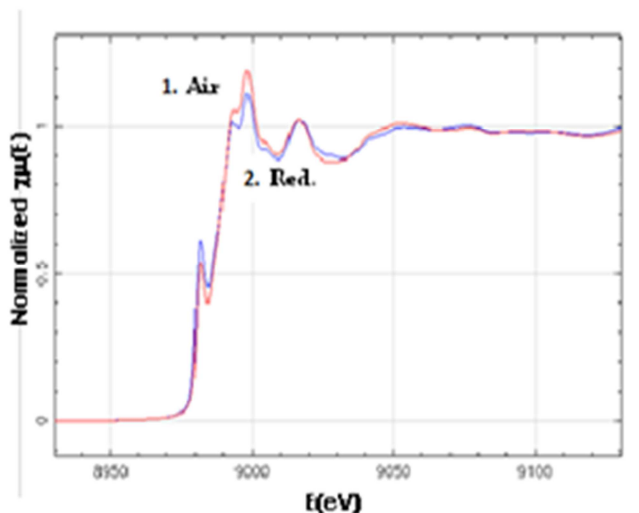


Figure 5C: XANES spectra of CuCr-0.8 catalyst : 1. catalyst reduction 2. Exposure to air after reaction.

The CuCr/Al catalyst, Figure 5D, shows a Cu edge XANES profile similar to the ones obtained for the CuCr-0.5 catalyst, i.e mainly oxidized in the fresh catalyst in air and mainly reduced after reduction, reaction and subsequent exposure to air. The Cu XANES spectrum of CuZn/Al catalyst (not shown) is basically the same as CuCr/Al and CuCr-0.5 showing no major effect of ZnO on the oxidation state of Cu.

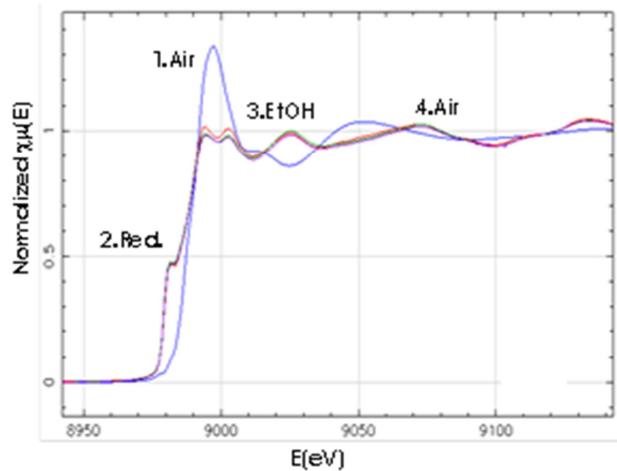


Figure 5D: XANES spectra of CuCr/Al catalyst :1. Exposure to the air. 2. catalyst reduction. 3. Ethanol decomposition. 4. Exposure to air after reaction.

C-3.3 Catalytic tests

According to the literature, the reforming reactions are catalyzed by metals of Groups 8–10 of the Periodic Table and in particular nickel being preferred for industrial applications [11]. However, early studies on ethanol reforming were carried out over copper-based catalysts [12]. The copper is active and selective phase to produce hydrogen, but promoters and supports are necessary to prevent both metal sintering and fouling the surface due to the acetaldehyde adsorption. Copper, initially present in the fresh catalysts composition in the form of oxide, was previously reduced to metal to be active in a flow of hydrogen for about 3h at 300°C. In this section the performances of two series of catalysts have been studied:

- A. Catalysts prepared by combustion
- B. Commercial catalysts

C-3.3.1 Copper based catalysts prepared by combustion

At first, the individuation of the best "phi" ratio necessary to obtain the most active and selective catalyst have been done. Figure 6A shows the ethanol conversion versus the temperature profiles for three different catalysts profiles for CuCr-0.5, CuCr-0.8 and CuCr-3 catalysts with the corresponding selectivity shown in Figure 6B. The runs were performed in a constant flow of ethanol ($2.2 \text{ cm}^3/\text{min}$) diluted in $38 \text{ cm}^3/\text{min}$ of nitrogen, at atmospheric pressure and by changing the temperature of reaction in the range $50\text{-}500^\circ\text{C}$. The Figure 6A shows the conversion for each three catalysts examined at different temperature of reaction. At high temperature ($>500^\circ\text{C}$) a conversion of about 95-100% was obtained for all catalyst. At an intermediate temperature of about 250°C the conversion is about 77-80% for CuCr-0.5 and CuCr-0.8 and is only 10% for CuCr_2O_4 . It follows that, by increasing phi value decreases conversion at intermediate temperatures. The hydrogen selectivity (Figure 6B) defined as the ratio of the amount of hydrogen produced to the total amount of hydrogen that can be produced from the reacted ethanol, is very different among the three catalysts.

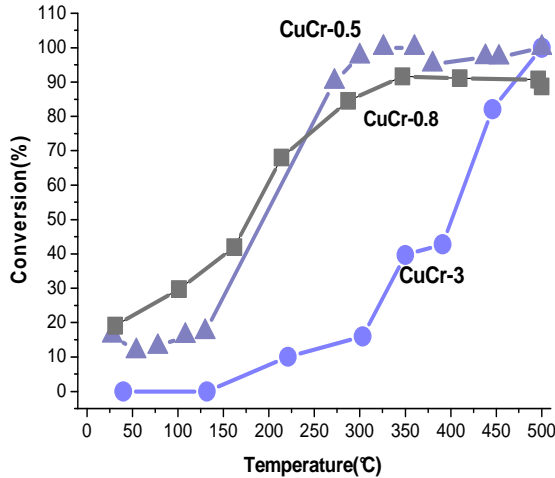


Figure 6A: conversion profiles for profiles for CuCr-0.5, CuCr-0.8 and CuCr-3 catalysts.

Up to 100°C hydrogen selectivity is low leading to the formation of CO_x and water. As temperature increases, H₂ selectivity increases and at 300°C the order of selectivity ranks as follows: CuCr-0.8 (40%)>CuCr-0.3 (27%) whereas the CuCr-0.5 is nearly unselective for H₂ producing mainly acetaldehyde ($S_{ACH}=85-90\%$ at $200 < T < 300^{\circ}\text{C}$), as shown in Figure 6C, along with water, CO_x and methane.

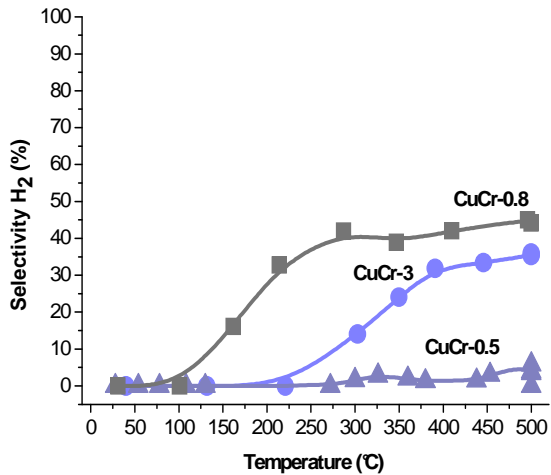


Figure 6B: hydrogen selectivities profiles for CuCr-0.5, CuCr-0.8 and CuCr-3 catalysts

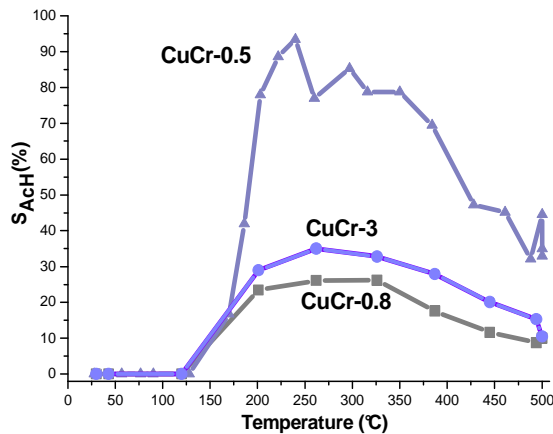


Figure 6C: acetaldehyde selectivity profiles of CuCr-0.5, CuCr-0.8 and CuCr-3 copper chromite catalysts.

Acetaldehyde selectivity for CuCr-3 is about 25-30% in the temperature range of 200-300°C. In the same temperature range the acetaldehyde selectivity of CuCr-0.8 is almost the same (22-25%). For each studied catalysts CuCr-0.5, CuCr-0.8 and CuCr-3.0, the

acetaldehyde selectivity reaches a maximum and then decreases as temperature increases. At temperatures higher than 300°C, H₂ selectivity levels off at about 47% for CuCr-0.8 and 33% for CuCr-3.0 and remains low for CuCr-0.5. The results, in Figure 6, indicate that the optimum value of phi is 0.8, which was used in subsequent preparations. Several studies have shown good activity for CuO-ZnO and CuCr₂O₄ catalysts in the ethanol steam reforming reaction [13-15]. On behalf of this purpose, the effect of zinc oxide on unsupported, CuCr-0.5 and CuCr-0.8, and supported on alumina, CuZn/Al and CuCr/Al, was studied (Figure 7).

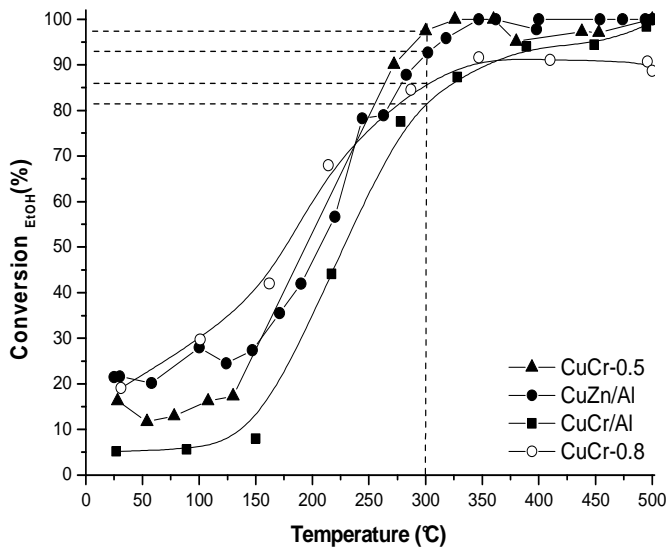


Figure 7A: comparison of the activity profiles CuCr-0.5, CuCr-0.8, CuCr/Al and CuZn-Al.

Figure 7A shows that at 300°C the conversion is in the 85-95% range for the unsupported CuCr-0.5/0.8 and about 92% for the supported Zn promoted catalysts CuZn/Al and slightly lower (~80%) for the supported CuCr/Al catalyst.

As it can be appreciated by the profiles of Figure 7B at 300°C, hydrogen selectivity is the highest for the supported CuCr/Al catalysts (48%) followed by the unsupported CuCr-O.8 (40 %) and the CuZn/Al (31%).

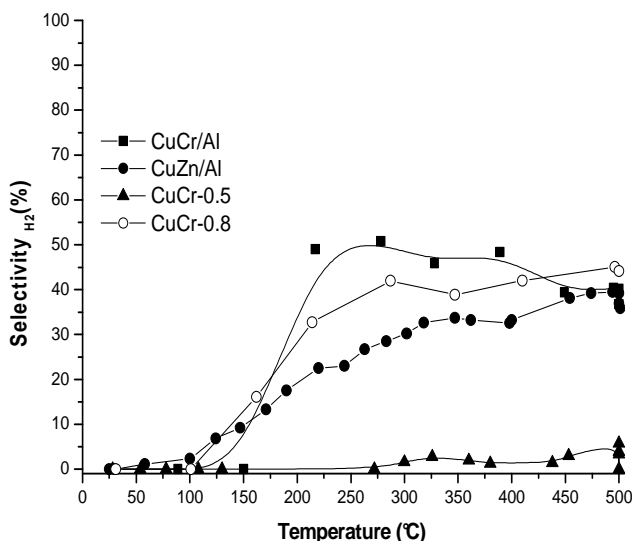


Figure 7B: comparison of the hydrogen selectivity profiles of CuCr-0.5, CuCr-0.8, CuCr/Al and CuZn/Al.

At 400°C, the hydrogen selectivity of these three catalysts is almost the same (40-45%) whereas the CuCr-0.5 catalyst exhibits no hydrogen selectivity in the whole temperature range. These results show that Zn promotion is not as effective as Cr promotion, in particular when the CuCr catalyst is dispersed in the Al support. Moreover, the deactivation resistance of the supported CuCr/Al catalyst was studied as a function of time-on-stream (TOS) (Figure 8). The conversion-temperature profile of the catalyst after used at different time on stream is shown in Figure 8A. As it can be appreciated, the conversion

at 300°C of the fresh catalysts (R1) and reactor used (R2: after 25 h TOS) decreased from 80% to about 51%.

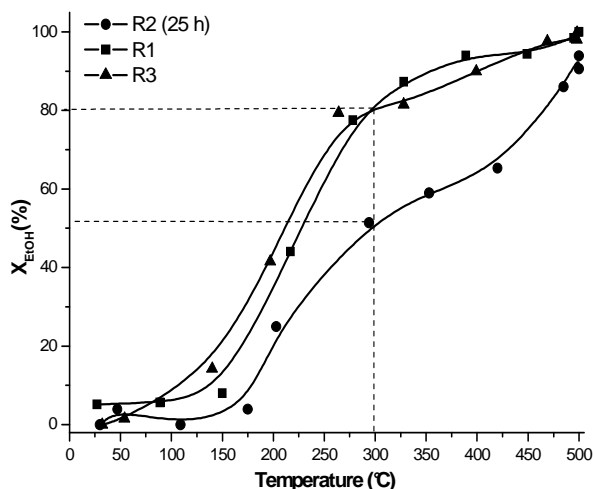


Figure 8A: comparison of the activity of CuCr/Al catalyst: (R1) fresh catalyst, (R2) used catalyst for about 25h, (R3) regenerate catalyst in oxygen flow of 2.2 cm³/min.

The activity, pull through after regeneration of the catalyst in hydrogen, gets about the same value as the fresh catalyst (R3). The selectivities at 300°C (Figure 8B), however, were about the same for the three cases reported. It is likely that the activity decrease after 25h of operation is due to the formation of coke from the partially dehydrogenated intermediates involved in the decomposition reaction. This is quite different that our previous results on Cu-Ni-Fe promoted multi-component catalysts [3], which show a significant decrease in activity with TOS for ethanol decomposition.

The H₂ selectivity remains constant during the time on stream studied which indicates that the sites involved in adsorption of ethanol are transformed by coke formation but the concentration of the

intermediates leading to their decomposition is not delayed in during the time-on-stream studied.

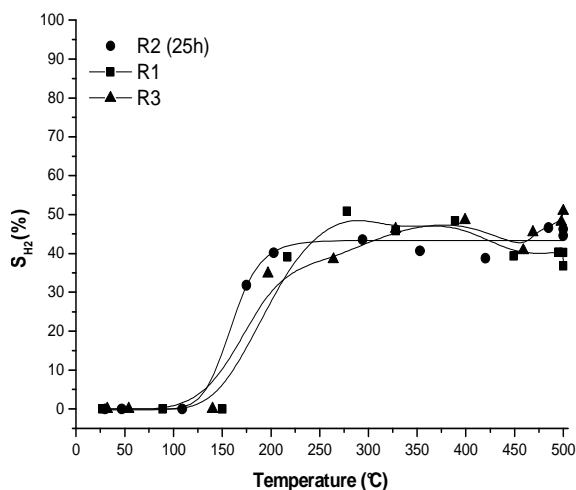


Figure 8B: comparison of the selectivity profiles of CuCr/Al catalyst: (R1) fresh catalyst, (R2) used catalyst for about 25h, (R3) regenerate catalyst in oxygen flow of 2.2 cm³/min.

The ethanol decomposition is a strongly endothermic reaction, which would require an additional energy source to sustain itself. The alternative use of oxidative reforming of ethanol, previously studied in the above mentioned Cu-Ni-Fe catalysts [3], has the advantage of being exothermic. Precisely, the use a low stream of oxygen, lowest than the stoichiometric one, has the possibility to keep clean the catalyst surface by coke deposition, the main cause, as above mentioned, of the catalyst deactivation.

At first the performances of CuZn/Al, CuCr/Al and CuCr-0.8 was investigated in a range 50-500°C of temperature, by using the same amount of catalyst and by using a mixture of ethanol and oxygen, diluted in 38 cm³/min of nitrogen, with molar ration of EtOH:O₂=0.6.

The results obtained in terms of ethanol conversion and hydrogen selectivity for these catalysts are reported in Figure 9.

Figure 9A shows that at 300°C CuCr-0.8 exhibits about 96% conversion while both supported CuCr/Al and CuZn/Al have conversions of about 68-72%.

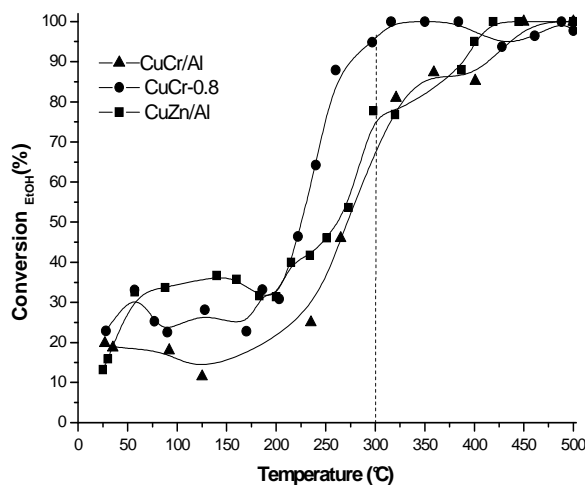


Figure 9A: comparison of activity profiles of CuZn/Al, CuCr/Al and CuCr-0.8 catalysts. The runs were performed in presence of a low quantity of oxygen EtOH:O₂=0.6 .

H₂ selectivities (Figure 9B), shows that until 200°C no hydrogen is produced and the main products of reaction are CO₂ and water. By increasing the temperature to 300°C CuZn/Al has a selectivity of 35% versus 28% obtained for CuCr/Al. At 300°C, in presence of oxygen CuCr-0.8 has a H₂ selectivity of only 10% indicating that in this catalyst the reaction pathway favors the total oxidation of ethanol to CO₂ and water. At temperature higher than 300°C, the H₂ selectivity of CuZn/Al is nearly constant in the 30-35% and 25-28%, for CuCr/Al.

It follows that in the presence of oxygen Zn promotion does not increase that total oxidation of the intermediates leading to CO₂ and water but rather this catalyst, retain sites selective for partial oxidation

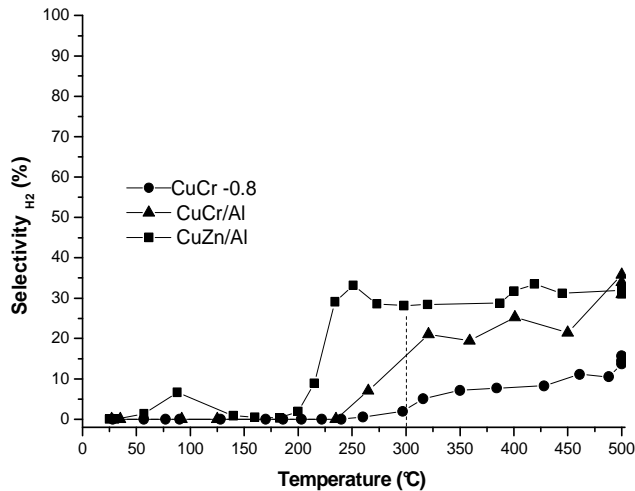


Figure 9B: comparison of selectivities profiles of CuZn/Al, CuCr/Al and CuCr-0.8 catalysts. The runs were performed in presence of a low quantity of oxygen EtOH:O₂=0.6

Further increase of the oxygen concentration to O₂/EtOH =1.2 decreases the selectivity for all catalysts even further (not shown) favoring the combustion of hydrogen to water. The increase of oxygen concentration promotes an increase of the catalysts activity. The hydrogen selectivity decreases drastically as O₂ concentration increase because the secondary reactions of combustion to CO_x are favored. The use of small amount of oxygen EtOH:O₂=0.6 should be a good compromise to obtain high activity, decreases catalysts deactivation and increases hydrogen selectivity. In OPX (oxidative partial oxidation) reactions, Cu/Cr with phi ratio=0.8 has shown very scarce performances in terms of hydrogen selectivity that was less than 10%.

A further increase of the ratio $\text{EtOH}:\text{O}_2=1.2$ corresponds to a considerably decrement of the hydrogen selectivity, since in that conditions the secondary combustion reaction are the favored side reactions. This behavior is, well, understood by the profiles reported in Figure 10A and 10B.

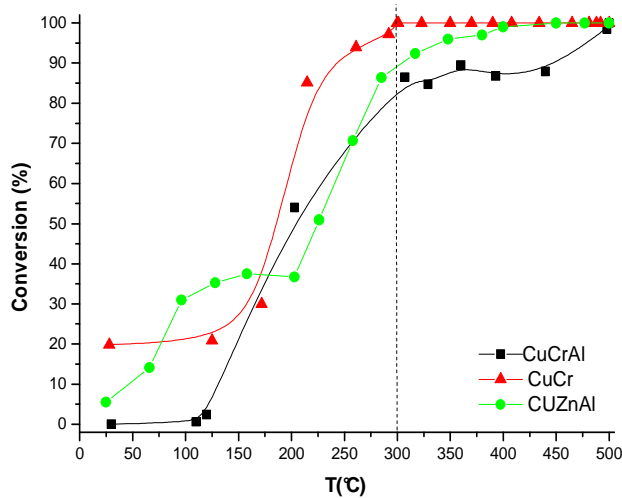


Figure 10A: comparison of activity profiles of copper based catalysts prepared by combustion. The runs were performed in presence of a high amount of oxygen $\text{EtOH}:\text{O}_2=1.2$.

The catalysts CuZnAl and CuCr-0.8 show a relatively high activity also at low temperature due to burning of coke depositions. At a temperature of 300°C the CuCr-0.8 shown an higher activity (95%) respect to CuZnAl (87%) and CuCrAl (81%). At temperature higher than 400°C the activity of CuCr and CuZnAl is almost the same (100%). In Figure 10B the profiles of hydrogen selectivity have been represented. It follows that the use of higher amount of oxygen could promote the formation of several co-products such CO_2 , CH_4 and acetaldehyde, rather than hydrogen.

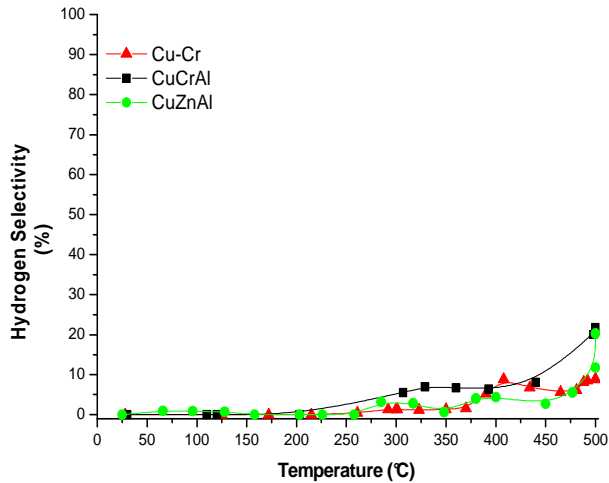


Figure 10B: comparison of selectivity profiles of copper based catalysts prepared by combustion. The runs were performed in presence of a high amount of oxygen EtOH:O₂=1.5.

By considering the several results obtained the use of small amount of oxygen EtOH:O₂=0.6 should be a good compromise to obtain high activity, decreases catalysts deactivation and increases hydrogen selectivity. The interesting result is that all these system are very selective to produce acetaldehyde. In Figure 11, the profiles of acetaldehyde selectivity as function of the reaction temperature for each catalyst at three different ratios EtOH:O₂=0/0.6/1.2 have been represented. In figure 11 A, the profiles of acetaldehyde selectivities have been reported related to the catalyst CuCrAl performance in both, ethanol decomposition reaction and in partial oxidative reforming. In Figure 11 B and in Figure 11 C the profiles of acetaldehyde selectivity for respectively CuCr-0.8 and CuZnAl have been reported.

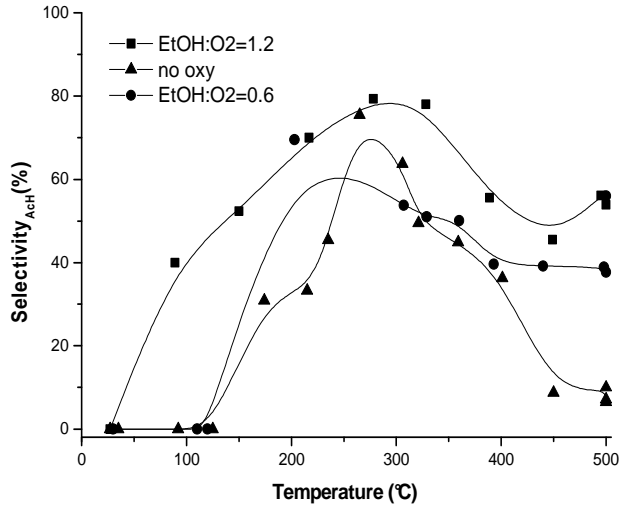


Figure 11A: acetaldehyde selectivity of the catalyst CuCrAl in ethanol decomposition (no oxy) and in partial oxidative reforming (EtOH:O₂=0.6/1.2).

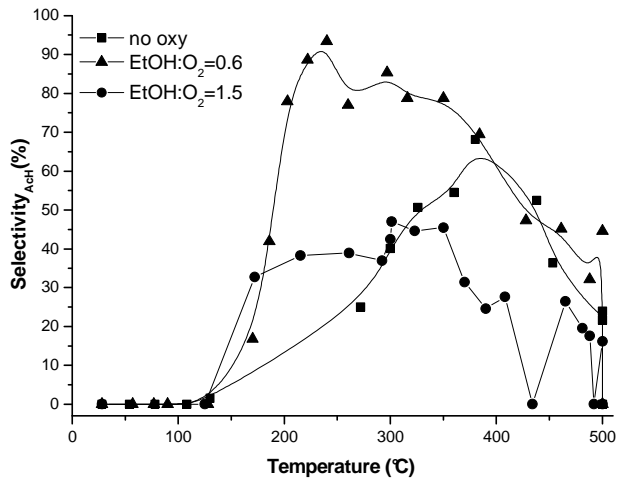


Figure 11B: acetaldehyde selectivity of the catalyst CuCr-0.8 in ethanol decomposition (no oxy) and in partial oxidative reforming (EtOH:O₂=0.6/1.2).

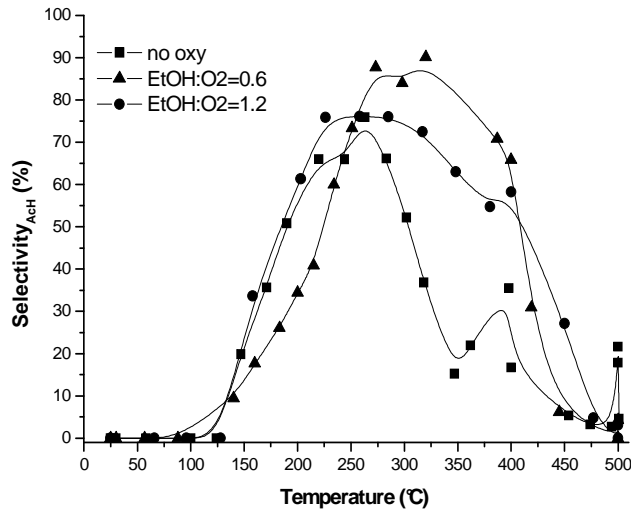


Figure 11C: acetaldehyde selectivity of the catalyst CuZnAl in ethanol decomposition (no oxy) and in partial oxidative reforming (EtOH:O₂=0.6/1.2).

In each case, the acetaldehyde production is higher at higher ratio EtOH:O₂. Moreover, in the ethanol decomposition reaction it should be possible to individuate the acetaldehyde formation only at higher temperature ($T > 250^{\circ}\text{C}$). This bearing is due to the endothermic nature of the reaction, so a high energy supply is necessary to favor the acetaldehyde formation. The exothermic nature of the OPX reaction, thanks to the small amount of oxygen employed, shifts the acetaldehyde production to low temperature range. The acetaldehyde observed is in all the cases very high (70-90%) and this consideration leads to conclude that these catalysts favor the dehydrogenation

reaction. This aspect is agreement with the results obtained by the ethanol dehydrogenation at high pressure.

C-3.4 Commercial catalysts

The behavior of commercial copper chromite and copper zinc catalysts have been already studied in the ethanol dehydrogenation reaction at high pressure (10-30 bar) and in a range of temperature of 200-260°C, with the aim to improve the ethyl acetate, in spite of acetaldehyde, and pure hydrogen production. In this section, dedicated wholly to the hydrogen production, these same catalysts have been studied in conditions of high temperature (50-500°C) and atmospheric pressure (1 atm). To ensure an easier understanding of the results below, a summary table of the composition of all the examined catalysts has been reported (Table 3).

Table 3: composition of the proven catalysts

Sample	Composition given by the companies
BASF K-310	CuO-ZnO-Al ₂ O ₃ (40-40-20 % b.w.)
Sud-Chemie T-4466	CuO/CuCr ₂ O ₄ (CuO/Cr ₂ O ₃ = 53/45)
Cu-0203	CuO/CuCr ₂ O ₄ (CuO/Cr ₂ O ₃ = 64/36)
BASF Cu-1234	CuCr ₂ O ₄ -CuO-Cu-BaCrO ₄ -Al ₂ O ₃ (45-1-13-11-30 % b.w.)

At first, a comparison of the activities and hydrogen and acetaldehydes selectivities profiles was done, between the four mentioned catalysts into the ethanol decomposition reaction (see Figure 12). Precisely, Figure 12A shows the high activity of both K-310 and Cu-1234 catalysts a relatively low temperature of reaction (10-20% at T<100°C). This feature could be justified by the presence of acidic sites of alumina in both the systems, on which the residual coke depositions burn and successively, in the first step of reaction, moderate quantity of CO₂ could be observed. At a temperature of

300°C, Cu-0203 containing an higher copper content (64%) has shown a very poor activity. Moreover, the Figure 12B point out the high hydrogen selectivity of Cu-1234, T-4466 and K-310 catalysts (82-91%).

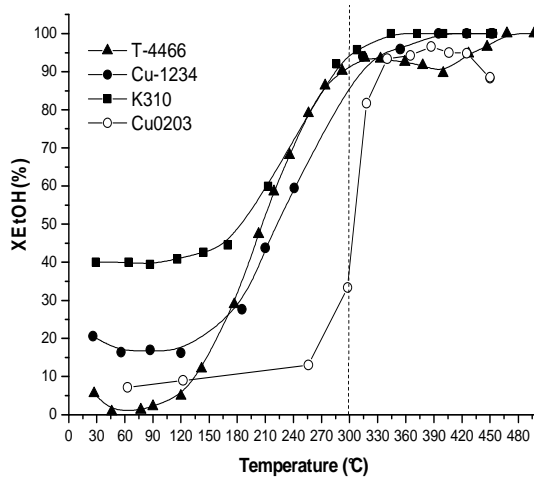


Figure 12A: conversion variation with the temperature for T-4466, Cu-1234, Cu-0203, and K-310.

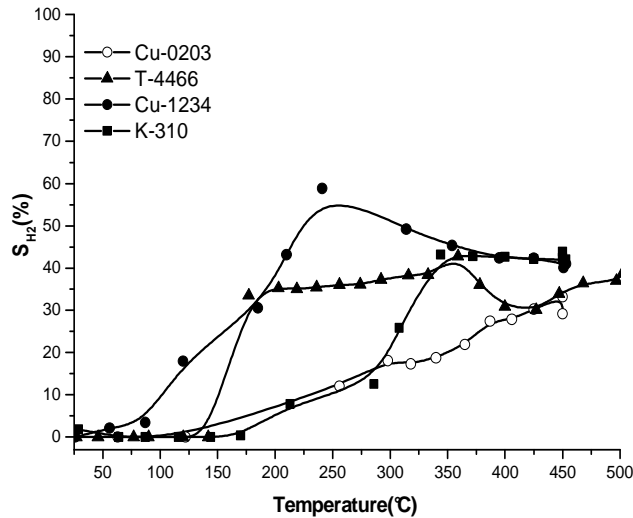


Figure 12B: hydrogen selectivity profiles of T-4466, Cu-1234, Cu-0203, and K-310.

In more detail, as it can be seen by the profiles of Figure 12B, the catalyst Cu-1234 shows, at temperature lower than 200°C, hydrogen selectivity of about 30%. This feature is very interesting because, the use of low temperature, provides several economics advantages generally related to the low cost of process. By a further increase of the reaction temperature to 250°C, a maximum of hydrogen selectivity of about 58-59% was reached. At temperature higher than 250°C, the hydrogen selectivity slightly decreases to 40-42%, a value that remains constant in all the explored range of temperature. The catalyst T-4466 has hydrogen selectivity of about 35-40% at temperature higher than 250°C. At the same temperature, Cu-0203 and K-310 show very low selectivity value of about 10%. At temperature higher than 300°C the hydrogen selectivity, for the last two mentioned catalysts, is of about 30%. The main reaction co-product of in each catalysts studied is the acetaldehyde as it can be appreciated by Figure 12C.

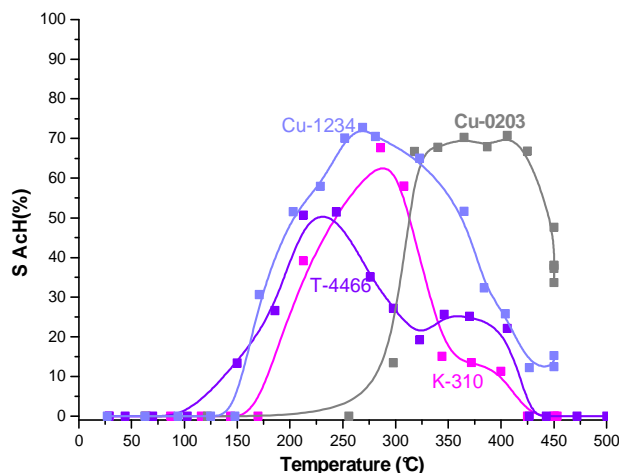


Figure 12C: acetaldehyde selectivity profiles of T-4466, Cu-1234, Cu-0203, and K-310.

As it can be appreciated by the profiles of Figure 12C, Cu-1234, T-4466 and K-310 show a selectivity of 40-65% in the range of temperature of 150-250°C. Cu-1234 has shown the better performances and it has proven to be a good system in dehydrogenation reaction at low temperature. The acetaldehyde selectivity rises up to a 72% at a temperature of 250°C and slightly decreases to a value of 35-40% at temperature of 400°C due to the effect of decomposition of acetaldehyde to CH_4 and CO . The catalyst Cu-0203 shows a discrete selectivity to acetaldehyde only at temperature reaction higher than 300°C, at which the catalyst has also shown a moderately activity (15%). The investigation is going on by studying the catalysts features in the partial oxidative reforming reaction. Firstly, the reaction has been performed by using a ratio $\text{CH}_3\text{CH}_2\text{OH}:\text{O}_2=0.6$ (Figure 13). In these conditions, the catalysts show a very scarce tendency to deactivate and no cycles of oxidation/reduction have been required.

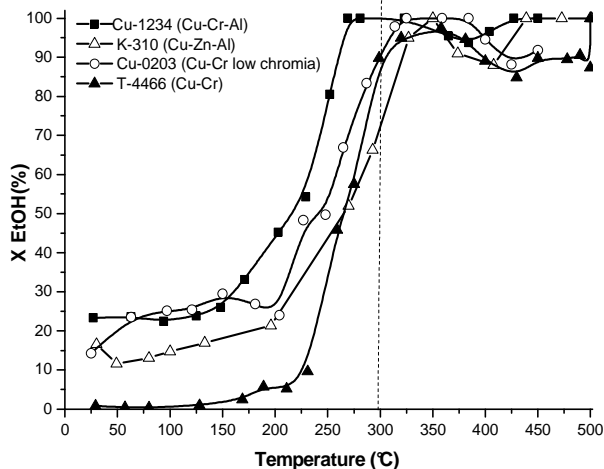


Figure 13 A: comparison of activity profiles of T-4466, Cu-1234, Cu-0203, and K-310. The runs were performed by using a ratio $\text{CH}_3\text{CH}_2\text{OH}:\text{O}_2=0.6$.

In figure 13 A is proven that at temperature of 300°C the activity of all the examined catalyst, except 300°C, is higher (90-100%) respect the ones obtained in ethanol decomposition reaction. The use of small amount of oxygen is useful to escape the coke deposition on the active sites of the catalysts used.

In Figure 13 B the hydrogen selectivities for each catalyst examined have been represented.

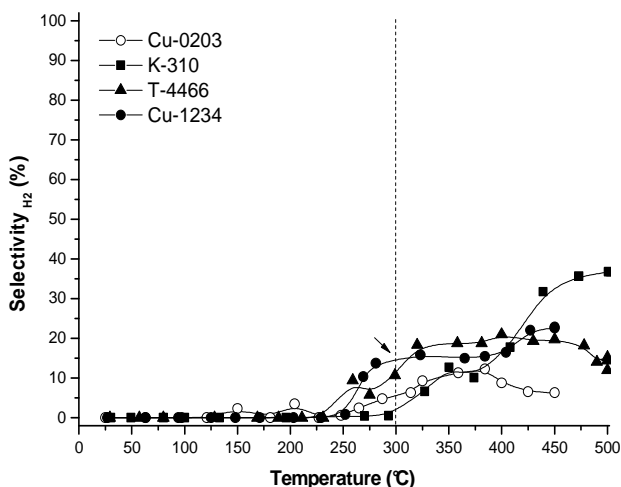


Figure 13 B: comparison of hydrogen selectivity's profiles of T-4466, Cu-1234, Cu-0203, and K-310. The runs were performed by using a ratio $\text{CH}_3\text{CH}_2\text{OH}=0.6$.

The use of small amount of oxygen provokes the sharp decrement of the selectivity to hydrogen that at 300°C is for the best catalyst Cu-1234 of about 18%. The other studied systems have shown selectivity values less than 15%. By increasing the temperature until 450°C, both Cu-1234 and T-4466 show a selectivity of 25-26% while K-310 of 35%. In this condition, the most favored product of reaction is the acetaldehyde as demonstrated by Figure 13C in which the profiles of

selectivity to acetaldehyde for each catalyst have been reported. Cu-1234 displays a very high selectivity to acetaldehyde narrow to the range of 50-60%, at low temperature ($T < 100^\circ\text{C}$). Whilst, as demonstrated by the activity profiles the catalyst has a conversion of 20-25% at a temperature of 50°C .

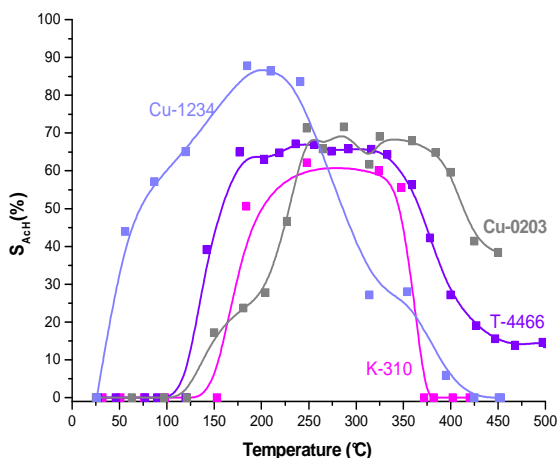


Figure 13C: comparison of acetaldehyde selectivities profiles of T-4466, Cu-1234, Cu-0203, and K-310. The runs were performed by using a ratio $\text{CH}_3\text{CH}_2\text{OH}:\text{O}_2=0.6$.

The catalysts Cu-0203, T-446 and K-310 reach a maximum of selectivity, 60-70%, in a broad range of temperature of about 200-350°C. Moreover Cu-0203 and T-4466, the only two catalysts that do not contain alumina, show an high ability to preserve the C-C bound at higher temperature, as demonstrated by the high selectivity values at $T > 400^\circ\text{C}$. By considering the several results obtained the use of small amount of oxygen $\text{EtOH}:\text{O}_2=0.6$ should be a good compromise to obtain high activity, decreases catalysts deactivation and increases hydrogen selectivity. The increase of oxygen fed could promote a significantly increase of the activity and of the stability of the used

catalysts (figure 14). At a temperature of 300°C, all the catalysts studied have demonstrated to hold a conversion of 87-92% (Figure 14A).

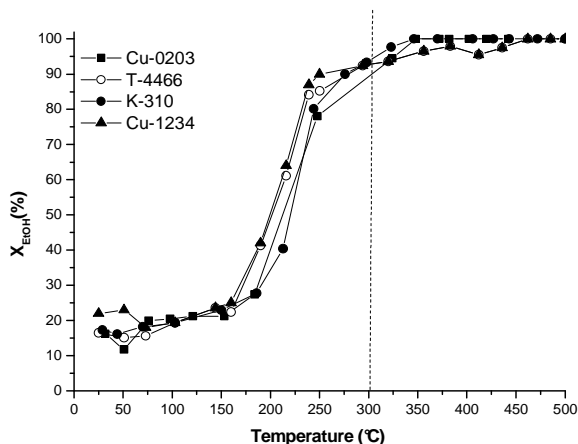


Figure 14 A: comparison of activity profiles of T-4466, Cu-1234, Cu-0203, and K-310. The runs were performed by using a ratio $\text{CH}_3\text{CH}_2\text{OH}:\text{O}_2=1.2$.

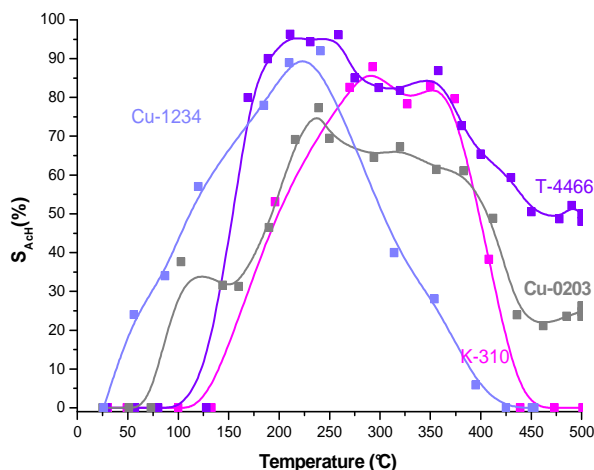


Figure 14 B: comparison of selectivity acetaldehyde profiles of T-4466, Cu-1234, Cu-0203, and K-310. The runs were performed by using a ratio $\text{CH}_3\text{CH}_2\text{OH}:\text{O}_2=1.2$.

In addition, the acetaldehyde profiles of Figure 14B show the high selectivity (60%) at low temperature ($T < 150^{\circ}\text{C}$) of the Cu-1234 catalyst. Also in this case, by operating at this ethanol oxygen ratio the selectivities in the range of temperature higher than 200°C the selectivity is 70-90%.

It follows that the use of higher amount of oxygen could promote reaction of formation of several co-products such CO_2 , CH_4 and acetaldehyde, rather than hydrogen. Moreover, these catalysts in low pressure condition, favor the acetaldehyde as main product of a dehydrogenation process. The main advantage is related to the low presence of CO , CO_2 and CH_4 gases that should be separate by hydrogen to obtain high grade of purity, necessary to fuel cells application.

C-3.4 Discussion

In this chapter, two series of catalysts have been examined respectively prepared by combustion and commercial ones, supplied by BASF (K-310, Cu-1234, Cu-0203) and Sud-Chemie (T-4466).

In spite of the various characterization methods utilized, each requires different conditions, like the standard ex-situ XRD vs. the more complicated in-situ experiments. Each method probe different properties and material volumes giving results that are often not consistent as discussed in detail below, so only qualitative conclusions can be reached.

In addition, there are multiple phases in these catalysts, as demonstrated by several characterization techniques, involving several oxidation states so more than one site could be involved. This is a complex reaction network, involving multiple sites that would require detailed kinetic evaluation, to correlate quantitatively active sites and material properties with the activity-selectivity trends.

Several considerations, about the correlation of the oxidation state with the properties of this material, have been done.

Firstly, the study of Cu-Cr prepared by using three different oxidizer/fuel ratio has shown that the preparation methodology could affect the catalysts textural properties. In a first phase of this research work, the best value phi to prepare the catalysts has been identified. The increase of phi ratio gets catalysts with a very low surface area due to the sintering and collapsing of the catalyst structure by the effect of the high temperature reached during the combustion synthesis reactions. BET area varies inversely with the fuel/oxidizer ratio increasing as phi decreases.

Highest BET area is obtained in the supported catalyst prepared by impregnation in a high area alumina as opposed to one prepared including the alumina precursor in the CS (CuZn/Al).

The ex-situ XRD examination in air shows the presence of several oxide phases including copper chromite, CuO, ZnO and Cr₂O₃ depending on the fuel/oxidizer and support used. As the XRD patterns have shown, the increase of fuel ratio can affect significantly the final crystalline structure of the catalysts. In more detail, the catalyst CuCr-3 shows well defined and closed diffraction peaks indicative of higher crystallite size. This feature is a direct effect of the high temperature reached during the combustion synthesis cause of eventually sintering and growing by aggregation of the crystallites.

Another important structural aspect that emerges by the XPS analysis is the presence of copper chromite at lowest phi ratio due to the identification of Cu²⁺/Cu⁺. Finally, the prepared catalysts show a very high porosity that makes these catalysts particularly active in the reaction in exam. All the consideration made on fresh catalysts cannot give clear info about the really behavior of the catalysts during the reaction. In matter of fact, the catalysts, during the reaction, are in

pre-reduced form and, thus, the active phase could be very different by the once identified on fresh catalysts. The use of in-situ investigation in conjunction with the results of activities and selectivities can help to the well interpretation of the obtained results. The ethanol decomposition was studied also on copper metallic phase, to understand the contributing of this metal in the ethanol decomposition reaction. In Figure 15 the profile of activity and selectivity has been reported.

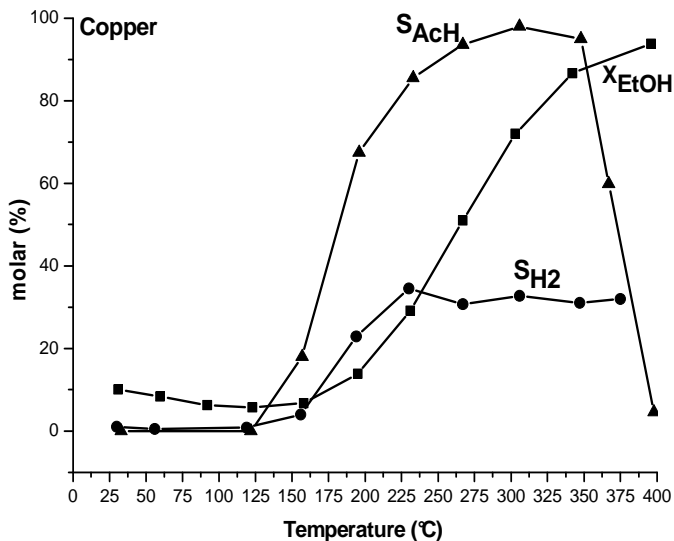


Figure 15: activity and selectivity respectively to hydrogen and acetaldehyde for metallic copper in ethanol decomposition reactions.

At low temperature ($T < 150^{\circ}\text{C}$) the copper activity is in truth poor. Only at a temperature higher than 250°C a modest activity, 40%, is detected. The scarce activity of the copper is due to the high endothermicity of ethanol decomposition reaction. At low temperature, less than 250°C , the acetaldehyde selectivity is very high of about 90%. This feature reflects the dehydrogenating character of

the copper. Another aspect should be considered, on the basis of the thermodynamic study realized on the dehydrogenation reaction (see chapter3-section B), the fact that, despite of low temperature the acetaldehyde is produced with high selectivity. This contradiction could be justified by the infinite residence time assumed in Gibbs free energy minimization. As matter of fact, all the runs reported in this chapter were performed at a very low ethanol residence time of about 0.18 ghmol^{-1} . By comparing the results obtained respectively with commercial and prepared by combustion catalysts, about the activity and selectivity performances, to the one obtained with pure metallic copper, it would be demonstrate its the contribute in the final results. As matter of fact, all the catalysts are active for ethanol decomposition at $T > 250^\circ\text{C}$, except CuCr-3.0 the less active. Mainly the activity of all the examined system is due to the contributing of metallic copper on the catalysts surface. The catalysts selectivity, in turn, varies with the fuel to oxidizer ratio and the presence of Cr or Zn. The use of two different promoters could give different performances in terms of hydrogen and acetaldehyde selectivity. As shown by the obtained results the unsupported CuCr-0.8 and the supported version CuCr/Al are the most active and selective catalysts. The performances of these catalysts are comparable with the corresponding commercial ones, respectively, T-4466 and Cu-1234.

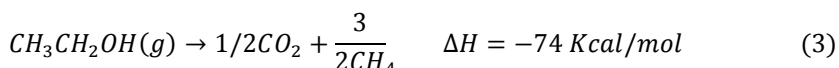
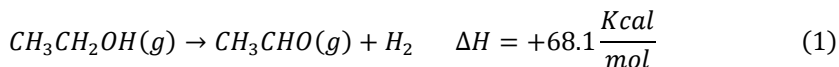
Surely, a better way to understand the behavior of the catalysts during the reaction is the use of in-situ characterization. In-situ XANES, contrary to ex-situ investigations, indicates that there is a significant difference in oxidation state between the fresh samples and those reduced before, during, and after reaction. Moreover, the CuCr-0.8 catalyst shows the presence of a mixed $\text{Cu}^0/\text{Cu}^{+1}$ mixture, whereas the other catalysts show mainly the presence of Cu^0 .

In addition, the in-situ FTIR could give a suggestion about such a possible pathway of reaction. Several adsorbed species have been detected such as OH^- , COO^- , CO and CO_2 as well as $-\text{CH}_3$ and C_2H_2 . The results have been studied in deep by examining the behavior of these adsorbed species on the catalysts surface. In particular, by increasing the reaction temperature, the ethanol adsorption peaks disappear in favor of the acetaldehyde and esters adsorption. While, all the above products are detected in the gas phase and as adsorbed species by FTIR, the reaction pathways involves the formation of partially dehydrogenated intermediates and the breaking of different bonds such as C-C, COO, C-OH and C-H bonds requiring different type of sites. After this overview about the main results obtained, a more detailed examination on the overall results has been made.

By examining each system, one clear result is the activity-selectivity of the CuCr-3.0 which appears correlated with the larger crystallite sizes in this catalyst as detected by XRD, SEM, and its low BET area. The presence of Cr_2O_3 in this catalyst, which is difficult to reduce, is also consistent with studied showing high decarbonylation activity [16-18]. It follows that the excess fuel used in the preparation of CuCr-3.0 led to a temperature increase during combustion synthesis that resulted in larger crystallites with fewer selective active sites for ethanol adsorption-formation of ethoxy and acetaldehyde intermediates followed by dehydrogenation. On the opposite side of the activity-selectivity results are those of CuCr-0.5 catalyst which although active, has low hydrogen selectivity but instead high acetaldehyde selectivity and high surface area. In this case, in-situ XANES shows that a reduced Cu phase is present during reaction, which is consistent with the well-known selectivity of Cu towards acetaldehyde formation [3,19]. Unfortunately, due to its dark color the FTIR results on this sample are too weak to show a good correlation with the adsorbed acetyl species.

CuCr-0.8 has intermediate properties but show higher activity towards hydrogen production and exhibits a distinct mixture of Cu^0 and Cu^{+1} oxidation states during reaction. The CuCr/Al catalyst exhibits similar XANES spectra than the CuCr-0.5 catalyst, whereas one would have expected more similarities with CuCr-0.8 due to its similar synthesis conditions activity-selectivity behavior. The nature of photoelectron emission detected in the XANES spectra is different in unsupported and supported samples because since X-rays are used in this method, the unsupported material reflects more bulk properties whereas the supported one are more surface because of its higher dispersion on the alumina support. Due to the noisy signal of the results obtained in the bending magnet beam line EXAFS fits were not reliable to estimate coordination numbers. CuCr/Al, while exhibiting similar oxidation state than the bulk of CuCr-0.5 it should have exhibited some Cu^{+1} sites similar than CuCr-0.8 based on the similar activity selectivity behavior. It follows that such sites are probably located on the surface of the dispersed phase and are not detected by the XANES results. As demonstrated in literature works^{18,19} [18-19] the ethanol is mainly adsorbed on Cu^0 phase and then easily dehydrogenated to acetyl species derived by adsorbed acetaldehyde. This aspect, demonstrated also by our results obtained by studying the metallic copper behavior, emerges by Figure 15.

The metallic copper favors the hydrogen selectivity (30%) at a temperature of about 200°C. The main co-product of reaction, in all the runs performed, is acetaldehyde that in turn could decomposes at high temperature to give hydrogen and carbon monoxide. Relatively scarce amount of methane, carbon dioxide have also been observed. To well understanding the products formation, the stoichiometric reactions involved in ethanol decomposition and the corresponding heats of reaction are as follows:



In addition, ethanol and acetaldehyde can undergo to further oxidation and decomposition by gas phase or adsorbed oxygen to yield CO₂ and water. The methane selectivity at temperature higher than about 300°C is about 27-30% and the other main product of reaction is CO (23-26%), according to the reaction (4). This behavior is due to the acetaldehyde decomposition affected by the high temperature and in agreement with the work of Luengo et al. [20], in which has been described that both Cu and Cr are responsible for the subsequent alcohol decomposition into CO and H₂.

Reactions leading to carbon formation also occur, especially at high temperature. While all the above products are seeing in the gas phase and some as adsorbed species by FTIR, the reaction pathways involves the formation of partially dehydrogenated intermediates and the breaking of different bonds such as C-C, COO, C-OH and C-H bonds requiring different type of sites. In addition there are multiple phases in these catalysts involving several oxidation states so more than one site could be involved. This is a complex reaction network, involving multiple sites that would require detailed kinetic evaluation to correlate quantitatively active sites and material properties with the activity-selectivity trends. In addition, in spite of the various characterization methods utilized, each requires different conditions, like the ex-situ XRD vs. the more complicated in-situ experiments. Each method probe different properties and material volumes giving results that appear inconsistent, so only qualitative conclusions can be

reached. The activity-selectivity of the CuCr-3.0 appears to correlate well with the larger crystallite sizes in this catalyst as detected by XRD, SEM, and its low BET area. The presence of Cr_2O_3 in this catalyst is also consistent with studied showing high decarbonylation activity [16-18]. It follows that the excess fuel used in the preparation of CuCr-3.0 led to temperature increases during combustion synthesis that resulted in larger crystallites with fewer selective active sites for ethanol adsorption-formation of ethoxy and acetaldehyde intermediates followed by dehydrogenation.

On the opposite side of the activity-selectivity results are those of CuCr-0.5 catalyst which although active, has low hydrogen selectivity but instead high acetaldehyde selectivity and the highest surface area among the unsupported catalysts. In this case, in-situ XANES shows that a reduced Cu phase is present during reaction, which is consistent with the well-known selectivity of Cu towards acetaldehyde formation [19]. Unfortunately, due to its dark color the FTIR results on this sample are too weak to show a good correlation with the adsorbed acetyl species. CuCr-0.8 has intermediate properties but show higher activity towards hydrogen production and exhibits a distinct mixture of Cu^0 and Cu^{+1} oxidation states during reaction. Previous studies in our group show that the more selective catalysts for hydrogen production show a mixture of oxidation states. The CuCr/Al catalyst exhibits similar XANES spectra than the CuCr-0.5 catalyst, whereas one would have expected more similarities with CuCr-0.8 due to its similar synthesis conditions activity-selectivity behavior. The excitation volume of x-ray absorption detected in the XANES spectra is different in unsupported and supported samples because X-rays absorption in the unsupported material reflects more bulk properties whereas in the supported one it reflects more surface properties because of its higher dispersion on the alumina support. Due to the noisier signal of the

results obtained in the bending magnet beam line, EXAFS fits were not reliable to estimate coordination numbers. CuCr/Al, while exhibiting similar oxidation state than the bulk of CuCr-0.5 should have exhibited some Cu^{+1} sites similar than CuCr-0.8 based on the similar activity selectivity behavior. It follows that such sites are probably located on the surface of the dispersed phase and are not detected by the XANES results. As reported using in-situ FTIR studies Zhang et al [6] shows that ethanol is mainly adsorbed on reduced Cu^0 phase and then easily dehydrogenated to acetyl species derived from adsorbed acetaldehyde. Colley et al [19] used TPR-TPD to study a copper chromite catalysts previously reduced in hydrogen flow. After that, a 12% $\text{C}_2\text{H}_5\text{OH}/\text{He}$ stream was fed to the reactor. The cracking patterns of the reactant ethanol ($\text{C}_2\text{H}_5\text{OH}$) and product ethyl ethanoate ($\text{CH}_3\text{CO}_2\text{C}_2\text{H}_5$) together with those of possible intermediates e.g., (CH_3CHO , ($\text{CH}_3\text{COC}_2\text{H}_5$ and crotonaldehyde) were all determined on the mass spectrometry, by which studies details on the elementary steps of reaction on copper/chromia catalysts was deduced. The existence of CuCr_2O_4 phase might contribute to the dispersion and stabilization of Cu^0 phase in Cu-Cr and suppress or limits the catalyst deactivation. Thus the Cu- CuCr_2O_4 are both active phase for the first step of ethanol decomposition to acetaldehyde and esters (ethyl acetate) compounds. The formation of the above mentioned compound has been confirmed by the in-situ DRIFT spectra. The chromia sites probably break the C-H and C-C bonds of adsorbed ethoxy that further decomposes to form hydrogen, methane and CO and consequently the acetaldehyde selectivity decreases by increasing the reaction temperature as confirmed for the copper-chromite catalysts (Figure 7). These results are in perfect agreement with those reported in the literature [21-23], in which is demonstrated that is generally accepted that Ni promotes C-C bond scission whereas

additives like Cr, Cu are the active agents for subsequent oxidation to produce CO and H₂. Freni et al. [24] found that the copper chromite exhibited high activity and selectivity to H₂ due to the lower tendency of Cu to re-oxidize during the reaction. These aspects have been demonstrated by our investigations and the low tendency of metallic copper to re-oxidize during the reaction and after exposure to the air (150 min) have been demonstrated by XANES spectra (Figure 5), in which the oxidation state of the catalyst during the reaction and after next exposure to the air have been shown. The copper oxidation state of all the fresh catalysts is +2 and +1. The XANES spectra of copper chromite catalysts have shown that after reduction and ethanol reforming the oxidation state of the copper is Cu⁰ or Cu⁺¹. These active phase have shown a high selectivity to acetaldehyde and hydrogen, as demonstrated in a previously study [3]. On the other hand, the nature of the support affects the performance of the catalyst, especially coke formation. Acidic supports, such as γ - alumina favors ethanol dehydration resulting in the formation of ethylene, which is a coke precursor. Dehydration can be reduced by using basic supports such as ZnO [25,26]. The DRIFT spectra suggest a possible mechanism of involving ethanol adsorption, decomposition to ethoxy intermediate that in a second step of reaction could transform to aldehydes and acetate, by reaction with adsorbed acetaldehyde species at higher temperature. These species at temperature higher than 300°C decompose to give hydrogen and a series of undesirable reaction products. Chromia has a role of structural promoter its presence prevents the copper mobility on the catalysts surface [22,23]. Moreover, the use of chromia as promoter has the effect to decrease deactivation due to C formation, commonly obtained in CuNiFe catalysts in which the selectivity decreased drastically with TOS although the conversion stays nearly constant. The reduction of coke

formation is due to the basicity of chromium oxide that could create a good environment to reduce the coke deposition principally favored by acidic Bronsted sites [6]. In summary, the picture that emerges from this study is the formation of reduced Cu probably on the surface of CuCr_2O_4 . Ethanol interacts preferentially with Cu and form ethoxy species that decompose sequentially to the various products observed. The presence of chromia provides structural stability to Cu sites and in addition reduces coke formation.

C-3.6 References

- [1] Kansin et al. Russian Journal of General Chemistry, 2008, Vol. 78, No. 11, pp. 2203–2213.
- [2] R.B.C Pillay Catalysis Letters 26 (1994) 365–371
- [3] A.Kumar, A.S.Mukasyan, E.E.Wolf, under revision, submitted to Applied Catalysis.
- [4] A. Kumar et al. / Applied Catalysis A: General 401 (2011) 20– 28
- [5] Brooks, A. R.; Clayton, C. R.; Doss, K.; Lu, Y. C. J. Electrochem.Soc. 1986, 133, 2459.
- [6] M.Zhang, G.Li H.Jiang, catal.lett. (2011) 141:1104-1110
- [7] J. Llorca et al. / Journal of Catalysis 227 (2004) 556–560
- [8] A. Yee, S.J. Morrison, H. Idriss, J. Catal. 186 (1999) 279.
- [9] G.B. Deacon, R.J. Phillips, J. Coord. Chem. Rev. 33 (1980) 227.
- [10] H. Idriss, C. Diagne, J.P. Hindermann, A. Kiennemann, M.A. Barteau, J. Catal. 155 (1995) 219.
- [11] Rostrup-Nielsen, J.R., Conversion of hydrocarbons and alcohols for fuel cells, Phys. Chem. Chem. Phys., 3, 283–288, 2001.
- [12] Iwasa, N. and Takezawa, N., Reforming of ethanol. Dehydrogenation to ethyl acetate and steam reforming to acetic acid over copper-based catalysts, Bull. Chem.Soc. Jpn., 64, 2619–2623, 1991.
- [13] E.Santacesaria, S.Carrà, Applied catalysis, 5, 345-358 (1983)
- [14] M. Turco et al. / Journal of Catalysis 228 (2004) 43–55.

- [15] Prasad Bulletin of Chemical Reaction Engineering & Catalysis, x (x), 2011, p.1 - p.51.
- [16] Igdon, B. W.; Hobbs, C. C.; Onore, M. U. U.S. Patent 3812210, 1974.
- [17] Stephen P. Tonner, David L. Trlmm, and Mark S. Walnwrlght, Ind. Eng. Chem. Prod. Res. ev. 1984, 23, 384-388.
- [18] M.Zhang, G.Li H.Jiang, catal.lett. (2011) 141:1104-1110
- [19] Colley SW, Tabatabei J, Wang KC, Wood MA (2005) J.Catal. 236:21-33
- [20] C.A. Luengo, G. Ciampi, M.O. Cencig, C. Steckelberg, M.A. Laborde, Int. J. Hydrogen Energy 17 (9) (1992) 677–681.
- [21] Klouz, V., V. Fierro, P. Denton, H. Katz, J.P. Lisse, S.B. Mauduit and C. Mirodatos, 2004, J. Power Sources, 105, 26.
- [22] Comas, J., F. Marino, M. Laborde and N. Amadeo, 2004, Chem. Eng. J., 98, 61.
- [23] Fastikostas, A.N. and X.E. Verykios, 2004, J. Catal., 225, 439.
- [24] Frusteri, F., S. Freni, V. Chiodo, L. Spadaro, O. Di Blasi, G. Bonura and S. Cavallaro, 2004a, Appl. Catal. A: Gen., 270, 1.
- [25] Aupretre, F., C. Descorme and D. Duprez, 2002, Catal. Commun., 3, 263.
- [26] Fierro, V., O. Akadim, H. Provendier and C. Mirodatos, 2005, J. Power Sources, 145, 659.
- [27] M.Zhang, G.Li H.Jiang, catal.lett. (2011) 141:1104-1110

SECTION C

Conclusions

As shown by the literature investigation the commonly catalytic phases employed for the hydrogen production by steam reforming, steam oxidative or partial oxidative reforming are copper, nickel, ruthenium and platinum. In this research, we focused our attention on the performances of copper based catalysts promoted with chromia and zinc oxide prepared by combustion synthesis. Recently, combustion synthesis techniques have gained attention for material synthesis on account of being an economical, fast, and energy efficient process. Typically, CS involves a self-sustained reaction in a solution of metal nitrates and an oxygen containing fuel. The reaction between the fuel, oxygen, and specie formed during decomposition of nitrates provides conditions for rapid high-temperature propagating reacting front and the final combustion products are a metal oxide.

We use combustion synthesis techniques to prepare catalysts for hydrogen production from ethanol reforming reactions. SCS is energy efficient and less time consuming process in comparison to other techniques such as co-precipitation, which requires the separation of products after precipitation. Furthermore, in co-precipitation, these products are calcined separately, which leads to sintering and a decrease in the surface area. The potential advantage of CS is that it can yield oxides with larger surface areas than co-precipitated-calcined catalysts. Apart from its simplicity and rapidness, SCS has other advantages. The combustion is exothermic, which in some cases can result in local temperatures as high as 1000 °C that can provide enough energy to evaporate volatile impurities as well as for

calcination of the product. Thus a pure crystalline product is obtained in a single step avoiding any other thermal treatment. Also, all other reaction products, except the metal oxide, are gas phase products which form channels while escaping, contributing towards the porosity of the solid products and potentially to a higher surface area. In particular active and selective copper-zinc and copper-chromite based catalysts for ethanol decomposition and oxidative reforming were prepared by using combustion synthesis. The catalysts preparation, the use of Zinc or Chromia as promoters, and the use supports have a significant effect on the activity and selectivity of the catalysts. The investigation on the use of an optimum ratio the fuel/oxidizer suggests the possibility, as demonstrated by ex-situ characterization, to have catalysts with a particular morphology, oxidation state and specific surface area. All catalysts are active for ethanol decomposition at $T > 250^{\circ}\text{C}$, except for the catalyst prepared by using an high ratio glycine/fuel. On the other hand the catalysts selectivity varies with the fuel to oxidizer and the presence Zn. The unsupported CuCr-0.8 and the supported version CuCr/Al are the most active and selective catalysts. The supported CuCr/Al catalyst, while it deactivates with TOS it maintains its selectivity in a 25 h TOS run. The activity can be recovered by re-reduction. The ex-situ characterization has suggested differences in oxidation state between the fresh samples and those reduced before, during, and after reaction. The CuCr-0.8 catalyst shows the presence of a mixed $\text{Cu}^0/\text{Cu}^{+1}$ mixture, whereas the other catalysts show mainly the presence of Cu^0 . The DRIFT investigation suggested the formation of several species adsorbed on the catalyst surface that at higher temperature could decompose by forming coke that could deactivate the catalysts surface. Chromia improves the catalyst stability by limiting coke deposition on the catalysts surface. In addition the use of alumina as support is useful to disperse the active phase. The partial oxidative reforming of ethanol, i.e in the presence

of oxygen at lower than the stoichiometric values, could be an alternative to the reforming reaction.

GENERAL CONCLUSION

By concluding, as well understood by our research, the future goal is to convert biomass into products that can compete with corresponding products derived from fossil resources with a focus on sustainability, resource availability and supply reliability. At this purpose, the use of bio-ethanol produced by second generation raw materials represents actually the great challenge of the research world. Since, by future forecasts, the quantity of ethanol will be in the last few years increasing, its use as “future building blocks” will be useful to produce chemicals.

At this purpose, the research work, described in this thesis, has shown the wide range of application of bioethanol and in particular its use for the production of high commodities chemicals, such as acetaldehyde and ethyl acetate, and moreover of pure hydrogen. As well known, about 90 % of chemicals are nowadays produced *via* a catalytic process and in this thesis, several heterogeneous phases have been studied. In particular the performances of two different phases, vanadia and of copper based catalysts, have been investigated in the oxidative dehydrogenation reaction (ODH), dehydrogenation at low and high pressure. Finally the copper chromite performances have been evaluated also in the ethanol partial oxidative reforming (OPX) to produce hydrogen.

The individuation and use of efficient heterogeneous catalytic systems represent a great challenge and their design is crucial to promote innovations in the chemical industry.

The heterogeneous systems are characterized by a very complex architecture, referred to chemicals, structural and textural levels, which all have a deep impact on the final catalytic performances. This research has been provide to the understanding of the relationships between the textural and surface chemical properties of vanadia and copper based catalysts and their catalytic performances, by investigating mainly the effect of preparation method, of the reaction temperature, pressure, ethanol residence time, oxygen concentration and hydrogen partial pressure on the catalytic behaviour.

The first part of this research works was entirely dedicated to the examinations of the catalytic performances of V_2O_5/TiO_2-SiO_2 prepared by grafting in the ethanol ODH. Moreover the performances of Cu/ZnO , Cu/ZrO_2 and of commercial $Cu-ZnO-Al_2O_3$ (K-310) have been studied at low pressure ethanol dehydrogenation reaction. In each mentioned case the interest is focused on the production of acetaldehyde. Indeed, the interest toward the acetaldehyde is also due to its use for the production of ethyl acetate, ethylene, and acetic acid. The experimental results have shown that the redox mixed metal oxide V_2O_5/TiO_2-SiO_2 are very active and selective catalysts in the oxidative dehydrogenation of the ethanol to acetaldehyde. In particular, by operating at relatively low residence time and at a temperature of 140-180°C, it is possible obtain ethanol conversion of about 80% and acetaldehyde selectivity of 90-95%. In particular, for the given support (TiO_2/SiO_2), the catalysts prepared by *grafting* resulted more active and selective and this behaviour would be find enlightenment in the higher surface molecular dispersion of vanadium sites that is possible to achieve by using the grafting preparation method. A high surface dispersion of supported vanadium sites is fundamental to improve both the activity and the selectivity to the desired products. It was found that the coating of the silica carrier with a monolayer of TiO_2 increases the vanadia active phase dispersion and consequently the selectivity towards the desired reaction product. As demonstrated in previous works, conducted in this research group, by

supporting directly the vanadia on the silica, due to the effects of the strong acidic sites of the support, the vanadia can agglomerate on the support surface and for this particular reason the Titania was used. On the other hand the use of silica as support is fundamental to preserve the mechanical and thermal strength of the catalysts. The results obtained into ethanol dehydrogenation by using copper based catalysts are very promising but, because of the high endothermicity of the reaction, a higher range of temperature should be used to sustain the reaction. An interesting result is associated to the production of small amount of ethyl acetate by using of copper based catalysts in low pressure dehydrogenation reaction in one step reaction. At this purpose the research, in a second phase, was dedicated to the development of a new process for the ethyl acetate and pure hydrogen production directly by ethanol in only one step dehydrogenation reaction by using copper commercial catalysts. The ethanol dehydrogenation is in general a low selectivity reaction and the C₃-C₄ products derived by the acetaldehyde condensation can shatter the industrial target of purity required. The Davy solved this problem by using a further reactor of hydrogenation of C₃-C₄ aldehydes and ketones to the corresponding alcohols that can easily separate, in the purification section, from ethyl acetate. The section B represents the core of this research work in which has been illustrated very interesting and innovative results. All the paths followed to realize an innovative industrial process from the laboratory, to the kinetic study toward the final industrial plant design proposal have been illustrated in detail in each chapter of this section. Interesting results of selectivity and activity have been obtained in particular operative conditions by using a commercial copper chromite catalyst (Cu-1234) able to convert ethanol 65% to ethyl acetate, with a selectivity of 97.8%. According to the obtainment of high selectivity results during the dehydrogenation step, the use of a further hydrogenating reactor was ruled out. Thus, the key factor of our invention is the development of an innovative simplified process to

produce ethyl acetate by ethanol in one step reaction. The main peculiarities of this process is related to the use of a copper/copper chromite catalyst, containing an opportune support, like alumina, and different structural promoters such as barium oxide and chromium oxide, having as main scope the prevention of the sintering of the metals and the subsequent catalyst deactivation. Moreover these oxide are able to create an acid-base environment favorable to the desired reaction. We have observed, in agreement with the current literature, that the operative conditions are very important for obtaining high activities and selectivities. In particular, at low pressure (1-5 bars) acetaldehyde is the main reaction product but moderately increasing the pressure up to 20-30 bars the selectivity is shifted toward the formation of ethyl acetate as main product. Afterword, by operating in the conditions unfavorable to ethyl acetate formation, the selectivity could be lowered by the presence of a competitive reaction pathway originated by the acetaldehyde self-condensation. At last, it is important to point out that activity and selectivity are also promoted by the hydrogen partial pressure. Hydrogen keep the catalyst in the reduced form and limit the acetaldehyde formation maintaining low its concentration so disfavoring the auto-condensation. This last observation opens the possibility in an industrial plant to use a stream of recycled hydrogen as carrier gas. Finally, in this process pure hydrogen (exempt of CO) is produced in mild conditions as by products. With the aim to sizing the reactor modeling, several kinetic models have been study and as demonstrated the Langmuir-Hinshelwood-Hougen-Watson (LHHW) is the ones to well fitting the experimental kinetic runs. It has been shown that the runs with the lowest amount of catalyst have been performed in chemical regime and have been used to identify the best kinetic model, while, the runs performed with 50 g of catalyst give data that are near the equilibrium conditions and allow to verify both the model goodness and the validity of the equilibrium constants. The obtained agreements are satisfactory, considering the approximations

introduced as the assumption of isothermal conditions and the use of the equilibrium constants directly derived from theoretical calculations. Nevertheless, in a first phase of this work a simplified power law was used at first to realize the sizing of the plant equipment. As already mentioned, the proposed new ethyl acetate process produces a high quality ethyl acetate product without, in spite of the already commercialized Davy proves, the use of hydrogenation unit, necessary to convert MEK or C₃-C₄ in ethanol. Thus, the proposed process is more simple and able to produce high quality ethyl acetate in only one step of reaction. Furthermore, the use of pressure changes to break the ethyl acetate/ ethanol / water azeotrope leads to an inherently cleaner product than processes such as esterification or direct addition that operate separation systems in water rich regions of the phase diagram. The scale up of this process, on the basis of the obtained results, should be improved and refined, possibly by using kinetic laws able to describe as well the experimental data and devoting a greater attention to the purification sections that should be analyzed and evaluated in all their peculiarities in more detail. The development and use, of an adequate kinetic expression, is necessary, fundamental to develop tubular, and multiple adiabatic bed reactor models. On the basis of the obtained results, in terms of hydrogen productivity, in the high pressure ethanol dehydrogenation, the last section of this research work was addressed to the investigation of the performances of copper chromite and copper-zinc based catalysts, prepared by using the innovative combustion synthesis, in the partial oxidative reforming (OPX) reaction to produce hydrogen. The combustion synthesis techniques have gained attention for material synthesis on account of being an economical, fast, and energy efficient process. Typically, CS involves a self-sustained reaction in a solution of metal nitrates and an oxygen containing fuel. The reaction between the fuel, oxygen, and specie formed during decomposition of nitrates provides conditions for rapid high-temperature propagating reacting front and the final combustion products are a metal oxide. The CS is

energy efficient and less time consuming process in comparison to other techniques such as co-precipitation, which requires the separation of products after precipitation. Furthermore, in co-precipitation, these products are calcined separately, which leads to sintering and a decrease in the surface area. The potential advantage of CS is that it can yield oxides with larger surface areas than co-precipitated-calcined catalysts. Apart from its simplicity and rapidness, SCS has other advantages. The combustion is exothermic, which in some cases can result in local temperatures as high as 1000 °C that can provide enough energy to evaporate volatile impurities as well as for calcination of the product. Thus a pure crystalline product is obtained in a single step avoiding any other thermal treatment. Also, all other reaction products, except the metal oxide, are gas phase products which form channels while escaping, contributing towards the porosity of the solid products and potentially to a higher surface area. In particular active and selective copper-zinc and copper-chromite based catalysts for ethanol decomposition and oxidative reforming were prepared by using combustion synthesis. The catalysts preparation, the use of Zinc or Chromia as promoters, and the use supports have a significant effect on the activity and selectivity of the catalysts. The investigation on the use of an optimum ratio the fuel/oxidizer suggests the possibility, as demonstrated by ex-situ characterization, to have catalysts with a particular morphology, oxidation state and specific surface area. All catalysts are active for ethanol decomposition at $T > 250^{\circ}\text{C}$, except for the catalyst prepared by using an high ratio glycine/fuel. On the other hand the catalysts selectivity varies with the fuel to oxidizer and the presence Zn. The unsupported CuCr-0.8 and the supported version CuCr/Al are the most active and selective catalysts. The supported CuCr/Al catalyst, while it deactivates with TOS it maintains its selectivity in a 25 h TOS run. The activity can be recovered by re-reduction. The ex-situ characterization has suggested differences in oxidation state between the fresh samples and those reduced before, during, and after reaction. The CuCr-0.8 catalyst

shows the presence of a mixed C^0/Cu^{+1} mixture, whereas the other catalysts show mainly the presence of Cu^0 . The DRIFT investigation suggested the formation of several species adsorbed on the catalyst surface that at higher temperature could decompose by forming coke that could deactivate the catalysts surface. Chromia improves the catalyst stability by limiting coke deposition on the catalysts surface. In addition the use of alumina as support is useful to disperse the active phase. The partial oxidative reforming of ethanol, i.e in the presence of oxygen at lower than the stoichiometric values, could be an alternative to the reforming reaction.

By concluding this PhD thesis highlights the main results obtained are related to development of a new process for the ethyl acetate and pure hydrogen production by using of copper/copper chromite catalysts in only one step ethanol dehydrogenation reaction. The commercial copper catalyst Cu-1234 has shown surprising performances in terms of ethyl acetate selectivity and resistance to sintering, that represent the main drawback of the copper based catalysts. The use of chromia improves the structural properties of the catalyst and limits the copper mobility at temperature of almost 300°C. The very promising results should be induced to an improvement of the process plant design, proposed in a very simplified form in the last part of this thesis. Moreover, a preliminary study of the performances of copper-chromite catalysts in the OPX of ethanol to produce hydrogen was realized. Also in this case very interesting results have been obtained and the best operative conditions to obtain the higher yield to hydrogen have been distinguished. The use of copper chromite is in this case fundamental to limits the catalyst fouling due to the coke deposition.

APPENDIX A

Catalysts Characterization Techniques

A.1 Spectroscopic UV-Vis

A.1.1 Determination of titanium content

The quantity of Titania graphed on silica surface could be evaluated by using the colorimetric method UV-VIS proposed in literature[1,2]. The method consists in the formation of a yellow complex between the Ti and H_2O_2 in a solution of diluted sulphuric acid (0.75-1.75M). In a preliminary phase by using standard of titanium with a concentration of the element included in the range 10-40mg/mL H_2O , a calibration curve was built. By the curve it is possible calculate the concentration of titanium known the absorbance at 397 nm. The quantity of supported TiO_2 could be evaluated by both the filtration solution or directly on the solid sample, by using a mineralization procedure. In the first case a ratio 1:5 between the filtration solution and sulphuric acid 1.69M could be used. In the second case, the solid (0.1 g) should be firstly mineralized with 9.41 mL of H_2SO_4 (96 wt%), under stirring, at 180°C for 4 h. After the filtration, the solution was diluted with H_2O to 100 mL to obtain a solution with a concentration 1.69 M of H_2SO_4 .

¹ F.Snell and L.S.Ettré Enciclopedia of industrial chemical analysis vol 19 (1974) 107 interscience New York.

² I.M. Kolthoff and P.J.Elving: " Treatise on Analytical Chemistry", II, vol8 (1963).

In each case, by adding some drops of H_2O_2 , a complex was formed and individuated at ≈ 397 nm.

A.1.2 Determination of vanadium content

Also in this case the method employed to evaluate the quantity of vanadium supported on $\text{TiO}_2/\text{SiO}_2$ was evaluate by applying a colorimetric methodology [1,2]. In this case a complex red-brown between the vanadium and the hydrogen peroxide in a perchloric acid solution was formed and individuated at wavelength of $\lambda_{\text{max}}=460\text{nm}$. Also in this case the evaluation is quantitative and obtained by built a calibration curve. Several solution was prepared by dilution of a standard solution of $1020 \mu\text{g}/\text{mL}$ (Aldrich) with 10 mL of HClO_4 70% wt to 50 cm^3 of water. The complex was formed by using a solution at 35%wt of hydrogen peroxide.

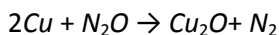
A.2 BET and pore size distribution.

The total area of the catalysts was evaluated by using two different apparatus Sorptomatic 1990 and Quantachrome Monosorb. The total area of the catalysts was measured on a direct reading dynamic flow surface area analyzer (Quantachrome Monosorb) using a single point N_2 isotherm, operating at a nitrogen partial pressure of 0.3 in He. Approximately 50 mg of sample is placed in a U-tube and out-gassed in the built-in degassing instrument port at 200°C for 1 h prior the measurement. This pretreatment assures that weakly adsorbed water and other adsorbates are fully eliminated from the sample surface. Then the dried sample is moved to the adsorption port where, after flowing a mixture of 30% N_2/He , the sample in the U-tube is immersed in a liquid nitrogen bath to allow nitrogen condensation on the sample surface. After reaching equilibrium, the liquid nitrogen dewar is removed and the sample is exposed to room temperature causing the physisorbed nitrogen to be desorbed from the sample

surface. The total volume of nitrogen released from the sample is detected by a thermal conductivity detector and a built-in integrator automatically computes the total specific surface area, S_g . Such value is calculated as $S_g = v_m N_A N_2 / V$, where v_m is the monolayer volume of the adsorbed gas as calculated from the BET isotherm, N is the Avogadro's number, AN_2 the adsorption cross section of a N_2 molecule, and V is the molar volume of nitrogen. The resulting specific surface area, S_g , is divided by the amount of mass used in the analysis and the BET area is obtained. The analysis was repeated for each sample several times to ensure reproducibility. In the case of Sorptomatic the solid were degased overnight at 180°C under vacuum. By using this instrument the pore size distribution was also evaluated.

A.3 Copper dispersion TPO-N₂O

The determination of the copper surface area and copper dispersion has been performed, with the N₂O method. A known amount of the catalyst, about 100 mg, was first of all reduced with a flow stream of 25 cm³/min of a mixture of 5% v/v H₂ in N₂ at 300°C for 2 hours. Afterwards, a flow stream (45 cm³/min) of pure N₂ was sent for about 20 minutes to remove residual hydrogen and water and then the catalyst was cooled to 60°C maintaining constant this temperature during the oxidation experiment. The N₂O experiments were conducted using a pulse method. Precisely several pulses of 1 cm³ of 5% N₂O in N₂ were injected into a carrier stream of N₂ flowing at 50 cm³/min until no further N₂O was reacted. Uptake of N₂O was monitored with a gold plated tungsten filament thermal conductivity detector (TCD) with a current of 130 mA. Dispersion and Cu specific surface area were calculated assuming a Cu surface atomic density of 1.47*10¹⁹ atoms/m². Mean and specific Cu surface areas were measured by a well-known chemisorption method where N₂O reacts with surface CuO with the following stoichiometry:



After that, the sample was subjected to hydrogen flow to reduce the surface. Precisely, the experiments have been conducted by using a constant flow of 5% of H_2 in Argon. About 6-8 areas, corresponding to the oxidation of the reduced surface, have been collected until the area of the chromatograms were constant and a maximum area has been achieved. The loop volume in which the N_2O is collected, first to be sent on the sample by using an automatically six way valve, is of about 1cc. Once known the areas related to the completely oxidation of copper is possible define the volume of hydrogen adsorbed by the following equation:

$$\text{Volume of } H_2\text{ads} = \frac{\sum(A_{max} - A_i)}{A_{max}} * \text{Loop Vol} * \%H_2 \text{ in Ar}$$

The dispersion of copper is expressed by the ratio between the mols of copper exposed divided by the mols of copper loaded.

$$\text{Cu dispersion} = \frac{n_{\text{Cu exposed}}}{n_{\text{Cu loaded}}}$$

By considering a temperature of 25°C a pressure of hydrogen of 1 bar is possible to calculate the mols of copper exposed.

$$n_{\text{Cu exposed}} = 2 \text{ mol } H_2\text{ads} = \left(\frac{P_{H_2} * V_{H_2\text{ads}}}{R_{\text{gas}} * T} \right)$$

For 100g of catalysts the mols of copper loaded are expressed by the equation x, function of the total mols of copper, obtained known the composition of the catalysts, of the molecular weight of copper, of the grams of catalyst charged into the oxidation reactor (about 0.1g).

$$n_{\text{Cu loaded}} = \frac{n_{\text{Cu Tot}} * PM_{\text{Cu}} * g_{\text{cat}}}{100 \text{ g cat}}$$

The copper specific surface areas were calculated assuming a Cu surface atomic density of 1.47×10^{19} atoms·m⁻² as it follows:

$$\text{Copper specific surface area} \left[\frac{\text{m}^2}{\text{g}} \right] = \frac{1}{g_{cat}} \left[\frac{\text{atoms Cu}}{\text{Cu atomic density}} \right]$$

Where the atoms of Cu have been calculated by considering the number of Avogadro 6.023×10^{23} and the mols of copper exposed.

$$\text{atoms Cu} = N_{\text{avogadro}} * \text{mols Cu exposed}$$

A-4 Crystalline structure characterization. X-ray diffraction spectroscopy (XRD)

X-ray analysis of powders is a technique extensively used for characterization and identification of polycrystalline phases. Incident X-rays waves interact with atoms in crystalline structures causing destructive and constructive interference of the reflected beam, resulting in the appearance of diffraction lines. This phenomenon occurs because X-rays with short wavelengths in the keV range have wavelengths that are approximately of the same order of magnitude of atomic distances in crystalline solids. Since the arrangement of atoms varies for different crystal structures, the diffraction patterns are characteristic of the solid and widely used to identify bulk materials. If we assume that atoms are ordered in sets of symmetrical planes forming lattices, then, for a set of planes with an inter-plane distance “d”, the condition for a diffraction to occurs is $2dsin\theta=n\lambda$, which is known as Bragg’s law. In this equation, λ is the wavelength of the x-ray, θ the scattering angle and n is an integer representing the 14 order of the diffraction peak. If the angle is varied, a set of sharp lines are observed for a single crystal. In samples in the form of powder, a small fraction of atoms in the sample will be oriented in such a way

that a certain crystal plane will be at the right angle with the incident beam for giving constructive and destructive interference. The diffraction angle that allows having maximum diffraction in a sample enables one to calculate the spacing between the lattice planes and allows phase identification. Furthermore if the crystallites in a sample have sizes below 50 Å, the diffraction lines broaden up due to the elimination of crystal planes causing destructive interference. The width of a diffraction peak can be used to estimate the average crystallite size, D , according the Debye-Scherrer equation: $D = k\lambda/(\beta\cos\vartheta)$, where λ is the wavelength of the radiation (commonly $\lambda_{\text{Cu}} = 1.54056 \text{ \AA}$ for a Cu-K α radiation), β is the full width at half maximum of the diffraction peak in radians, ϑ is the position of the maximum diffraction, and the constant k is the Scherrer constant ($k = 0.89 - 1.39$). The x-ray diffractometer utilized in this work was a Scintag X-1 to produce Cu K α radiation at a wavelength of 0.1540562 nm. Approximately 100 mg of a finely crushed and sieved sample were homogenously dispersed onto a silica or glass holder. The diffracted x-rays from the sample were detected by a Peltier cooled solid-state detector moving in a circular pattern (see Figure 2.1). 2θ scan angle was ranged from 20 degrees to 90 degrees with a step size of .05 degrees. Depending on the analysis the scan rate was constant at 0.1 degrees per second or 0.5 seconds per step.

A.5 Reducibility, basic and acid sites quantification TPR/ TPD-CO₂/ TPD-NH₃

The TPR experiments were carried out using a quartz U-tube reactor with an internal diameter of 10 mm. The powdered catalyst was loaded on a sintered quartz wool disk placed inside the reactor. The catalyst formed a bed of less than 5 mm in thickness (0.1-0.2 g) on which a glass wool plug was added. The samples were initially

pretreated in N_2 flow of $20 \text{ cm}^3/\text{min}$, at a temperature of 100°C , for about 1 h, to remove any trace of moisture. The samples were then cooled at room temperature. Always under nitrogen stream the temperature was then gradually increased with a scanning rate of $10^\circ\text{C}/\text{min}$ until reaching 300°C . After this pre-treatment the hydrogen TPR were performed using a flow stream of 6% of H_2 in N_2 ($60 \text{ cc}/\text{min}$). The gas stream was split in two flows one leading to the reference arm of a thermal conductivity detector (TCD) and the other one passing through the reactor before going to the detector. The water produced during the TPR was trapped by a dry trap located between the detector and the reactor. After the reduction pre-treatment the catalysts were subjected to a Programmed Desorption of NH_3 or to a Programmed Desorption of CO_2 to evaluate respectively the overall surface acidity and basicity of the studied catalysts. The overall surface acidity of the prepared catalysts was determined by a Temperature-Programmed Desorption of ammonia (NH_3 -TPD) in a fixed-bed continuous flow micro-reactor system. Before the NH_3 -TPD measurement, a sample of powdered catalyst ($0.1\text{-}0.2\text{g}$) was out-gassed in a flow of pure helium ($20 \text{ ml}/\text{min}$), at 300°C for 30 minutes. Then, the sample was cooled at 40°C and saturated with a stream of 10% NH_3 in He ($20 \text{ ml}/\text{min}$) for about 30 min. Afterward, the catalyst was purged in a helium flow until a constant baseline was attained. The ammonia desorption was determined in the temperature range of $40\text{-}500^\circ\text{C}$ with a linear heating rate of $10^\circ\text{C min}^{-1}$ in a flow of He ($10 \text{ ml}/\text{min}$). Desorbed NH_3 was detected by a thermal conductivity Detector (TCD). Then, the surface basicity of the prepared catalysts was determined by TPD of CO_2 performed in the same fixed-bed micro-reactor used for ammonia TPD. The fresh catalysts were subjected to a pre-reduction, as previously described. Before the CO_2 -TPD measurement, a sample of powdered catalyst ($0.1\text{-}0.2 \text{ mg}$) was out-gassed in a flow stream of pure helium ($20 \text{ ml}/\text{min}$), at 300°C for

30 min. Subsequently, the sample was cooled at 40 °C and saturated with a stream of CO₂ (10 ml/min) for about 30 min. Then, the catalyst was purged with a helium flow until a constant baseline level was attained. The carbon dioxide desorption was evaluated in the temperature range of 100–500 °C with a linear heating rate of 10 °C min⁻¹ in a flow stream of He (20 ml/min). Desorbed CO₂ was detected by a thermal conductivity detector (TCD).

A.6 Near surface structure analysis: X-ray photoelectron spectroscopy (XPS).

X-ray photoelectron spectroscopy (XPS) is a technique also based on photoelectron emission. This effect consists on the excitation of electrons from a sample subjected to electromagnetic radiation. As stated by the Einstein photoelectron law, the energy of the incident radiation must surpass a minimum energy in order to delocalize and eject inner electrons from the sample with a kinetic energy E_k .

$$E_k = h\nu - E_b$$

The binding energy of the excited electron, E_b , corresponds to the minimum energy required to eject the electron from the sample. The product between the Planck's constant (h) and the frequency of the incident photon (ν) is the energy of the x-ray striking the surface of the sample. Once the energy of the incident x-ray is bigger than the electron's binding energy, a core or valence electron will be emitted from the sample with a kinetic energy E_k . The emitted electrons are focused by an array of magnetic lenses into a series of slits on hemispherical electrodes. The concentric electrodes are set at a differential voltage that directs electrons with different kinetic energies to follow specific radii before reaching the detector. In this way the electrons are energetically dispersed and an energy spectrum can be recorded. An XPS spectrum consists of a set of peaks with

different intensities at different energies. Binding energies are characteristic of the elements under study and therefore each element provides electrons with specific kinetic energies, which allows direct identification of the atomic composition of materials. The intensity of each peak is proportional to the concentration of the corresponding atom. Therefore, quantitative information of the surface concentration can be also obtained from the XPS signal. Consider for example a copper sample subjected to x-rays of 1486.6 eV, which is the energy of a typical spectrometer using a monochromated Al K- α radiation. The complete electronic distribution on atomic Cu is $1s^2 2s^2 2p^6 3s^2 3p^6 3d^{10} 4s^1$ with a total of 29 electrons, but for simplicity Figure 2.5A shows only some of the quantized energy levels of Cu. Under such radiation electrons with binding energies lower than the incident beam are excited and removed from the corresponding orbital. Some of the removed electrons are backscattered into the unfilled orbitals while others are able to reach the Fermi level (Fermi energy is the energy of the highest occupied state at 0°K). Since the 2s electrons have lower energy than the incident x-ray, electron from the 2s orbital will be excited and removed from the 2s level. Alternatively, any other electron with a binding energy lower than 1486.6 eV will be excited as well. Since the incident energy is known, 1486.6 eV, the x-axis scale can be easily converted to binding energies, E_b , by using that $E_b = h\nu - E_k$. The differences in intensity for electrons from different energy levels are due to unequal probabilities for photoejection. The presence of gas in the analysis chamber can scatter the ejected electrons and hinder them from reaching the detector. Therefore, the quantification of the number of emitted electrons at each binding energy requires ultra-high vacuum conditions (UHV). Depending on the sample, the photo-emitted electrons reaching the vacuum are originated from a layer of approximately 10 nm of the sample. This is because the emitted photoelectrons have low kinetic energies (0 -

1500 eV) and the depth from which they can emerge is therefore very limited. For this reason, XPS is a surface-sensitive technique and the sample depth is in the range of few nanometers. X-ray photoelectron spectroscopy measurements were carried out in a Kratos XSAM-800 spectrometer utilizing Al-K α radiation source operating at 1486.6 eV and a 90-degree takeoff angle.. The binding energies (BE) were calibrated with the C 1s peak fixed at 285.0 eV as an internal reference standard. Fresh ground powder catalyst samples were adhered to brass mounts with double-sided carbon tape prior to loading into the analysis chamber. Samples were left to degas overnight while the vacuum system maintained a pressure less than 1×10^{-8} torr. Control and data collection was data was done using Vision2 software running on Sun workstations. Normally each element of interest was scanned 10 times with a range of ~ 20 eV and an acquisition time of ~ 1 minute, elements with low concentrations were scanned more times. Raw data was processed with CasaXPS software package, with relative sensitivity factors obtained from the Kratos XSAM library.

A.7 Surface topography characterization: Scanning Electron Microscopy (SEM)

Scanning electron microscope (SEM) provides images of magnified three-dimensional objects with high depth of field quality. An SEM microscope consists of an electron gun (tungsten filament) able to generate an electron beam in the range of energy of 0.1-30 keV. The generated electrons are accelerated by magnetic lenses, which direct the electron beam into a specific path downward the evacuated column (see Figure 2.6). 25

The vacuum inside the column, usually of about 10^{-6} torr, assures that the scattering of electrons by remaining gases inside the column is minimized. The magnetic lenses are able to focus the electron beam onto the specimen on a spot of less than 10 nm. A pair of scanning

coils causes the beam to deflect back and forth following a line pattern. One line is scanned after another until a rectangular region has been completely scanned. When the electron beam impacts the surface of the sample backscattered and secondary electrons escape from the specimen. Backscattered electrons are electrons from the beam able to escape the specimen because of elastic scattering. Secondary electrons are electrons from the specimen having enough kinetic energy, from the inelastic collision with electrons beam, to escape from the sample surface. These two types of electrons are collected by a positively charge detector. The detector consist of a scintillator that when struck with an energetic electron (~ 10 keV) photons are emitted. The emitted photons are directed to a multiplier and back converted into a current. This current differs depending of the energy of the electrons captured by the detector, which allows forming a contrast image map of the specimen surface. Prior the analysis the samples were finely grounded and mounted in a carbon tape on the specimen holder. Alternatively, to improve the particle dispersion on the holder, 2 mg of the grounded sample was diluted in distilled water. Then, a drop of this suspension was set on the clean holder surface and evaporated at room temperature. The analysis was done in Magellan field emission SEM at 30 keV under a vacuum of 10^{-6} torr.

A-8. Nearest neighbor characterization by Extended X-ray Absorption Fine Structure (EXAFS)

X-rays are an important tool to probe the structure of solids. During X-ray absorption experiments, an X-ray having a given wavelength, or monochromatic beam, is directed into a sample. Then, the energy of the X-ray beam is gradually increased in order to reach the absorption energy of the photoelectrons of the element being analyzed. When the X-ray energy is equal to the binding energy of a core electron from

an inner shell, it is adsorbed causing a sharp jump (absorption *edge*) in the adsorption energy occurs and a 16 photoelectron is emitted. The absorption edge corresponds to the energy required to excite and emit an electron from an inner shell of the atom. Below that edge energy the X-ray absorption is low and no electron excitation is observed. The particle-wave duality of the emitted photoelectron allows one to visualize it as a propagating wave interacting with the surrounding atoms. The constructive and destructive interference between the outgoing and back-scattered electron waves results in a series of oscillations on the high photon energy side of the adsorption edge. If the outgoing and backscattered photoelectron waves are out of phase and thus interfere destructively, it will be a local minimum in the spectrum. In contrast, constructive interference will give a local maximum. These oscillations are related to the atomic structure information of the scattering atoms. Using a scattering model it is possible to fit the data to the model and obtain information such as the atomic number, scattering distance, and coordination number of the atoms surrounding the element being studied. Depending on the energy range beyond the ionization edge, the absorption spectrum is classified between 5 and 150eV as X-ray Absorption Near Edge Structure (XANES), and above 150 eV as X-ray Absorption Fine Structure (EXAFS). The XANES region provides information of the oxidation state of the atom and the local geometry around the atom. The EXAFS region provides detailed information on the local environment of the target atom, coordination numbers and scattering lengths. Since the X-ray energy must be varied in the range close to the edge energy, EXAFS experiments require a tunable high intensity x-ray source, which are best attained with the use of synchrotrons. In a typical synchrotron, electrons are accelerated at high speed by magnetic fields so that they follow a circular trajectory. During this process the particles emit synchrotron radiation which typically

includes radio waves, infrared light, visible light, ultraviolet light, and x-rays. The latter, being several orders of magnitude greater than the radiation from a typical laboratory X-ray source. Measurements using extended x-ray absorption spectroscopy focusing on near edge spectroscopy were carried out at the Advanced Photon Source (APS) at Argonne National Laboratory (ANL). The measurements were made in transmission mode with ionization chambers optimized for the maximum current with linear response (~1010 photons detected/sec). A cryogenically cooled double-crystal Si (111) monochromator with resolution (ΔE) better than 2.5 eV at 8.979 keV (Cu K edge) was used in conjunction with a Rh-coated mirror to minimize the presence of harmonics. The integration time per data point was 1-3 sec, and three scans were obtained for each processing condition. Standard procedures based on WINXAS97 software were used to extract the XANES spectra. Phase shifts and backscattering amplitudes were obtained from XANES data obtained for the following reference compounds: CuO and Cu₂O for Cu-O and Cu foil for Cu-Cu while Cr₂O₃ and CrO₃ for Cr-O and Cr foil for Cr-Cr. The sample was pressed into a cylindrical holder with a thickness chosen to give an absorbance ($\Delta\mu x$) of about 1.0 in the Cu edge region. Due to the high density of the Cu based catalysts; the fresh powder was diluted by a factor of 10 with fumed silica prior to being pressed into a wafer. The sample holder was centered in a continuous-flow EXAFS reactor tube 18 inches long and 0.75 inches diameter. The tube was fitted at both ends with polyimide windows to allow transmission of the x-ray beam with gas valves fitted perpendicular to the tube. The reactor was fitted into a clamshell style electrical furnace, which was controlled and monitored with three type K thermocouples located inside the reactor tube and furnace assembly (see figure 1).



Figure 1: reactor assembly and sample holders.

This furnace, window, and valve configuration allowed isolation of the reactor from the atmosphere and the ability to flow various reducing, reactant, and oxidizing gas mixtures at elevated temperatures, all while being probed by the x-ray beam, meaning the catalyst under operando reaction conditions could be monitored. The catalysts were studied under reaction and reducing conditions. Spectrum was first recorded with the catalyst in its untreated state at room temperature (in air). All samples were previously reduced by heating in a reducing atmosphere of pure H_2 to a temperature of 300°C , then scanned after cooling to room temperature. For reaction studies under ethanol decomposition reaction conditions the temperature was changed to the desired set point and a reaction mixture of $2.2 \text{ cm}^3/\text{min}$ of $\text{CH}_3\text{CH}_2\text{OH}$ in He was flowed over the catalyst for 30 minutes. After that the XANES spectrum was recorded with the aim of evaluating the variation of the oxidation state during the reaction.

A-9 DRIFT: Characterization of adsorbed species on surfaces. Fourier Transform Infrared Spectroscopy

Atoms in a molecule have a periodic motion while the molecule as a whole has translational and rotational motion. The frequency of that periodic motion is known as a vibration frequency. Vibrations in a molecule are quantized and can be excited to higher energies by adsorbing photons of similar energy. This adsorbing process changes the rotational and vibrational energy state of the molecule from a ground state to an excited state. The energy transition between the two states occurs at specific photon energies (wavelength), which are characteristic of the atoms or molecular groups under involved. As a result, a group of several bonded atoms or chemical functional group, being studied in a specific infrared energy can absorb radiation at specific energies, which are almost independent of the structure of the rest of the molecule. This absorption process produces specific spectral bands which allow identifying the groups present in the studied molecule and thus determining the molecular structure. This fingerprint character of infrared absorption allows one to use this technique for identifying types of chemical bonds present in molecules. To generate the spectra, the sample is illuminated with an infrared beam having a variable energies and thus frequencies. In this way, excited functional groups present in the sample can be identified. Depending on the wavelength frequency, infrared light can be divided in three main energy regions, far infrared ($4 \sim 400\text{cm}^{-1}$, $\lambda=2500\text{-}25 \mu\text{m}$), mid infrared ($400 \sim 4,000\text{cm}^{-1}$, $\lambda=25\text{-}2.5 \mu\text{m}$) and near infrared ($4,000 \sim 14,000\text{cm}^{-1}$, $\lambda=2.5\text{-}0.7 \mu\text{m}$). For the purpose of catalysis, the mid infrared region is mostly used since it gives information about molecular vibrations of adsorbed molecules. 28

Fourier Transform Infrared (FTIR) spectrometers are widely used to study the infrared absorption of adsorbed species on solid surfaces. Such spectrometers are designed to be able to measure all infrared frequencies simultaneously in the range studied. This is achieved by an internal arrangement of mirrors known as interferometer, which is

able to produce an interference pattern. The Michelson interferometer consists of four arms. The first arm consists of an infrared source usually a carbon rod heated to high temperature, the second arm contains a fixed mirror, the third arm contains a moving mirror, and at the fourth is focused on a detector. At the intersection of the four arms a beamsplitter is located, which is designed to transmit half the radiation that impinges upon it, and reflect half of it. With this setup, the transmitted part of the beam from the beamsplitter is directed to the moving mirror and the reflected part from the beamsplitter directed to the fixed mirror. Both beams recombine at the beam splitter, producing an interferogram which illuminates the sample and then directed to the detector. A sample can be located between the IR reflected from the fourth arm, and then the resulting infrared beam directed to a detector. The transmission mode of operation is the most common experimental arrangement used for solid powders. In this technique, a sample is pressed into a thin self-supported wafer through which the infrared beam is transmitted and captured by a detector. The interference pattern produced is fitted to a Fourier transform series and then deconvoluted to yield a spectrum of adsorbed energy versus frequency. In the present study transmission infrared spectra of pressed disks (~20 mg) were collected in-situ in an IR reactor cell. The cell is placed in an FTIR spectrometer and the spectra were collected at a resolution of 2 cm^{-1} upon collection of 100 scans per spectrum. The spectrometer was equipped with a KBr beamsplitter and a deuterated triglycine sulfate (DTGS) detector. As the amount of radiation striking the detector changes, the temperature of the DTGS element change. This change in temperature is measured in terms of voltage across the detector element. The IR cell is equipped with CsI windows, has connections for inlet and outlet flows, and thermocouples connected to a temperature controller to monitor and control its temperature. The spectra were

obtained in absorbance mode after subtraction of the background spectrum of the catalyst's disk under He atmosphere at the corresponding 30 °C temperature. The samples were pretreated at various conditions prior to study adsorptions and reactions. After pretreatment, the catalyst was cooled down to room temperature in He, and the reaction mixture with a given composition was introduced and spectra collected at different temperatures (example for the PROX reaction: 0.8% CO, 0.8% oxygen, and 51% H₂, with He as balance was added at a total flow rate of 195 cc/min). Transmission IR can be obtained with samples that are partially transparent to IR radiation. When the sample is opaque and infrared transmittance is low, spectra can be collected in diffuse reflectance mode, better known as Diffuse Reflectance Infrared Fourier Transform Spectroscopy or DRIFTS. This mode does not require that the infrared beam goes through the bulk sample as in transmission mode. In the diffuse reflectance mode the infrared beam illuminates a shallow bed of catalyst powder penetrating 1-10 microns into it and it is then reflected back to an optical system. An arrangement of mirrors allows directing the incident infrared beam to a couple of parallel elliptical mirrors. One side of this elliptical mirror direct the incident beam to the sample and then the reflected radiation from the sample is collected by the second elliptical mirror and directed to a detector. The DRIFT spectra of ethanol on copper based catalysts were obtained in a Bruker Equinox 55 spectrometer equipped with a DTSG detector and a moving interferometer with a scanner velocity of 2-30 KHz, a Mid-IR source and a beam splitter. A weighted quantity of catalyst powder was mixed with fumed silica, used to prevent the total adsorption of IR radiation by the black powder characteristic of our samples. The diluted sample was charged in an IR-cell-reactor (Harrick) equipped with a CaF₂ windows and thermostated heaters, and connected to heated inlets and outlet lines to allow ethanol/He flow into the cell.

The samples were pre-treated in-situ by heating under Helium flow ($25 \text{ cm}^3 \text{ min}^{-1}$), then reduced at 300°C in a flow of 20% H_2 in He for about 1h. The system was rapidly cooled and ethanol flow was introduced in the cell and contacted with the pre-treated sample at three different temperature 100; 200; 300°C and at atmospheric pressure. For each spectrum 128 scans in the range $4000\text{--}370 \text{ cm}^{-1}$ frequency range were recorded at a resolution of 4 cm^{-1} (see Figure 2).

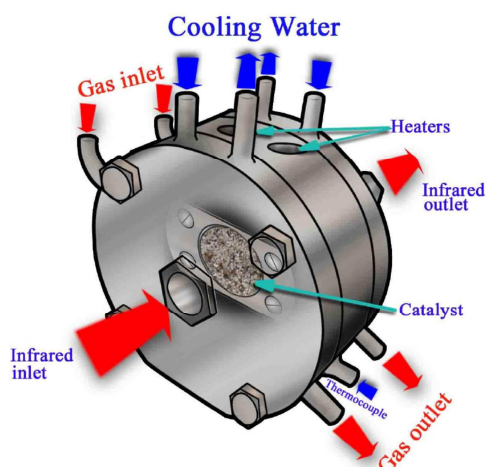


Figure 2: DRIFT cell apparatus

APPENDIX B

MATLAB CODE

B.1 MATLAB CODE to evaluated the kinetic parameters.

B.1.1 Main

```
clc
clear
warning('off','MATLAB:dispatcher:InexactCaseMatch')
% format long
format short

global x0                                % parameters
del modello
global Data                              % data
sperimentali
global nd id
global temper wcat pres
global fe0 fa0 fin0 fh20 fac0 fo0
global xe_sp sa_sp sac_sp so_sp
global it                                % contator
iterazioni
global n_prove                           % exp runs
global i_mod
global xData yData

% choosing model
% i_mod=4 LHHW
%-----
i_mod=4;

% experimental data reading
```

```

%-----
Data=lettura();           % experimental
nd=Data(:,1);            % index exp.run(-)
id=Data(:,2);            % (0=no)exclusion of the run
wcat=Data(:,3);          % catalyst(g)
temper=Data(:,4);        % temperature(°C)
pres=Data(:,5);          % Pressure(atm)
fe0=Data(:,6);           % EtOH(mols/h)
fa0=Data(:,7);           % AcH (mols/h)
fin0=Data(:,8);          % Inert(mols/h)
fh20=Data(:,9);          % Hydrogen(mols/h)
fac0=Data(:,10);         % Ethyl acetate(mols/h)
fo0=Data(:,11);          % Others(mols/h)
xe_sp=Data(:,13);        % EtOH conversion
sac_sp=Data(:,14);       % AcH selectivity
sa_sp=Data(:,15);        % AcOEt selectivity
so_sp=Data(:,16);        % Others selectivity
NP=size(Data);
n_prove=NP(1);
%-----
xData=[wcat temper pres fe0 fa0 fin0 fh20 fac0 fo0];
yData=[xe_sp sac_sp sa_sp so_sp] ;
ySp=xe_sp;

% Parameters
%-----
if i_mod==4
    x0(1)=+97.10; % INIZIALI
    x0(2)=+8.62833e-002 ;
    x0(3)= +9.16221e-004 ;
    x0(4)= 3.62595e+004 ;
    x0(5)= 1.22523e+004 ;
    x0(6)= 1.66183e-004 ;
    x0(7)= 1.03309e+001 ;
    x0(8)= +0.98872e+002 ;
    x0(9)= +4.13585e+001 ;
    x0(10)= 2.66350e-004 ;
    x0(11)= 2.51384e+004 ;
    x0(12)= 7.17526e+003 ;
    x0(13)= 1.39557e+004 ;
    x0(14)= 1.33489e+004 ;
end

```

```

npar=length(x0);

% parameters constraints
%-----

if
elseif i_mod==4
    xbound=[40      100
            0       0.5
            0       0.1
            34000   36000
            13000   14000
            0       0.001
            8       11
            98      120
            36      42
            0       0.01
            24000   26000
            7000    7500
            14000   18000
            11000   14000];

end
xmin=xbound(:,1);
xmax=xbound(:,2);
% reset
%-----
it=0;
% parameters optimization
%-----
OPTIONS1=optimset('MaxFunEvals',1, ...
                  'Display','On',...
                  'TolFun',1.e-8, ...
                  'Tolx',1.e-8,...
                  'LevenbergMarquardt','Off',...
                  'TolCon',1.e-8,...
                  'MaxIter',300);

% [x,resnorm,resid] =
lsqcurvefit('objfun',x0,xData,yData,xmin,xmax,OPTION
S1);
%
% resnorm

```

```

%
jopt=1;
if jopt==1;
[x,resnorm,resid] =
lsqcurvefit('objfun',x0,xData,yData,xmin,xmax,OPTION
S1);
    resnorm;
end
if jopt==2;
    [x,fval] = fminsearch('objfun_fx',x0,OPTIONS1);
    x
    fval
end
if jopt==3;
    [x,fval] =
lsqnonlin('objfun_fx',x0,xmin,xmax,OPTIONS1);
    x
    fval
end
disp ('-----')
-----')

```

B.1.1.2 Objfun

```

% parameters optimizations
%-----
function f=objfun2(par,xData)
global y0                    % conditions
global x0                    % parameters
global it                    %
global temp_i                % temp.(°C)
global wcat_i                % cat.(g)
global pres_i                % press (atm)
global n_prove                % exp.Runs
global i_mod                  % index
global xe_sp sa_sp sac_sp so_sp
x0=par;
zspan=[0 0.5 1];           %
for i=1:n_prove;
wcat_i=xData(i,1);
temp_i=xData(i,2);
pres_i=xData(i,3);

```

```

y0(1)=xData(i,4);    % ethanol
y0(2)=xData(i,5);    % acetaldehyde
y0(3)=xData(i,6);    % inert
y0(4)=xData(i,7);    % hydrogen
y0(5)=xData(i,8);    % ethyl acetate
y0(6)=xData(i,9);    % others
options=odeset('RelTol',0.001);
[z,ycz]=ode45('odesis',zspan,y0,options);
for j=1:6;
    f_out(j)=ycz(3,j);
end
r_a = (2*f_out(2)) / (2*f_out(1));
r_ac = (4*f_out(5)) / (2*f_out(1));
r_o = (4*f_out(6)) / (2*f_out(1));
r_e = (2*f_out(1)) / (2*f_out(1));
sum_r= r_a + r_ac + r_o + r_e;
sum_r
xe_cal(i)=1 - (1/sum_r) ;
if xe_cal(i)~=0
    fatt_sel=(1-xe_cal(i))/xe_cal(i);
else
    fatt_sel=1;
end
sa(i) = r_a*fatt_sel;
sac(i)= r_ac*fatt_sel;
so(i) = r_o*fatt_sel;
sum_sel(i)=sa(i)+sac(i)+so(i);
end
% sa, sac, so, sum_sel
yData_cal(:,1)=xe_cal;
yData_cal(:,2)=sac;
yData_cal(:,3)=sa;
yData_cal(:,4)=so;
f=yData_cal;
sum_err=0;
for i=1:n_prove;
    delta_conv(i)=100*abs(xe_cal(i)-
xe_sp(i))/abs(xe_cal(i));
    sum_err=sum_err+delta_conv(i);
    delta_sac(i) =100*abs(sac(i)-
sac_sp(i))/abs(sac_sp(i));
    delta_sa(i) =100*abs(sa(i)-
sa_sp(i))/abs(sa_sp(i));

```



```

i_prove=0;
for i=1:n_rows
    if Data1(i,2)~=0
        i_prove=i_prove+1;
        for j=1:n_columns
            Data(i_prove,j)=Data1(i,j);
        end
    end
end
end

```

B.1.2 Model LHHW

```

function fdot = modello_4( fmol )
global x0
global temp_
global wcat_i
global pres_i
% ---- gas constant ----
rgas=1.987; % calK?1mol?1;
% ---- molar flow rates ----
fe = fmol(1);
fa = fmol(2);
fi = fmol(3);
fh2 = fmol(4);
fac = fmol(5);
fo = fmol(6);
ftot= fe+fa+fi+fh2+fac+fo;
% ---- molar fraction----
ye = fe/ftot;
ya = fa/ftot;
yi = fi/ftot;
yh2 = fh2/ftot;
yac = fac/ftot;
yo = fo/ftot;
% ---- partial pressure----
ptot=pres_i;
pe = ptot*ye;
pa = ptot*ya;
pi = ptot*yi;
ph2 = ptot*yh2;
pac = ptot*yac;
po = ptot*yo;

```

```

% ----Kinetic constants, activation energies and
equilibrium constants----
tk=temp_i+273.15;
trif=220+273.15;
kr1 =x0(1); % kinetic constant
kr2 =x0(2);
kr3 =x0(3);
ea1 =x0(4); % activation energies
ea2 =x0(5);
ea3 =x0(6);
ker =x0(7); %adsorption constants
kar =x0(8);
kaer=x0(9);
kh2r=x0(10);
de =x0(11);
da =x0(12);
dae =x0(13);
dh2 =x0(14);
%-----ki vs T-----
inv_t=(1/trif)-(1/tk);
k1=kr1*exp((ea1/rgas)*inv_t);
k2=kr2*exp((ea2/rgas)*inv_t);
k3=kr3*exp((ea3/rgas)*inv_t);
%----- Keq vs T by ASPEN-----
ke1=exp((-9136.40/tk)+15.434+1.17);
ke2=exp(+ (4386.003/tk)-4.79);
%----kads vs T-----
ke=ker*exp((de/rgas)*inv_t);
ka=kar*exp((da/rgas)*inv_t);
kae=kaer*exp((dae/rgas)*inv_t);
kh2=kh2r*exp((dh2/rgas)*inv_t);

% ---- reaction rates-----
te1=(1/ke1)*(pa*ph2);
if te1>pe
    te1=pe;
end
te2=(1/ke2)*(pac*ph2);
if te2>pe*pa
    te2=pe*pa;
end

```

```
tads=(1+ke*pe+ka*pa+kh2*ph2+kae*pac)^2;
r1=k1*ke*(pe-te1)/tads;
r2=k2*ka*ke*(pa*pe-te2)/tads;
r3=k3*pa^2;

% ---- mass balance ----
fdot(1)= wcat_i*(-r1-r2);           % ethanol
fdot(2)= wcat_i*(r1-r2-2*r3);      % acetaldehyde
fdot(3)= wcat_i*(0);               % inert
fdot(4)= wcat_i*(r1+r2);           % hydrogen
fdot(5)= wcat_i*(r2);              % ethyl acetat
fdot(6)= wcat_i*(r3);              % others
end
```

APPENDIX C

Plant equipment

Summary of the employed equipment and of the operative conditions used to sizing them.

Table 1: Pump-section 100

Equip. No.	23
Pump	P-101
Output pressure bar	1.0000
Efficiency	1.0000
Calculated Pout bar	1.0000
Vol. flow rate m ³ /h	29.0403
Mass flow rate kg/h	23000.0020

Table 2: Heat exchangers-section 100

Equip.	24	38	37
Heat Ex.	E-101	E-102	E-103
1st Stream T Out (kcal/h)	80.0000 1.3633e+007	80.0000 1.2354e+007	80.0000 -3.2005e+006
LMTD Corr Factor (bar)	1.0000	1.0000	1.0000
	1.0000	1.0000	1.0000

Table 3: compressor-section 100

Compressor	
Equip. No. Compressor	8
Name	C-101
Pressure out (bar)	20.0000
Type of Compressor	1
Efficiency	0.7500
Actual power (kcal/h)	3.9664e+006
Cp/Cv	1.1452
Theoretical power (kcal/h)	2.9748e+006
Ideal Cp/Cv	1.1242
Calc Pout (bar)	20.0000
Calc. mass flowrate (kg/h)	59192

Table 4: distillation towers (TWRS)-section 100

Equip. No.	33	34
Name: distillation towers	T-101	T-102
No. of stages	30	15
1st feed stage	3	7
2nd feed stage	22	0
Top pressure (bar)	1.0000	1.0000
Condenser mode	7	7
Condenser spe	0.9990	0.9990

Cond comp i	1	6
Reboiler mode	7	7

Table 5: heat exchangers- section 200

Eq.n	13	5	6	7	21
H.Ex.	E-201	E-202	E-203	E-204	E-205
TOut (°C)	220.0000	220.0000	230.0000	230.0000	5.0000
(kcal/h)	-801018	351190	496704	106195	-1.6345E7
LMDT	1.0000	1.0000	1.0000	1.0000	1.0000
P _{out} (bar)	20.0000	20.0000	20.0000	20.0000	20.0000

Table 6: kinetics reactors- section 200

Equip. No.	1	2	3	4
Name Reactors	R-201	R-202	R-203	R-204
Reactor type	2	2	2	2
Reaction phase	1	1	1	1
Thermal mode	2	2	2	2
Pressure (bar)	20.0000	20.0000	20.0000	20.0000
T _{out} C	209.2982	214.9438	226.8005	227.6552
Reactor vol. (m ³)	10.0000	10.0000	10.0000	10.0000
C.flag	1	1	1	1
Number of steps	300	300	300	300
No.of Reactions	3	3	3	3
Molar Flow Unit	2	2	2	2
Activ. E/H	6	6	6	6
Volume Unit	3	3	3	3
U(kcal/h-m ² -C)	10.0000	10.0000	10.0000	10.0000
(kcal/h)	-13946.4883	-3941.0779	-713.1607	-215.2497
Mass unit	2	2	2	2
Partial P unit	2	2	2	2

Table 7: flash- section 300

Equip. No.	14	30
Name Flash	V-301	V-302
Flash Mode	0	2
Param	5.0000	-20.0000
Param 2	20.0000	50.0000
Heat duty (kcal/h)	0.0230	
K values:		
Ethanol	1.513E-003	1.076E-004
Ethyl Acetate	5.352E-003	1.080E-003
Hydrogen	200.719	102.824
Acetaldehyde	0.025	4.952E-003
Nitrogen	87.669	56.335
Water	1.153E-003	6.742E-005
Cis-Crotonaldehy	1.654E-003	2.053E-004
Ethylene Glycol	1.846E-006	7.770E-008

Table 8: compressor-section 300

Equip.No.	27
Name Compressor	C-301
Pressure out bar	50.0000

Type of Compressor	1
Efficiency	0.7500
Actual power (kcal/h)	378150.0313
Cp/Cv	1.3991
Theoretical power (kcal/h)	283612.5313
Ideal Cp/Cv	1.3891
Calc Pout bar	50.0000
Calc. mass flowrate (kg/h)	1584

Table 9: heat exchanger-section 300

Equip. No.	39	11	15
Name H.ex	E-301	E-302	E-303
1st Stream T _{out} (°C)	-20.0000	20.0000	200.0000
Ht Duty(kcal/h)	-472920.0000	137214.7188	1.4464e+007
LMTD Corr Factor	1.0000	1.0000	1.0000
1st Stream P _{out} (bar)	50.0000	50.0000	20.0000

Table 10: valve-section 300

Equip. No.	29
Name Valve	
Pressure out bar	50.0000

Table 11: expander-section 300

Equip. No.	41
Pressure out bar	20.0000
Type of Expander	1
Efficiency	0.7500
Actual power kcal/h	-505.6559
Cp/Cv	1.1836
Theoretical power (kcal/h)	-674.2078
Ideal Cp/Cv	1.0386
Calc Pout bar	20.0000

Table 12: component separator-section 3

Equip. No.	10
Name Separator	T-302
Top Temp Spec	200.0000
Bottom Temp Spec	200.0000
Heat duty kcal/h	-5152.8140
Component No. 3	1.0000
Component No. 4	1.0000

Table 13: distillation towers-section 4

Equip. No.	9	16
Name	T-401	T-402
No. of stages	30	30
1st feed stage	20	10
Top pressure bar	20.0000	1.0000
Condenser mode	1	1
Condenser spec.	3.0000	0.5000
Reboiler mode	3	3
Reboiler spec.	206.0000	77.0000
Initial flag	1	1
Calc cond duty (kcal/h)	-5.5480e+007	-2.0983e+007

Calc rebr duty kcal/h	3.9099e+007	9.6528e+006
Est. Dist. rate (kmol/h)		151.4930
Est. Reflux rate(kmol/h)		75.7465
Est. T top C	173.4420	95.9732
Est. T bottom C	184.5531	77.0000
Est. T 2 C	178.8442	76.3716
Column diameter m		2.2860
Tray space m		0.6096
No of sections	0	1
Calc Reflux ratio	3.0000	0.5000
Calc Reflux mole (kmol/h)	6888.0435	749.7289
Calc Reflux mass kg/h	373542.6250	43941.1211
No of passes (S1)	0	1
Weir side width cm		13.9700
Weir height cm		5.0800
System factor		1.0000
Optimization flag	1	1

Table 14: compressor-section 4

Equip. No.	20
Name Compressor	C-401
Pressure out bar	20.0000
Type of Compressor	1
Efficiency	0.7500
Actual power (kcal/h)	78649.6328
Cp/Cv	1.1302
Theoretical power(kcal/h)	58987.2227
Ideal Cp/Cv	1.1054
Calc Pout bar	20.0000
Calc. mass flowrate(kg/h)	87881

Table 15: valve-section 4

Equip. No.	28
Name Valve	
Pressure out bar	1.0000

Table 16: separator-section 4

Equip. No.	22
Name Separator	T-403
Heat duty kcal/h	181769.7500
Component No. 2	0.9950